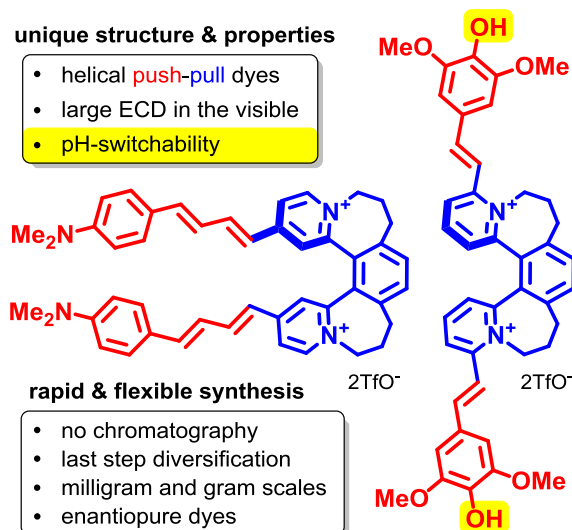


# Electronic Supplementary Information

## Functional helquats: cationic dyes with marked, switchable chiroptical properties in the visible region

Paul E. Reyes-Gutiérrez, Michael Jirásek, Lukáš Severa, Pavlína Novotná, Dušan Koval, Petra Sázelová, Jan Vávra, Andreas Meyer, Ivana Čísařová, David Šaman, Radek Pohl, Petr Štěpánek, Petr Slaviček, Benjamin J. Coe, Miroslav Hájek, Václav Kašička, Marie Urbanová, and Filip Teplý\*



## Table of contents

1) General information	S3
2) Materials	S5
3) Procedures and analytical data	S8
Part A: Synthesis of racemic [6]helquat ( <i>rac</i> )- <b>6</b>	S9
Part B: Synthesis of racemic [5]helquat ( <i>rac</i> )- <b>3</b>	S14
Part C: Synthesis of racemic [5]helquat ( <i>rac</i> )- <b>7</b>	S20
Part D: Resolution of racemic [5]helquats ( <i>rac</i> )- <b>3</b>	S24
Part E: Resolution of racemic [5]helquats ( <i>rac</i> )- <b>7</b>	S31
Part F: Synthesis of racemic dyes <b>6a-h</b> from ( <i>rac</i> )- <b>6</b>	S38
Part G: Synthesis of racemic dyes ( <i>rac</i> )- <b>3a</b> , ( <i>rac</i> )- <b>3i</b> , ( <i>rac</i> )- <b>3j</b> and non-racemic dyes (+)-( <i>P</i> )- <b>3a</b> , (-)-( <i>P</i> )- <b>3i</b> , (-)-( <i>P</i> )- <b>3j</b> and (-)-( <i>M</i> )- <b>3a</b> , (+)-( <i>M</i> )- <b>3i</b> , (+)-( <i>M</i> )- <b>3j</b> ....	S50
Part H: Synthesis of racemic dyes ( <i>rac</i> )- <b>7a</b> , ( <i>rac</i> )- <b>7i</b> , ( <i>rac</i> )- <b>7j</b> and non-racemic dyes (-)-( <i>P</i> )- <b>7a</b> , (-)-( <i>P</i> )- <b>7i</b> , (-)-( <i>P</i> )- <b>7j</b> and (+)-( <i>M</i> )- <b>7a</b> , (+)-( <i>M</i> )- <b>7i</b> , (+)-( <i>M</i> )- <b>7j</b> ...	S58
Part I: Synthesis of racemic pH-switchable dyes ( <i>rac</i> )- <b>3k</b> and non-racemic dyes (+)-( <i>P</i> )- <b>3k</b> , (-)-( <i>M</i> )- <b>3k</b>	S67
Part J: Synthesis of racemic pH-switchable dyes ( <i>rac</i> )- <b>7k</b> and non-racemic dyes (-)-( <i>P</i> )- <b>7k</b> , (+)-( <i>M</i> )- <b>7k</b>	S72
4) Capillary electrophoresis (CE)	S76
5) Experimental UV-Vis absorption and ECD spectra	S99
6) Calculated UV-Vis absorption and ECD spectra	S123
7) X-ray analysis	S142
8) References	S157
9) <sup>1</sup> H and <sup>13</sup> C NMR spectra	S160

## 1) General information

Liquids and solutions were transferred via needle and syringe under inert atmosphere unless otherwise stated. Melting points were determined on a Wagner & Munz PolyTherm A micro melting point apparatus and on a Stuart melting point SMP30 apparatus, and are uncorrected. Thin-layer chromatography (TLC) analysis was performed on silica gel plates (Silica gel 60 F<sub>254</sub>-coated aluminium sheets, Merck, cat. no. 1.05554.0001) and visualized by UV (UV lamp 254/365 nm, Spectroline<sup>®</sup> Model ENF – 240C/FE) and/or chemical staining with KMnO<sub>4</sub> [KMnO<sub>4</sub> (1% aq.), Na<sub>2</sub>CO<sub>3</sub> (2% aq.)]. TLC analysis of dications was achieved using Stoddart's magic mixture<sup>1</sup> (MeOH : NH<sub>4</sub>Cl aq (2M) : MeNO<sub>2</sub> 7 : 2 : 1) as eluent on silica gel plates. If necessary, DMSO was removed from samples using a Labconco evaporator (Refrigerated CentriVap Benchtop Vacuum Concentrator, cat. no. 7310031). Sonication was conducted with a BANDELIN SONOREX sonicator. NMR spectra were measured on a Bruker Avance 600 (600 MHz for <sup>1</sup>H, 151 MHz for <sup>13</sup>C) or Bruker Avance 400 (400 MHz for <sup>1</sup>H, 101 MHz for <sup>13</sup>C) NMR spectrometer. In <sup>1</sup>H and <sup>13</sup>C NMR spectra, chemical shifts are referenced as follows (ppm): in acetone-*d*<sub>6</sub> the peaks were referenced relative to the solvent peak  $\delta_{\text{H}} = 2.09$  ppm and  $\delta_{\text{C}} = 29.80$  ppm; in CDCl<sub>3</sub> relative to Me<sub>4</sub>Si signals  $\delta_{\text{H}} = 0.00$  ppm or the solvent peak  $\delta_{\text{H}} = 7.26$  ppm and  $\delta_{\text{C}} = 77.00$  ppm; acetonitrile-*d*<sub>3</sub> relative to the solvent peak  $\delta_{\text{H}} = 1.94$  ppm and  $\delta_{\text{C}} = 118.26$  ppm; and DMSO-*d*<sub>6</sub>  $\delta_{\text{H}} = 2.50$  ppm and  $\delta_{\text{C}} = 39.50$  ppm. Chemical shifts are given in  $\delta$ -scale as parts per million (ppm); coupling constants (*J*) are given in Hertz. IR spectra were recorded on a Bruker EQUINOX55 (IFS55) spectrometer in KBr pellets. Mass spectral data were obtained at the Mass Spectrometry Facility operated by the Institute of Organic Chemistry and Biochemistry, Academy of Sciences of the Czech Republic, v.v.i. (IOCB ASCR). Electrospray ionization (ESI) mass spectra were recorded using a Thermo Scientific LCQ Fleet mass spectrometer equipped with an electrospray ion source and controlled by Xcalibur software. The mobile phase consisted of MeOH : water (9 : 1), flow rate of 200  $\mu\text{L}\cdot\text{min}^{-1}$ . The sample was dissolved, diluted with the mobile phase and injected using a 5  $\mu\text{L}$  loop. Spray voltage, capillary voltage, tube lens voltage and capillary temperature were 5.5 kV, 5 V, 80 V and 275°C, respectively. High-resolution mass spectra (HR MS) were obtained with the ESI instrument. Specific rotation values were determined with an Autopol IV (Rudolph Research Analytical, USA, 2001) polarimeter. Specific rotation values  $[\alpha]_{\text{D}}^{20}$  were measured in MeOH unless stated otherwise (concentrations units: g/100 mL). Molar rotation values  $[\phi]_{\text{D}}^{20}$  (units: deg cm<sup>2</sup> dmol<sup>-1</sup>) were calculated from specific

rotation values  $[\alpha]_D^{20}$  according to the following formula  $[\phi]_D^{20} = [\alpha]_D^{20} \cdot M_w / 100$  (where  $M_w$  is molecular weight in g/mol). For general information about capillary electrophoresis (CE), see Section S4 (p. S76). For general information related with Electronic Circular Dichroism (ECD) and UV-Vis, see Section S5 (p. S99). X-ray general information is shown in Section S7 (p. S142).

## 2) Materials

Demineralized water obtained from the Water Purification Facility at the IOCB ASCR was used unless otherwise stated. Demineralization was accomplished via filtration through ion exchange columns (Lewatit S100 for catex column, Lewatit MP500 for anex column) in a demineralization ion exchange station type ID-PP and IDKP (Kavalier, Votice, Czech Republic).

Dichloromethane and triethylamine were purified via distillation under argon over CaH<sub>2</sub> and were used directly after distillation. MeOH was distilled from Mg/I<sub>2</sub> as follows. MeOH (100 mL) was charged into a 1 L round-bottomed flask. Then, 5 g of Mg was added followed by addition of I<sub>2</sub> (500 mg). The mixture was heated to reflux under Ar atmosphere for 15 min. Then, more I<sub>2</sub> (500 mg) and MeOH (500 mL) were added and the mixture was refluxed under Ar atmosphere for 2h.

Degassed solvents were obtained via the freeze-pump-thaw method. The solvent was frozen under argon, and then thawed under vacuum. This process was repeated (3×). Finally the thawed solvent was purged with argon. DMSO-*d*<sub>6</sub> was dried over 4 Å molecular sieves. Unless otherwise stated, all other starting materials and reagents were obtained from commercial suppliers and used without further purification.

Stoddart's magic mixture<sup>1</sup> = MeOH : 2 M NH<sub>4</sub>Cl : MeNO<sub>2</sub> = 7 : 2 : 1

Pent-3-yn-1-yl trifluoromethanesulfonate was prepared according to previous report<sup>2</sup> and was then used without further purification.

Trifluoromethanesulfonic anhydride (Alfa Aesar, 98%, 658-23-6)

Trifluoromethanesulfonic acid (Sigma-Aldrich, ReagentGrade<sup>®</sup>, 98%, 158534)

1-Chloroisoquinoline (Aldrich, 95%, 19493-44-8)

Acetylene gas (Dissolved, Messer Technogas, UN1001)

CuI (Aldrich, 99.999%, 7681-65-4)

Bis(triphenylphosphine)palladium (II) dichloride [PdCl<sub>2</sub>(PPh<sub>3</sub>)<sub>2</sub>] (Aldrich, 98%, 208671)

[Pd(PPh<sub>3</sub>)<sub>4</sub>] (Aldrich, 99%, 216666)

2-Bromo-4-methylpyridine (TCI, B2112)

2-Bromo-6-methylpyridine (TCI, B2114)

4-Pentyn-1-ol (Alfa Aesar, 98%, 5390-04-5)

Pyridine (Alfa Aesar, anhydrous 99.5%, 110-86-1)

Et<sub>3</sub>N (Alfa Aesar, 99%, 121-44-8)

Tris(triphenylphosphine)rhodium(I)chloride, [RhCl(PPh<sub>3</sub>)<sub>3</sub>] (Fluka, 97+%, 14694-95-2)  
*N,N*-Dimethylformamide (Aldrich, 99.8%, 319937)  
DMSO (Aldrich, 99%, 67-68-5)  
NaOH (Penta, 1310-73-2)  
Dowex<sup>®</sup> resin 1x2, 16-100, Supelco  
(-)-Dibenzoyl-L-tartaric acid (Anhydrous, 99%, Alfa Aesar, A16181)  
(+)-Dibenzoyl-D-tartaric acid (Anhydrous, 99%, Alfa Aesar, B24754)  
4-(Dimethylamino)benzaldehyde (ACS reagent, 99%, 156477 or Aldrich, 99%, 100-10-7)  
4-(Dimethylamino)cinnamaldehyde (Apollo Scientific Limited, 0R17035)  
2,3-Dimethoxybenzaldehyde (Aldrich, 98%, 86-51-1)  
4-(Diphenylamino)benzaldehyde (Acros Organics, 98%, 4181-05-9)  
9-Julolidine carboxaldehyde (Synthon, 98%, 33985-71-6)  
6-Methoxy-2-naphthaldehyde (Aldrich, 98%, 3453-33-6)  
9-Anthracenecarboxaldehyde (Aldrich, 97%, 642-31-9)  
*p*-Anisaldehyde (Aldrich, 123-11-5)  
4-*n*-Dodecyloxybenzaldehyde (Alfa Aesar, 98%, 24083-19-0)  
Syringaldehyde (Aldrich, S7602)  
Piperidine (ReagentPlus<sup>®</sup>, 99%, Sigma-Aldrich, 10409-4)  
Pyrrolidine (99%, Aldrich, P73803)  
Acetone, CH<sub>2</sub>Cl<sub>2</sub>, Et<sub>2</sub>O, hexane, cyclohexane, ethanol, 2-propanol, EtOAc, and MeOH were purchased from PENTA, Czech Republic ([www.pentachemicals.eu](http://www.pentachemicals.eu)).  
Ethanol (Merck, Uvasol<sup>®</sup>, 100980)  
Acetone-*d*<sub>6</sub> (Merck, 99.9%, 100021)  
DMSO-*d*<sub>6</sub> (Euriso-Top, C.E. Saclay, H<sub>2</sub>O < 0.02%, 99.80% D, D010H Z0331, 100 mL; with 4 Å molecular sieves added)  
CDCl<sub>3</sub> (Merck, 99.8%, 102450)  
Acetonitrile-*d*<sub>3</sub> (water < 0.05%, Euriso-Top, D021P)  
Methanol-*d*<sub>4</sub> (99.8 atom% D, Aldrich, 151947)  
CaH<sub>2</sub> (Alfa Aesar, coarse powder, 7789-78-8)  
Celite (Fluka, 512 medium, 91053-39-3)  
Universal pH paper strips for pH 0-12 (Lachner)  
MeOH for ECD measurements (Lachner)  
Centrifuge tubes, Sarstedt C-51588

Abbreviations:

BGE = background electrolyte (for capillary electrophoresis)

CE = capillary electrophoresis

DBT = dibenzoyl tartrate

DMSO = dimethylsulfoxide

Eq. = equation

equiv = equivalents

Et<sub>2</sub>O = diethyl ether

EtOAc = ethyl acetate

MeOH = methanol

PDA = photodiode array

SBE-β-CD = sulfobutyl-β-cyclodextrin (Section S4)

S-γ-CD = sulfated γ-cyclodextrin (Section S4)

Tf = CF<sub>3</sub>SO<sub>2</sub>

TfOH = trifluoromethanesulfonic acid

RT = room temperature

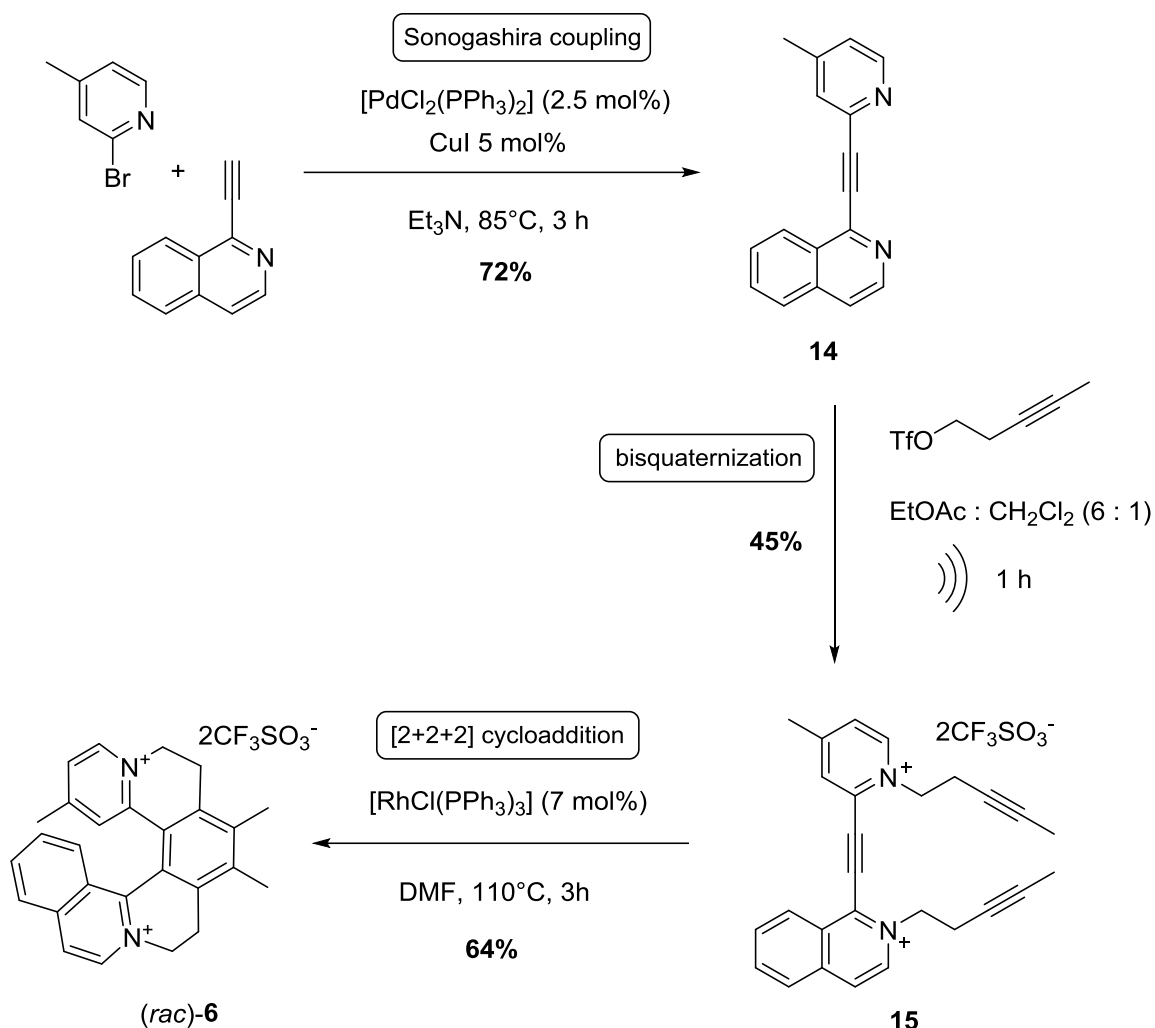
TLC = thin-layer chromatography

### 3) Procedures and analytical data

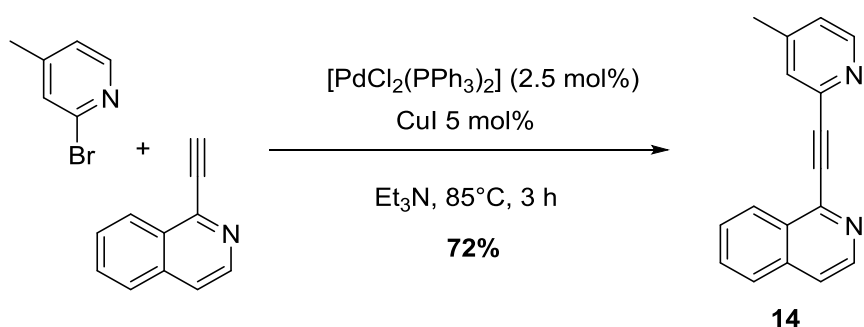
Part A: Synthesis of racemic [6]helquat ( <i>rac</i> )- <b>6</b> .....	S9
Part B: Synthesis of racemic [5]helquat ( <i>rac</i> )- <b>3</b> .....	S14
Part C: Synthesis of racemic [5]helquat ( <i>rac</i> )- <b>7</b> .....	S20
Part D: Resolution of racemic [5]helquat ( <i>rac</i> )- <b>3</b> .....	S24
Part E: Resolution of racemic [5]helquat ( <i>rac</i> )- <b>7</b> .....	S31
Part F: Synthesis of racemic dyes <b>6a-h</b> from common precursor ( <i>rac</i> )- <b>6</b> .....	S38
Part G: Synthesis of racemic dyes ( <i>rac</i> )- <b>3a</b> , ( <i>rac</i> )- <b>3i</b> , ( <i>rac</i> )- <b>3j</b> and non-racemic dyes (+)-( <i>P</i> )- <b>3a</b> , (-)-( <i>P</i> )- <b>3i</b> , (-)-( <i>P</i> )- <b>3j</b> and (-)-( <i>M</i> )- <b>3a</b> , (+)-( <i>M</i> )- <b>3i</b> , (+)-( <i>M</i> )- <b>3j</b> ...	S50
Part H: Synthesis of racemic dyes ( <i>rac</i> )- <b>7a</b> , ( <i>rac</i> )- <b>7i</b> , ( <i>rac</i> )- <b>7j</b> and non-racemic dyes (-)-( <i>P</i> )- <b>7a</b> , (-)-( <i>P</i> )- <b>7i</b> , (-)-( <i>P</i> )- <b>7j</b> and (+)-( <i>M</i> )- <b>7a</b> , (+)-( <i>M</i> )- <b>7i</b> , (+)-( <i>M</i> )- <b>7j</b> ...	S58
Part I: Synthesis of racemic pH-switchable dye ( <i>rac</i> )- <b>3k</b> and non-racemic dyes (+)-( <i>P</i> )- <b>3k</b> , (-)-( <i>M</i> )- <b>3k</b> .....	S67
Part J: Synthesis of racemic pH-switchable dye ( <i>rac</i> )- <b>7k</b> and non-racemic dyes (-)-( <i>P</i> )- <b>7k</b> , (+)-( <i>M</i> )- <b>7k</b> .....	S72



## Part A: Synthesis of racemic [6]helquat (*rac*)-6

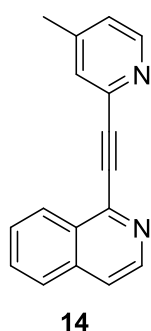


### 1-((4-Methylpyridin-2-yl)ethynyl)isoquinoline, 14



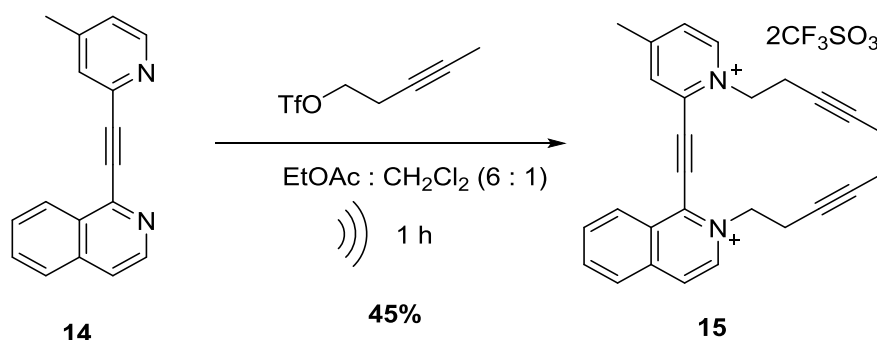
1-Ethynylisoquinoline (3.00 g, 19.60 mmol), 2-bromo-4-methylpyridine (2.7 mL, 23.50 mmol), [PdCl<sub>2</sub>(PPh<sub>3</sub>)<sub>2</sub>] (344 mg, 0.49 mmol, 2.5 mol%) and CuI (187 mg, 0.979 mmol) were added to a Schlenk flask. The flask was flushed with argon. Freshly distilled Et<sub>3</sub>N (100 mL) was added. Resulting mixture was stirred for a few minutes at RT, and then the

mixture was heated to 85°C for 3h. The reaction progress was monitored by TLC (mobile phase hexane : EtOAc = 2 : 1, starting bromopyridine  $R_f = 0.65$ , product **14**  $R_f = 0.3$ ). After the complete consumption of 1-ethynylisoquinoline (TLC,  $R_f = 0.4$ , hexane : EtOAc 2 : 1), the volatiles were removed on a rotary evaporator and resulting residue was dissolved in EtOAc. Solution was filtered through Celite® 512 layer on a sinter and the filtercake was washed with EtOAc. Filtrate was concentrated and the residue was purified by flash chromatography gradient (eluent – hexane : EtOAc, from 4 : 1 to pure EtOAc). Coupling product **14** was obtained as a yellowish solid in 72% yield (3.445 g, 14.10 mmol).



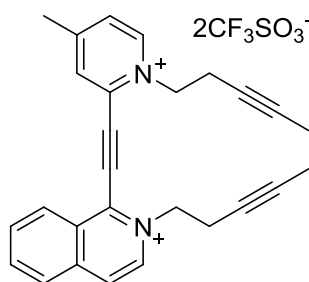
m.p. 115 – 116°C.  $^1\text{H NMR}$  (600 MHz, acetone- $d_6$ ): 2.47 (t,  $J = 0.8$  Hz, 3H); 7.35 (ddq,  $J = 0.8, 1.7, 5.0$  Hz, 1H); 7.73 (m, 1H); 7.86 (ddd,  $J = 1.4, 6.8, 8.33$  Hz, 1H); 7.89 (ddd,  $J = 1.3, 6.8, 8.1$  Hz, 1H); 7.92 (bdd (1.2, 5.7 Hz, 1H); 8.08 (ddt,  $J = 0.8, 1.3, 8.1$  Hz, 1H); 8.59 (dd,  $J = 0.7, 5.0$  Hz, 1H); 8.62 (ddt,  $J = 0.8, 1.3, 8.3$  Hz, 1H); 8.63 (d,  $J = 5.7$  Hz, 1H).  $^{13}\text{C NMR}$  (151 MHz, acetone- $d_6$ ):  $\delta = 20.65; 85.82; 93.50; 122.04; 125.70; 127.20; 128.10; 129.40; 129.45; 130.33; 131.72; 136.70; 143.18; 144.00; 144.19; 148.72; 151.03$ . IR (KBr):  $\nu$  ( $\text{cm}^{-1}$ ) 434; 461; 666; 754; 799; 831; 866; 877; 912; 1014; 1045; 1106; 1155; 1143; 1171; 1209; 1238; 1284; 1298; 1316; 1351; 1383; 1407; 1452; 1466; 1499; 1551; 1578; 1596; 1618; 2211; 2919; 3010; 3039; 3051; 3065; 3082. MS (ESI $^+$ )  $m/z$  (%): 245.1 (100), 267.1 (55), 268.1 (10). HRMS (ESI $^+$ )  $m/z$ : [(M+H) $^+$ ] ( $\text{C}_{17}\text{H}_{13}\text{N}_2$ ) calc.: 245.10732, found 245.10733. Elem. Anal. calc. for  $\text{C}_{17}\text{H}_{12}\text{N}_2$ : C, 83.58; H, 4.95; N, 11.47. Found: C, 83.35; H, 5.01; N, 11.07.

**1-((4-Methyl-1-(pent-3-yn-1-yl)pyridin-1-ium-2-yl)ethynyl)-2-(pent-3-yn-1-yl)isoquinolin-2-ium trifluoromethanesulfonate, **15****



Coupling product **14** (2.00 g, 8.19 mmol) was added to a Schlenk flask and the flask was purged with argon (3×vacuum/argon cycle). Then, freshly distilled  $\text{CH}_2\text{Cl}_2$  (150 mL, distilled from  $\text{CaH}_2$ ) was added under argon followed by alkyne triflate (3.9 mL, 24.56 mmol). The

reaction mixture was sonicated under argon for 1 h. The reaction progress was monitored by TLC (mobile phase hexane : EtOAc = 2 : 1, starting **14**  $R_f = 0.3$ , product **15**  $R_f = 0.4$ ). After that, the mixture was concentrated to a final volume of around 50 mL and then EtOAc (250 mL) was added. The dark precipitate was centrifuged and the supernatant was removed using a Pasteur pipette. The solids were then sonicated 3 times with EtOAc (3×30 mL) and again centrifuged and decanted to obtain a white powder (1.70 g, yield 31%). The residual supernatants were combined, the volatiles were removed by rotary evaporation and the residue dissolved in CH<sub>2</sub>Cl<sub>2</sub> (80 mL). This solution was mixed with water (1.5 L), extracted, and the CH<sub>2</sub>Cl<sub>2</sub> layer was removed. The aqueous layer, containing the dicationic tryne product **15**, was extracted several times with additional portions of CH<sub>2</sub>Cl<sub>2</sub> (3×80 mL). The last extraction led to colorless organic phase. Water from the aqueous layer was removed on rotary evaporator (maximum bath temperature was 50°C). Then, the residue was mixed with EtOAc (30 mL) and then sonicated and centrifuged to give second fraction of the product **15** as an off-white powder (0.75 g, yield 14%). Both solid fractions were combined and dried under vacuum to obtain a white solid in 45% yield (2.45 g, 3.62 mmol). Alternatively, it may be suitable to perform direct extraction with large amount of water right after the removal of volatiles from the reaction mixture. However, too large amount of water would probably be necessary for such extraction. Therefore, because of practical convenience, the precipitation procedure was used to purify the first major fraction of the product.

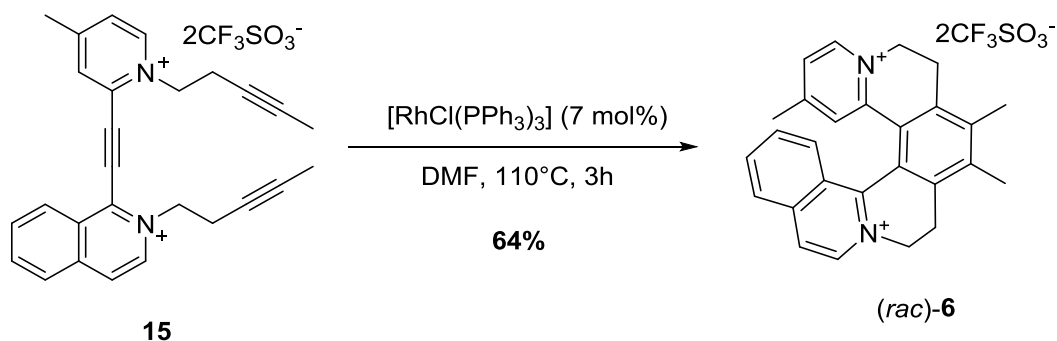


**15**

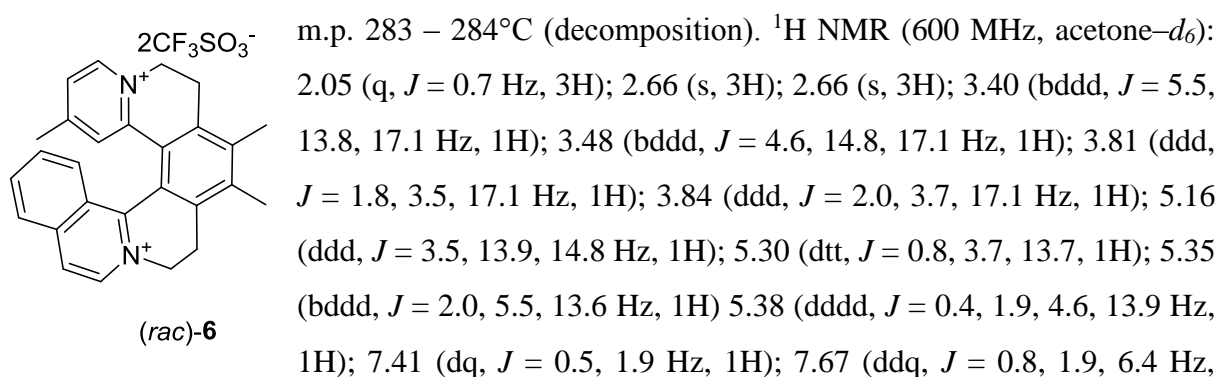
$2CF_3SO_3^-$  m.p. 168 – 170°C (decomposition). <sup>1</sup>H NMR (600 MHz, acetone-*d*<sub>6</sub>): 1.74 (t,  $J = 2.6$  Hz, 3H); 1.77 (t,  $J = 2.6$  Hz, 3H); 3.24 (tq,  $J = 2.6, 6.6$  Hz, 2H); 2.89 (t,  $J = 0.7$  Hz, 3H); 3.29 (tq,  $J = 2.6, 6.5$  Hz, 2H); 5.33 (t,  $J = 6.6$  Hz, 2H); 5.50 (t,  $J = 6.5$  Hz, 2H); 8.35 (ddd,  $J = 1.2, 7.0, 8.6$  Hz, 1H); 8.39 (ddq,  $J = 0.7, 2.0, 6.4$  Hz, 1H); 8.46 (ddd,  $J = 1.0, 7.0, 8.3$  Hz, 1H); 8.60 (dt,  $J = 1.1, 8.3$  Hz, 1H); 8.95 (dq,  $J = 0.7, 2.0$  Hz, 1H); 8.95 (dd,  $J = 1.0, 6.8$  Hz, 1H); 9.10 (dq,  $J = 0.9, 8.6$  Hz, 1H); 9.21 (d,  $J = 6.8$  Hz, 1H); 9.36 (d,  $J = 6.4$  Hz, 1H). <sup>13</sup>C NMR (151 MHz, acetone-*d*<sub>6</sub>):  $\delta = 3.14; 3.18; 21.62; 21.66; 22.00; 60.02; 61.11; 74.09; 74.27; 82.07; 82.24; 89.81; 98.39; 128.59; 129.25; 129.94; 130.92; 131.06; 134.41; 134.55; 136.14; 138.51; 138.61; 138.61; 138.86; 147.77; 161.79$ . IR (KBr):  $\tilde{\nu}$  (cm<sup>-1</sup>) 518; 573; 638; 670; 760; 786; 832; 881; 1030; 1159; 1223; 1258; 1272; 1351; 1386; 1408; 1430; 1460; 1492; 1517; 1565; 1573; 1605; 1627; 2194; 2332; 2863; 2927; 3056; 3082; 3094; 3127; 3146. MS (ESI)  $m/z$

(%): 409.2 (100), 311.1 (56), 377.2 (55), 343.2 (40), 395.2 (37), 410.2 (34), 296.1 (30).  
 HRMS (ESI)  $m/z$ :  $[(M)^{2+}]$  ( $C_{27}H_{26}N_2$ ) calc.: 189.10425, found: 189.10426.

**6,7,13-trimethyl-4,5,8,9-tetrahydroisoquinolino[1,2-a]pyrido[1,2-k][2,9]phenanthroline-3,10-diium trifluoromethanesulfonate, (*rac*)-6**

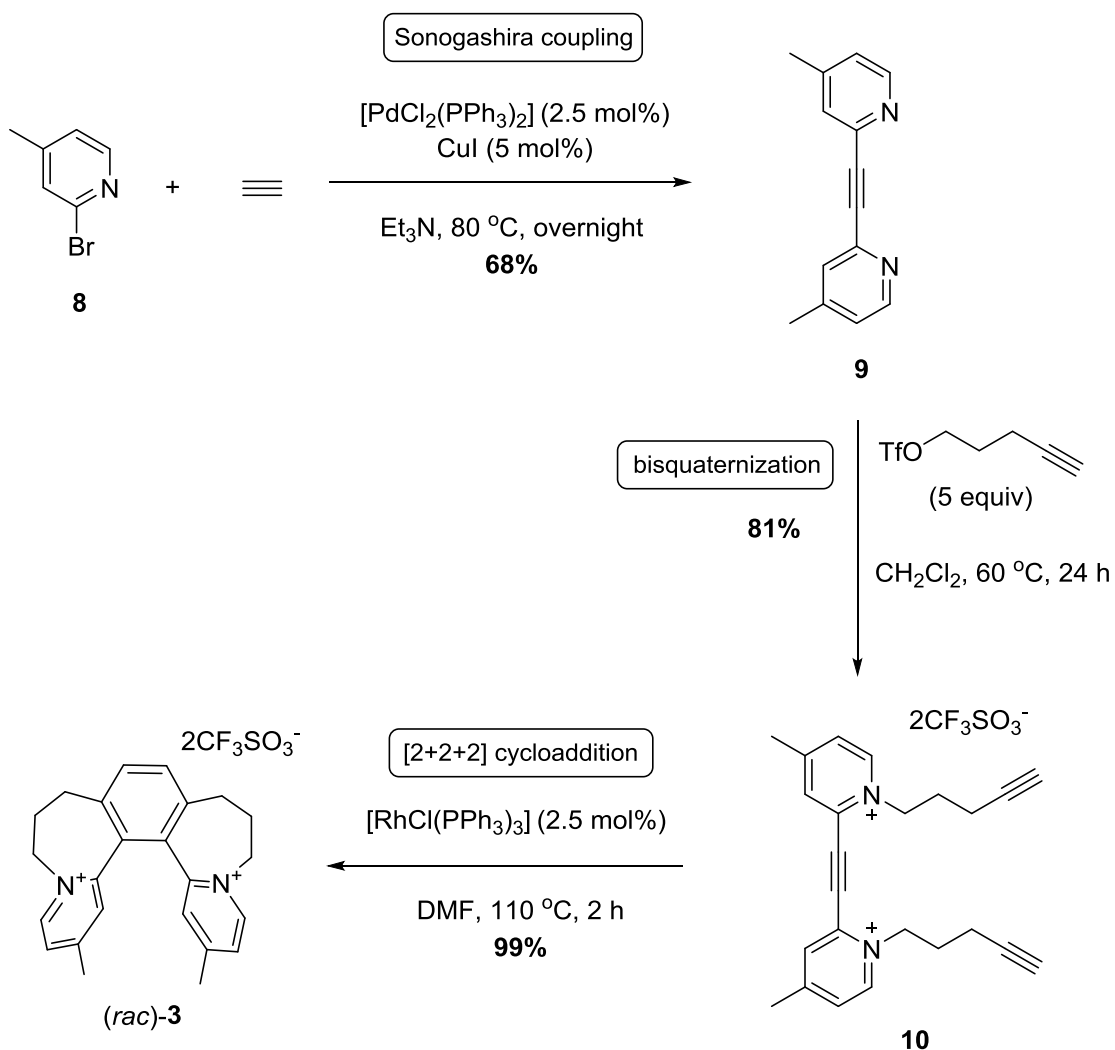


Triyne **15** (1.87 g, 2.77 mmol), Wilkinson's catalyst (179 mg, 0.19 mmol, 7 mol%) and DMF (300 mL) were added to a Schlenk flask. The reaction mixture was then stirred and heated at 110°C for 3h under argon while protected from ambient light using aluminium foil cover. After the reaction was complete according to the TLC (mobile phase Stoddart's magic mixture, starting material **15**  $R_f = 0.4$ , product (*rac*)-**6**  $R_f = 0.5$ ), DMF was removed by evaporation on rotary evaporator and residual solids were sonicated with EtOAc (150 mL) and the suspension was then centrifuged. The solids were separated and then EtOAc : acetone (45 mL, 6 : 1) was added. The resulting suspension was sonicated and then centrifuged to separate the solids. This solid was subsequently purified by sonication and centrifugation three more times using mixture EtOAc : acetone (45 mL, 5 : 1). Next sonication/centrifugation was further repeated with a mixture EtOAc : acetone (35 mL, 3 : 1) and then with EtOAc : acetone (35 mL, 2 : 1) to get an off-white solid. The resultant solid was dried under vacuum to obtain product (*rac*)-**6** as an off-white powder in 64% yield (1.2 g, 1.77 mmol).

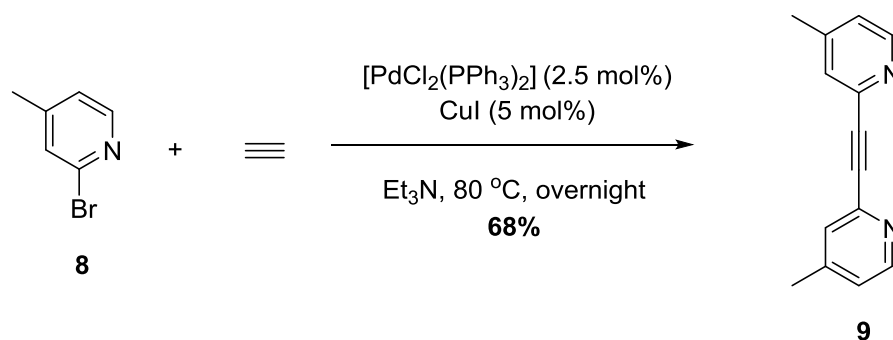


1H); 7.79 (ddd,  $J = 1.4, 7.0, 8.8$  Hz, 1H); 8.03 (ddd,  $J = 1.1, 7.0, 8.3$  Hz, 1H); 8.14 (dq,  $J = 0.9, 8.8$  Hz, 1H); 8.33 (ddt,  $J = 0.6, 1.4, 8.3$  Hz, 1H); 8.59 (dd,  $J = 0.6, 6.7$  Hz, 1H); 9.04 (d,  $J = 6.4$  Hz, 1H); 9.06 (d,  $J = 6.7$  Hz, 1H).  $^{13}\text{C}$  NMR (151 MHz, acetone- $d_6$ ):  $\delta = 16.92; 17.00; 21.06; 26.18; 26.65; 54.99; 56.18; 123.63; 125.58; 126.89; 127.11; 127.94; 128.82; 129.00; 130.61; 132.62; 136.22; 137.76; 139.02; 139.84; 141.15; 142.36; 142.47; 145.61; 147.19; 151.55; 159.47$ . IR (KBr):  $\tilde{\nu}$  ( $\text{cm}^{-1}$ ) = 518; 573; 638; 675; 756; 885; 1031; 1156; 1225; 1268; 1355; 1378; 1415; 1435; 1505; 1515; 1552; 1573; 1609; 1632; 3055; 3076; 3096; 3152. MS (ESI)  $m/z$ : 377.2 (100), 189.1 (92), 378.2 (34), 189.7 (28), 527.2 (28). HRMS (ESI)  $m/z$ :  $[(\text{M})^{2+}]$  ( $\text{C}_{27}\text{H}_{26}\text{N}_2$ ) calc.: 189.10425, found: 189.10405. Elem. Anal. calc. for  $\text{C}_{29}\text{H}_{26}\text{F}_6\text{N}_2\text{O}_6\text{S}_2$ : C, 51.22; H, 3.95; N, 3.86. Found: C, 51.48; H, 3.87; N, 4.14. X-ray crystal of [(*rac*)-**6**][**I**]<sub>2</sub>, see X-ray analysis (Section S7, pp. S142-143).

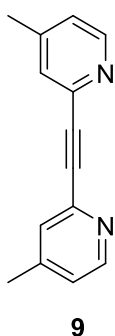
## Part B: Synthesis of racemic [5]helquat (*rac*)-3



## 1,2-Bis(4-methylpyridin-2-yl)ethyne, **9**

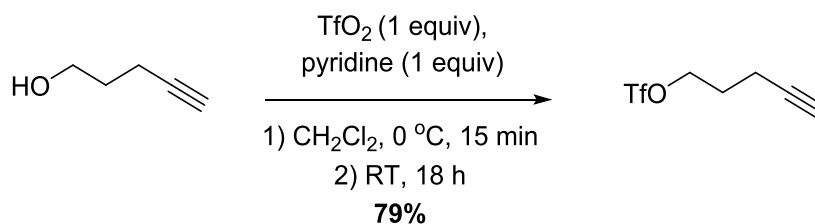


A mixture of  $[\text{PdCl}_2(\text{PPh}_3)_2]$  (2.00 g, 2.9 mmol, 2.5 mol%),  $\text{CuI}$  (1.1 g, 5.8 mmol, 5 mol%), and 2-bromo-4-methylpyridine (**8**, 13.1 mL, 116.2 mmol) in dry  $\text{Et}_3\text{N}$  (250 mL) was stirred at 80°C under an acetylene atmosphere (1 atm, balloon) overnight. The progress of the reaction was monitored by TLC (mobile phase hexane :  $\text{EtOAc}$  = 1 : 1, starting material **8**  $R_f$  = 0.9, product **9**  $R_f$  = 0.18). After filtration through a Celite<sup>®</sup> 512 layer on a sinter followed by washing with  $\text{EtOAc}$ , the volatiles were removed on a rotary evaporator to give a solid residue as a brown powder. Cyclohexane (150 mL) was added to the solid residue and the mixture was heated at 80°C on rotary evaporator without applying vacuum. After 1 minute of rotation, the insoluble residue was decanted and the hot solution was fast transferred to a new flask to complete the crystallization at RT. The procedure was repeated 20 times with 50 mL of cyclohexane each time. Crystals were separated from supernatant by vacuum filtration to get the 1,2-bis(4-methylpyridin-2-yl)ethyne (**9**) as a pale yellow solid (8.2 g, 39.4 mmol, 68%).

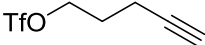


m.p. 132-134°C.  $^1\text{H}$  NMR (600 MHz,  $\text{acetone-}d_6$ ): 2.39 (t,  $J$  = 0.8 Hz, 6H); 7.25 (ddq,  $J$  = 0.8, 1.8, 5.0 Hz, 2H); 7.50 (m, 2H); 8.48 (dd,  $J$  = 0.9, 5.0 Hz, 2H).  $^{13}\text{C}$  NMR (151 MHz,  $\text{acetone-}d_6$ ):  $\delta$  = 20.64; 88.23; 125.34; 129.17; 143.42; 148.54; 150.87. IR (KBr):  $\tilde{\nu}$  ( $\text{cm}^{-1}$ ) 3044; 2920; 2851; 1925; 1817; 1654; 1624; 1598; 1549; 1469; 1499; 1408; 1285; 1183; 993; 954; 912; 831. MS (ESI)  $m/z$  (%): 209 (100). HRMS (ESI)  $m/z$ :  $[\text{M}+\text{H}^+]$  ( $\text{C}_{14}\text{H}_{13}\text{N}_2$ ) calc.: 209.1079, found: 209.1082.

### Pent-4-yn-1-yl trifluoromethanesulfonate

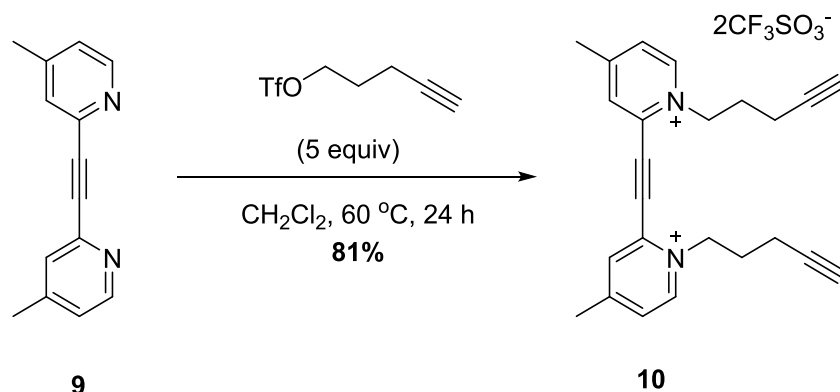


A solution of 4-pentyn-1-ol (25.0 mL, 270 mmol), and pyridine (22.0 mL, 270 mmol) in dry CH<sub>2</sub>Cl<sub>2</sub> (100 mL) was added dropwise to a solution of trifluoromethanesulfonic anhydride (45 mL, 269.5 mmol, 1 equiv) in dry CH<sub>2</sub>Cl<sub>2</sub> (100 mL) at 0°C. The reaction mixture was stirred for 15 min at 0°C and 18 h at RT under argon. The progress of the reaction was monitored by TLC (mobile phase hexane : EtOAc = 9 : 1, starting alcohol R<sub>f</sub> = 0.06, product R<sub>f</sub> = 0.58). After complete consumption of the starting 4-pentyn-1-ol (by TLC), the reaction mixture was washed with H<sub>2</sub>O (5×100mL). The organic layer was dried over Na<sub>2</sub>SO<sub>4</sub>. Na<sub>2</sub>SO<sub>4</sub> was then removed by filtration, volatiles from the filtrate were removed on a rotary evaporator, and the residue was dried under vacuum to get the pent-4-yn-1-yl trifluoromethanesulfonate as a brownish liquid (46.0 g, 213 mmol, 79% yield).<sup>2</sup>

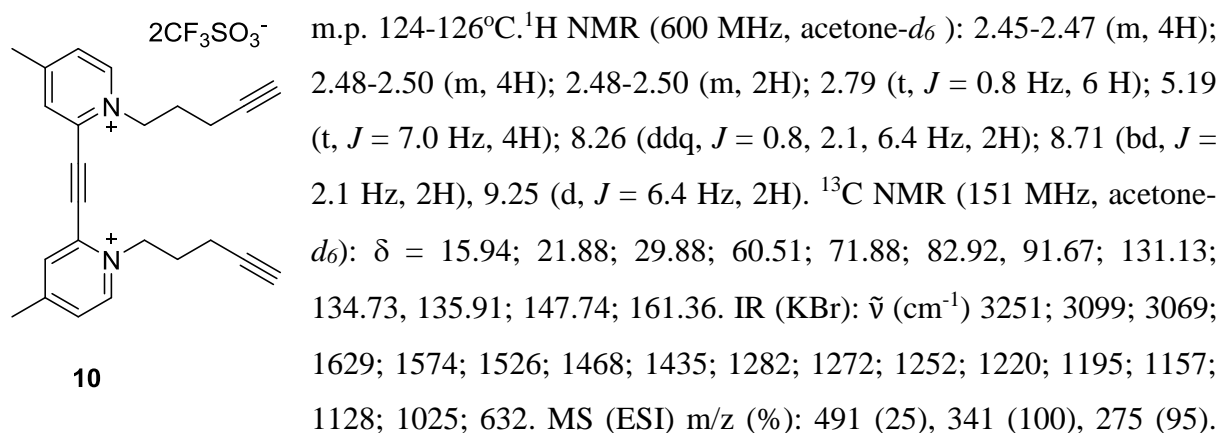
 <sup>1</sup>H NMR (400 MHz, CDCl<sub>3</sub>): δ 2.00-2.06 (m, 2H), 2.03 (t, *J* = 2.7 Hz, 1H), 2.38 (td, *J* = 2.7, 7.0 (2×) Hz, 2H), 4.67 (t, *J* = 6.0 Hz, 2H).<sup>2</sup>



**2,2'-(Ethyne-1,2-diyl)bis(4-methyl-1-(pent-4-yn-1-yl)pyridin-1-ium) trifluoromethanesulfonate, 10**

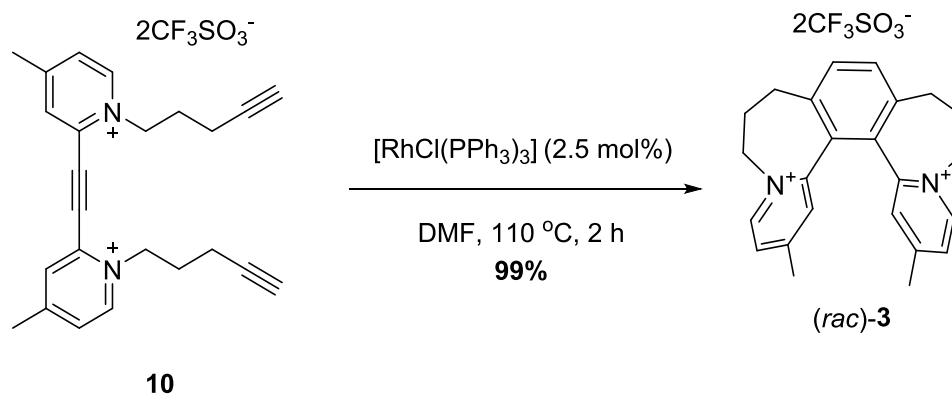


Pent-4-yn-1-yl trifluoromethanesulfonate (41.50 g, 192 mmol, 5 equiv) was added to a solution of 1,2-bis(4-methylpyridin-2-yl)ethyne (**9**, 8.0 g, 38.4 mmol) in dry CH<sub>2</sub>Cl<sub>2</sub> (100 mL) at RT. The resulting solution was stirred at 60°C for 24 h under argon while protected from ambient light using aluminium foil cover. The progress of the reaction was monitored by TLC (mobile phase Stoddart's magic mixture, starting material **9** R<sub>f</sub> = 0.85, product **10** R<sub>f</sub> = 0.48). The solvent was removed on a rotary evaporator and the resulting dark solid was then sonicated with EtOAc (150 mL), the resulting suspension was centrifuged, and the supernatant was removed. The solid was washed five more times with EtOAc (5×100 mL). Drying of the solids under vacuum led to the product **10** as a beige solid (20.0 g, 31.2 mmol, 81% yield).



HRMS (ESI) *m/z*: [(M-TfO)<sup>+</sup>] (C<sub>25</sub>H<sub>26</sub>F<sub>3</sub>N<sub>2</sub>O<sub>3</sub>S<sup>+</sup>) calc.: 491.16107, found: 491.16111. Elem. Anal. calc. for C<sub>26</sub>H<sub>26</sub>F<sub>6</sub>N<sub>2</sub>O<sub>6</sub>S<sub>2</sub>: C, 48.75; H, 4.09; N, 4.37; S, 10.01. Found: C, 48.41; H, 3.92; N, 4.12; S, 10.27.

**(rac)-2,17-Dimethyl-6,7,8,11,12,13-hexahydrodipyrido[1,2-a:1',2'-a']benzo[2,1-c:3,4-c']bisazepindium trifluoromethansulfonate, (rac)-3**



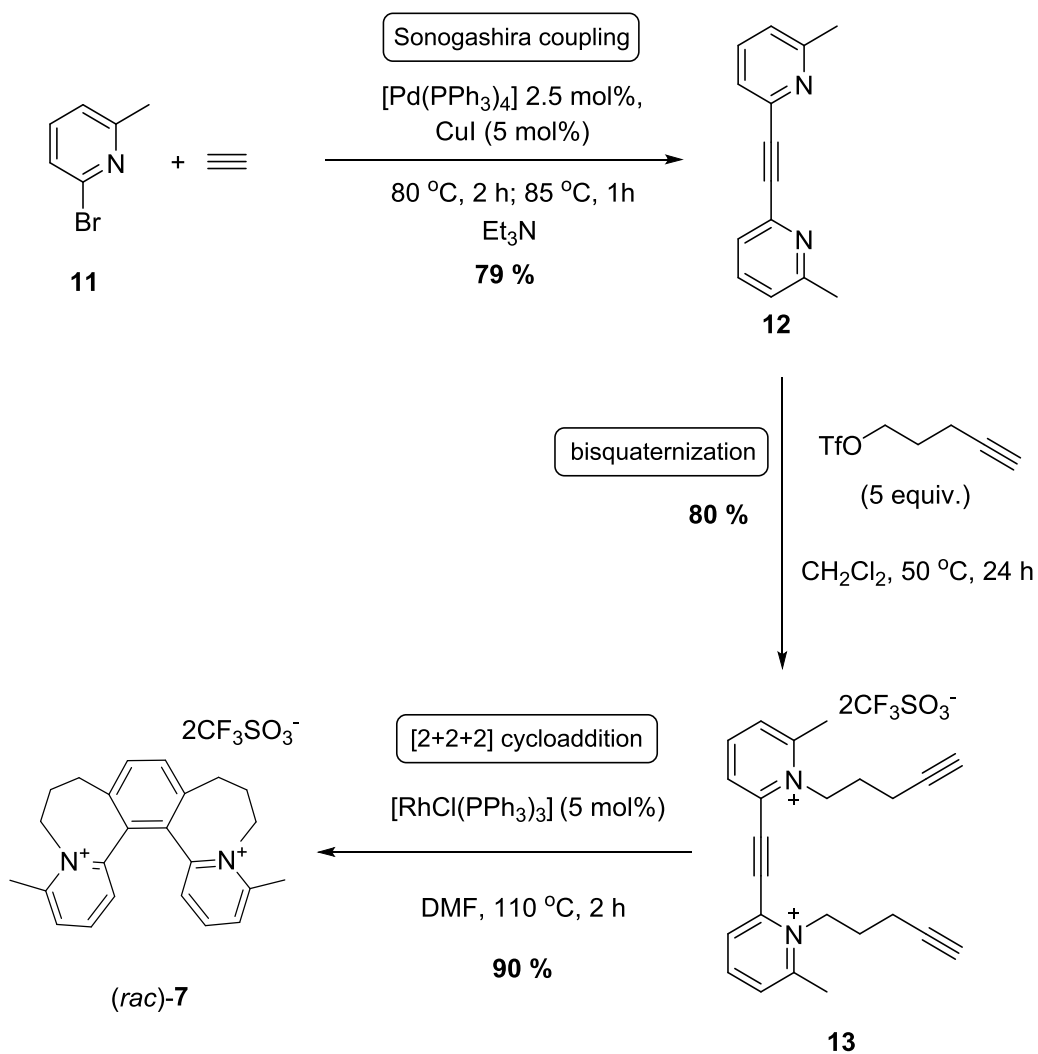
A mixture of triyne **10** (20.0 g, 31.2 mmol), and [RhCl(PPh<sub>3</sub>)<sub>3</sub>] (0.72 g, 0.78 mmol, 2.5 mol%) in degassed and dry DMF (200 mL) was stirred at 110°C for 2 h under argon while protected from ambient light using aluminium foil cover. The progress of the reaction was monitored by TLC (mobile phase Stoddart magic mixture, starting material **10** R<sub>f</sub> = 0.48, product (rac)-**3** R<sub>f</sub> = 0.39). The resulting dark green solution was cooled to RT and then transferred to a round-bottomed flask (using acetone for rinsing). All volatiles were then removed on a rotary evaporator and the residue was dried for 1 h under high vacuum to remove possibly all traces of DMF. Then, EtOAc (60 mL) was added, the mixture was sonicated, centrifuged, and the supernatant was separated from the resulting solids. The grey solid residue was washed five more times with EtOAc (5×60 mL). Removal of volatiles on rotary evaporator and drying under vacuum of an oil pump (3.0 mbar) led to (rac)-**3** which was isolated as a beige solid (20.0 g, 31.2 mmol, 99% yield).

**(rac)-3** 2CF<sub>3</sub>SO<sub>3</sub><sup>-</sup>

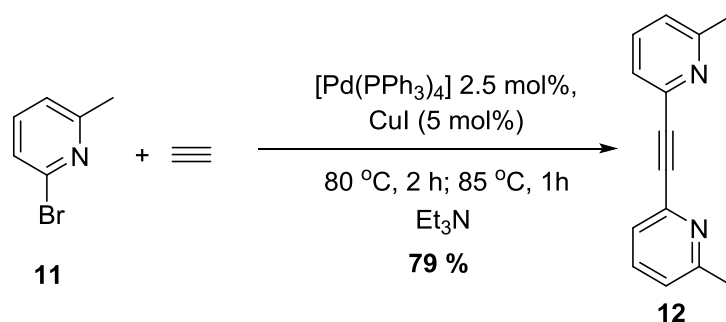
m.p. 332-335°C. <sup>1</sup>H NMR (600 MHz, acetone-*d*<sub>6</sub>): 2.49 (s, 6H); 2.51-2.58 (m, 2H); 2.64-2.66 (ddd, *J* = 7.2, 12.6, 13.9 Hz, 2H); 2.81-2.87 (m, 2H); 3.15 (ddd, *J* = 1.3, 6.8, 13.9 Hz, 2H); 4.78 (dt, *J* = 5.8, 13.6 Hz, 2H); 5.06 (bdd, *J* = 6.6, 13.8 Hz, 2H); 7.66 (dq, *J* = 0.6, 2.0 Hz, 2H); 7.87 (s, 2H); 8.07 (ddq, *J* = 0.6, 2.0, 6.4 Hz, 2H); 9.20 (bd, *J* = 6.4 Hz, 2H). <sup>13</sup>C NMR (151 MHz, acetone-*d*<sub>6</sub>): δ = 21.69; 29.39; 32.41; 58.55; 129.23; 131.31; 132.14; 134.15; 140.08; 146.79; 151.83; 160.94. IR (KBr):  $\tilde{\nu}$  (cm<sup>-1</sup>) 3159; 3097; 3043; 2935; 2869; 1633; 1571; 1515; 1458; 1262; 1227; 1152; 1035; 1026; 866;

831; 642. MS (ESI) m/z (%): 491 (100), 341 (85), 171 (45). HRMS (ESI) m/z: [(M-TfO<sup>-</sup>)<sup>+</sup>] (C<sub>25</sub>H<sub>26</sub>F<sub>3</sub>N<sub>2</sub>O<sub>3</sub>S<sup>+</sup>) calc.: 491.16107, found: 491.16118. Elem. Anal. calc. for C<sub>26</sub>H<sub>26</sub>F<sub>6</sub>N<sub>2</sub>O<sub>6</sub>S<sub>2</sub>: C, 48.75; H, 4.09; N, 4.37; S, 10.01. Found: C, 48.89; H, 4.03; N, 4.13; S, 10.27. X-ray crystal of [(*rac*)-**3**][TfO]<sub>2</sub>, see X-ray analysis (Section S7, p. S144).

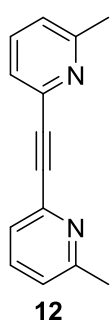
## Part C: Synthesis of racemic [5]helquat (*rac*)-7



## 1,2-Bis(6-methylpyridin-2-yl)ethyne, **12**



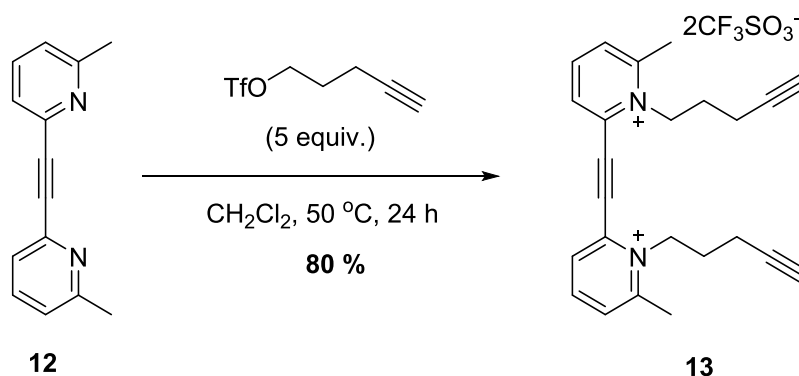
To a mixture of  $[Pd(PPh_3)_4]$  (2.85 g, 2.47 mmol, 2.5 mol%) and CuI (942 mg, 4.95 mmol, 5 mol%) in a Schlenk flask under argon was added dry  $Et_3N$  (200 mL). 2-Bromo-6-methylpyridine (**11**, 11.3 mL, 17.0 g, 98.8 mmol) was added to the stirring mixture via needle and syringe. Finally, argon atmosphere was exchanged for acetylene atmosphere by connecting a balloon with acetylene gas to the Schlenk flask and by piercing the septum with a needle for 10 seconds. The reaction mixture was stirred for 2 h at 80°C and then for 1 further hour at 85°C. The progress of the reaction was monitored by TLC (mobile phase hexane : EtOAc = 1 : 1, starting material **11**  $R_f$  = 0.88, product **12**  $R_f$  = 0.24). After filtration through a sinter with Celite<sup>®</sup> 512 layer and washing with EtOAc (500 mL), the volatiles were removed on a rotary evaporator and the residue was transferred to a 250 mL round-bottomed flask (using acetone for rinsing). After removing the acetone on a rotary evaporator, cyclohexane (150 mL) was added to the solid residue and the mixture was heated at 80°C on a rotary evaporator without applying vacuum. After 1 min of rotation and heating, the insoluble residue was decanted and the hot solution was fast and carefully transferred to a new flask to complete the crystallization at RT. The procedure was repeated four more times with cyclohexane (4×50mL). Crystals were separated from supernatant by vacuum filtration to get compound **12** as a yellowish powder (8.17 g, 39.3 mmol, 79%).



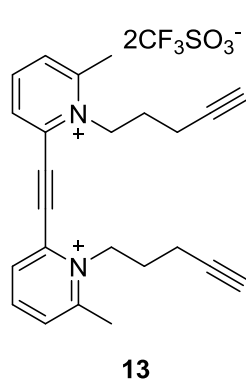
m.p. 135-137°C.  $^1H$  NMR (600 MHz, acetone- $d_6$ ): 2.55 (bs, 6H); 7.32 (qdd,  $J$  = 0.6, 1.0, 7.7 Hz, 2H); 7.50 (qdd,  $J$  = 0.7, 1.0, 7.7 Hz, 2H); 7.77 (t,  $J$  = 7.7 Hz, 2H).  $^{13}C$  NMR (151 MHz, acetone- $d_6$ ):  $\delta$  = 23.54; 87.31; 123.03; 124.57; 136.58; 141.92; 159.08. IR (KBr):  $\tilde{\nu}$  ( $cm^{-1}$ ) 3069; 3054; 2987; 2959; 2220; 1584; 1565;

1458; 1452; 1373; 1242; 1231; 1154; 1090; 793; 743; 736. MS (ESI)  $m/z$  (%) = 209 (100). HRMS (ESI)  $m/z$ :  $[M+H^+]$  ( $C_{14}H_{13}N_2^+$ ) calc.: 209.10732, found: 209.10732.

**6,6'-(Ethyne-1,2-diyl)bis(2-methyl-1-(pent-4-yn-1-yl)pyridin-1-ium) trifluoromethanesulfonate, 13**

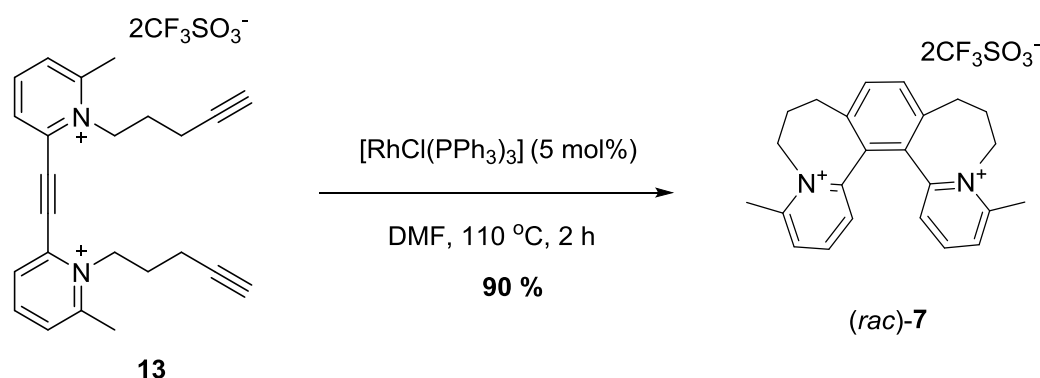


Pent-4-yn-1-yl trifluoromethanesulfonate (16.1 mL, 21.16 g, 97.9 mmol) was added to a solution of **12** (4.1 g, 19.6 mmol) in dry  $CH_2Cl_2$  (100 mL) at RT. The resulting solution was stirred at 50°C for 24 h under reflux condenser and under argon while protected from ambient light using aluminium foil cover. During the course of reaction, white precipitate was formed. It was then filtered through a sinter, and then washed with EtOAc (150 mL) followed by Et<sub>2</sub>O (100 mL). The resulting white powder was then dried under vacuum of an oil pump (3.0 mbar). Product **13** was obtained as a beige powder (10.04 g, 15.7 mmol, 80% yield).



m.p. 168-171°C. <sup>1</sup>H NMR (600 MHz, acetone-*d*<sub>6</sub>): 2.45-2.51 (m, 4H); 2.55 (t,  $J = 2.7$  Hz, 2H); 2.64 (dt,  $J = 2.7, 6.9$  Hz, 4H); 3.23 (bs, 6H); 5.25-5.27 (m, 4H); 8.38 (dd,  $J = 1.7, 8.1$  Hz, 2H); 8.68 (dd,  $J = 1.7, 7.9$  Hz, 2H); 8.73 (t,  $J = 8.0$  Hz, 2H). <sup>13</sup>C NMR (151 MHz, acetone-*d*<sub>6</sub>):  $\delta = 16.19; 21.73; 28.37; 56.90; 71.95; 83.06; 92.16; 133.24; 133.57; 136.06; 145.82; 160.12$ . IR (KBr):  $\tilde{\nu}$  (cm<sup>-1</sup>) 3237; 2114; 1614; 1580; 1498; 1262; 1224; 1198; 1156; 1030; 815; 638; 574. MS (ESI)  $m/z$  (%): 491 (5), 342 (100), 275 (50), 171 (5). HRMS (ESI)  $m/z$ :  $[(M-TfO^-)^+]$  ( $C_{25}H_{26}F_3N_2O_3S^+$ ) calc.: 491.16107, found: 491.16089.

**(rac)-4,15-Dimethyl-6,7,8,11,12,13-hexahydrodipyrido[1,2-a:1',2'-a']benzo[2,1-c:3,4-c']bisazepindium trifluoromethansulfonate, (rac)-7**



A mixture of triyne **13** (9.7 g, 15.2 mmol), and  $[\text{RhCl}(\text{PPh}_3)_3]$  (702 mg, 758  $\mu\text{mol}$ , 5 mol%) in degassed and dry DMF (150 mL) was stirred at 110°C for 2 h under argon while protected from ambient light using aluminium foil cover. The progress of the reaction was monitored by TLC (mobile phase Stoddart magic mixture, starting material **13**  $R_f = 0.48$  and  $0.67$ , product *(rac)*-**7**  $R_f = 0.31$ ). The resulting solution was cooled to RT and then transferred to a round-bottomed flask. All volatiles were then removed on a rotary evaporator and the residue was dried for 1 h under high vacuum to remove possibly all traces of DMF. The crude product was then sonicated with EtOAc (200 mL). The resulting suspension was filtered through a sinter, and the solids on the sinter were then washed with Et<sub>2</sub>O (50 mL), then EtOAc (100 mL) and finally with Et<sub>2</sub>O (100 mL). The solids were then dried under vacuum of an oil pump (3.0 mbar). Product *(rac)*-**7** was obtained as a beige powder (8.71 g, 13.6 mmol, 90% yield).

$2\text{CF}_3\text{SO}_3^-$

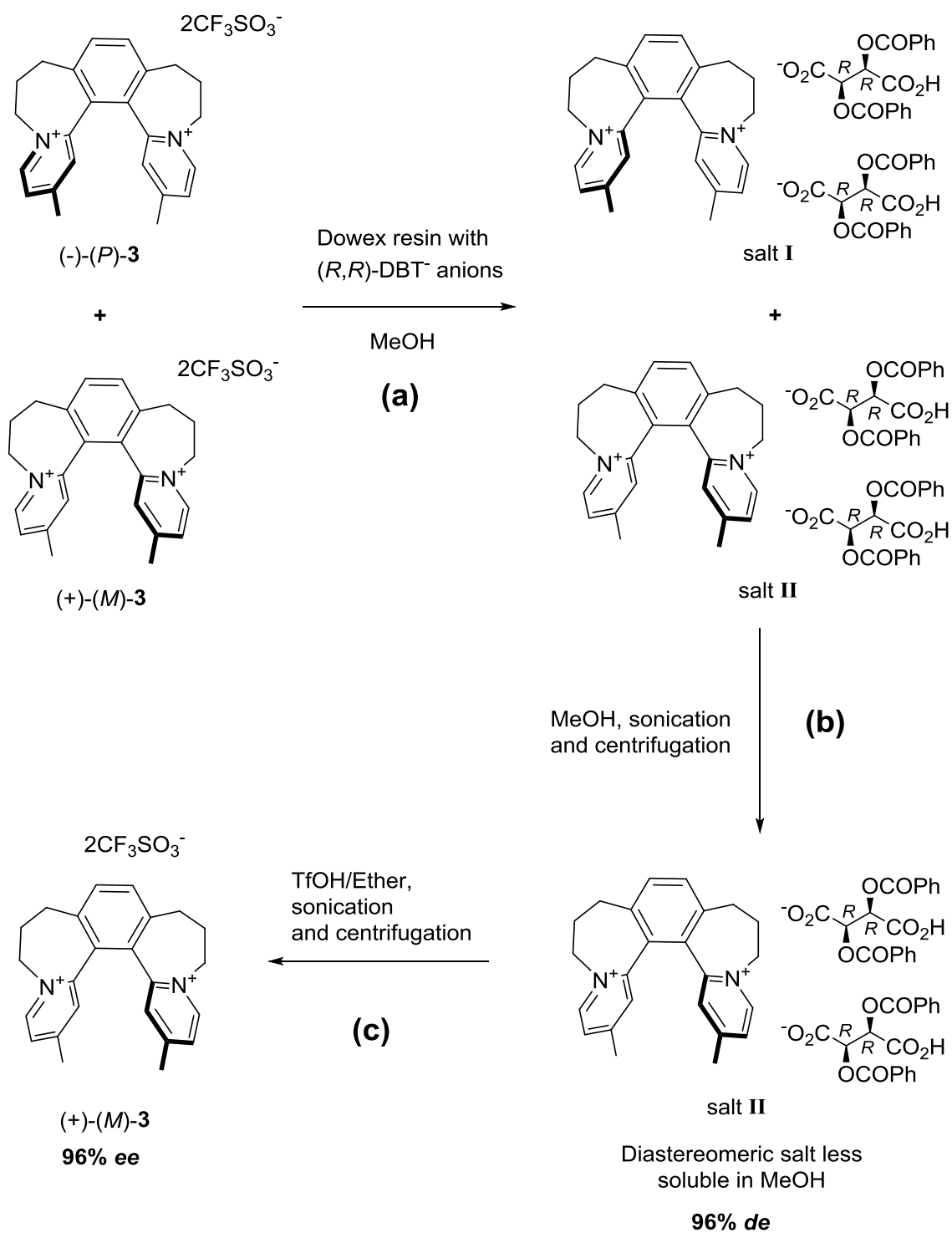
**(rac)-7**

m.p. 291-293°C. <sup>1</sup>H NMR (600 MHz, acetone-*d*<sub>6</sub>): 2.49-2.55 (m, 2H); 2.60 (dt, *J* = 6.8, 13.1 Hz, 2H); 2.86-2.93 (m, 2H); 3.15-3.19 (m, 2H); 3.16 (bs, 6H); 4.60 (dt, *J* = 5.0, 14.1 Hz, 2H); 5.19 (dd, *J* = 5.6, 14.1 Hz, 2H); 7.66 (dd, *J* = 1.4, 8.0 Hz, 2H); 7.85 (s, 2H); 8.09 (dd, *J* = 1.4, 8.0 Hz, 2H); 8.27 (t, *J* = 8.0 Hz, 2H). <sup>13</sup>C NMR (151 MHz, acetone-*d*<sub>6</sub>):  $\delta$  = 21.62; 29.35; 30.94; 53.89; 130.59; 130.62; 132.16; 133.76; 139.94; 145.29; 153.63; 158.05. IR (KBr):  $\tilde{\nu}$  (cm<sup>-1</sup>) 1621; 1580; 1495; 1266; 1225; 1159; 1032; 638; 573; 518. MS (ESI) *m/z* (%): 491 (10), 341 (100), 171 (6). HRMS (ESI) *m/z*: [(*M*-TfO<sup>-</sup>)<sup>+</sup>] (C<sub>25</sub>H<sub>26</sub>F<sub>3</sub>N<sub>2</sub>O<sub>3</sub>S<sup>+</sup>) calc.: 491.16107, found: 491.16126. Elem. Anal. calc. for C<sub>26</sub>H<sub>26</sub>F<sub>6</sub>N<sub>2</sub>O<sub>6</sub>S<sub>2</sub>: C, 48.75; H, 4.09; N, 4.37. Found: C, 48.66; H, 4.45; N, 3.98. X-ray crystal of [(*rac*)-**7**][TfO]<sub>2</sub>, see X-ray analysis (Section S7, p. S145).

## Part D: Resolution of racemic [5]helquats (*rac*)-3

Resolution of (*rac*)-3 to obtain (+)-(*M*)-3 via mixture of diastereomeric salts I and II

### I and II



**Scheme S1.** Resolution of (*rac*)-3 to obtain (+)-(*M*)-3 via mixture of diastereomeric salts I and II



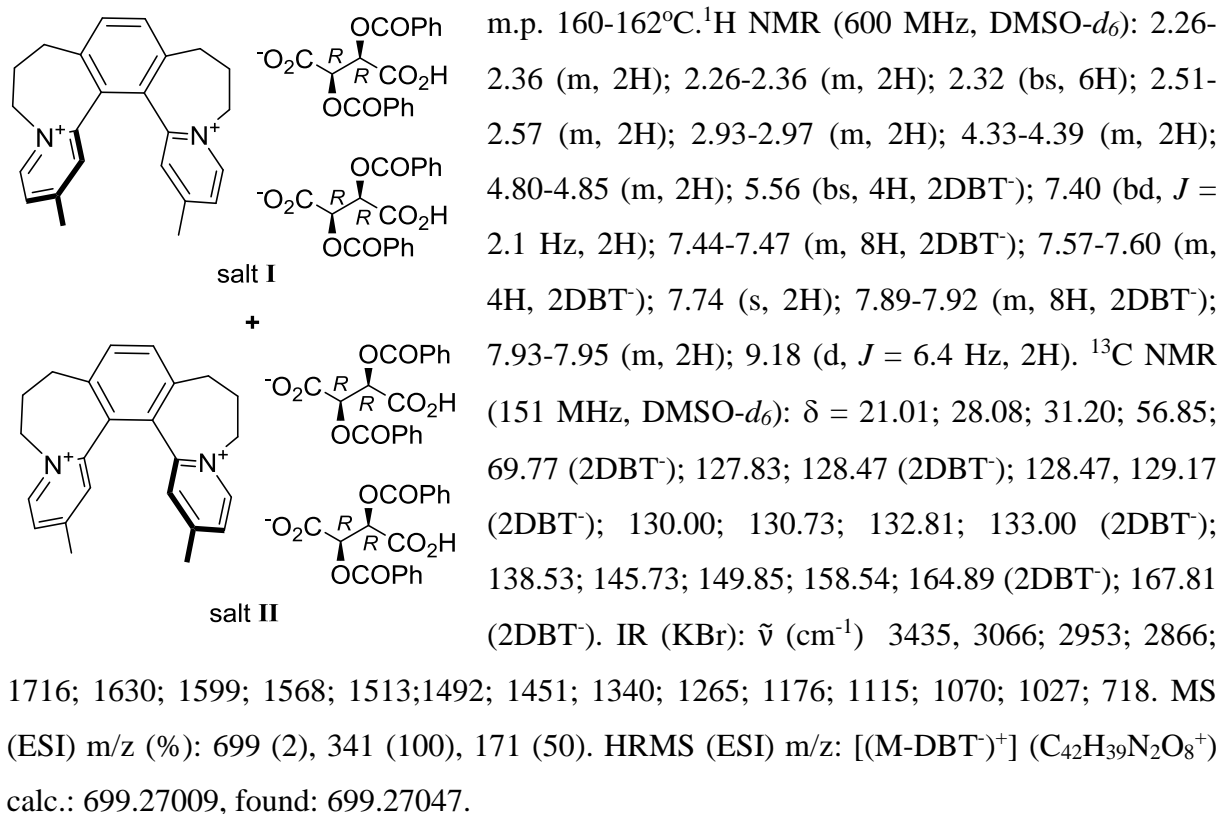
### 1. Preparation of the anion-exchange resin:

100 mL of basic anion exchange resin in Cl<sup>-</sup> cycle (Dowex 1×2, 16-100 mesh) was mixed with demineralized water in a column equipped with a sinter S0 and a teflon tap. Switching from Cl<sup>-</sup> cycle to OH<sup>-</sup> was performed by passing 2 M aqueous solution of NaOH (80 g/L, 4L) through the column. The absence of the Cl<sup>-</sup> anions was confirmed by taking a few drops from the column into a small vial, acidifying it with a few drops of aqueous HNO<sub>3</sub> (1:1) solution, and adding two drops of 0.1 M aqueous AgNO<sub>3</sub> solution. A completely clear solution indicates the absence of Cl<sup>-</sup> anions (absence of precipitated AgCl). Then, demineralized water (1 L) was added until neutralization was achieved. Water was exchanged with MeOH by passing sufficient amount of MeOH through the column. The anion exchange resin in OH<sup>-</sup> was loaded with 0.2 M methanolic solution of (-)-(R,R)-O,O'-dibenzoyltartaric acid (43 g, 120 mmol, 600 mL of MeOH). After addition of 200 mL of the methanolic solution, the column was stoppered and mixed by turning it upside down gently in order that all the resin beads mix with the methanolic solution. The rest of the 0.2 M methanolic solution of (-)-(R,R)-O,O'-dibenzoyltartaric acid, was slowly run through the column. MeOH (400 mL) was run through the column until the drops eluted were neutral (Step (a), Scheme S1).

### 2. Transformation of the (*rac*)-3 to mixture of salts I and II:

A solution of (*rac*)-3 (1.0 g, 1.56 mmol) in 80 mL of MeOH was slowly passed through the column loaded with (R,R)-O,O'-dibenzoyl tartrate anions (Step (a), Scheme S1). To elute the compound from the column, additional 100 mL of MeOH was used. Evaporation of the volatiles using a rotary evaporator (the bath temperature was kept at 30°C) and drying under vacuum led to the isolation of diastereomeric mixture of salts I and II as a beige solid (1.84 g). Complete exchange of the triflate anions was verified by the absence of a signal in <sup>19</sup>F NMR. TLC (mobile phase Stoddart's magic mixture, starting material R<sub>f</sub> = 0.39, product R<sub>f</sub> = 0.33).

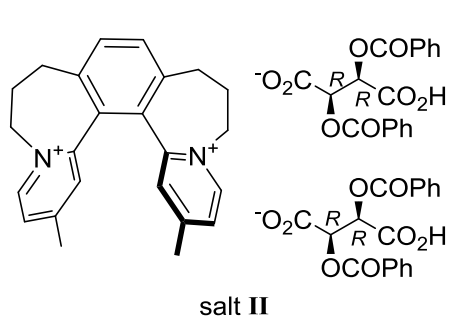
**Mixture of (-)-(P) and (-)-(M)-2,17-Dimethyl-6,7,8,11,12,13-hexahydrodipyrido[1,2-a:1',2'-a']benzo[2,1-c:3,4-c']bisazepindium (2R,3R)-2,3-bis(benzoyloxy)-3-carboxypropanoate, mixture of salts I and II**



### 3. Separation of the salt II and diastereoenriched salt I:

MeOH (2 mL) was added to the diastereomeric mixture of salt I and salt II (1.84 g, Step (b), Scheme S1). The suspension was sonicated, centrifuged, and the liquids were separated from the solid pellet (all liquids were collected to obtain (-)-(P)-3 enantiomer later on, see Scheme S2). This procedure consisting of MeOH addition, sonication, and centrifugation was repeated six more times. After drying the solid pellet under vacuum, salt II was obtained as a beige solid (0.77 g, 0.73 mmol, 47% yield, 96% *de*, CE). After evaporation of the volatiles from the solutions, diastereoenriched salt I was obtained as a dark brown solid (0.85 g, 0.804 mmol, 51% yield).

**(+)-(M)-2,17-Dimethyl-6,7,8,11,12,13-hexahydrodipyrido[1,2-a:1',2'-a']benzo[2,1-c:3,4-c']bisazepindium (2R,3R)-2,3-bis(benzoyloxy)-3-carboxypropanoate, salt II**

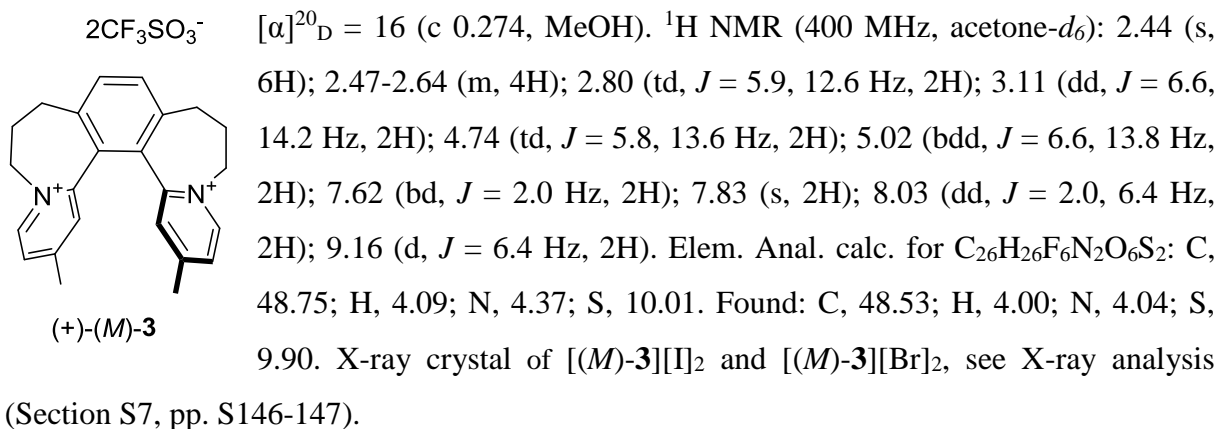


$[\alpha]_D^{20} = 10$  (c 0.278, DMSO). m.p. 158 – 159°C.  $^1\text{H}$  NMR (600 MHz, DMSO- $d_6$ ): 2.31-2.37 (m, 2H); 2.31-2.37 (m, 2H); 2.33 (bs, 6H); 2.52-2.56 (m, 2H); 2.94-2.97 (m, 2H); 4.38 (td,  $J = 13.3, 5.0$  Hz, 2H); 4.81 (dd,  $J = 13.7, 6.3$  Hz, 2H); 5.60 (bs, 4H, 2DBT $^-$ ); 7.37 (bd,  $J = 2.1$  Hz, 2H); 7.44 (tt,  $J = 7.8, 1.4$  Hz, 8H, 2DBT $^-$ ); 7.57-7.60 (m, 4H, 2DBT $^-$ ); 7.75 (s, 2H); 7.87-7.89 (m, 8H, 2DBT $^-$ ); 7.95 (dd,  $J = 6.3, 1.3$  Hz, 2H); 9.13 (d,  $J = 6.4$  Hz, 2H).  $^{13}\text{C}$  NMR (151 MHz, DMSO- $d_6$ ):  $\delta = 20.96; 28.01; 31.14; 40.06, 56.83; 70.87$  (2DBT $^-$ ); 127.79; 128.48 (2DBT $^-$ ); 129.04 (2DBT $^-$ ); 129.55; 129.91; 130.64, 132.77; 133.18 (2DBT $^-$ ); 138.47; 145.56; 149.82; 158.52; 164.68 (2DBT $^-$ ); 167.49 (2DBT $^-$ ). IR (KBr):  $\tilde{\nu}$  (cm $^{-1}$ ) 3422, 3063; 2958; 2867; 1721; 1632; 1602; 1572; 1514; 1492; 1452; 1337; 1265; 1176; 1112; 1070; 1027; 896; 847; 716. MS (ESI)  $m/z$  (%): 1057 (2); 699 (2), 341 (100), 171 (94). HRMS (ESI)  $m/z$ :  $[(M^+)]$  (C $_{60}$ H $_{53}$ N $_2$ O $_{16}$ ) calc.: 1057.33896, found: 1057.34025.

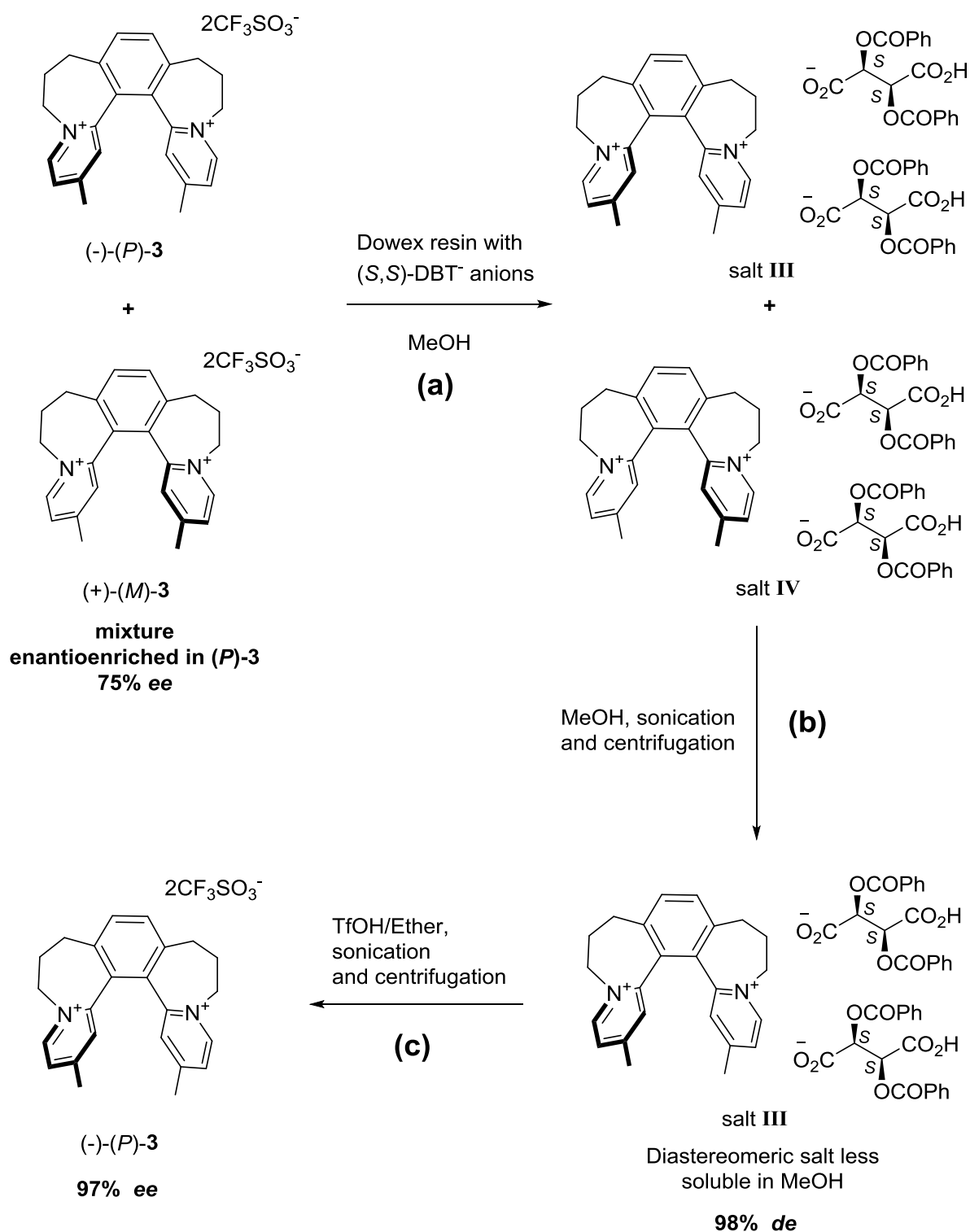
**4. Procedure to obtain (+)-(M)-3 and enantioenriched (-)-(P)-3:**

A mixture of TfOH : Et $_2$ O 1 : 99 (8 mL) was added to the salt II (0.70g). The solids softened after the addition of the TfOH solution, the mixture was sonicated for 5 min and the soft solids turned less soft and finally a beige solid resulted. The mixture was centrifuged, and the liquids were separated from the solid pellet. This procedure of TfOH : Et $_2$ O addition, sonication and centrifugation, was repeated nine more times (Step (c), Scheme S1). In order to remove the TfOH impurities, the solid pellet was additionally sonicated with pure Et $_2$ O (8 mL). After centrifugation, the liquid was separated from the solid pellet, which was then treated with more Et $_2$ O (3×8mL). After drying the solid pellet under vacuum, enantiomer (+)-(M)-3 was obtained as a beige solid (0.41 g, 0.64 mmol, 41% yield, 96% *ee*, see CE Section S4, Figure S1, S78). Analogous to the procedure described for (+)-(M)-3, the enantioenriched (-)-(P)-3 was obtained from enantioenriched salt I (0.85 g) as a greyish solid (0.47 g, 0.73 mmol, 47% yield, 75% *ee*, CE). Racemization barrier determination of (+)-(M)-3 is detailed in CE Section S4 (Figure S11, p. S85). For ECD and UV/Vis spectra, see Figure S19 (Section S5, p. S100).

**(+)-(M)-2,17-Dimethyl-6,7,8,11,12,13-hexahydrodipyrido[1,2-a:1',2'-a']benzo[2,1-c:3,4-c']bisazepindium trifluoromethansulfonate, (+)-(M)-3**



**Resolution of (*rac*)-3 to obtain (-)-(*P*)-3 via mixture of diastereomeric salts **III** and **IV****

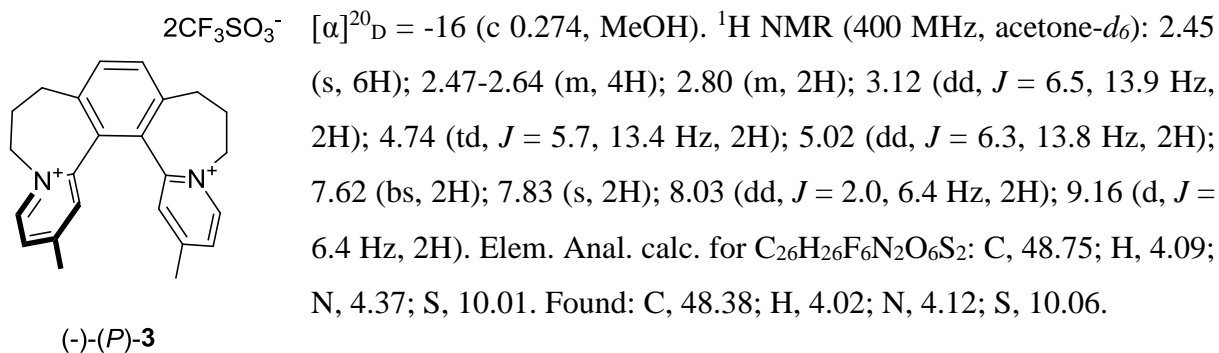


**Scheme S2.** Resolution of (*rac*)-3 to obtain (-)-(*P*)-3 via mixture of diastereomeric salts **III** and **IV**

### Procedure to obtain (-)-(P)-3:

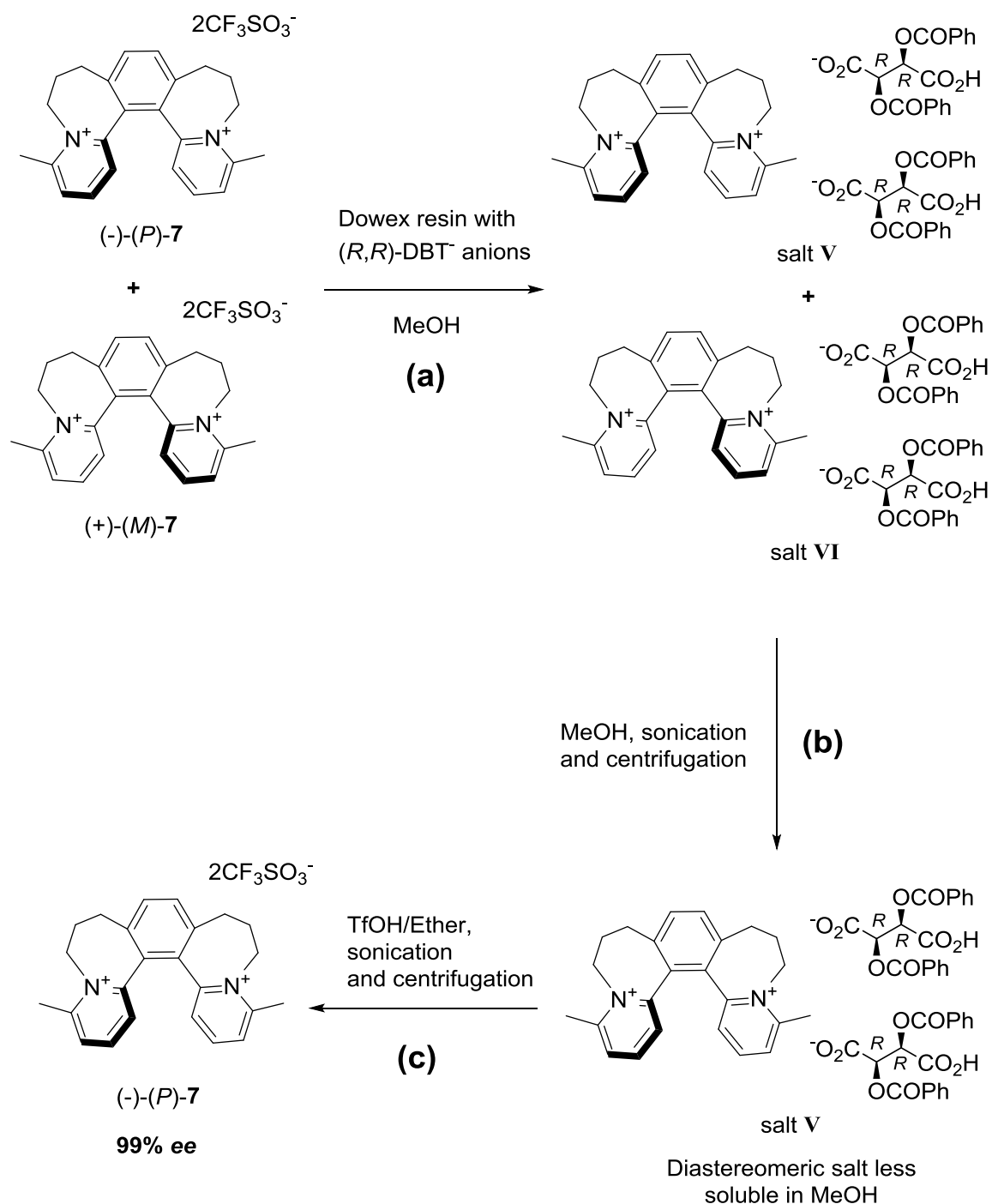
The procedure to obtain (-)-(P)-3 was analogous to that described for (+)-(M)-3 (Steps a-c, Scheme S1). (*S,S*)-dibenzoyltartrate anion was used instead of (*R,R*)-dibenzoyltartrate anion (Step (a), Scheme S2). Initial anion exchange started with enantioenriched (-)-(P)-3 (0.47 g, 0.73 mmol, 75% de) giving a crude of diastereoenriched mixture salt **III** and salt **IV** (0.95 g). Then, salt **III** (Step (b), Scheme 2) was isolated as a beige solid (0.60 g, 0.57 mmol, 77% yield, 98% *de*, CE). Finally, (-)-(P)-3 enantiomer (Step (c), Scheme 2) was obtained as a beige solid (0.28 g, 0.26 mmol, 60% yield, 98% *ee*, see CE Section S4, Figure S1, p. S78). For ECD and UV/Vis spectra, see Figure S19 (Section S5, p. S100).

### (-)-(P)-2,17-Dimethyl-6,7,8,11,12,13-hexahydrodipyrido[1,2-a:1',2'-a']benzo[2,1-c:3,4-c']bisazepindium trifluoromethanesulfonate, (-)-(P)-3



## Part E: Resolution of racemic [5]helquats (*rac*)-7

### Resolution of (*rac*)-7 to obtain (-)-(*P*)-7 via mixture of diastereomeric salts V and VI



**Scheme S3.** Resolution of (*rac*)-7 to obtain (-)-(*P*)-7 via mixture of diastereomeric salts V and VI

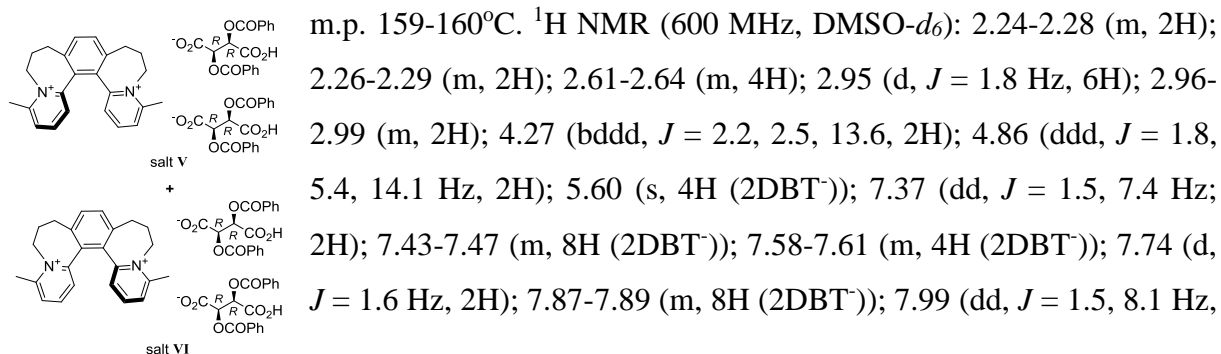
## 1. Preparation of the anion-exchange resin:

250 mL of strongly basic anion exchange resin in  $\text{Cl}^-$  cycle (Dowex 1×2, 16-100 mesh) in demineralized water was prepared in a column equipped with a sinter (porosity S1) and a teflon tap. Switching from  $\text{Cl}^-$  cycle to  $\text{OH}^-$  was performed by passing 2 M aqueous solution of NaOH (80 g/L, 6L) through the column. The absence of the  $\text{Cl}^-$  anions was confirmed by taking a few drops from the column into a small vial, acidifying it with a few drops of aqueous  $\text{HNO}_3$  (1:1) solution, and adding two drops of 0.1 M aqueous  $\text{AgNO}_3$  solution. A completely clear solution indicates the absence of  $\text{Cl}^-$  anions (absence of precipitated  $\text{AgCl}$ ). Then, demineralized water (1.5 L) was passed through until neutralization was achieved. Water was exchanged with MeOH by passing 500 mL of MeOH through the column. The anion exchange resin in  $\text{OH}^-$  cycle was loaded with 1500 mL of the 0.2 M MeOH solution of (-)-(R,R)-L-O,O'-dibenzoyltartaric acid (107.5 g, 300 mmol, 1500 mL of MeOH). After running three quarters of the solution, column was stoppered and mixed by turning it upside down gently in order that all the resin beads mix with the rest of methanolic solution. MeOH (750 mL) was run through the column until the drops eluted were neutral.

## 2. Transformation of the (rac)-7 to mixture of salts V and VI:

A solution of (rac)-7 (5.0 g, 7.81 mmol) in 400 mL of MeOH was slowly passed through the column loaded with (R,R)-L-O,O'-dibenzoyl tartrate anions (Step (a), Scheme 3). To elute the compound from the column, additional 250 mL of MeOH was used. Evaporation of the volatiles using a rotary evaporator (the bath temperature was kept at 30°C) and drying under vacuum led the diastereomeric mixture of salts V and VI as a greyish solid (9.42 g). Complete exchange of the triflate anions was verified by the absence of a signal in  $^{19}\text{F}$  NMR.

### Mixture of (-)-(P) and (+)-(M)-4,15-dimethyl-6,7,8,11,12,13-hexahydrodipyrido[1,2-a:1',2'-a']benzo[2,1-c:3,4-c']bisazepindium (2R,3R)-2,3-bis(benzoyloxy)-3-carboxypropanoate, salts V and VI



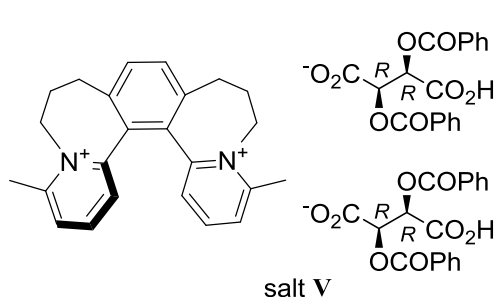


2H); 8.11 (t,  $J = 8.0$  Hz, 2H).  $^{13}\text{C}$  NMR (151 MHz,  $\text{DMSO-}d_6$ ):  $\delta = 20.94$ ; 28.05; 29.77; 52.46; 70.90 (2DBT $^-$ ); 128.59 (2DBT $^-$ ); 129.12 (2DBT $^-$ ); 129.35 (2DBT $^-$ ); 129.51; 130.83; 132.49; 133.32 (2DBT $^-$ ); 138.42 (2DBT $^-$ ); 143.77; 151.98; 156.47; 164.71 (2DBT $^-$ ); 167.53 (2DBT $^-$ ). IR (KBr):  $\tilde{\nu}$  ( $\text{cm}^{-1}$ ) 3436; 3064; 2870; 1719; 1620; 1582; 1494; 1451; 1316; 1264; 1176; 1264; 1176; 1113; 1070; 717. MS (ESI)  $m/z$  (%): 699 (2), 341 (100), 171 (80). HRMS (ESI)  $m/z$ : [(M-DBT $^-$ ) $^+$ ] ( $\text{C}_{42}\text{H}_{39}\text{N}_2\text{O}_8^+$ ) calc.: 699.27009, found: 699.27048.

### 3. Separation of the salt V and distereoenriched salt VI:

MeOH (30 mL) was added to the diastereomeric mixture of salts V and VI (7.45 g, Step (b), Scheme 3). The suspension was sonicated, centrifuged, and the liquid was separated from the solid pellet (all liquids were collected to obtain (+)-(*M*)-7 enantiomer later on, see Scheme S4). This procedure of MeOH addition, sonication and centrifugation was repeated five more times. After drying the solid pellet under vacuum, salt V was obtained as a white solid (2.34 g, 2.21 mmol, 100% *de*). After evaporation of the volatiles from the solutions, distereoenriched salt VI was obtained as a brown solid (57% *de*, CE).

#### (-)-(*P*)-4,15-Dimethyl-6,7,8,11,12,13-hexahydrodipyrido[1,2-*a*:1',2'-*a'*]benzo[2,1-*c*:3,4-*c'*]bisazepindium (2*R*,3*R*)-2,3-bis(benzoyloxy)-3-carboxypropanoate, salt V

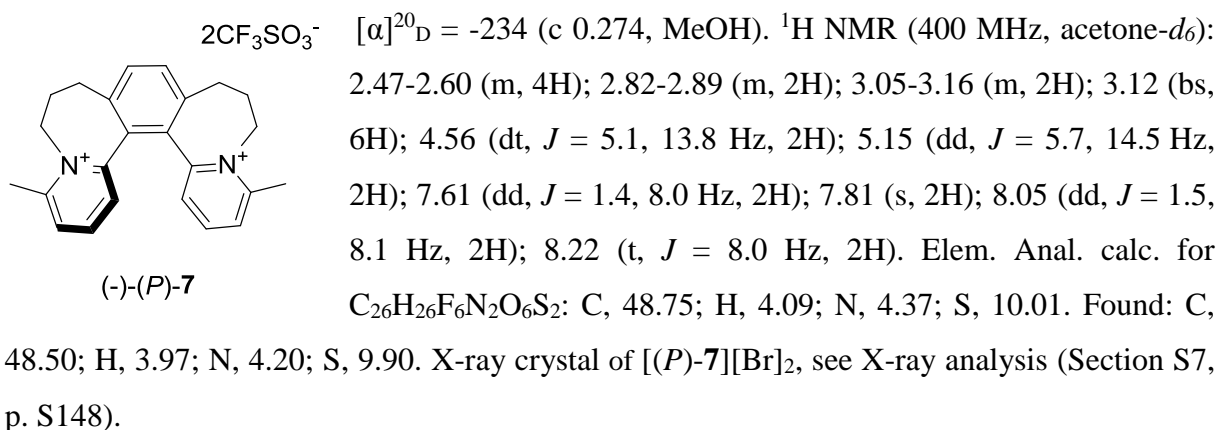


$[\alpha]_D^{20} = -161$  (c 0.218, DMSO). m.p. 160-161°C.  $^1\text{H}$  NMR (600 MHz,  $\text{DMSO-}d_6$ ): 2.23-2.26 (m, 2H); 2.26-2.28 (m, 2H); 2.60-2.63 (m, 4H); 2.94 (s, 6H); 2.96-3.00 (m, 2H); 4.27 (td,  $J = 14.0, 13.5, 4.7$  Hz, 2H); 4.86 (dd,  $J = 14.4, 5.7$  Hz, 2H); 5.60 (s, 4H (2DBT $^-$ )); 7.37 (dd,  $J = 1.5, 7.4$  Hz, 2H); 7.43-7.46 (m, 8H (2DBT $^-$ )); 7.58-7.60 (m, 4H (2DBT $^-$ )); 7.74 (s, 2H); 7.88 (dd,  $J = 8.3, 1.2$  Hz, 8H (2DBT $^-$ )); 7.98 (dd,  $J = 1.5, 8.1$  Hz, 2H); 8.11 (t,  $J = 8.0$  Hz, 2H).  $^{13}\text{C}$  NMR (151 MHz,  $\text{DMSO-}d_6$ ):  $\delta = 20.96$ ; 28.08; 29.79; 40.06; 52.48; 70.83 (2DBT $^-$ ); 128.60 (2DBT $^-$ ); 129.13 (2DBT $^-$ ); 129.37 (2DBT $^-$ ); 129.58; 130.85; 132.51; 133.31 (2DBT $^-$ ); 138.44 (2DBT $^-$ ); 143.80; 152.0; 156.49; 164.74 (2DBT $^-$ ); 167.56 (2DBT $^-$ ). (KBr):  $\tilde{\nu}$  ( $\text{cm}^{-1}$ ) 3435, 3064; 3009; 2974; 2867; 1719; 1620; 1602; 1582; 1493; 1451; 1331; 1316; 1265; 1194; 1176; 1114; 1070; 1027; 1001; 896; 848; 804; 764; 717; 688; 676; 554. MS (ESI)  $m/z$  (%): 341 (100), 171 (20). HRMS (ESI)  $m/z$ : [(M-2DBT $^-$ ) $^{2+}$ ] ( $\text{C}_{24}\text{H}_{26}\text{N}_2^{2+}$ ) calc.: 171.10425, found: 171.10428.

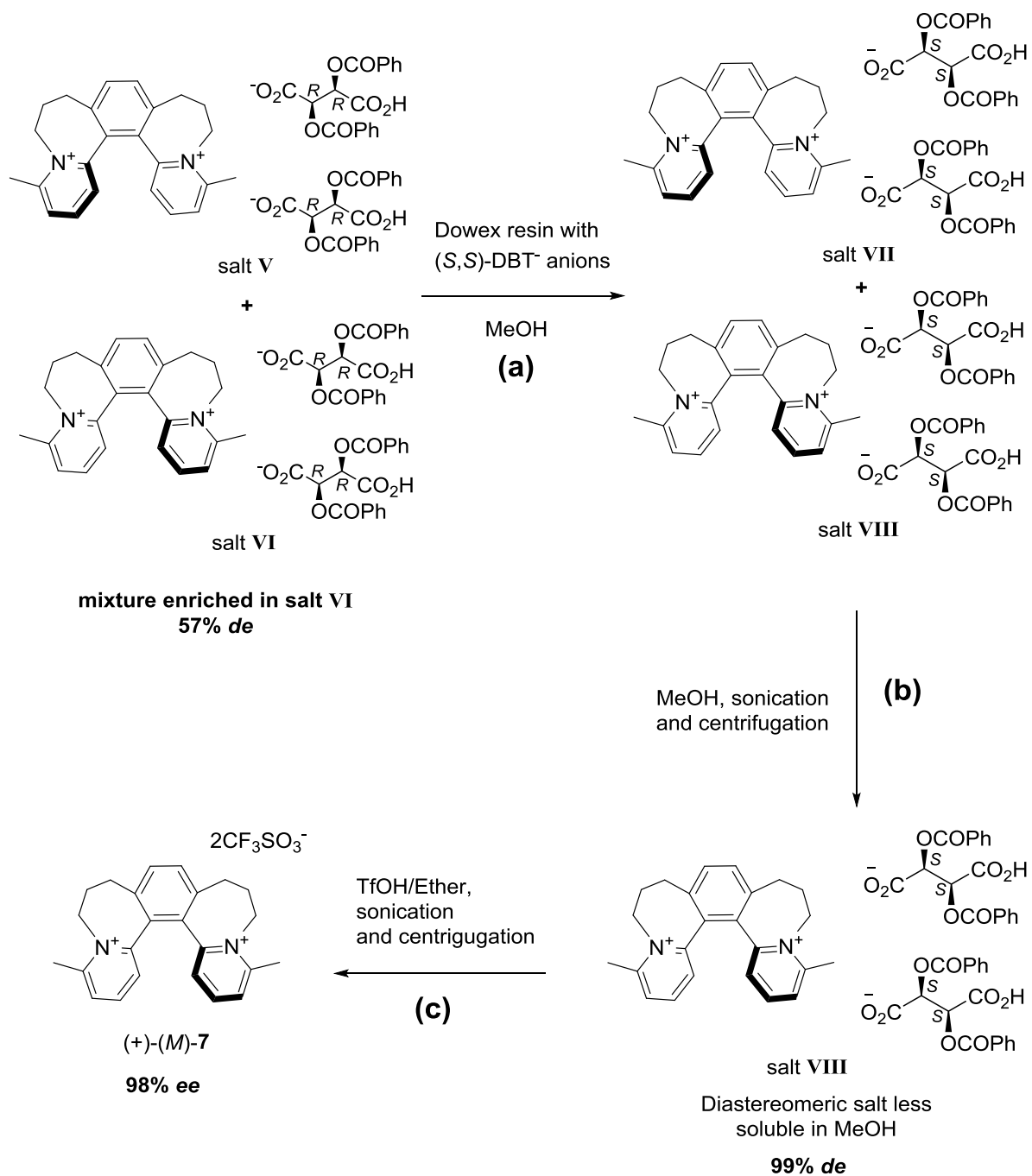
#### 4. Procedure to obtain (-)-(P)-7:

A mixture of TfOH : Et<sub>2</sub>O 1 : 50 (25 mL) and Et<sub>2</sub>O (10 mL) was added to the salt **V** (2.34 g, 2.21 mmol). The mixture was sonicated for 5 min, then the mixture was centrifuged, and the liquids were separated from the solid pellet (Step 3, Scheme 3). This procedure of TfOH : Et<sub>2</sub>O addition, sonication and centrifugation, was repeated three more times. In order to remove all the TfOH residues, the solid pellet was sonicated with pure Et<sub>2</sub>O (25 mL). After centrifugation, the liquids were separated from the solid pellet, and then the solid pellet was treated with more Et<sub>2</sub>O (four more times). After drying the solid pellet under vacuum, enantiomer (-)-(P)-**7** was obtained as a white solid (1.46 g, 2.28 mmol, 100% yield, 99% *ee*, see CE Section S4, Figure S6, p. S80). Racemization barrier determination of (-)-(P)-**7** is detailed in CE Section S4 (Figure S13, p. S89). For ECD and UV/Vis spectra, see Figure S24 (Section S5, p. S107).

#### (-)-(P)-4,15-Dimethyl-6,7,8,11,12,13-hexahydrodipyrido[1,2-a:1',2'-a']benzo[2,1-c:3,4-c']bisazepindium trifluoromethanesulfonate, (-)-(P)-7



**Resolution of (*rac*)-7 to obtain (+)-(*M*)-7 via mixture of diastereomeric salts VII and VIII**



**Scheme S4.** Resolution of (*rac*)-7 to obtain (+)-(*M*)-7 via mixture of diastereomeric salts VII and VIII

### 1. Transformation of the diastereoenriched salt VI to diastereoenriched salt VIII:

250 mL of strongly basic anion exchange resin in Cl<sup>-</sup> cycle (Dowex 1×2, 16-100 mesh) in demineralized water was loaded by (+)-(*S,S*)-*D-O,O'*-dibenzoyltartaric anions according to step (a), Scheme S4. Solution of diastereoenriched salt VI (57% *de*, CE) in 400 ml MeOH was slowly run through the column. Then, the column was washed with 250 mL MeOH and the volatiles from combined methanolic solutions were removed on a rotary evaporator to obtain diastereomerically enriched salt VIII as a brownish solid.

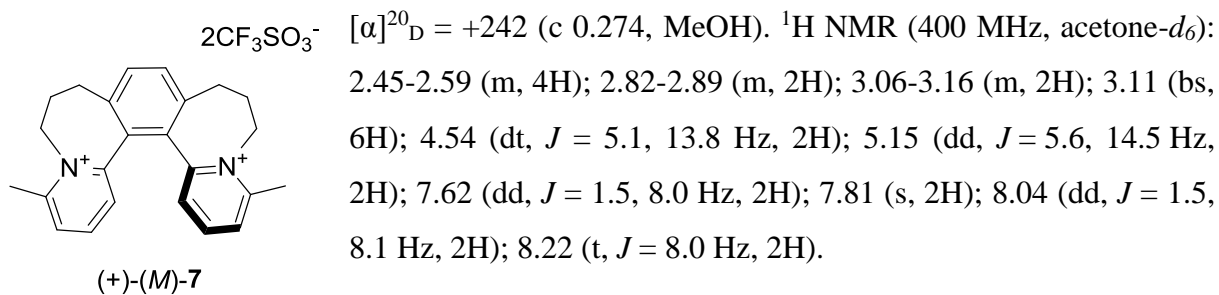
### 2. Separation of the salt VIII:

MeOH (30 mL) was added to the diastereomeric mixture of salt VII and salt VIII (5.89 g). The suspension was sonicated, centrifuged, and the liquids were separated from the solid pellet (Step (b), Scheme S4). This procedure of MeOH addition, sonication, and centrifugation was repeated six more times. After drying the solid pellet under vacuum, salt VIII was obtained as a white solid (2.06 g, 1.95 mmol, 99% *de*, CE).

### 3. Procedure to obtain (+)-(*M*)-7:

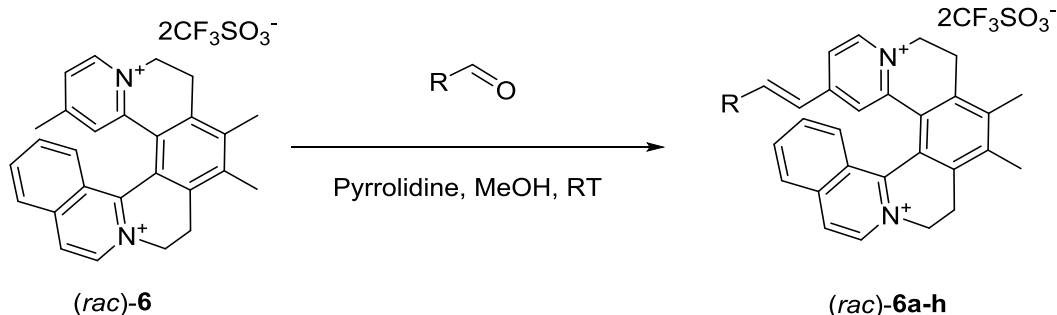
A mixture of TfOH : Et<sub>2</sub>O 1 : 50 (22 mL) and Et<sub>2</sub>O (10 mL) was added to the salt VIII (2.06 g, 1.95 mmol). The mixture was sonicated for 5 min, then the mixture was centrifuged, and the liquids were separated from the solid pellet (Step (c), Scheme S4). This procedure of TfOH : Et<sub>2</sub>O addition, sonication and centrifugation, was repeated three more times. In order to remove the TfOH impurities, the solid pellet was sonicated with pure Et<sub>2</sub>O (25 mL). After centrifugation, the liquids were separated from the solid pellet, and then the solid pellet was treated with more Et<sub>2</sub>O (five more times). After drying the solid pellet under vacuum, enantiomer (+)-(*M*)-7 was obtained as a white solid (1.34 g, 2.09 mmol, 100% yield, 99% *ee*, see CE Section S4, Figure S6, p. S80). For ECD and UV/Vis spectra, see Figure S24 (Section S5, p. S107).

**(+)-(M)-4,15-Dimethyl-6,7,8,11,12,13-hexahydrodipyrido[1,2-a:1',2'-a']benzo[2,1-c:3,4-c']bisazepindium trifluoromethansulfonate, (+)-(M)-7**

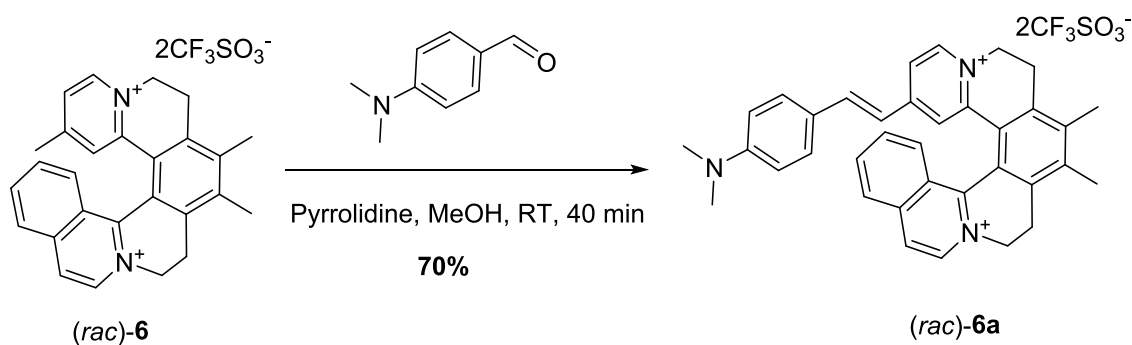


## Part F: Synthesis of racemic dyes 6a-h from common precursor

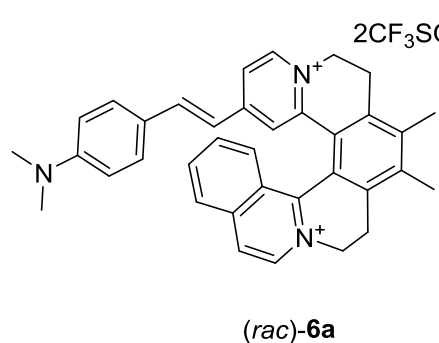
### (rac)-6



### (E)-13-(4-(Dimethylamino)styryl)-6,7-dimethyl-4,5,8,9-tetrahydroisoquinolino[1,2-a]pyrido[1,2-k][2,9]phenanthroline-3,10-dium trifluoromethanesulfonate, (rac)-6a

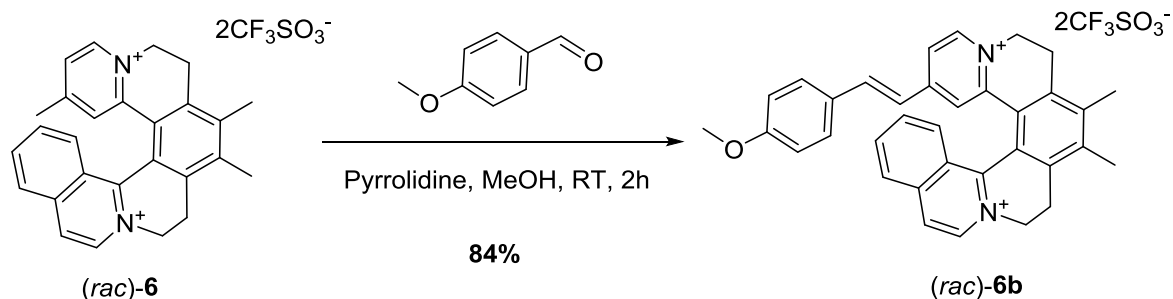


(rac)-6 (300 mg, 0.443 mmol), 4-dimethylaminobenzaldehyde (330 mg, 2.22 mmol, 5 equiv), pyrrolidine (0.185 mL, 2.22 mmol, 5 equiv) and MeOH (6 mL) were placed to 10 mL flask and stirred for 40 min at RT under argon while protected from ambient light using aluminium foil cover. Reaction progress was checked by TLC (mobile phase Stoddart's magic mixture, starting material (rac)-6  $R_f = 0.5$ , product (rac)-6a  $R_f = 0.7$ ). Crude product was transferred to 50 mL centrifuge tubes (3 tubes with 2 mL of reaction crude each one) and precipitated from reaction mixture by addition of Et<sub>2</sub>O (50 mL to each tube). The resulting suspensions were centrifuged and supernatants were removed. Residues were dissolved in a minimum amount of MeOH (2 mL added to each tube), afterward Et<sub>2</sub>O (30 mL) was added to each tube. Precipitates were centrifuged. This reprecipitation was repeated twice. Centrifuged solids were collected in a glass vial using Et<sub>2</sub>O. The resulting suspension was centrifuged and Et<sub>2</sub>O was removed. The solids were dried under vacuum to get pure (rac)-6a as a deep red solid in 70% yield (250.7 mg, 0.310 mmol).



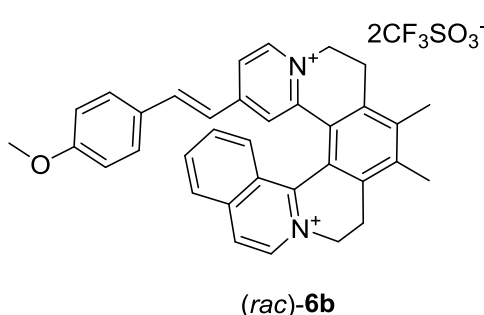
m.p. 269°C (decomposition). <sup>1</sup>H NMR (600 MHz, acetone-*d*<sub>6</sub>): 2.58 (s, 3H); 2.59 (s, 3H); 3.06 (s, 6H); 3.32 (ddd, *J* = 5.2, 14.4, 16.9 Hz, 1H); 3.42 (bdt, *J* = 3.5, 16.0, 16.6 Hz, 1H); 3.73 (ddd, *J* = 1.9, 3.5, 16.9 Hz, 2H); 5.07 - 5.19 (m, 3H); 5.34 (ddd, *J* = 1.9, 3.6, 14.0 Hz, 1H); 6.56 (d, *J* = 16.0 Hz, 1H); 6.70 - 6.72 (m, 2H); 7.15 (d, *J* = 16.0 Hz, 1H); 7.21 (d, *J* = 2.0 Hz, 1H); 7.40 (m, 2H); 7.70 (dd, *J* = 2.0, 6.7 Hz, 1H); 7.75 (ddd, *J* = 1.3, 6.9, 8.7 Hz, 1H); 7.92 (ddd, *J* = 1.1, 6.9, 8.11 Hz, 1H); 8.09 (dq, *J* = 1.0, 8.7 Hz, 1H); 8.16 (bdt, *J* = 0.7, 1.3, 8.1 Hz, 1H); 8.52 (bd, *J* = 6.7 Hz, 1H); 8.74 (d, *J* = 6.7 Hz, 1H); 9.04 (d, *J* = 6.7 Hz, 1H). <sup>13</sup>C NMR (100 MHz, acetonitrile-*d*<sub>3</sub>): δ = 17.15; 17.16; 26.32; 26.67; 40.34; 54.09; 56.17; 112.87; 116.77; 120.10; 123.15; 123.26; 125.34; 125.54; 126.89; 128.16; 128.83; 128.93; 131.36; 132.69; 136.41; 137.35; 138.56; 139.70; 141.05; 142.16; 142.65; 143.20; 144.72; 146.67; 151.95; 153.55; 154.63. MS (ESI) *m/z* (%): 509.5 (20), 508.5 (56), 255.2 (41), 254.7 (100). HRMS (ESI) *m/z*: [(M-TfO<sup>-</sup>)<sup>+</sup>] (C<sub>37</sub>H<sub>35</sub>F<sub>3</sub>N<sub>3</sub>O<sub>3</sub>S<sup>+</sup>) calc.: 658.23457, found: 658.23429; [(M-2TfO<sup>-</sup>)<sup>2+</sup>] (C<sub>36</sub>H<sub>35</sub>N<sub>3</sub><sup>2+</sup>) calc.: 254.64100, found: 254.64102. Elem. Anal. calc. for C<sub>38</sub>H<sub>35</sub>F<sub>6</sub>N<sub>3</sub>O<sub>6</sub>S<sub>2</sub>: C, 56.50; H, 4.37; N, 5.20; S, 7.94. Found: C, 56.35; H, 4.20; N, 5.09; S, 7.62. For UV/Vis molar absorption coefficient ( $\epsilon$ ) and corresponding absorption wavelength ( $\lambda_{\max}$ ), see Table S7 (Section S5, p. S99). X-ray crystal of [(*rac*)-6a][NapSO<sub>3</sub>]<sub>2</sub>, see X-ray analysis (Section S7, p. S149).

**(*E*)-13-(4-Methoxystyryl)-6,7-dimethyl-4,5,8,9-tetrahydroisoquinolino[1,2-*a*]pyrido [1,2-*k*][2,9 phenanthroline-3,10-diium trifluoromethansulfonate, (*rac*)-6b**



(*rac*)-6 (80.0 mg, 0.12 mmol), *p*-anisaldehyde (29  $\mu$ L, 0.24 mmol, 2 equiv), pyrrolidine (69  $\mu$ L, 0.83 mmol, 7 equiv) and MeOH (1.5 mL) were placed to 10 mL flask and stirred for 2 h at RT under argon while protected from ambient light using aluminium foil cover. Reaction

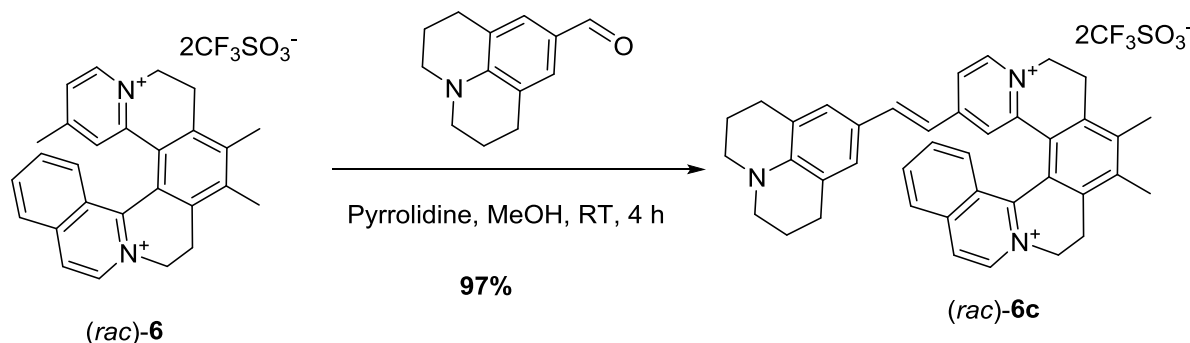
progress was checked by TLC (mobile phase Stoddart's magic mixture, starting material (*rac*)-**6**  $R_f = 0.5$ , product (*rac*)-**6b**  $R_f = 0.7$ ). Crude product was transferred to 50 mL centrifuge tubes (2 tubes with 0.75 mL of reaction crude each one) and precipitated by addition of Et<sub>2</sub>O (45 mL to each tube). Suspensions were centrifuged and supernatants were removed. Residues were dissolved in MeOH (3 mL to each tube) and then Et<sub>2</sub>O (20 mL) was added to each tube. Solids were reprecipitated 3 more times to get pure product and then collected in a glass vial using Et<sub>2</sub>O. The resulting suspension was centrifuged and Et<sub>2</sub>O was removed. The solid was dried under vacuum to get pure (*rac*)-**6b** as a nicely yellow solid in 84% yield (78.9 mg, 0.10 mmol).



$2CF_3SO_3^-$  m.p. 277°C (decomposition). <sup>1</sup>H NMR (600 MHz, acetone-*d*<sub>6</sub>): 2.60 (s, 3H); 2.61 (s, 3H); 3.32-3.44 (m, 2H); 3.77 (ddd,  $J = 1.9, 3.6, 17.0$  Hz, 2H); 3.85 (s, 3H); 5.14 - 5.21 (m, 3H); 5.35 (ddd,  $J = 1.9, 4.6, 14.1$  Hz, 1H); 6.76 (d,  $J = 16.3$  Hz, 1H); 6.94 (m, 2H); 7.24 (d,  $J = 16.3$  Hz, 1H); 7.37 (d,  $J = 2.0$  Hz, 1H); 7.52 (m, 2H); 7.75 (ddd,  $J = 1.3, 6.9, 8.7$  Hz, 1H); 7.86 (dd,  $J = 2.0, 6.6$  Hz, 1H); 7.93 (ddd,  $J = 1.1, 6.9, 8.1$  Hz, 1H); 8.10 (dq,  $J = 0.9, 8.7$  Hz, 1H); 8.18 (bdt,  $J = 0.7, 1.3, 8.1$  Hz, 1H); 8.54 (bd,  $J = 6.7$  Hz, 1H); 8.89 (d,  $J = 6.6$  Hz, 1H); 9.06 (d,  $J = 6.7$  Hz, 1H). <sup>13</sup>C NMR (100 MHz, acetonitrile-*d*<sub>3</sub>):  $\delta = 17.17; 17.22; 26.21; 26.66; 54.56; 56.17; 56.31; 115.58; 120.36; 121.25; 123.37; 125.46; 126.27; 126.91; 127.95; 128.39; 128.77; 128.99; 131.09; 132.79; 136.49; 137.44; 138.74; 139.77; 141.40; 141.94; 142.32; 142.75; 145.40; 147.33; 151.78; 154.24; 163.01$ . MS (ESI)  $m/z$  (%): 645.2 (43), 496.3 (43), 495.3 (100), 248.1 (40). HRMS (ESI)  $m/z$ : [(M-TfO<sup>-</sup>)<sup>+</sup>] (C<sub>36</sub>H<sub>32</sub>F<sub>3</sub>N<sub>2</sub>O<sub>4</sub>S<sup>+</sup>) calc.: 645.20294, found: 645.20339. Elem. Anal. calc. for C<sub>37</sub>H<sub>32</sub>F<sub>6</sub>N<sub>2</sub>O<sub>7</sub>S<sub>2</sub>: C, 55.92; H, 4.06; N, 3.52; S, 8.07. Found: C, 55.70; H, 3.94; N, 3.40; S, 7.84. For UV/Vis molar absorption coefficient ( $\epsilon$ ) and corresponding absorption wavelength ( $\lambda_{max}$ ), see Table S7 (Section S5, p. S99). X-ray crystal of [(*rac*)-**6b**][TfO]<sub>2</sub>, see X-ray analysis (Section S7, p. S150).



**(E)-13-(2-(1,2,3,5,6,7-Hexahydropyrido[3,2,1-ij]quinolin-9-yl)vinyl)-6,7-dimethyl-4,5,8,9-tetrahydroisoquinolino[1,2-a]pyrido[1,2-k][2,9]phenanthroline-3,10-dium trifluoromethanesulfonate, (*rac*)-6c**



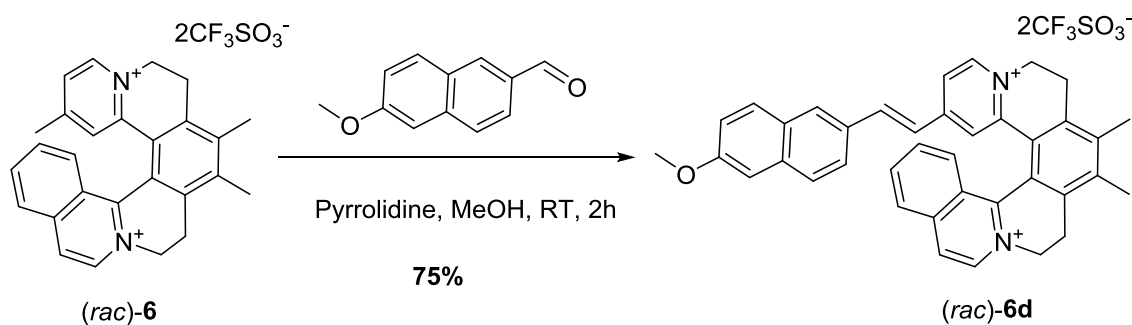
*(rac)*-6 (260 mg, 0.38 mmol), 9-julolidinecarboxaldehyde (387 mg, 1.92 mmol, 5 equiv), pyrrolidine (0.16 mL, 1.92 mmol, 5 equiv) and MeOH (8 mL) were placed to small flask and stirred for 4h at RT under argon while protected from ambient light using aluminium foil cover. Reaction progress was checked by TLC (mobile phase Stoddart's magic mixture, starting material *(rac)*-6  $R_f = 0.5$ , product *(rac)*-6c  $R_f = 0.6$ ). Crude product was transferred to 50 mL centrifuge tubes (4 tubes with 2 mL of reaction crude each one) and precipitated by addition of Et<sub>2</sub>O (45 mL added to each tube). Suspensions were centrifuged and supernatants were removed. Residues were dissolved in a minimum amount of MeOH and precipitated by addition of Et<sub>2</sub>O (35 mL added to each tube). Solids were reprecipitated once more time to get pure product. Solids were collected in a glass vial using Et<sub>2</sub>O. The resulting suspension was centrifuged and Et<sub>2</sub>O was removed. The solid was dried under vacuum to get pure *(rac)*-6c as a deep blue solid in 97% yield (320.0 mg, 0.372 mmol).

$2\text{CF}_3\text{SO}_3^-$   
*(rac)*-6c

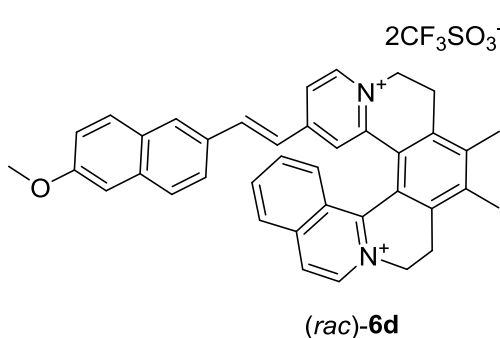
m.p. 242 – 244°C (decomposition). <sup>1</sup>H NMR (600 MHz, acetone-*d*<sub>6</sub>): 1.89 – 1.95 (m, 4H); 2.57 (s, 3H); 2.59 (s, 3H); 2.67 – 2.70 (m, 4H); 3.29 – 3.32 (m, 4H); 3.31 (bddd,  $J = 5.1, 14.5, 16.8$  Hz, 1H); 3.40 (bdt,  $J = 4.8, 15.9$  Hz, 1H); 3.71 (ddd,  $J = 2.0, 3.6, 16.8$  Hz, 2H); 5.01 - 5.11 (m, 2H); 5.18 (dt,  $J = 3.8, 14.8$  Hz, 1H); 5.34 (ddd,  $J = 1.9, 4.8, 14.0$  Hz, 1H); 6.45 (d,  $J = 15.9$  Hz, 1H); 6.96 (s, 2H); 7.07 (d,  $J = 15.9$  Hz, 1H); 7.14 (d,  $J = 2.0$  Hz, 1H); 7.62 (dd,  $J = 2.0, 6.8$  Hz, 1H); 7.76 (ddd,  $J = 1.3, 6.9, 8.1$  Hz, 1H); 7.93 (ddd,  $J = 1.1, 6.9, 8.1$  Hz, 1H);

8.09 (dq,  $J = 0.9, 8.7$  Hz, 1H); 8.18 (bddd,  $J = 0.7, 1.3, 8.1$  Hz, 1H); 8.50 (bd,  $J = 6.7$  Hz, 1H); 8.67 (d,  $J = 6.8$  Hz, 1H); 9.04 (d,  $J = 6.7$  Hz, 1H).  $^{13}\text{C}$  NMR (151 MHz, acetone- $d_6$ ):  $\delta = 16.97; 17.00; 22.16; 26.57; 26.74; 28.21; 50.61; 53.80; 56.37; 115.72; 119.33; 122.62; 123.50; 125.21; 125.62; 126.93; 128.63; 128.96; 129.02; 129.30; 132.52; 136.15; 137.82; 138.66; 139.77; 140.59; 142.17; 142.25; 143.85; 144.45; 146.59; 146.76; 152.02; 154.92$ . IR (KBr):  $\tilde{\nu}$  ( $\text{cm}^{-1}$ ) 2935; 2842; 1631; 1573; 1562; 1522; 1508; 1378; 1355; 1316; 1275; 1260; 1221; 1208; 1157; 1108; 1084; 1052; 1030; 819; 754; 730; 679; 637; 573; 517. HRMS (ESI)  $m/z$ :  $[(\text{M-TfO}^-)^+]$  ( $\text{C}_{41}\text{H}_{39}\text{F}_3\text{N}_3\text{O}_3\text{S}^+$ ) calc.: 710.26587, found: 710.26598. For UV/Vis molar absorption coefficient ( $\epsilon$ ) and corresponding absorption wavelength ( $\lambda_{\text{max}}$ ), see Table S7 (Section S5, p. S99).

**(*E*)-13-(2-(6-Methoxynaphthalen-2-yl)vinyl)-6,7-dimethyl-4,5,8,9-tetrahydro-isoquinolino[1,2-a]pyrido[1,2-k][2,9]phenanthroline-3,10-dium trifluoromethanesulfonate, (*rac*)-6d**

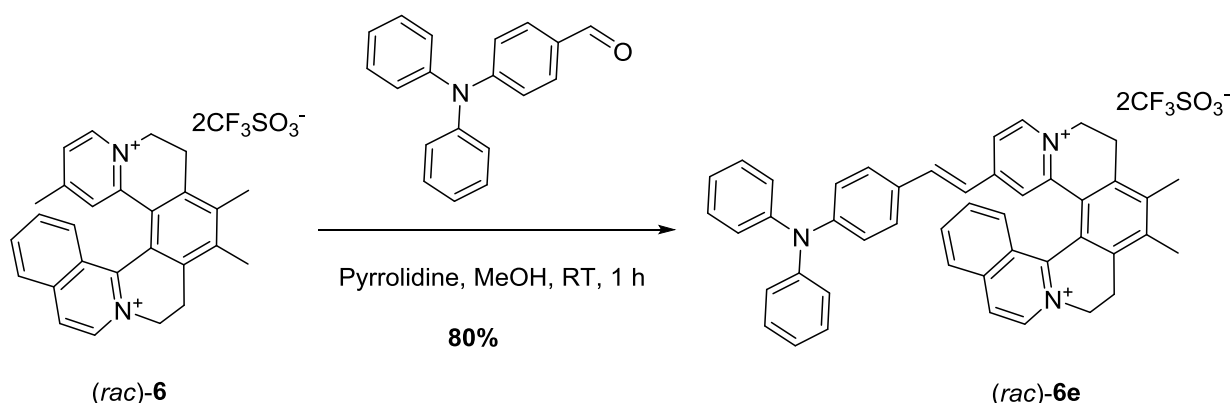


(*rac*)-**6** (300 mg, 0.44 mmol), 6-methoxy-2-naphthaldehyde (412.8 mg, 2.22 mmol, 5 equiv), MeOH (6 mL) and pyrrolidine (0.185 mL, 2.22 mmol, 5 equiv) were placed to 10 mL flask and stirred for 2 h at RT under argon while protected from ambient light using aluminium foil cover. Reaction was checked by TLC (mobile phase Stoddart's magic mixture, starting material (*rac*)-**6**  $R_f = 0.5$ , product (*rac*)-**6d**  $R_f = 0.6$ ). Crude product was transferred to 50 mL centrifuge tubes (3 tubes with 2 mL of reaction crude each one) and precipitated by addition of Et<sub>2</sub>O (45 mL added to each tube). Suspensions were centrifuged and supernatants were removed. Residues were dissolved in a minimum amount of MeOH (3 mL) and precipitated by addition of Et<sub>2</sub>O (35 mL added to each tube). This reprecipitation was repeated two more times to get pure product. Solids were collected in a glass vial using Et<sub>2</sub>O. The resulting suspension was centrifuged and Et<sub>2</sub>O was removed. The solid was dried under vacuum to get pure (*rac*)-**6d** as an orange solid in 75% yield (281 mg, 0.333 mmol).

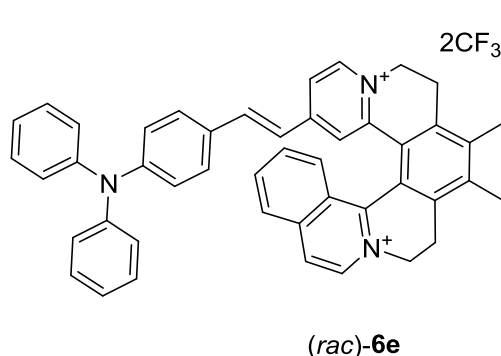


$2\text{CF}_3\text{SO}_3^-$  m.p. 318 – 320°C (decomposition).  $^1\text{H}$  NMR (600 MHz, acetonitrile- $d_3$ ): 2.44 (s, 3H); 2.45 (s, 3H); 3.05 (ddd,  $J = 5.0, 14.2, 17.1$  Hz, 1H); 3.15 (bdt,  $J = 4.6, 15.5$  Hz, 1H); 3.52 (ddd,  $J = 1.9, 3.5, 16.8$  Hz, 2H); 3.93 (s, 3H); 4.80 (ddd,  $J = 3.8, 13.6, 14.2$  Hz, 1H); 4.88 (ddd,  $J = 1.8, 5.0, 13.6$  Hz, 1H); 4.93 (ddd,  $J = 3.5, 14.0, 14.7$  Hz, 1H); 5.07 (ddd,  $J = 1.9, 4.6, 14.0$  Hz, 1H); 6.73 (d,  $J = 16.3$  Hz, 1H); 6.94 (d,  $J = 2.0$  Hz, 1H); 7.07 (d,  $J = 16.3$  Hz, 1H); 7.21 (dd,  $J = 2.6, 8.8$  Hz, 1H); 7.29 (d,  $J = 2.6$  Hz, 1H); 7.54 (dd,  $J = 1.8, 8.6$  Hz, 1H); 7.57 (dd,  $J = 2.0, 6.6$  Hz, 1H); 7.60 (ddd,  $J = 1.2, 6.9, 8.8$  Hz, 1H); 7.75 (dd,  $J = 4.6, 8.9$  Hz, 2H); 7.80 – 7.85 (m, 3H); 7.99 (d,  $J = 8.2$  Hz, 1H); 8.30 (d,  $J = 6.7$  Hz, 1H); 8.49 (d,  $J = 6.6$  Hz, 1H); 8.71 (d,  $J = 6.7$  Hz, 1H).  $^{13}\text{C}$  NMR (151 MHz, acetone- $d_6$ ):  $\delta = 17.01; 17.09; 26.00; 26.53; 54.49; 56.05; 56.17; 107.14; 120.47; 121.31; 121.81; 123.20; 124.90; 125.36; 126.44; 126.75; 127.69; 128.51; 128.60; 128.88; 129.40; 130.96; 130.96; 131.19; 132.67; 136.36; 136.89; 137.37; 138.51; 139.65; 141.30; 142.11; 142.20; 142.56; 145.41; 147.19; 151.61; 153.75; 160.20$ . IR (KBr):  $\tilde{\nu}$  ( $\text{cm}^{-1}$ ) 518; 573; 638; 679; 755; 818; 980; 1030; 1117; 1164; 1224; 1265; 1352; 1381; 1393; 1411; 1439; 1484; 1508; 1552; 1573; 1602; 1629; 2843. HRMS (ESI)  $m/z$ : [(M-TfO) $^+$ ] ( $\text{C}_{40}\text{H}_{34}\text{F}_3\text{N}_2\text{O}_4\text{S}^+$ ) calc.: 695.21859, found: 695.21812; [(M-2TfO) $^{2+}$ ] ( $\text{C}_{39}\text{H}_{34}\text{N}_2\text{O}^{2+}$ ) calc.: 273.13301, found: 273.13304. Elem. Anal. calc. for  $\text{C}_{41}\text{H}_{34}\text{F}_6\text{N}_2\text{O}_7\text{S}_2$ : C, 58.29; H, 4.06; N, 3.32; S, 7.59. Found: C, 58.20; H, 3.88; N, 3.16; S, 7.31. For UV/Vis molar absorption coefficient ( $\epsilon$ ) and corresponding absorption wavelength ( $\lambda_{\text{max}}$ ), see Table S7 (Section S5, p. S99). X-ray crystal of [(rac)-6d][I] $_2$ , see X-ray analysis (Section S7, p. S151).

**(E)-13-(4-(Diphenylamino)styryl)-6,7-dimethyl-4,5,8,9-tetrahydroisoquinolino[1,2-a]pyrido[1,2-k][2,9]phenanthroline-3,10-dium trifluoromethanesulfonate, (rac)-6e**



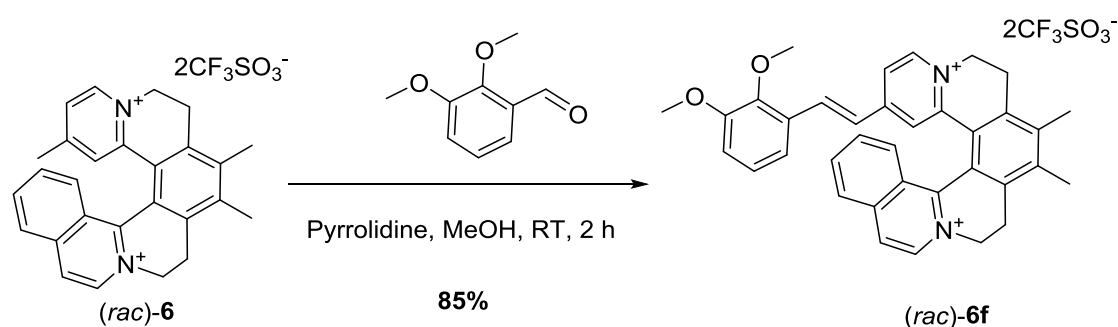
(rac)-6 (50 mg, 0.074 mmol), 4-(diphenylamino)benzaldehyde (101 mg, 0.37 mmol, 5 equiv), pyrrolidine (0.031 mL, 0.37 mmol, 5 equiv) and MeOH (1.3 mL) were placed to 10 mL flask and stirred for 1 h at RT under argon while protected from ambient light using aluminium foil cover. Reaction progress was checked by TLC (mobile phases Stoddart's magic mixture, starting material (rac)-6  $R_f = 0.5$ , product (rac)-6e  $R_f = 0.6$ ). Crude product was transferred to 50 mL centrifuge tube and precipitated by addition of Et<sub>2</sub>O (45 mL). Suspension was centrifuged and supernatants were removed. Residue was dissolved in a minimum amount of MeOH (2 mL) and precipitated by addition of Et<sub>2</sub>O (40 mL). This reprecipitation was repeated two more times to get pure product. Solid was collected in a glass vial using Et<sub>2</sub>O and the resulting suspension was centrifuged. The Et<sub>2</sub>O was removed and the solid was dried under vacuum to get pure (rac)-6e as a deep red solid in 80% yield (55 mg, 0.059 mmol).



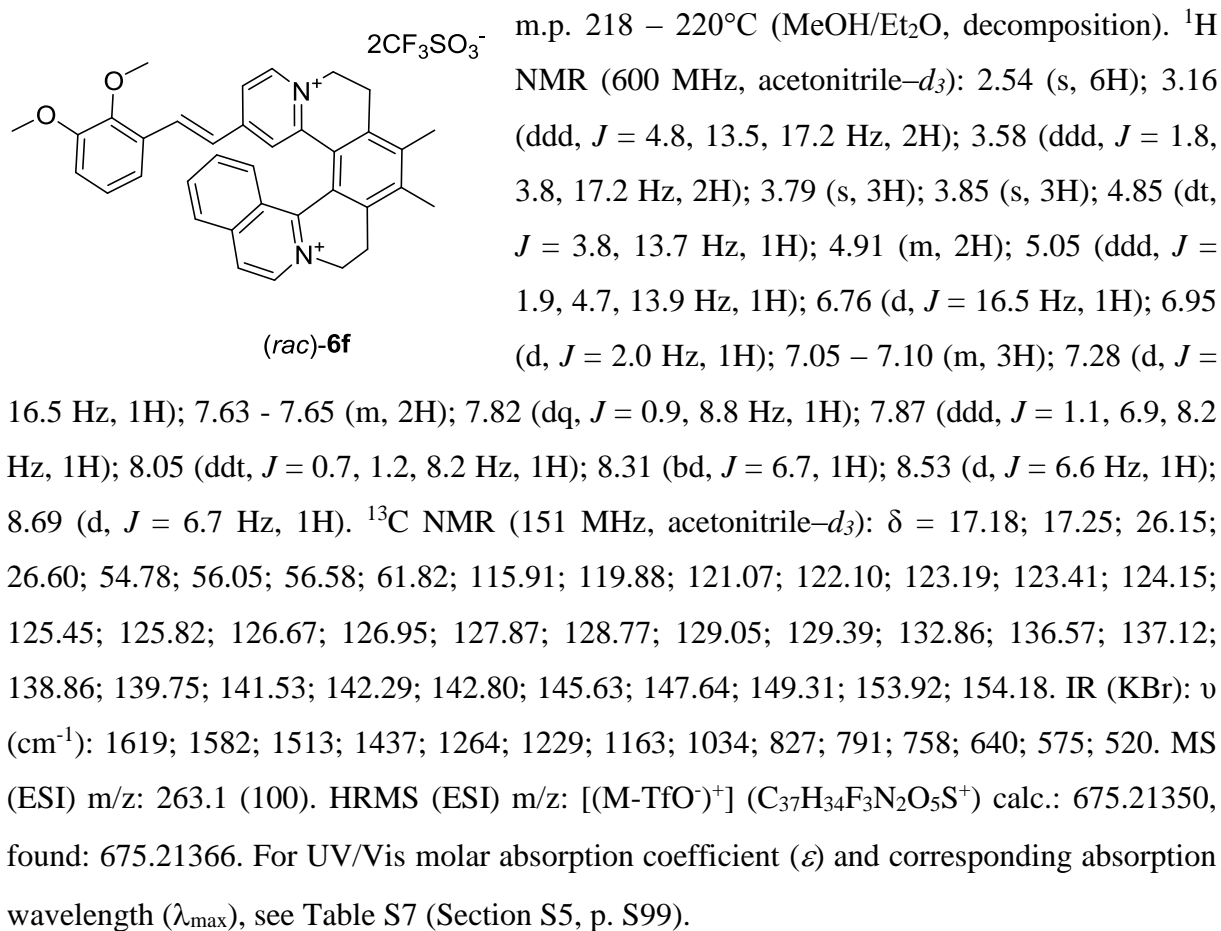
m.p. 218 – 220°C (decomposition). <sup>1</sup>H NMR (600 MHz, acetone-*d*<sub>6</sub>): 2.62 (s, 6H); 3.34 - 3.46 (m, 2H); 3.75 - 3.80 (m, 2H); 5.16 - 5.24 (m, 3H); 5.34 (ddd,  $J = 1.8, 4.5, 14.1$  Hz, 1H); 6.78 (d,  $J = 16.2$  Hz, 1H); 6.88 - 6.90 (m, 2H); 7.13 - 7.15 (m, 4H); 7.16 - 7.19 (m, 2H); 7.25 (d,  $J = 16.2$  Hz, 1H); 7.36 - 7.39 (m, 5H); 7.43 - 7.45 (m, 2H); 7.78 (ddd,  $J = 1.3, 6.9, 8.8$  Hz, 1H); 7.86 (dd,  $J = 2.0, 6.7$  Hz, 1H); 7.96 (ddd,  $J = 1.1, 6.9, 8.2$  Hz, 1H); 8.13 (dq,  $J = 0.9, 8.8$  Hz, 1H); 8.21 (ddt,  $J = 0.7, 1.3, 8.2$  Hz, 1H); 8.54 (bdd,  $J = 0.8, 6.7$  Hz, 1H); 8.88 (d,  $J = 6.7$  Hz, 1H); 9.03 (d,  $J = 6.7$  Hz, 1H). <sup>13</sup>C NMR

(151 MHz, acetone-*d*<sub>6</sub>):  $\delta$  = 16.98; 17.05; 26.38; 26.67; 30.35; 54.40; 56.32; 120.22; 120.75; 121.18; 121.47; 123.32; 123.61; 125.34; 125.49; 126.61; 126.92; 128.31; 128.66; 128.97; 130.58; 130.79; 132.63; 136.24; 137.97; 138.90; 139.82; 140.99; 141.91; 142.34; 145.36; 147.43; 147.54; 151.22; 151.79; 154.41. IR (KBr):  $\tilde{\nu}$  (cm<sup>-1</sup>) 1616; 1578; 1510; 1490; 1450; 1330; 1278; 1259; 1153; 1029; 974; 889; 755; 679; 637; 573; 517. TOF MS (ESI) m/z (%): 783.2 (26), 782.2 (47), 317.1 (52), 316.6 (100). HRMS (ESI) m/z: [(M-TfO)<sup>+</sup>] (C<sub>47</sub>H<sub>39</sub>F<sub>3</sub>N<sub>3</sub>O<sub>3</sub>S<sup>+</sup>) calc.: 782.26587, found: 782.26561. For UV/Vis molar absorption coefficient ( $\epsilon$ ) and corresponding absorption wavelength ( $\lambda_{\max}$ ), see Table S7 (Section S5, p. S99).

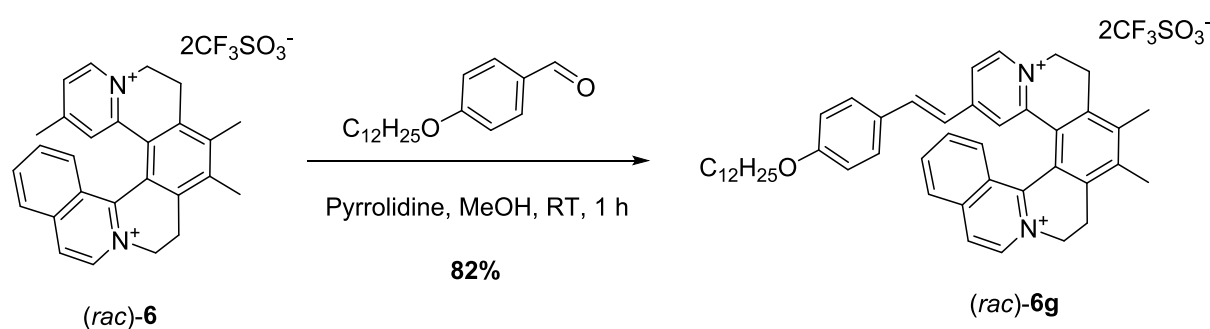
**(*E*)-13-(2,3-Dimethoxystyryl)-6,7-dimethyl-4,5,8,9-tetrahydroisoquinolino[1,2-a]pyrido[1,2-k][2,9]phenanthroline-3,10-dium trifluoromethanesulfonate, (*rac*)-6f**



(*rac*)-**6** (50.0 mg, 0.074 mmol), 2,3-dimethoxybenzaldehyde (61.4 mg, 0.369 mmol, 5 equiv), pyrrolidine (0.031 mL, 0.369 mmol, 5 equiv) and MeOH (1.3 mL) were placed to small flask and stirred for 2 h at RT under argon while protected from ambient light using aluminium foil cover. Reaction progress was checked by TLC (mobile phase Stoddart's magic mixture, starting material (*rac*)-**6**  $R_f$  = 0.5, product (*rac*)-**6f**  $R_f$  = 0.7). Crude product was transferred to 50 mL centrifuge tube and precipitated by addition of Et<sub>2</sub>O (45 mL). Suspension was centrifuged and supernatant was removed. Residue was dissolved in a minimum amount of MeOH (2 mL) and precipitated by Et<sub>2</sub>O (40 mL). This reprecipitation was repeated three more times to get pure product. Solids were collected in a glass vial using Et<sub>2</sub>O and the resulting suspension was centrifuged. The Et<sub>2</sub>O was removed and the solid was dried under vacuum to get pure (*rac*)-**6f** as a yellow solid in 85% yield (52.0 mg, 0.063 mmol).

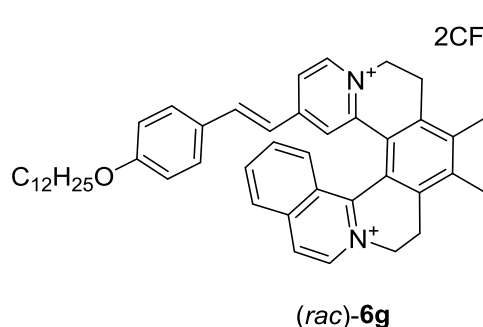


**(*E*)-13-(4-Methoxystyryl)-6,7-dimethyl-4,5,8,9-tetrahydroisoquinolino[1,2-*a*]pyrido [1,2-*k*][2,9 phenanthroline-3,10-diium trifluoromethansulfonate, (*rac*)-6g**



(*rac*)-**6** (50 mg, 0.074 mmol), 4-dodecyloxybenzaldehyde (107 mg, 0.37 mmol, 5 equiv), pyrrolidine (0.031 mL, 0.37 mmol, 5 equiv) and MeOH (1 mL) were placed to 10 mL flask and stirred for 1 h at RT under argon while protected from ambient light using aluminium foil cover. Reaction progress was checked by TLC (mobile phase Stoddart's magic mixture, starting material (*rac*)-**6** *R<sub>f</sub>* = 0.5, product (*rac*)-**6g** *R<sub>f</sub>* = 0.7). Crude product was transferred to 50 mL centrifuge tube and precipitated by addition of Et<sub>2</sub>O (45 mL). Suspension was

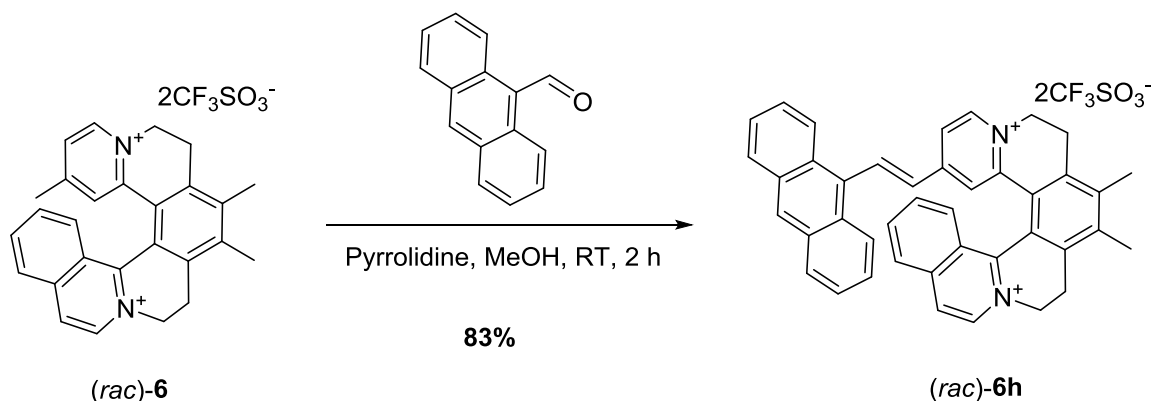
centrifuged and supernatant was removed. Residue was dissolved in a minimum amount of MeOH (1 mL) and precipitated by Et<sub>2</sub>O (40 mL). This reprecipitation was repeated two more times to get pure product. Solids were collected in a glass vial using Et<sub>2</sub>O and the resulting suspension was centrifuged. The Et<sub>2</sub>O was removed and the solid was dried under vacuum to get pure (*rac*)-**6g** as a yellow solid in 82% yield (57.5 mg, 0.061 mmol).



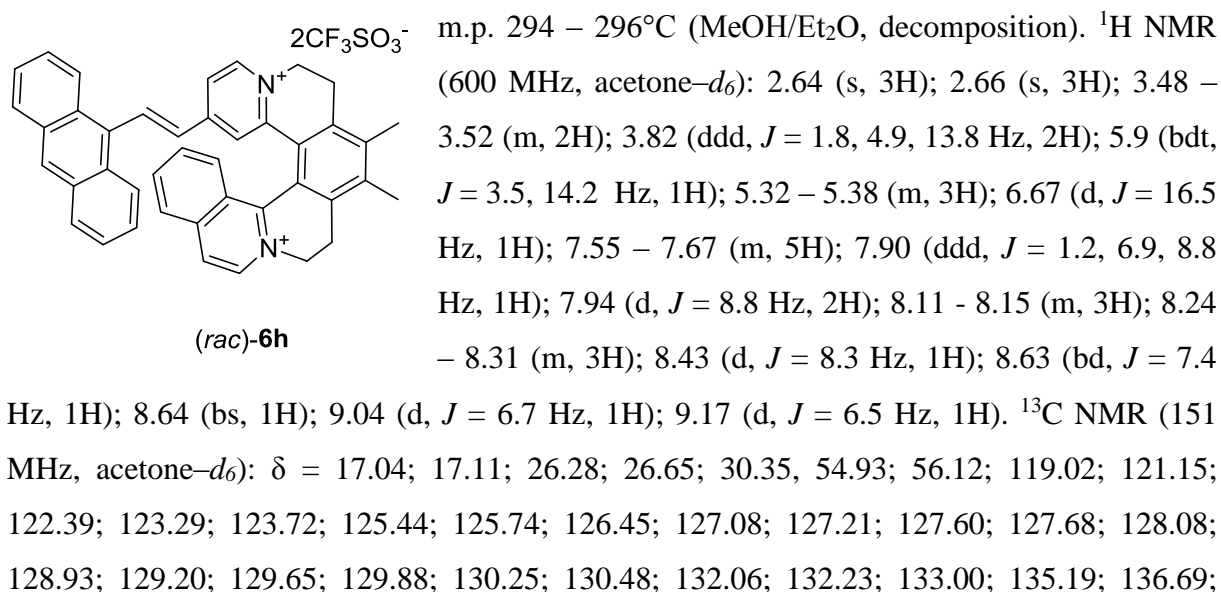
2CF<sub>3</sub>SO<sub>3</sub><sup>-</sup> m.p. 265-267°C. <sup>1</sup>H NMR (600 MHz, acetone-*d*<sub>6</sub>): 0.88 (t, *J* = 6.0 Hz, 3H); 1.29 – 1.38 (m, 14 H); 1.48 – 1.51 (m, 2H); 1.77 – 1.81 (m, 2H); 2.59 (s, 3H); 2.60 (s, 3H); 2.80 – 2.82 (m, 2H); 3.33 (td, *J* = 5.3, 15.7 Hz, 1H); 3.42 (td, *J* = 16.0, 4.3 Hz, 1H); 3.76 (d, *J* = 17.0 Hz, 2H);

4.06 (t, *J* = 6.0 Hz, 2H); 5.14 – 5.23 (m, 3H); 5.34 (ddd, *J* = 13.8, 4.3, 1.4 Hz, 1H); 6.74 (d, *J* = 16.2 Hz, 1H); 6.93 (m, 2H); 7.23 (d, *J* = 16.2 Hz, 1H); 7.34 (d, *J* = 1.8 Hz, 1H); 7.49 (m, 2H); 7.75 (ddd, *J* = 8.3, 6.9, 1.2 Hz, 1H); 7.84 (dd, *J* = 6.6, 1.9 Hz, 1H); 7.92 (t, *J* = 8.1 Hz, 1H); 8.08 (d, *J* = 8.8 Hz, 1H); 8.16 (d, *J* = 8.2 Hz, 1H); 8.52 (d, *J* = 6.7 Hz, 1H); 8.87 (d, *J* = 6.7 Hz, 1H); 9.04 (d, *J* = 6.7 Hz, 1H). <sup>13</sup>C NMR (151 MHz, acetone-*d*<sub>6</sub>): δ = 14.35; 16.99; 17.03; 23.32; 26.31; 26.69; 26.72; 29.84; 30.07; 30.33; 30.33; 30.35; 30.38; 32.63; 54.44; 56.33; 68.89; 115.77; 120.45; 120.80; 121.19; 123.33; 123.59; 125.30; 126.84; 126.87; 128.16; 128.38; 128.93; 131.18; 132.60; 136.20; 137.95; 138.81; 139.80; 141.03; 141.96; 142.30; 142.34; 145.48; 147.41; 151.75; 154.38; 162.40. IR (KBr):  $\tilde{\nu}$  (cm<sup>-1</sup>) 2926; 2854; 1618; 1594; 1571; 1553; 1514; 1469; 1379; 1328; 1264; 1170; 1031; 979; 890; 755; 679; 638; 573; 518. MS (ESI) *m/z*: 800.3 (23), 799.3 (39), 325.7 (54), 325.2 (100). HRMS (ESI) *m/z*: [(M-2TfO<sup>-</sup>)<sup>2+</sup>] (C<sub>46</sub>H<sub>54</sub>N<sub>2</sub>O<sup>2+</sup>) calc.: 325.21126, found: 325.21128. Elem. Anal. calc. for C<sub>48</sub>H<sub>54</sub>F<sub>6</sub>N<sub>2</sub>O<sub>7</sub>S<sub>2</sub>: C, 60.75; H, 5.74; N, 2.95; S, 6.76. Found: C, 60.64; H, 5.71; N, 2.80; S, 6.77. For UV/Vis molar absorption coefficient ( $\epsilon$ ) and corresponding absorption wavelength ( $\lambda_{\max}$ ), see Table S7 (Section S5, p. S99).

**(E)-13-(2-(Anthracen-9-yl)vinyl)-6,7-dimethyl-4,5,8,9-tetrahydroisoquinolino[1,2-a]pyrido[1,2-k][2,9]phenanthroline-3,10-dium trifluoromethanesulfonate, (*rac*)-6h**



*(rac)*-6 (50.0 mg, 0.074 mmol), 9-anthracenecarboxaldehyde (76 mg, 0.37 mmol, 5 equiv), pyrrolidine (0.031 mL, 0.37 mmol, 5 equiv) and MeOH (1.3 mL) were placed to small flask and stirred for 2 h at RT under argon while protected from ambient light using aluminium foil cover. Reaction progress was checked by TLC (mobile phase Stoddart's magic mixture, starting material *(rac)*-6  $R_f = 0.5$ , product *(rac)*-6h  $R_f = 0.6$ ). Crude product was transferred to 50 mL centrifuge tube and precipitated by addition of Et<sub>2</sub>O (45 mL). Suspension was centrifuged and supernatant was removed. Residue was dissolved in a minimum amount of MeOH (1 mL) and precipitated by Et<sub>2</sub>O (40 mL). This reprecipitation was repeated three more times to get pure product. Solids were collected in a glass vial using Et<sub>2</sub>O and the resulting suspension was centrifuged. The Et<sub>2</sub>O was removed and the solid was dried under vacuum to get pure *(rac)*-6h as an orange solid in 83% yield (53.0 mg, 0.061 mmol).

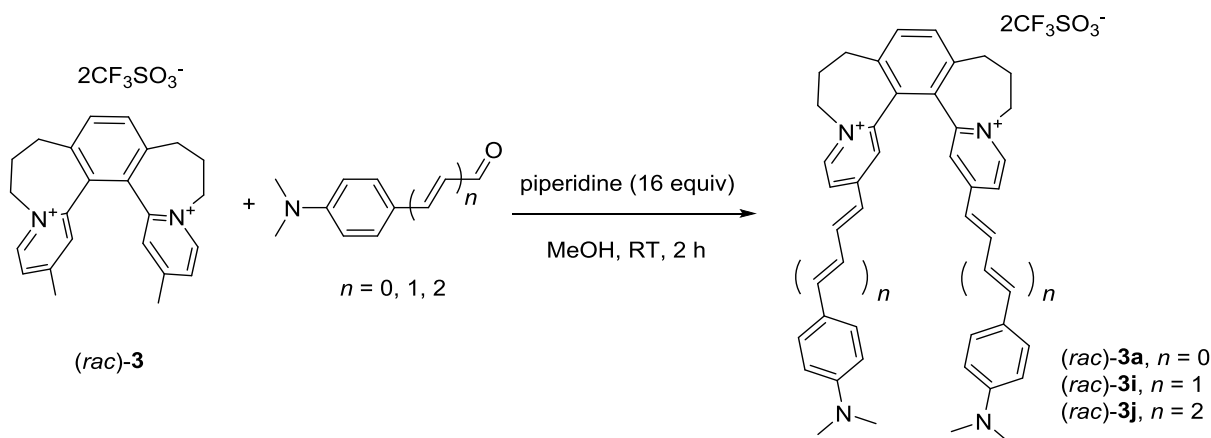




137.79; 138.74; 139.08; 139.88; 141.38; 142.52; 142.55; 146.40; 148.07; 151.81; 152.73. IR (KBr):  $\tilde{\nu}$  (cm<sup>-1</sup>) 1625; 1610; 1571; 1552; 1508; 1432; 1408; 1379; 1357; 1273; 1259; 1223; 1153; 1030; 962; 890; 845; 820; 788; 754; 742; 637; 679; 573; 517. MS (ESI) m/z: 715.1 (41), 283.6 (52), 283.1 (100). HRMS (ESI) m/z: [(M-TfO<sup>-</sup>)<sup>+</sup>] (C<sub>43</sub>H<sub>34</sub>F<sub>3</sub>N<sub>2</sub>O<sub>3</sub>S<sup>+</sup>) calc.: 715.22367, found: 715.22281. For UV/Vis molar absorption coefficient ( $\epsilon$ ) and corresponding absorption wavelength ( $\lambda_{\max}$ ), see Table S7 (Section S5, p. S99). X-ray crystal of [(*rac*)-**6h**][I]<sub>2</sub>, see X-ray analysis (Section S7, p. S152).

**Part G: Synthesis of racemic dyes (*rac*)-3a, (*rac*)-3i, (*rac*)-3j and non-racemic dyes (+)-(*P*)-3a, (-)-(*P*)-3i, (-)-(*P*)-3j and (-)-(*M*)-3a, (+)-(*M*)-3i, (+)-(*M*)-3j**

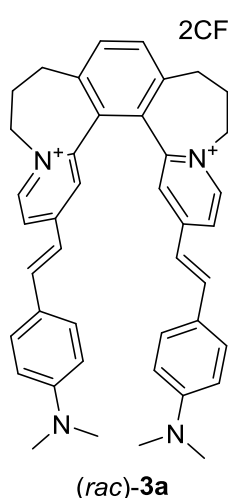
**1. General procedure for the synthesis of (*rac*)-3a, (*rac*)-3i, and (*rac*)-3j dyes:**



Starting helquat (*rac*)-3 (10 mg, 0.016 mmol) and the respective aldehyde (30 equiv) were placed in a 10 mL glass-vial equipped with a stirring bar and a teflon cap. Dry MeOH (0.5 mL) and piperidine (25  $\mu\text{L}$ , 0.25 mmol, 16 equiv) were added, and the resulting mixture was stirred 2 h at RT under argon while protected from ambient light using aluminium foil cover. A color change was observed immediately after the piperidine was added. Progress of the reaction was monitored by TLC (mobile phase Stoddart's magic mixture). After the indicated time, crude product was precipitated from the reaction mixture by addition of Et<sub>2</sub>O (8 mL). The suspension was sonicated, centrifuged, and the liquids were separated from the solid pellet. MeOH (0.5 mL) and Et<sub>2</sub>O (8 mL) were added to the solid pellet. The resulting suspension was sonicated, centrifuged, and the liquid was separated from the solid pellet. The purification process was repeated 4 to 6 more times until the absence of the starting aldehyde according to TLC. Et<sub>2</sub>O (8 mL) was added and the suspension was sonicated and then centrifuged. After separation of the liquids from the solid pellet, the sample was treated three more times with Et<sub>2</sub>O (8 mL). Removal of the liquid, and drying of the solid product at RT (5-10 min) and then under vacuum of an oil pump (3.0 mbar) led to pure Knoevenagel-König condensation products (*rac*)-3a, (*rac*)-3i, and (*rac*)-3j.

**(rac)-2,17-Bis((E)-4-(dimethylamino)styryl)-6,7,8,11,12,13-hexahydrodipyrido[1,2-a:1',2'-a']benzo[2,1-c:3,4-c']bisazepindium trifluoromethansulfonate, (rac)-3a**

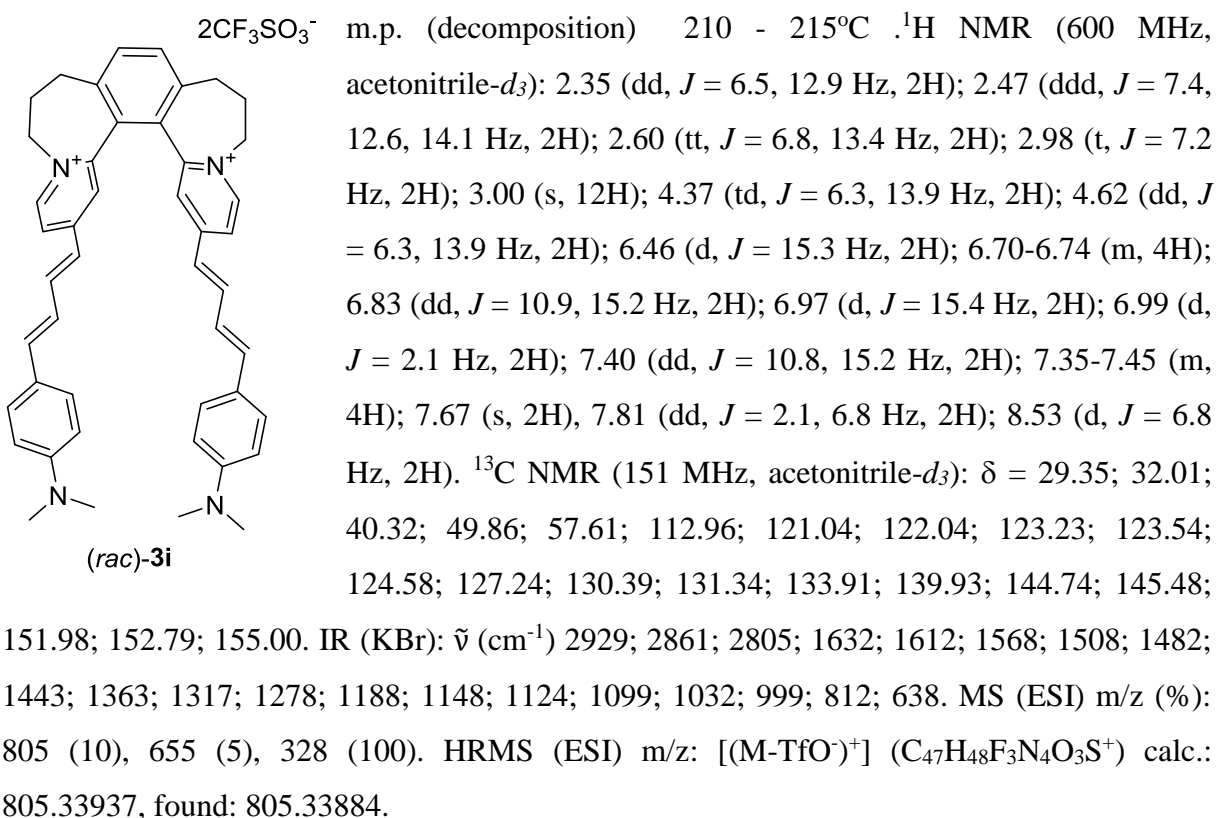
Compound (rac)-3a was isolated as a red-violet solid (13 mg, 0.014 mmol, 94% yield) from (rac)-3 (10 mg, 0.016 mmol) and 4-(dimethylamino)benzaldehyde (0.070 g, 0.47 mmol, 30 equiv), following the procedure described above. Progress of the reaction was monitored by TLC (mobile phase Stoddart's magic mixture, starting material (rac)-3  $R_f = 0.39$ , product (rac)-3a  $R_f = 0.71$ ).



$2CF_3SO_3^-$  m.p. 310-313°C.  $^1H$  NMR (600 MHz, acetonitrile- $d_3$ ): 2.35 (tt,  $J = 6.5, 13.0$  Hz, 2H); 2.49 (ddd,  $J = 7.5, 13.5, 14.1$  Hz, 2H); 2.61 (tt,  $J = 6.8, 13.3$  Hz, 2H); 2.99 (dd,  $J = 6.7, 14.1$  Hz, 2H); 3.03 (s, 12H); 4.39 (td,  $J = 5.7, 13.4$  Hz, 2H); 4.62 (dd,  $J = 6.3, 13.9$  Hz, 2H); 6.74 (d,  $J = 8.9$  Hz, 4H); 6.84 (d,  $J = 16.0$  Hz, 2H); 7.00 (d,  $J = 2.0$  Hz, 2H); 7.47 (d,  $J = 8.9$  Hz, 4H); 7.51 (d,  $J = 16.0$  Hz, 2H); 7.68 (s, 2H); 7.84 (dd,  $J = 2.1, 6.4$  Hz, 2H); 8.51 (d, 6.8 Hz, 2H).  $^{13}C$  NMR (151 MHz, acetonitrile- $d_3$ ):  $\delta = 29.35; 31.93; 40.25; 57.40; 112.92; 117.13; 121.42; 123.21; 127.14; 131.42; 131.46; 133.83; 139.88; 144.19; 145.26; 151.96; 153.66; 155.48$ . IR (KBr):  $\tilde{\nu}$  ( $cm^{-1}$ ) 3082; 2909; 2866; 2809; 1633; 1571; 1546; 1546; 1529; 1508; 1484; 1440; 1423; 1374; 1332; 1272; 1259; 1223; 1189; 1170; 1156; 1099; 1029; 638. MS (ESI)  $m/z$  (%): 753 (35), 302 (100). HRMS (ESI)  $m/z$ : [(M-TfO $^-$ )] $^+$  ( $C_{43}H_{44}F_3N_4O_3S^+$ ) calc.: 753.30807, found: 753.30858. Elem. Anal. calc. for  $C_{44}H_{44}F_6N_4O_6S_2$ : C, 58.53; H, 4.91; N, 6.20; S, 7.10. Found: C, 58.86; H, 4.84; N, 5.98; S, 7.08. X-ray crystal of [(rac)-3a][TfO] $_2$ , see X-ray analysis (Section S7, p. S153).

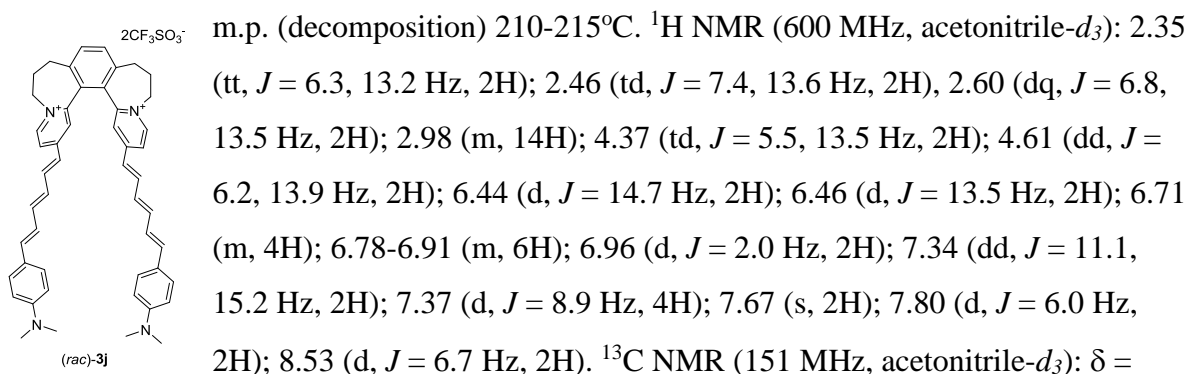
**(rac)-2,17-Bis((1E,3E)-4-((dimethylamino)phenyl)buta-1,3-dien1-yl)-6,7,8,11,12,13-hexahydrodipyrido[1,2-a:1',2'-a']benzo[2,1-c:3,4-c']bisazepindium trifluoromethansulfonate, (rac)-3i**

Compound (rac)-3i was isolated as a purple solid (9 mg, 0.009 mmol, 60% yield) from (rac)-3 (10 mg, 0.016 mmol) and 4-(dimethylamino)cinnamaldehyde (0.082 g, 0.47 mmol, 30 equiv), following the procedure described above. Progress of the reaction was monitored by TLC (mobile phase Stoddart's magic mixture, starting material (rac)-3  $R_f = 0.39$ , product (rac)-3i  $R_f = 0.75$ ).



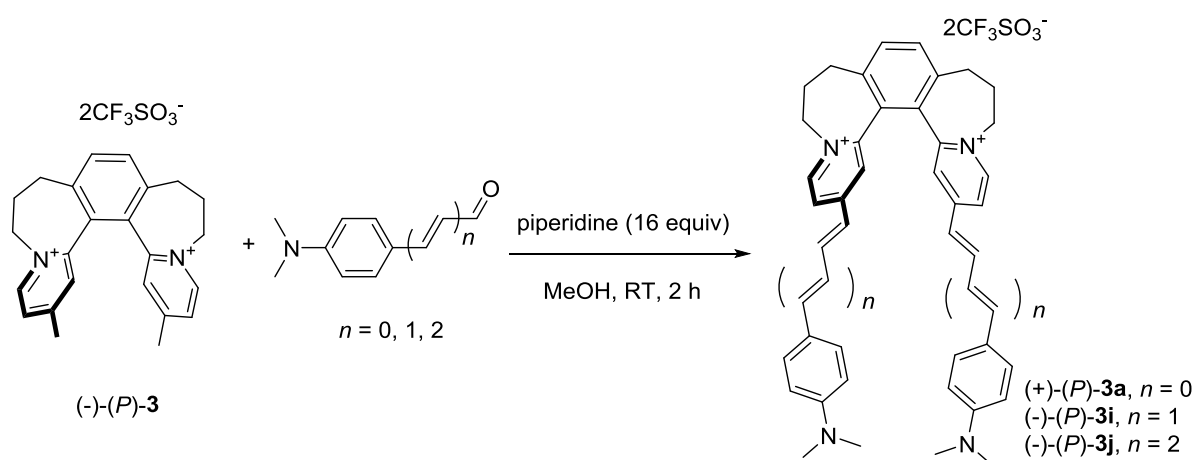
**(rac)-2,17-Bis((1E,3E,5E)-6-(4-(dimethylamino)phenyl)hexa-1,3,5-trien-1-yl)-6,7,8,11,12,13-hexahydrodipyrido[1,2-a:1',2'-a']benzo[2,1-c:3,4-c']bisazepindium trifluoromethanesulfonate, (rac)-3j**

Compound (rac)-**3j** was isolated as a violet solid (5 mg, 0.005 mmol, 31% yield) from (rac)-**3** (10 mg, 0.016 mmol) and (2E,4E)-5-(4-(dimethylamino)phenyl)penta-2,4-dienal <sup>3</sup> (0.070 g, 0.47 mmol, 30 equiv), following the procedure described above. Progress of the reaction was monitored by TLC (mobile phase Stoddart's magic mixture, starting material  $R_f = 0.39$ , product  $R_f = 0.77$ ).



29.33; 32.04; 40.37; 57.71; 113.09; 122.26; 124.35; 124.59; 125.32; 127.46; 129.60; 129.77; 131.29; 133.98; 139.96; 140.67; 144.56; 145.60; 152.06; 152.26; 154.79. IR (KBr):  $\tilde{\nu}$  (cm<sup>-1</sup>) 3074; 3022; 2925; 2857; 2802; 1630; 1617; 1559; 1544; 1522; 1443; 1362; 1258; 1224; 1187; 1145; 1123; 1099; 1079; 1061; 1030; 1001; 945; 819; 637. MS (ESI) m/z (%): 857 (5), 763 (10), 354 (100). HRMS (ESI) m/z: [(M-2TfO)<sup>2+</sup>] (C<sub>50</sub>H<sub>52</sub>N<sub>4</sub><sup>2+</sup>) calc.: 354.20905, found: 354.20917. Elem. Anal. calc. for C<sub>52</sub>H<sub>52</sub>F<sub>6</sub>N<sub>4</sub>O<sub>6</sub>S<sub>2</sub>: C, 62.02; H, 5.20; N, 5.56. Found: C, 62.08; H, 5.28; N, 5.22.

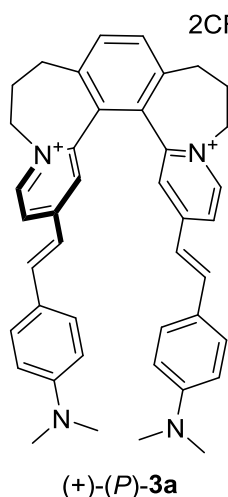
## 2. General procedure for the synthesis of (+)-(*P*)-3a, (-)-(*P*)-3i, and (-)-(*P*)-3j dyes:



Starting enantiopure helquat (-)-(*P*)-3 (10 mg, 0.016 mmol) and the respective aldehyde (30 equiv) were placed in a 10 mL glass-vial equipped with a stirring bar and a teflon cap. Dry MeOH (0.5 mL) and piperidine (25  $\mu$ L, 0.25 mmol, 16 equiv) were added, and the resulting mixture was stirred 2 h at RT under argon while protected from ambient light using aluminium foil cover. A color change was observed immediately after the piperidine was added. Progress of the reaction was monitored by TLC (mobile phase Stoddart's magic mixture). After the indicated time, crude product was precipitated from the reaction mixture by addition of Et<sub>2</sub>O (8 mL). The suspension was sonicated, centrifuged, and the liquids were separated from the solid pellet. MeOH (0.5 mL) and Et<sub>2</sub>O (8 mL) were added to the solid pellet. The resulting suspension was sonicated, centrifuged, and the liquids were separated from the solid pellet. The purification process was repeated 4 to 6 more times until the absence of starting aldehyde according to TLC. Et<sub>2</sub>O (8 mL) was added and the suspension was sonicated and then centrifuged. After separation of the liquids from the solid pellet, the sample was treated three more times with Et<sub>2</sub>O (8 mL). Removal of the liquid, and drying of

the solid product at RT (5-10 min) and then under vacuum of an oil pump (3.0 mbar) led to pure Knoevenagel-König condensation products (+)-(*P*)-**3a**, (-)-(*P*)-**3i**, and (-)-(*P*)-**3j**.

**(+)-(*P*)-2,17-Bis((*E*)-4-(dimethylamino)styryl)-6,7,8,11,12,13-hexahydrodipyrido[1,2-*a*:1',2'-*a'*]benzo[2,1-*c*:3,4-*c'*]bisazepindium trifluoromethansulfonate, (+)-(*P*)-**3a****

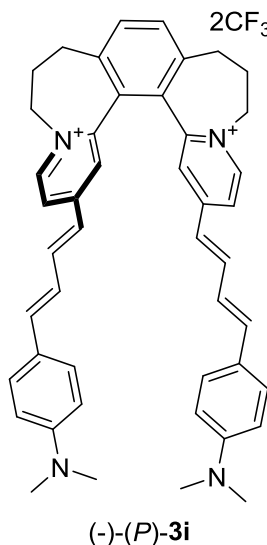


2CF<sub>3</sub>SO<sub>3</sub><sup>-</sup>

Compound (+)-(*P*)-**3a** was isolated as a red-violet solid (13 mg, 0.014 mmol, 94% yield,  $[\alpha]_D^{20} = +24788$  (c 3x10<sup>-4</sup>, MeOH), 95% *ee*) from (-)-(*P*)-**3** (10 mg, 0.016 mmol, 97% *ee*) and 4-(dimethylamino)benzaldehyde (0.070 g, 0.47 mmol, 30 equiv), following the procedure described above. Progress of the reaction was monitored by TLC (mobile phase Stoddart's magic mixture, starting material (-)-(*P*)-**3** *R<sub>f</sub>* = 0.39, product (+)-(*P*)-**3a** *R<sub>f</sub>* = 0.71). Chemical structure of the product was verified by <sup>1</sup>H NMR (400 MHz, acetonitrile-*d*<sub>3</sub>) and compared with (*rac*)-**3a** (See <sup>1</sup>H and <sup>13</sup>C NMR spectra Section S9, p. S184). The enantiopurity of (+)-(*P*)-**3a**

was determined by capillary electrophoresis (Section S4, Figure S2, p. S78). For ECD and UV/Vis spectra, see Figure S21 (Section S5, p. S103).

**(-)-(*P*)-2,17-Bis((1*E*,3*E*)-4-((dimethylamino)phenyl)buta-1,3-dien1-yl)-6,7,8,11,12,13-hexahydrodipyrido[1,2-*a*:1',2'-*a'*]benzo[2,1-*c*:3,4-*c'*]bisazepindium trifluoromethansulfonate, (-)-(*P*)-**3i****

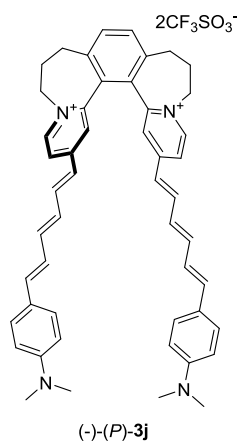


2CF<sub>3</sub>SO<sub>3</sub><sup>-</sup>

Compound (-)-(*P*)-**3i** was isolated as a purple solid (9 mg, 0.009 mmol, 60% yield,  $[\alpha]_D^{20} = -10533$  (c 3x10<sup>-4</sup>, MeOH), 99% *ee*) from (-)-(*P*)-**3** (10 mg, 0.016 mmol, 97% *ee*) and 4-(Dimethylamino)cinnamaldehyde (0.082 g, 0.47 mmol, 30 equiv), following the procedure described above. Progress of the reaction was monitored by TLC (mobile phase Stoddart's magic mixture, starting material (-)-(*P*)-**3** *R<sub>f</sub>* = 0.39, product (-)-(*P*)-**3i** *R<sub>f</sub>* = 0.75). Chemical structure of the product was verified by <sup>1</sup>H NMR (400 MHz, ) and compared with (*rac*)-**3i** (See <sup>1</sup>H and <sup>13</sup>C NMR spectra Section S9, p. S186). The enantiopurity of (-)-(*P*)-**3i** was

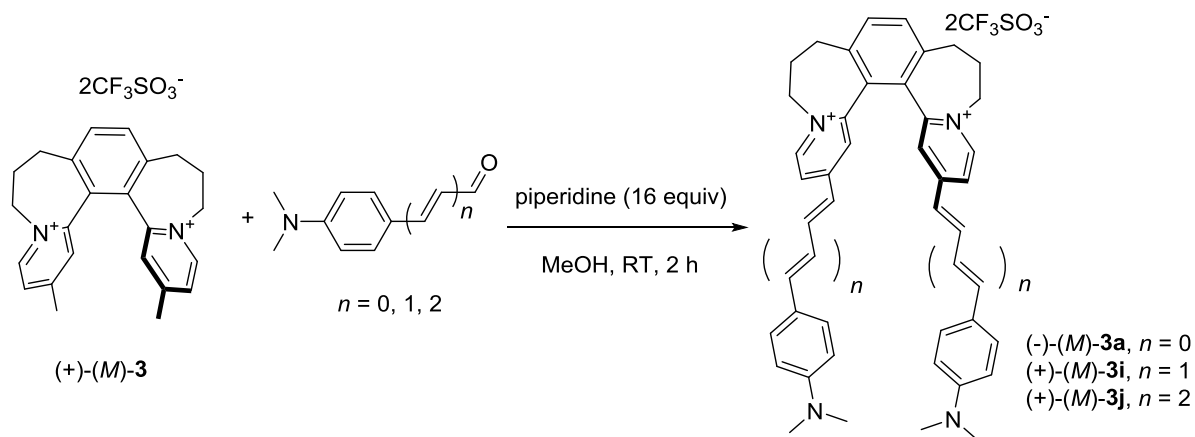
determined by capillary electrophoresis (Section S4, Figure S3, S79). For ECD and UV/Vis spectra, see Figure S22 (Section S5, p. S104).

**(-)-(P)-2,17-Bis((1E,3E,5E)-6-(4-(dimethylamino)phenyl)hexa-1,3,5-trien-1-yl)-6,7,8,11,12,13-hexahydrodipyrido[1,2-a:1',2'-a']benzo[2,1-c:3,4-c']bisazepindium trifluoromethansulfonate, (-)-(P)-3j**



Compound (-)-(P)-**3j** was isolated as a violet solid (10 mg, 0.010 mmol, 62% yield,  $[\alpha]_D^{20} = -17067$  (c  $3 \times 10^{-4}$ , MeOH), 94% *ee*) from (-)-(P)-**3** (10 mg, 0.016 mmol, 97% *ee*) and (2E,4E)-5-(4-(dimethylamino)phenyl)penta-2,4-dienal <sup>3</sup> (0.070 g, 0.47 mmol, 30 equiv), following the procedure described above. Progress of the reaction was monitored by TLC (mobile phase Stoddart magic mixture, starting material (-)-(P)-**3**  $R_f = 0.39$ , product (-)-(P)-**3j**  $R_f = 0.77$ ). Chemical structure of the product was verified by <sup>1</sup>H NMR (400 MHz, acetonitrile-*d*<sub>3</sub>) and compared with (*rac*)-**3j** (See <sup>1</sup>H and <sup>13</sup>C NMR spectra Section S9, p. S188). The enantiopurity of (-)-(P)-**3j** was determined by capillary electrophoresis (Section S4, Figure S4, p. S79). For ECD and UV/Vis spectra, see Figure S23 (Section S5, p. S105).

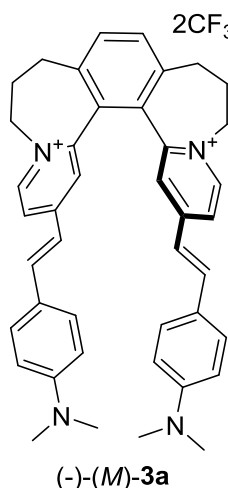
**3. General procedure for the synthesis of (-)-(M)-3a, (+)-(M)-3i, and (+)-(M)-3j dyes:**



Starting enantiopure helquat (+)-(M)-**3** (10 mg, 0.016 mmol) and the respective aldehyde (30 equiv) were placed in a 10 mL glass-vial equipped with a stirring bar and a teflon cap. Dry MeOH (0.5 mL) and piperidine (25  $\mu\text{L}$ , 0.25 mmol, 16 equiv) were added, and the resulting mixture was stirred 2 h at RT under argon while protected from ambient light using aluminium foil cover. A color change was observed immediately after the piperidine was added. Progress of the reaction was monitored by TLC (mobile phase Stoddart's magic mixture). After the indicated time, crude product was precipitated from the reaction mixture by addition of Et<sub>2</sub>O (8 mL). The suspension was sonicated, centrifuged, and the liquids were separated from the solid pellet. MeOH (0.5 mL) and Et<sub>2</sub>O (8 mL) were added to the solid

pellet. The resulting suspension was sonicated, centrifuged, and the liquids were separated from the solid pellet. The purification process was repeated 4 to 6 more times until the absence of starting aldehyde according to TLC. Et<sub>2</sub>O (8 mL) was added and the suspension was sonicated and then centrifuged. After separation of the liquids from the solid pellet, the sample was treated three more times with Et<sub>2</sub>O (8 mL). Removal of the liquids, and drying of the solid product at RT (5-10 min) and then under vacuum of an oil pump (3.0 mbar) led to pure Knoevenagel-König condensation products (-)-(M)-**3a**, (+)-(M)-**3i**, and (+)-(M)-**3j**.

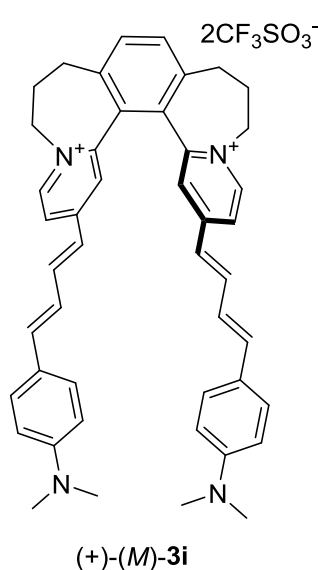
**(-)-(M)-2,17-Bis((E)-4-(dimethylamino)styryl)-6,7,8,11,12,13-hexahydrodipyrido[1,2-a:1',2'-a']benzo[2,1-c:3,4-c']bisazepindium trifluoromethanesulfonate, (-)-(M)-**3a****



$2\text{CF}_3\text{SO}_3^-$  Compound (-)-(M)-**3a** was isolated as a red-violet solid (12 mg, 0.013 mmol, 86% yield,  $[\alpha]_D^{20} = -23563$  (c  $3 \times 10^{-4}$ , MeOH), 92% *ee*) from (+)-(M)-**3** (10 mg, 0.016 mmol, 96% *ee*) and 4-(dimethylamino)benzaldehyde (0.070 g, 0.47 mmol, 30 equiv), following the procedure described above. Progress of the reaction was monitored by TLC (mobile phase Stoddart's magic mixture, starting material (+)-(M)-**3**  $R_f = 0.39$ , product (-)-(M)-**3a**  $R_f = 0.71$ ). Chemical structure of the product was verified by <sup>1</sup>H NMR (400 MHz, acetonitrile-*d*<sub>3</sub>) and compared with (*rac*)-**3a** (See <sup>1</sup>H and <sup>13</sup>C NMR spectra Section S9, p. S184). The enantiopurity of (-)-(M)-**3a** was determined by capillary electrophoresis (Section S4, Figure S2, S78). For racemization barrier determination of (-)-(M)-**3a**, see CE Section S4 (Figure S15, p. S93). For ECD and UV/Vis spectra, see Figure S21 (Section S5, p. S103). X-ray crystal of [(M)-**3a**][ClO<sub>4</sub>]<sub>2</sub>, see X-ray analysis (Section S7, p. S155).



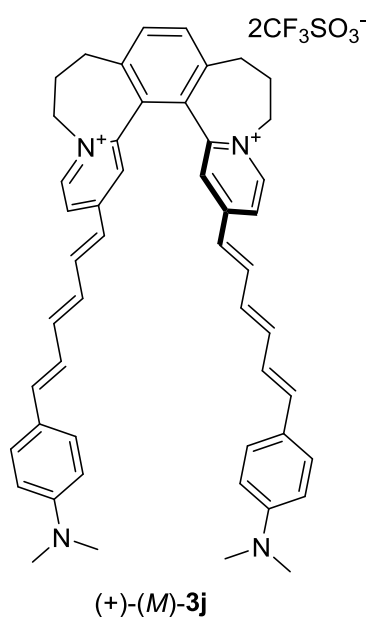
**(+)-(M)-2,17-Bis((1E,3E)-4-((dimethylamino)phenyl)buta-1,3-dien1-yl)-6,7,8,11,12,13-hexahydrodipyrido[1,2-a:1',2'-a']benzo[2,1-c:3,4-c']bisazepindium trifluoromethansulfonate, (+)-(M)-3i**



Compound (+)-(M)-**3i** was isolated as a purple solid (5 mg, 0.005 mmol, 33% yield,  $[\alpha]_D^{20} = +9640$  (c  $3 \times 10^{-4}$ , MeOH), 97% *ee*) from (+)-(M)-**3** (10 mg, 0.016 mmol, 96% *ee*) and 4-(dimethylamino)cinnamaldehyde (0.082 g, 0.47 mmol, 30 equiv), following the procedure described above. Progress of the reaction was monitored by TLC (mobile phase Stoddart's magic mixture, starting material (+)-(M)-**3**  $R_f = 0.39$ , product (+)-(M)-**3i**  $R_f = 0.75$ ). Chemical structure of the product was verified by <sup>1</sup>H NMR (400 MHz, acetonitrile-*d*<sub>3</sub>) and compared with (*rac*)-**3i** (See <sup>1</sup>H and <sup>13</sup>C NMR spectra Section S9, p. S186). The enantiopurity of (+)-(M)-**3i** was determined by capillary electrophoresis (Section S4,

Figure S3, p. S79). For ECD and UV/Vis spectra, see Figure S22 (Section S5, p. S104).

**(+)-(M)-2,17-Bis((1E,3E,5E)-6-(4-(dimethylamino)phenyl)hexa-1,3,5-trien-1-yl)-6,7,8,11,12,13-hexahydrodipyrido[1,2-a:1',2'-a']benzo[2,1-c:3,4-c']bisazepindium trifluoromethansulfonate, (+)-(M)-3j**

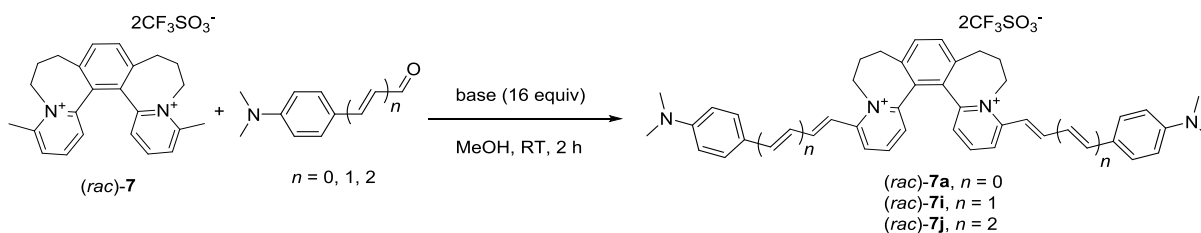


Compound (+)-(M)-**3j** was isolated as a violet solid (9 mg, 0.009 mmol, 57% yield,  $[\alpha]_D^{20} = +21250$  (c  $3 \times 10^{-4}$ , MeOH), 98% *ee*) from (+)-(M)-**3** (10 mg, 0.016 mmol, 96% *ee*) and (2E,4E)-5-(4-(dimethylamino)phenyl)penta-2,4-dienal <sup>3</sup> (0.070 g, 0.47 mmol, 30 equiv), following the procedure described above. Progress of the reaction was monitored by TLC (mobile phase Stoddart's magic mixture, starting material (+)-(M)-**3**  $R_f = 0.39$ , product (+)-(M)-**3j**  $R_f = 0.77$ ). Chemical structure of the product was verified by <sup>1</sup>H NMR (400 MHz, acetonitrile-*d*<sub>3</sub>) and compared with (*rac*)-**3j** (See <sup>1</sup>H and <sup>13</sup>C NMR spectra Section S9, p. S188). The enantiopurity of (+)-(M)-**3j** was determined by capillary electrophoresis (Section S4, Figure S4,

p. S79). For ECD and UV/Vis spectra, see Figure S23 (Section S5, p. S105).

## Part H: Synthesis of racemic dyes (*rac*)-7a, (*rac*)-7i, (*rac*)-7j and non-racemic dyes (-)-(*P*)-7a, (-)-(*P*)-7i, (-)-(*P*)-7j and (+)-(*M*)-7a, (+)-(*M*)-7i, (+)-(*M*)-7j

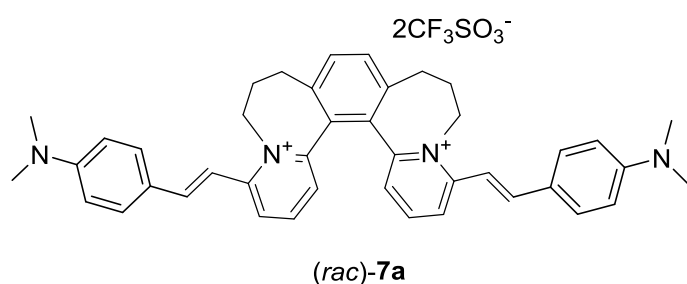
### 1. General procedure for the synthesis of (*rac*)-7a, (*rac*)-7i, and (*rac*)-7j dyes:



Starting helquat (*rac*)-7 (10 mg, 0.016 mmol) and the respective aldehyde (30 equiv) were placed in a 10 mL glass-vial equipped with a stirring bar and a teflon cap. Dry MeOH (0.5 mL) and the respective amine base (16 equiv) were added, and the resulting mixture was stirred 2 h at RT under argon while protected from ambient light using aluminium foil cover. A color change was observed immediately after the piperidine was added. Progress of the reaction was monitored by TLC (mobile phase “Stoddart’s magic mixture”). After the indicated time, crude product was precipitated from the reaction mixture by addition of Et<sub>2</sub>O (8 mL). The suspension was sonicated, centrifuged, and the liquids were separated from the solid pellet. MeOH (0.5 mL) and Et<sub>2</sub>O (8 mL) were added to the solid pellet. The resulting suspension was sonicated, centrifuged, and the liquid was separated from the solid pellet. The purification process was repeated 4 to 6 more times until the absence of starting aldehyde according to TLC. Et<sub>2</sub>O (8 mL) was added and the suspension was sonicated and then centrifuged. After separation of the liquids from the solid pellet, the sample was treated three more times with Et<sub>2</sub>O (8 mL). Removal of the liquids, and drying of the solid product at RT (5-10 min) and then under vacuum of an oil pump (3 mbar) led to pure Knoevenagel-König condensation products (*rac*)-7a, (*rac*)-7i, and (*rac*)-7j.

**(rac)-4,15-Bis((E)-4-(dimethylamino)styryl)-6,7,8,11,12,13-hexahydrodipyrido[1,2-a:1',2'-a']benzo[2,1-c:3,4-c']bisazepindium trifluoromethansulfonate, (rac)-7a**

Compound (rac)-7a was isolated as a brown-red solid (11 mg, 0.012 mmol, 78% yield) from (rac)-7 (10 mg, 0.016 mmol) and 4-(dimethylamino)benzaldehyde (0.070 g, 0.47 mmol, 30 equiv). Pyrrolidine was used as a base (0.21  $\mu$ L, 0.25 mmol, 16 equiv), and the procedure was as it is described above. Progress of the reaction was monitored by TLC (mobile phase Stoddart's magic mixture, starting material (rac)-7  $R_f$  = 0.31, product (rac)-7a  $R_f$  = 0.82).



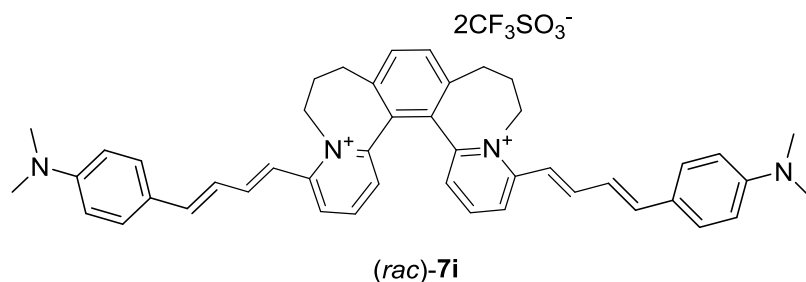
m.p. 320-322°C.  $^1\text{H}$  NMR (600 MHz, acetonitrile- $d_3$ ): 2.35 (ddt,  $J$  = 6.5, 7.3, 13.2 Hz, 2H); 2.4 (ddd,  $J$  = 7.2, 13.6 Hz, 2H); 2.73 (tt,  $J$  = 6.2, 13.0 Hz, 2H); 3.03 (dd,  $J$  = 6.3, 14.0 Hz, 2H); 3.08 (s, 12H); 4.29 (ddd,  $J$  = 5.1, 14.1,

14.2 Hz, 2H); 5.01 (dd,  $J$  = 5.7, 14.6 Hz, 2H); 6.82 (d,  $J$  = 7.8 Hz, 4H); 6.96 (d,  $J$  = 7.6 Hz, 2H); 7.18 (d,  $J$  = 15.6 Hz, 2H); 7.67 (s, 2H); 7.72 (d,  $J$  = 7.7 Hz, 4H); 7.77 (d,  $J$  = 15.5 Hz, 2H); 7.92 (t,  $J$  = 8.0 Hz, 2H); 8.16 (d,  $J$  = 8.5 Hz, 2H).  $^{13}\text{C}$  NMR (151 MHz, acetonitrile- $d_3$ ):  $\delta$  = 29.40; 30.99; 40.33; 53.22; 111.23; 112.87; 123.10; 125.57; 128.47; 131.86; 132.38; 133.62; 139.79; 142.92; 146.93; 152.82; 153.87; 156.15. IR (KBr):  $\tilde{\nu}$  ( $\text{cm}^{-1}$ ) 3065; 2912; 2863; 2810; 1592; 1556; 1529; 1485; 1461; 1440; 1410; 1370; 1330; 1272; 1256; 1190; 1168; 1152; 1084; 1032; 946; 819; 638. MS (ESI)  $m/z$  (%): 753 (5), 302 (100). HRMS (ESI)  $m/z$ : [(M-TfO) $^{2+}$ ] ( $\text{C}_{42}\text{H}_{44}\text{N}_4^{2+}$ ) calc.: 302.17775, found: 302.17792. Elem. Anal. calc. for  $\text{C}_{44}\text{H}_{44}\text{F}_6\text{N}_4\text{O}_6\text{S}_2$ : C, 58.53; H, 4.91; N, 6.20; S, 7.10. Found: C, 58.49; H, 5.04; N, 5.82; S, 7.09. X-ray crystal of [(rac)-7a][TfO] $_2$ , see X-ray analysis (Section S7, p. S154).

**(rac)-4,15-Bis((1E,3E)-4-((dimethylamino)phenyl)buta-1,3-dien1-yl)-6,7,8,11,12,13-hexahydrodipyrido[1,2-a:1',2'-a']benzo[2,1-c:3,4-c']bisazepindium trifluoromethansulfonate, (rac)-7i**

Compound (rac)-7i was isolated as a purple solid (10 mg, 0.01 mmol, 67% yield) from (rac)-7 (10 mg, 0.016 mmol) and 4-(dimethylamino)cinnamaldehyde (0.082 g, 0.47 mmol, 30 equiv). Piperidine was used as a base (0.25  $\mu$ L, 0.25 mmol, 16 equiv), and the procedure was

as it is described above. Progress of the reaction was monitored by TLC (mobile phase Stoddart's magic mixture, starting material (*rac*)-**7**  $R_f = 0.31$ , product (*rac*)-**7i**  $R_f = 0.85$ ).

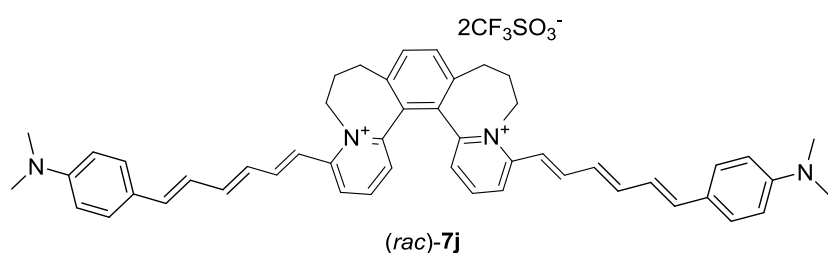


m.p. (decomposition) 210-213°C. <sup>1</sup>H NMR (600 MHz, acetonitrile-*d*<sub>3</sub>): 2.34 (tt, *J* = 6.2, 12.8 Hz, 2H); 2.44 (ddd, *J* = 7.4, 13.8, 14.0 Hz, 2H); 2.65 (tt, *J* = 6.8, 13.8 Hz,

2H); 3.00 (d, *J* = 6.8 Hz, 2H); 3.03 (s, 12H); 4.27 (td, *J* = 5.2, 14.1 Hz, 2H); 4.88 (dd, *J* = 5.8, 14.9 Hz, 2H), 6.77 (d, *J* = 8.3 Hz, 4H); 6.95 (d, *J* = 8.2 Hz, 2H), 6.97 (d, *J* = 15.2 Hz, 2H); 7.11-7.14 (m, 4H); 7.49 (d, *J* = 8.3 Hz, 4H); 7.65-7.69 (m, 4H); 7.91 (t, *J* = 8.5 Hz, 2H); 8.11 (d, *J* = 8.5 Hz, 2H). <sup>13</sup>C NMR (151 MHz, acetonitrile-*d*<sub>3</sub>): δ = 29.35; 30.85; 40.34; 53.29; 113.05; 117.36; 123.45; 124.45; 125.61; 128.86; 130.38; 132.30; 133.73; 139.83; 142.95; 144.95; 147.75; 152.90; 155.43. IR (KBr):  $\tilde{\nu}$  (cm<sup>-1</sup>) 3067; 3022; 2987; 2925; 2860; 2806; 1582; 1552; 1486; 1461; 1444; 1412; 1365; 1324; 1276; 1257; 1224; 1186; 1147; 1084; 1031; 1000; 944; 831; 638. MS (ESI) *m/z* (%): 805 (15), 328 (100). HRMS (ESI) *m/z* : [(M-2TfO<sup>-</sup>)<sup>+2</sup>] (C<sub>46</sub>H<sub>48</sub>N<sub>4</sub><sup>2+</sup>) calc.: 328.19340, found: 328.19363. Elem. Anal. calc. for C<sub>48</sub>H<sub>48</sub>F<sub>6</sub>N<sub>4</sub>O<sub>6</sub>S<sub>2</sub>: C, 60.37; H, 5.07; N, 5.87. Found: C, 59.93; H, 5.23; N, 5.77.

**(*rac*)-4,15-Bis((1*E*,3*E*,5*E*)-6-(4-(dimethylamino)phenyl)hexa-1,3,5-trien-1-yl)-6,7,8,11,12,13-hexahydrodipyrido[1,2-*a*:1',2'-*a'*]benzo[2,1-*c*:3,4-*c'*]bisazepindium trifluoromethansulfonate, (*rac*)-**7j****

Compound (*rac*)-**7j** was isolated as a dark-violet solid (12.0 mg, 0.012 mmol, 75% yield) from (*rac*)-**7** (10 mg, 0.016 mmol) and (2*E*,4*E*)-5-(4-(dimethylamino)phenyl)penta-2,4-dienal<sup>3</sup> (0.070 g, 0.47 mmol, 30 equiv). Piperidine was used as a base (0.25 μL, 0.25 mmol, 16 equiv), and the procedure was as it is described above. Progress of the reaction was monitored by TLC (mobile phase Stoddart's magic mixture, starting material (*rac*)-**7**  $R_f = 0.31$ , product

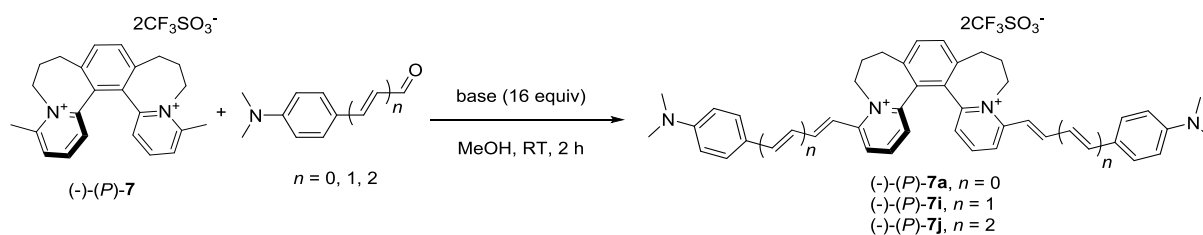


(*rac*)-**7j**  $R_f = 0.86$ ).

m.p. (decomposition) 217-219°C. <sup>1</sup>H NMR (600 MHz, acetonitrile-*d*<sub>3</sub>): 2.32 (dd, *J*

= 6.5, 12.8 Hz, 2H); 2.42 (ddd,  $J = 7.3, 13.4$  Hz, 2H); 2.63 (tt,  $J = 6.2, 13.6$  Hz, 2H); 2.97-3.02 (m, 2H); 2.99 (s, 12H); 4.26 (ddd,  $J = 5.1, 14.0, 14.4$  Hz, 2H); 4.87 (td,  $J = 5.7, 14.4$  Hz, 2H); 6.70-6.75 (m, 6H), 6.87 (d,  $J = 15.2$  Hz, 2H); 6.91 (d,  $J = 10.2$  Hz, 2H); 6.94-6.96 (m, 4H); 7.02 (dd,  $J = 10.2, 14.2$  Hz, 2H); 7.42 (d,  $J = 8.52$  Hz, 4H); 7.60 (dd,  $J = 11.3, 14.6$  Hz, 2H); 7.66 (s, 2H); 7.91 (t,  $J = 8.0$  Hz, 2H); 8.10 (d,  $J = 8.2$  Hz, 2H).  $^{13}\text{C}$  NMR (151 MHz, acetonitrile- $d_3$ ):  $\delta = 29.33; 30.94; 40.38; 53.35; 113.10; 121.07; 124.44; 125.30; 125.77; 129.14; 129.46; 129.67; 132.25; 133.77; 139.85; 140.97; 143.10; 145.96; 146.95; 152.30; 152.98; 155.26$ . IR (KBr):  $\tilde{\nu}$  ( $\text{cm}^{-1}$ ) 3077; 3021; 2925; 2804; 1614; 1584; 1548; 1523; 1485; 1460; 1445; 1363; 1329; 1275; 1253; 1224; 1207; 1188; 1144; 1085; 1031; 1003; 945; 813; 637. MS (ESI)  $m/z$  (%): 857 (5), 354 (100). HRMS (ESI)  $m/z$ :  $[(M-2\text{TfO}^-)^{2+}]$  ( $\text{C}_{50}\text{H}_{52}\text{N}_4^{2+}$ ) calc.: 354.20905, found: 354.20910. Elem. Anal. calc. for  $\text{C}_{52}\text{H}_{52}\text{F}_6\text{N}_4\text{O}_6\text{S}_2$ : C, 62.02; H, 5.20; N, 5.56. Found: C, 62.03; H, 5.30; N, 5.27.

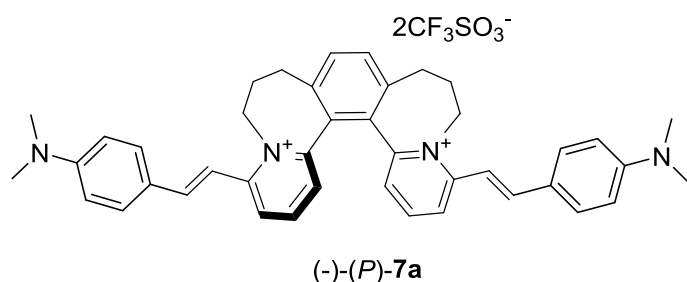
## 2. General procedure for the synthesis of (-)-(P)-7a, (-)-(P)-7i, and (-)-(P)-7j:



Starting enantiopure helquat (-)-(P)-7 (10 mg, 0.016 mmol) and the respective aldehyde (30 equiv) were placed in a 10 mL glass-vial equipped with a stirring bar and a teflon cap. Dry MeOH (0.5 mL) and the respective amine base (16 equiv) were added, and the resulting mixture was stirred 2 h at RT under argon while protected from ambient light using aluminium foil cover. A color change was observed immediately after the piperidine was added. Progress of the reaction was monitored by TLC (mobile phase Stoddart's magic mixture). After the indicated time, crude product was precipitated from the reaction mixture by addition of  $\text{Et}_2\text{O}$  (8 mL). The suspension was sonicated, centrifuged, and the liquids were separated from the solid pellet. MeOH (0.5 mL) and  $\text{Et}_2\text{O}$  (8 mL) were added to the solid pellet. The resulting suspension was sonicated, centrifuged, and the liquids were separated from the solid pellet. The purification process was repeated 4 to 6 more times until the absence of starting aldehyde according to TLC.  $\text{Et}_2\text{O}$  (8 mL) was added and the suspension

was sonicated and then centrifuged. After separation of the liquids from the solid pellet, the sample was treated three more times with Et<sub>2</sub>O (8 mL). Removal of the liquids, and drying of the solid product at RT (5-10 min) and then under vacuum of an oil pump (3 mbar) led to pure Knoevenagel-König condensation products (-)-(P)-7a, (-)-(P)-7i, and (-)-(P)-7j.

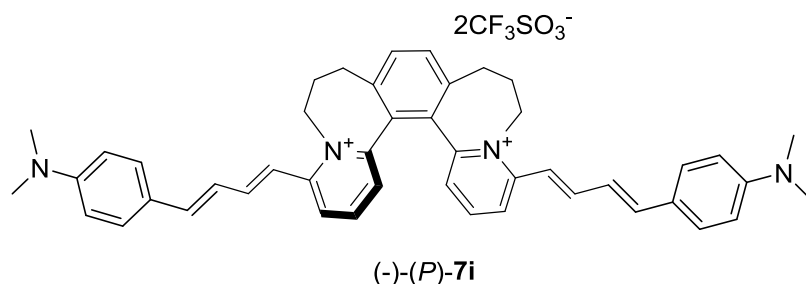
**(-)-(P)-4,15-Bis((E)-4-(dimethylamino)styryl)-6,7,8,11,12,13-hexahydrodipyrido[1,2-a:1',2'-a']benzo[2,1-c:3,4-c']bisazepindium trifluoromethanesulfonate, (-)-(P)-7a**



Compound (-)-(P)-7a was isolated as a red solid (5 mg, 0.005 mmol, 35% yield,  $[\alpha]_D^{20} = -11172$  (c  $3 \times 10^{-4}$ , MeOH), 96% *ee*) from (-)-(P)-7 (10 mg, 0.016 mmol, 99% *ee*) and 4-(dimethylamino)benzaldehyde (0.070

g, 0.47 mmol, 30 equiv). Pyrrolidine was used as a base (0.21  $\mu$ L, 0.25 mmol, 16 equiv), and the procedure was as it is described above. Progress of the reaction was monitored by TLC (mobile phase Stoddart's magic mixture, starting material (-)-(P)-7  $R_f = 0.31$ , product (-)-(P)-7a  $R_f = 0.82$ ). Chemical structure of the product was verified by <sup>1</sup>H NMR (400 MHz, acetonitrile-*d*<sub>3</sub>) and compared with (*rac*)-7a (See <sup>1</sup>H and <sup>13</sup>C NMR spectra Section S9, p. S190). The enantiopurity of (-)-(P)-7a was determined by capillary electrophoresis (Section S4, Figure S7, p. S81). For racemization barrier determination of (-)-(P)-7a, see CE Section S4 (Figure S17, p. S97). For ECD and UV/Vis spectra, see Figure S26 (Section S5, p. S110).

**(-)-(P)-4,15-Bis((1E,3E)-4-((dimethylamino)phenyl)buta-1,3-dien1-yl)-6,7,8,11,12,13-hexahydrodipyrido[1,2-a:1',2'-a']benzo[2,1-c:3,4-c']bisazepindium trifluoromethanesulfonate, (-)-(P)-7i**

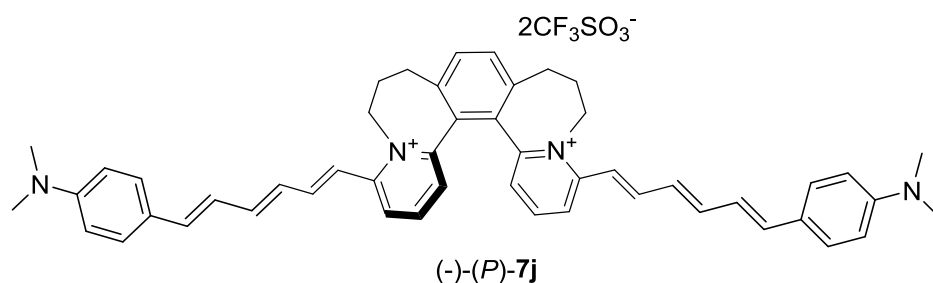


Compound (-)-(P)-7i was isolated as a purple solid (11 mg, 0.011 mmol, 73% yield,  $[\alpha]_D^{20} = -8255$  (c  $3 \times 10^{-4}$ , MeOH), 98% *ee*) from (-)-(P)-7 (10 mg, 0.016 mmol,

99% *ee*) and 4-(dimethylamino)cinnamaldehyde (0.082 g, 0.47 mmol, 30 equiv). Piperidine was used as a base (0.25  $\mu$ L, 0.25 mmol, 16 equiv), and the procedure was as it is described

above. Progress of the reaction was monitored by TLC (mobile phase Stoddart's magic mixture, starting material (-)-(P)-**7**  $R_f = 0.31$ , product (-)-(P)-**7i**  $R_f = 0.85$ ). Chemical structure of the product was verified by  $^1\text{H}$  NMR (400 MHz, acetonitrile- $d_3$ ) and compared with (*rac*)-**7i** (See  $^1\text{H}$  and  $^{13}\text{C}$  NMR spectra Section S9, p. S192). The enantiopurity of (-)-(P)-**7i** was determined by capillary electrophoresis (Section S4, Figure S8, p. S81). For ECD and UV/Vis spectra, see Figure S27 (Section S5, p. S111).

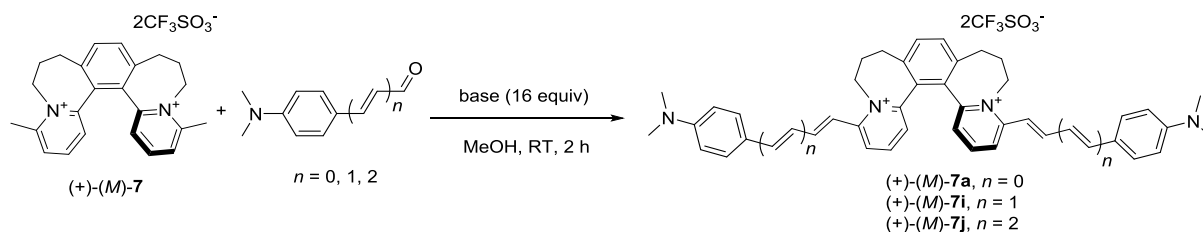
**(-)-(P)-4,15-bis((1E,3E,5E)-6-(4-(dimethylamino)phenyl)hexa-1,3,5-trien-1-yl)-6,7,8,11,12,13-hexahydrodipyrido[1,2-a:1',2'-a']benzo[2,1-c:3,4-c']bisazepindium trifluoromethanesulfonate, (-)-(P)-**7j****



Compound (-)-(P)-**7j** was isolated as a dark-violet solid (7 mg, 0.007 mmol, 44% yield,  $[\alpha]_D^{20} = -1160$  (c

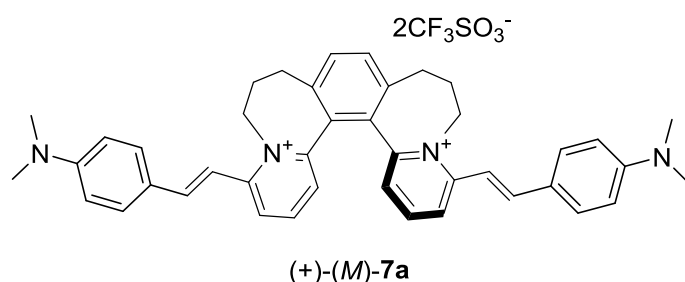
$3 \times 10^{-4}$ , MeOH), 99% *ee*) from (-)-(P)-**7** (10 mg, 0.016 mmol 99% *ee*) and (2E,4E)-5-(4-(dimethylamino)phenyl)penta-2,4-dienal <sup>3</sup> (0.070 g, 0.47 mmol, 30 equiv). Piperidine was used as a base (0.25  $\mu\text{L}$ , 0.25 mmol, 16 equiv), and the procedure was as it is described above. Progress of the reaction was monitored by TLC (mobile phase Stoddart's magic mixture, starting material (-)-(P)-**7**  $R_f = 0.31$ , product (-)-(P)-**7j**  $R_f = 0.86$ ). Chemical structure of the product was verified by  $^1\text{H}$  NMR (400 MHz, acetonitrile- $d_3$ ) and compared with (*rac*)-**7j** (See  $^1\text{H}$  and  $^{13}\text{C}$  NMR spectra Section S9, p. S194). The enantiopurity of (-)-(P)-**7j** was determined by capillary electrophoresis (Section S4, Figure S9, p. S82). For ECD and UV/Vis spectra, see Figure S28 (Section S5, p. S112).

### 3. General procedure for the synthesis of (+)-(*M*)-7a, (+)-(*M*)-7i, and (+)-(*M*)-7j dyes:



Starting enantiopure helquat (+)-(*M*)-7 (10 mg, 0.016 mmol) and the respective aldehyde (30 equiv) were placed in a 10 mL glass-vial equipped with a stirring bar and a teflon cap. Dry MeOH (0.5 mL) and the respective amine base (16 equiv) were added, and the resulting mixture was stirred 2 h at RT under argon while protected from ambient light using aluminium foil cover. A color change was observed immediately after the piperidine was added. Progress of the reaction was monitored by TLC (mobile phase Stoddart's magic mixture). After the indicated time, crude product was precipitated from the reaction mixture by addition of Et<sub>2</sub>O (8 mL). The suspension was sonicated, centrifuged, and the liquids were separated from the solid pellet. MeOH (0.5 mL) and Et<sub>2</sub>O (8 mL) were added to the solid pellet. The resulting suspension was sonicated, centrifuged, and the liquids were separated from the solid pellet. The purification process was repeated 4 to 6 more times until the absence of starting aldehyde according to TLC. Et<sub>2</sub>O (8 mL) was added and the suspension was sonicated and then centrifuged. After separation of the liquids from the solid pellet, the sample was treated three more times with Et<sub>2</sub>O (8 mL). Removal of the liquid, and drying of the solid product at RT (5-10 min) and then under vacuum of an oil pump (3 mbar) led to pure Knoevenagel-König condensation products (+)-(*M*)-7a, (+)-(*M*)-7i, and (+)-(*M*)-7j.

#### (+)-(*M*)-4,15-Bis((*E*)-4-(dimethylamino)styryl)-6,7,8,11,12,13-hexahydrodipyrido[1,2-*a*:1',2'-*a'*]benzo[2,1-*c*:3,4-*c'*]bisazepindium trifluoromethansulfonate, (+)-(*M*)-7a

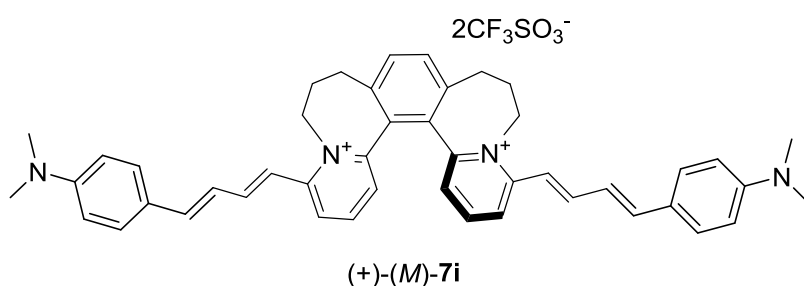


Compound (+)-(*M*)-7a was isolated as a red solid (6 mg, 0.007 mmol, 42% yield,  $[\alpha]_{\text{D}}^{20} = 11188$  (c  $3 \times 10^{-4}$ , MeOH), 98% *ee*) from (+)-(*M*)-7 (10 mg, 0.016 mmol, 98% *ee*) and 4-



(dimethylamino)benzaldehyde (0.070 g, 0.47 mmol, 30 equiv). Pyrrolidine was used as a base (0.21  $\mu\text{L}$ , 0.25 mmol, 16 equiv), and the procedure was as it is described above. Progress of the reaction was monitored by TLC (mobile phase Stoddart's magic mixture, starting material (+)-(*M*)-**7**  $R_f = 0.31$ , product (+)-(*M*)-**7a**  $R_f = 0.82$ ). Chemical structure of the product was verified by  $^1\text{H}$  NMR (400 MHz, acetonitrile- $d_3$ ) and compared with (*rac*)-**7a** (See  $^1\text{H}$  and  $^{13}\text{C}$  NMR spectra Section S9, p. S190). The enantiopurity of (+)-(*M*)-**7a** was determined by capillary electrophoresis (Section S4, Figure S7, p. S81). For ECD and UV/Vis spectra, see Figure S26 (Section S5, p. S110).

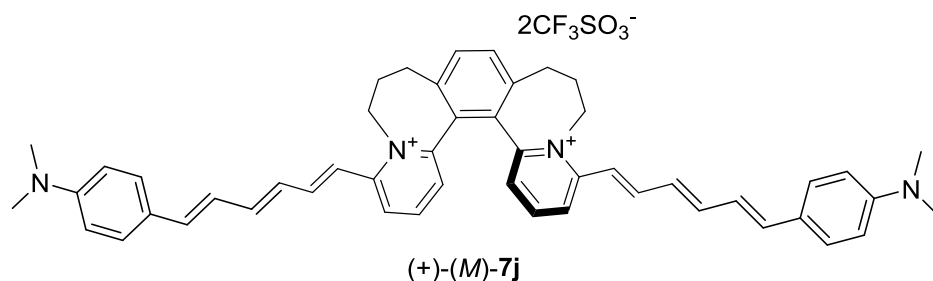
**(+)-(*M*)-4,15-Bis((1*E*,3*E*)-4-((dimethylamino)phenyl)buta-1,3-dien1-yl)-6,7,8,11,12,13-hexahydrodipyrido[1,2-*a*:1',2'-*a'*]benzo[2,1-*c*:3,4-*c'*]bisazepindium trifluoromethanesulfonate, (+)-(*M*)-**7i****



Compound (+)-(*M*)-**7i** was isolated as a dark solid (10 mg, 0.010 mmol, 67% yield,  $[\alpha]^{20}_{\text{D}} = +7975$  (c  $3 \times 10^{-4}$ , MeOH), 99% *ee*) from (+)-(*M*)-**7** (10 mg, 0.016 mmol,

98% *ee*) and 4-(dimethylamino)cinnamaldehyde (0.082 g, 0.47 mmol, 30 equiv). Piperidine was used as a base (0.25  $\mu\text{L}$ , 0.25 mmol, 16 equiv), and the procedure was as it is described above. Progress of the reaction was monitored by TLC (mobile phase Stoddart's magic mixture, starting material (+)-(*M*)-**7**  $R_f = 0.31$ , product (+)-(*M*)-**7i**  $R_f = 0.85$ ). Chemical structure of the product was verified by  $^1\text{H}$  NMR (400 MHz, acetonitrile- $d_3$ ) and compared with (*rac*)-**7i** (See  $^1\text{H}$  and  $^{13}\text{C}$  NMR spectra Section S9, p. S192). The enantiopurity of (+)-(*M*)-**7i** was determined by capillary electrophoresis (Section S4, Figure S8, p. S81). For ECD and UV/Vis spectra, see Figure S27 (Section S5, p. S111).

**(+)-(M)-4,15-bis((1E,3E,5E)-6-(4-(dimethylamino)phenyl)hexa-1,3,5-trien-1-yl)-6,7,8,11,12,13-hexahydrodipyrido[1,2-a:1',2'-a']benzo[2,1-c:3,4-c']bisazepindium trifluoromethanesulfonate, (+)-(M)-7j**



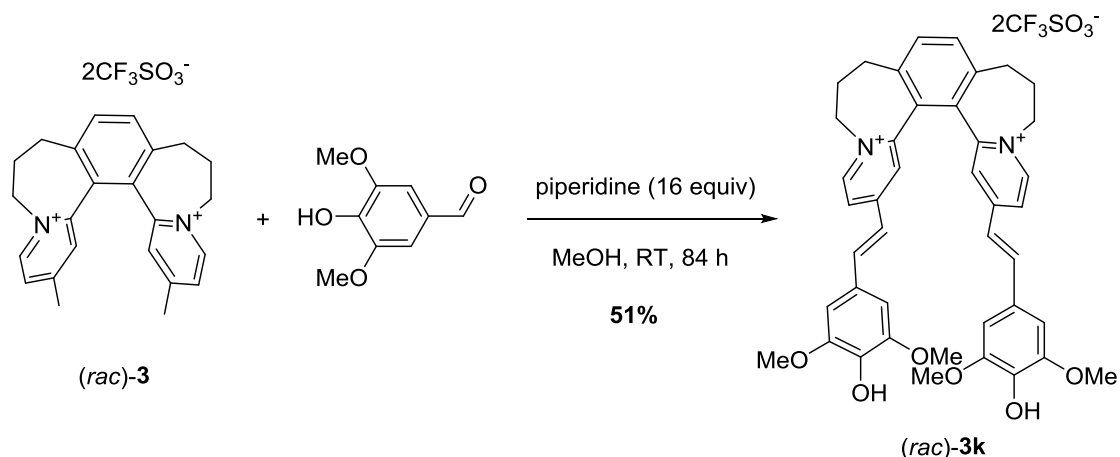
Compound (+)-(M)-7j was isolated as a dark solid (8 mg, 0.008 mmol, 50% yield,  $[\alpha]_D^{20} = +1560$  (c

$3 \times 10^{-4}$ , MeOH), 99% *ee*) from (+)-(M)-7 (10 mg, 0.016 mmol, 98% *ee*) and (2E,4E)-5-(4-(dimethylamino)phenyl)penta-2,4-dienal <sup>3</sup> (0.070 g, 0.47 mmol, 30 equiv). Piperidine was used as a base (0.25  $\mu$ L, 0.25 mmol, 16 equiv), and the procedure was as it is described above. Progress of the reaction was monitored by TLC (mobile phase Stoddart's magic mixture, starting material (+)-(M)-7  $R_f = 0.31$ , product (+)-(M)-7j  $R_f = 0.86$ ). Chemical structure of the product was verified by <sup>1</sup>H NMR (400 MHz, acetonitrile-*d*<sub>3</sub>) and compared with (*rac*)-7j (See <sup>1</sup>H and <sup>13</sup>C NMR spectra Section S9, p. S194). The enantiopurity of (+)-(M)-7j was determined by capillary electrophoresis (Section S4, Figure S9, p. S82). For ECD and UV/Vis spectra, see Figure S28 (Section S5, p. S112).

## Part I: Synthesis of racemic pH-switchable dye (*rac*)-3k and non-racemic dyes (+)-(*P*)-3k and (-)-(*M*)-3k.

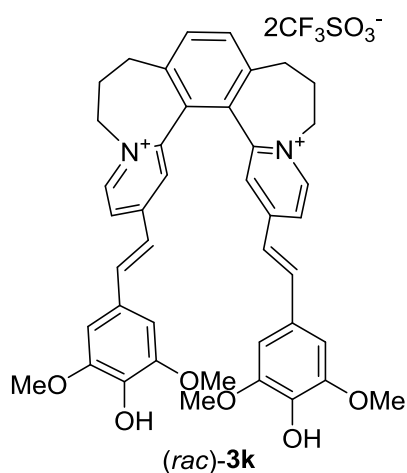
### 1. Procedure for the synthesis of (*rac*)-3k

(*rac*)-2,17-Bis((*E*)-4-hydroxy-3,5-dimethoxystyryl)-6,7,8,11,12,13-hexahydrodipyrido[1,2-*a*:1',2'-*a'*]benzo[2,1-*c*:3,4-*c'*]bisazepindium trifluoromethansulfonate, (*rac*)-3k



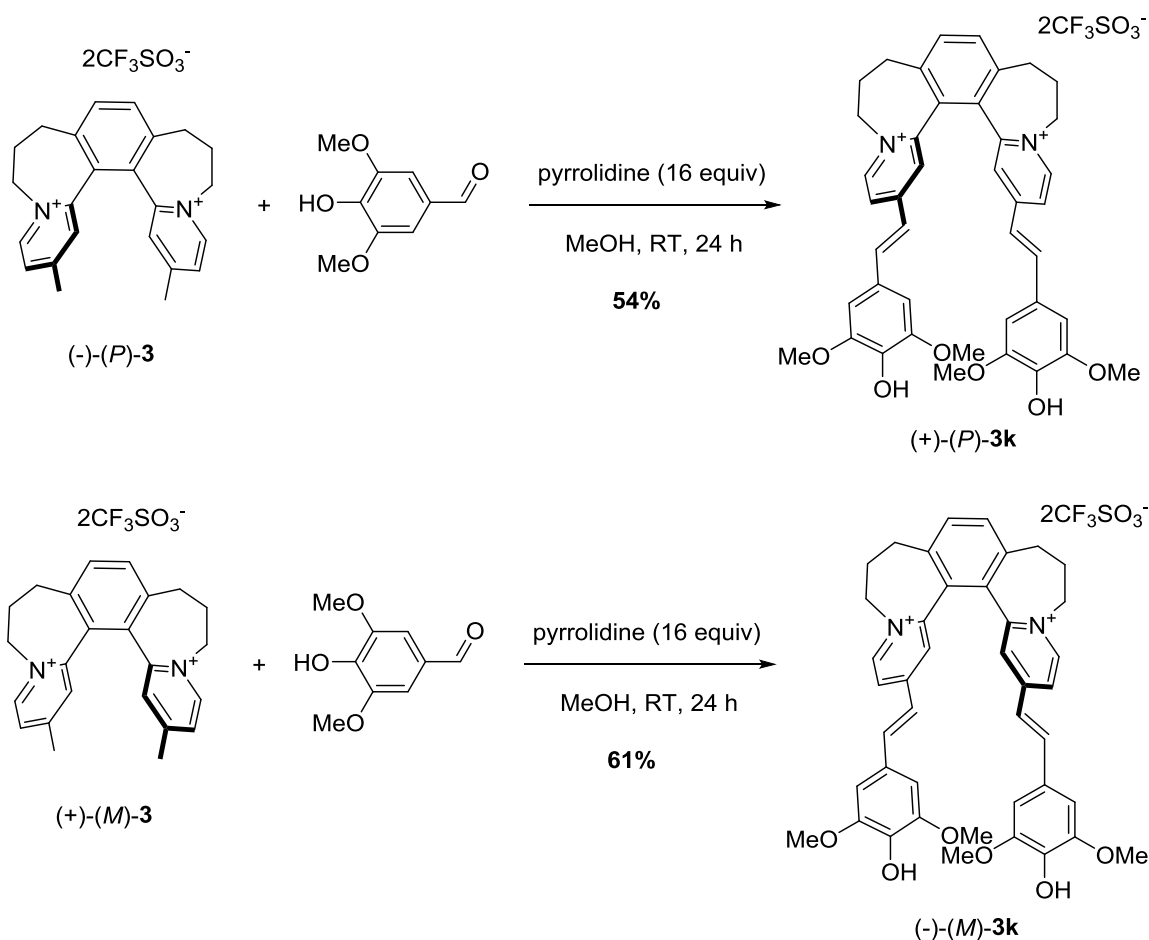
Starting helquat (*rac*)-3 (30 mg, 0.047 mmol) and 4-hydroxy-3,5-dimethoxybenzaldehyde (0.26 g, 1.4 mmol, 30 equiv) were placed in a 50 mL plastic-centrifuge tube (SARSTEDT, cat. num. 62.547.254) equipped with a stirring bar and a cap. Dry MeOH (1.5 mL) and piperidine (74  $\mu$ L, 0.75 mmol, 16 equiv) were added, and the resulting mixture was stirred 84 h at RT under argon while protected from ambient light using aluminium foil cover. A color change was observed immediately after the piperidine was added. After the indicated time, TLC (mobile phase Stoddart's magic mixture, starting material (*rac*)-3  $R_f = 0.39$ , product (*rac*)-3k  $R_f = 0.71$ ) showed total consumption of the starting material (*rac*)-3 and no presence of the monocondensated product ( $R_f = 0.4$ ). Crude product was precipitated from the reaction mixture by addition of Et<sub>2</sub>O (33 mL). The suspension was sonicated, centrifuged, and the liquids were separated from the solid pellet. MeOH (2 mL) and Et<sub>2</sub>O (33 mL) were added to the solid pellet. The resulting suspension was sonicated, centrifuged, and the liquids were separated from the solid pellet. The solids were dissolved in MeOH (10 mL approx.) and precipitated by addition of Et<sub>2</sub>O (25 mL). The suspension was sonicated, centrifuged, and the liquids were separated from the solid pellet. The addition of MeOH (10 mL) and Et<sub>2</sub>O (25 mL) was repeated two more times. After the suspension was centrifuged by the last time, Et<sub>2</sub>O (35 mL) was added to the solid pellet, sonicated and then centrifuged. After separation of the

liquids from the solid pellet, the sample was dried at RT (5-10 min) and then use of vacuum of an oil pump led (3 mbar) to a pure Knoevenagel-König condensation product (*rac*)-**3k** as an olive green solid (0.023 g, 0.024 mmol, 51% yield).



m.p. (decomposition) 322-324°C. <sup>1</sup>H NMR (600 MHz, 0.1 M TfOH / methanol-*d*<sub>4</sub> + 2 drops of DMSO-*d*<sub>6</sub>): 2.46 (dq, *J* = 6.1, 12.6 Hz, 2H); 2.55-2.59 (m, 2H); 2.73 (dq, *J* = 6.55, 6.7, 13.2 Hz, 2H); 3.09 (dd, *J* = 6.7, 14.3 Hz, 2H); 3.89 (s, 12H); 4.59 (td, *J* = 5.8, 13.5, 2H); 4.8 (dd, *J* = 6.5, 13.9 Hz, 2H); 6.96 (s, 4H); 7.07 (d, *J* = 16.0 Hz, 2H); 7.41 (d, *J* = 2.1 Hz, 2H); 7.67 (d, *J* = 16.0 Hz, 2H); 7.79 (s, 2H); 8.15 (dd, *J* = 2.1, 6.8 Hz, 2H); 8.9 (d, *J* = 6.7 Hz, 2H). <sup>13</sup>C NMR (151 MHz, 0.1 M TfOH / methanol-*d*<sub>4</sub> + 2 drops of DMSO-*d*<sub>6</sub>): δ = 29.76; 32.66; 56.98; 57.93; 107.57; 120.65; 122.76; 127.25; 128.12; 131.75; 134.42; 140.41; 140.80; 144.66; 146.14; 149.62; 152.79; 155.95. IR (KBr):  $\tilde{\nu}$  (cm<sup>-1</sup>) 2952; 1614; 1587; 1553; 1513; 1459; 1429; 1418; 1338; 1274; 1262; 1224; 1154; 1113; 1031; 988; 972; 912; 840; 638. MS (ESI) *m/z* (%): 819 (30), 669 (25), 335 (100). HRMS (ESI) *m/z*: [M<sup>+</sup>] (C<sub>42</sub>H<sub>42</sub>N<sub>2</sub>O<sub>6</sub><sup>2+</sup>) calc.: 335.15160, found: 335.15171. Elem. Anal. calc. for C<sub>44</sub>H<sub>42</sub>F<sub>6</sub>N<sub>2</sub>O<sub>12</sub>S<sub>2</sub>: C, 54.54; H, 4.37; N, 2.89; S, 6.62. Found: C, 54.34; H, 4.62; N, 2.48; S, 6.40.

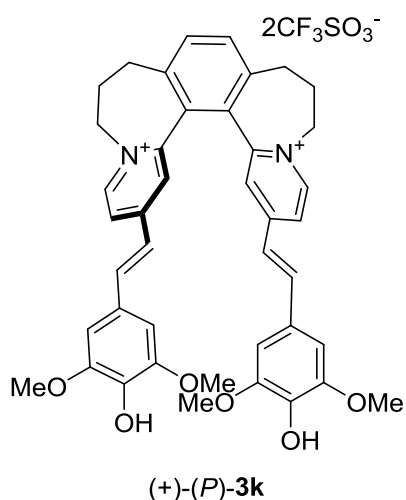
## 2. General procedure for the synthesis of (+)-*(P)*-3k and (-)-*(M)*-3k:



Starting enantiopure helquat (-)-*(P)*-3 or (+)-*(M)*-3 (10 mg, 0.016 mmol) and 4-hydroxy-3,5-dimethoxybenzaldehyde (0.085 g, 0.47 mmol, 30 equiv) were placed in a 10 mL glass-vial equipped with a stirring bar and a teflon cap. Dry MeOH (0.5 mL) and pyrrolidine (21  $\mu$ L, 0.25 mmol, 16 equiv) were added, and the resulting mixture was stirred 24 h at RT under argon while protected from ambient light using aluminium foil cover. A color change was observed immediately after the piperidine was added. After the indicated time, TLC (mobile phase Stoddart's magic mixture) showed total consumption of the starting material (-)-*(P)*-3 or (+)-*(M)*-3, and no presence of the monocondensated product. Crude product was precipitated from the reaction mixture by addition of Et<sub>2</sub>O (8 mL). The suspension was agitated using a vortex, centrifuged, and the liquids were separated from the solid pellet. MeOH (0.5 mL) and Et<sub>2</sub>O (8 mL) were added to the solid pellet. The resulting suspension was shaken, centrifuged, and the liquids were separated from the solid pellet. The MeOH (0.5 mL) and Et<sub>2</sub>O additions (8 mL) were repeated two more times. Then, acetonitrile was added (0.5 mL) and the solid was precipitated by addition of Et<sub>2</sub>O (5.5 mL). The suspension was shaken, centrifuged, and the liquids were separated from the solid pellet. Et<sub>2</sub>O (8 mL) was added and the suspension

was sonicated and then centrifuged. After separation of the liquids from the solids, the sample was dried at RT (5-10 min) and then use of vacuum of an oil pump (3 mbar) led to pure Knoevenagel-König condensation products (+)-(*P*)-**3k** and (-)-(*M*)-**3k** as green solids.

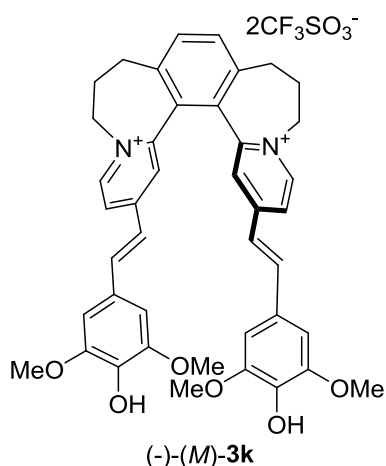
**(+)-(*P*)-2,17-Bis((*E*)-4-hydroxy-3,5-dimethoxystyryl)-6,7,8,11,12,13-hexahydrodipyrido[1,2-*a*:1',2'-*a'*]benzo[2,1-*c*:3,4-*c'*]bisazepindium trifluoromethanesulfonate, (+)-(*P*)-**3k****



Compound (+)-(*P*)-**3k** was isolated as a green solid (10 mg, 0.010 mmol, 67% yield,  $[\alpha]_D^{20} = +2703$  (c  $3 \times 10^{-4}$ , MeOH), 85% *ee*) from (-)-(*P*)-**3** (10 mg, 0.016 mmol 97% *ee*), following the procedure described above. Progress of the reaction was monitored by TLC (mobile phase Stoddart's magic mixture, starting material (-)-(*P*)-**3**  $R_f = 0.39$ , product (+)-(*P*)-**3k**  $R_f = 0.71$ ). Chemical structure of the product was verified by  $^1\text{H}$  NMR (400 MHz, DMSO- $d_6$  + 2 drops of 0.1 M solution of TfOH in methanol- $d_4$ ) and compared with (*rac*)-**3k** (See  $^1\text{H}$  and  $^{13}\text{C}$  NMR spectra Section S9, p. S196).

The enantiopurity of (+)-(*P*)-**3k** was determined by capillary electrophoresis (Section S4, Figure S5, p. S80). For ECD and UV/Vis absorption spectra for pH-switching with dye (+)-(*P*)-**3k**, see Figure S29 (p. S115).

**(-)-(*M*)-2,17-Bis((*E*)-4-hydroxy-3,5-dimethoxystyryl)-6,7,8,11,12,13-hexahydrodipyrido[1,2-*a*:1',2'-*a'*]benzo[2,1-*c*:3,4-*c'*]bisazepindium trifluoromethanesulfonate, (-)-(*M*)-**3k****



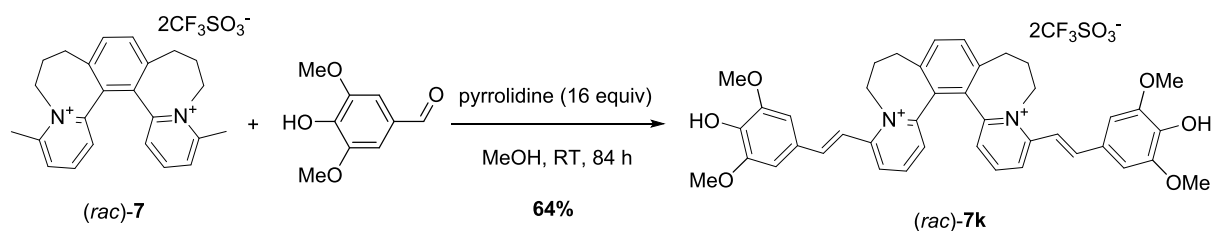
Compound (-)-(*M*)-**3k** was isolated as an olive green solid (9 mg, 0.009 mmol, 60% yield,  $[\alpha]_D^{20} = -2621$  (c  $3 \times 10^{-4}$ , MeOH), 80% *ee*) from (+)-(*M*)-**3** (10 mg, 0.016 mmol, 96% *ee*), following the procedure described above. Progress of the reaction was monitored by TLC (mobile phase Stoddart's magic mixture, starting material (+)-(*M*)-**3**  $R_f = 0.39$ , product (-)-(*M*)-**3k**  $R_f = 0.71$ ). Chemical structure of the product was verified by  $^1\text{H}$  NMR (400 MHz, DMSO- $d_6$  + 2 drops of 0.1 M

solution of TfOH in methanol- $d_4$ ) and compared with (*rac*)-**3k** (See  $^1\text{H}$  and  $^{13}\text{C}$  NMR spectra Section S9, p. S196). The enantiopurity of (-)-(*M*)-**3k** was determined by capillary electrophoresis (Section S4, Figure S5, p. S80). For ECD and UV/Vis absorption spectra for pH-switching with dye (-)-(*M*)-**3k**, see Figures S29-30 (pp. S115-116).

## Part J: Synthesis of racemic pH-switchable dye (*rac*)-7k and non-racemic dyes (-)-(*P*)-7k and (+)-(*M*)-7k

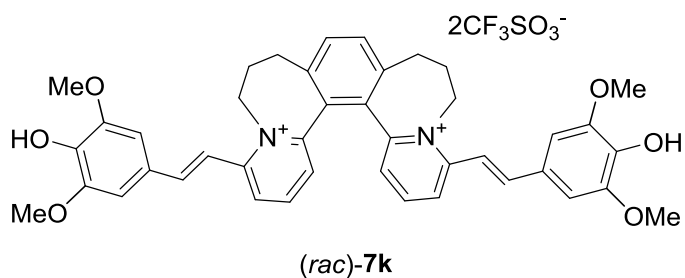
### 1. Procedure for the synthesis of (*rac*)-7k

(*rac*)-4,15-Bis((*E*)-4-hydroxy-3,5-dimethoxystyryl)-6,7,8,11,12,13-hexahydrodipyrido[1,2-*a*:1',2'-*a'*]benzo[2,1-*c*:3,4-*c'*]bisazepindium trifluoromethansulfonate, (*rac*)-7k



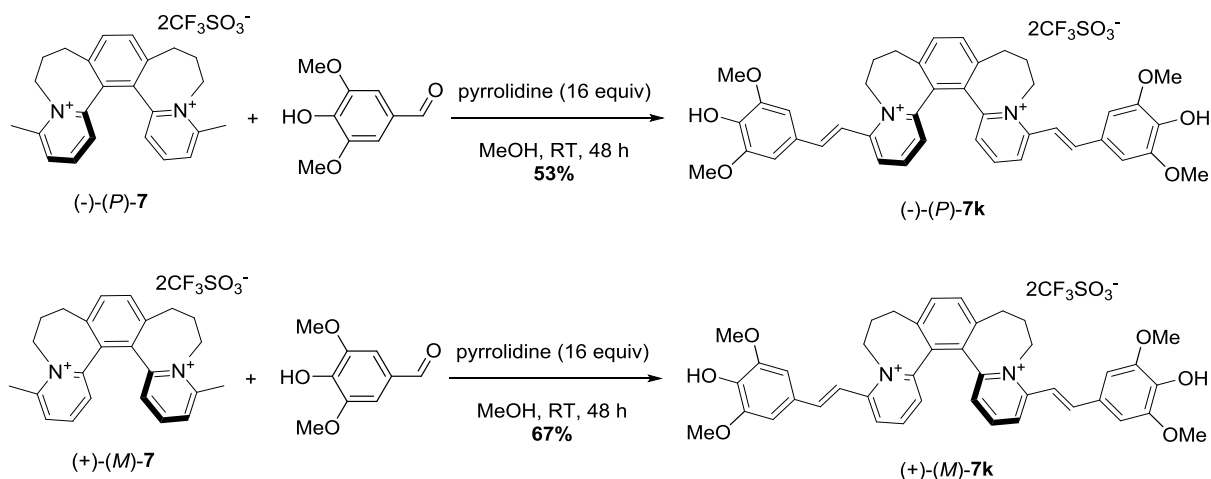
Starting helquat (*rac*)-7 (30 mg, 0.047 mmol) and 4-hydroxy-3,5-dimethoxybenzaldehyde (0.26 g, 1.4 mmol, 30 equiv) were placed in a 50 mL plastic-centrifuge tube (SARSTEDT, cat. num. 62.547.254) equipped with a stirring bar and a cap. Dry MeOH (1.5 mL) and pyrrolidine (62  $\mu$ L, 0.75 mmol, 16 equiv) were added, and the resulting mixture was stirred 84 h at RT under argon while protected from ambient light using aluminium foil cover. A color change was observed immediately after the piperidine was added. After the indicated time, TLC (mobile phase Stoddart's magic mixture, starting material (*rac*)-7  $R_f = 0.31$ , product (*rac*)-7k  $R_f = 0.76$ ) showed total consumption of the starting material (*rac*)-7 and no presence of the monocondensated product ( $R_f = 0.6$ ). Crude product was precipitated from the reaction mixture by addition of Et<sub>2</sub>O (33 mL). The suspension was sonicated, centrifuged, and the liquids were separated from the solid pellet. Acetonitrile (2 mL) and Et<sub>2</sub>O (33 mL) were added to the solid pellet. The resulting suspension was sonicated, centrifuged, and the liquids were separated from the solid pellet. The addition of acetonitrile followed by sonication, and centrifugation, was repeated two more times. Then, the solids were dissolved in MeOH (10 mL approx.) and precipitated by addition of Et<sub>2</sub>O (25 mL). The suspension was sonicated, centrifuged, and the liquids were separated from the solid pellet. The addition of MeOH (10 mL) and Et<sub>2</sub>O (25 mL) was repeated two more times. After the suspension was centrifuged for the last time, Et<sub>2</sub>O (35 mL) was added to the solid pellet, sonicated and then centrifuged. After separation of the liquids from the solid pellet, the sample was dried at RT (5-10 min) and then use of vacuum of an oil pump (3 mbar) led to pure Knoevenagel-König condensation product (*rac*)-7k as dark green flakes (0.029 g, 0.03 mmol, 64% yield).





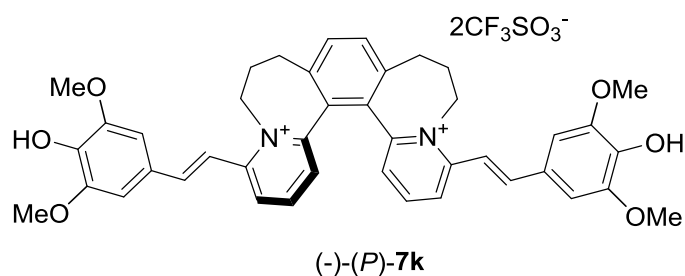
m.p. (decomposition) 210-215°C.  $^1\text{H}$  NMR (600 MHz, 0.1M TfOH / methanol- $d_4$  + 5 drops of DMSO- $d_6$ ): 2.44-2.49 (m, 2H); 2.53 (td,  $J = 13.5$ , 13.3, 6.8 Hz, 2H); 2.80-2.88 (m, 2H); 3.12 (dd,  $J = 13.7$ , 6.0 Hz, 2H); 3.97 (s, 12H); 4.45 (td,  $J = 14.0$ , 5.0 Hz, 2H); 5.26 (dd,  $J = 14.5$ , 6.0 Hz, 2H); 7.21 (s, 4H); 7.33 (dd,  $J = 7.8$ , 1.3 Hz, 2H); 7.53 (d,  $J = 16.0$  Hz, 2H); 7.78 (s, 2H); 7.86 (d,  $J = 16.0$  Hz, 2H); 8.16 (t, 8.1 Hz, 2H); 8.38 (d,  $J = 8.4$ , 1.2 Hz, 2H).  $^{13}\text{C}$  NMR (151 MHz, 0.1M TfOH / methanol- $d_4$  + 5 drops of DMSO- $d_6$ ):  $\delta = 29.76$ , 31.78, 53.80, 57.14, 108.03, 115.13, 120.79, 122.9, 126.88, 127.19, 129.53, 132.52, 134.19, 140.34, 140.96, 144.31, 147.65, 149.73, 153.55, 156.40. IR (KBr):  $\tilde{\nu}$  ( $\text{cm}^{-1}$ ) 3071; 2950; 2929; 2838; 1611; 165; 1504; 1489; 1456; 1414; 1326; 1272; 1234; 1164; 1234; 1164; 1145; 1114; 1074; 1030; 988; 832; 637. MS (ESI)  $m/z$  (%): 819 (15), 669 (25), 335 (100). HRMS (ESI)  $m/z$ :  $[(\text{M}-2\text{TfO}^-)^{2+}]$  ( $\text{C}_{42}\text{H}_{42}\text{N}_2\text{O}_6^{2+}$ ) calc.: 335.15160, found: 335.15168.

## 2. General procedure for the synthesis of (-)-(P)-7k and (+)-(M)-7k:



Starting enantiopure helquat (-)-(P)-7 or (+)-(M)-7 (10 mg, 0.016 mmol) and 4-hydroxy-3,5-dimethoxybenzaldehyde (0.085 g, 0.47 mmol, 30 equiv) were placed in a 10 mL glass-vial equipped with a stirring bar and a teflon cap. Dry MeOH (0.5 mL) and pyrrolidine (21  $\mu$ L, 0.25 mmol, 16 equiv) were added, and the resulting mixture was stirred 24 h at RT under argon while protected from ambient light using aluminium foil cover. A color change was observed immediately after the piperidine was added. After the indicated time, TLC (mobile phase "Stoddart's magic mixture") showed total consumption of the starting material (-)-(P)-7 or (+)-(M)-7, and no presence of the monocondensated product. Crude product was precipitated from the reaction mixture by addition of Et<sub>2</sub>O (7.5 mL). The suspension was agitated using a vortex, centrifuged, and the liquids were separated from the solid pellet. The solids were dissolved in MeOH (0.7 mL approx.) and Et<sub>2</sub>O (7.5 mL) was added. The resulting suspension was shaken, centrifuged, and the liquids were separated from the solid pellet. The MeOH (0.7 mL) and Et<sub>2</sub>O additions (7.5 mL) were repeated four more times. Et<sub>2</sub>O (8 mL) was added and the suspension was sonicated and then centrifuged. After separation of the liquids from the solids, the sample was dried at RT (5-10 min) and then use of vacuum of an oil pump (3 mbar) led to pure Knoevenagel-König condensation products (-)-(P)-7k and (+)-(M)-7k as dark green flakes.

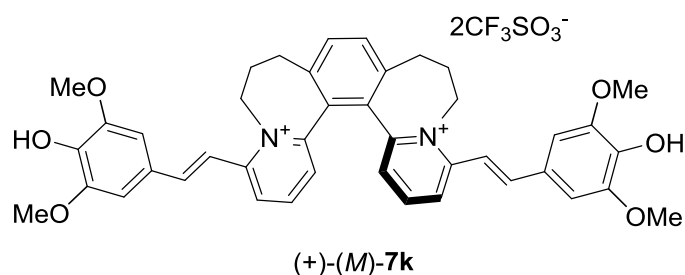
**(-)-(P)-4,15-bis((E)-4-hydroxy-3,5-dimethoxystyryl)-6,7,8,11,12,13-hexahydrodipyrido[1,2-a:1',2'-a']benzo[2,1-c:3,4-c']bisazepindium trifluoromethanesulfonate, (-)-(P)-7k**



Compound (-)-(P)-7k was isolated as dark-green flakes (8 mg, 0.008 mmol, 53% yield,  $[\alpha]_D^{20} = -1929$  (c  $3 \times 10^{-4}$ , MeOH), 99% *ee*) from (-)-(P)-7 (10 mg, 0.016 mmol, 99% *ee*), following the procedure described

above. Progress of the reaction was monitored by TLC (mobile phase Stoddart's magic mixture, starting material (-)-(P)-7  $R_f = 0.31$ , product (-)-(P)-7k  $R_f = 0.76$ ). Chemical structure of the product was verified by <sup>1</sup>H NMR (400 MHz, DMSO-*d*<sub>6</sub> + 2 drops of 0.1 M solution of TfOH in methanol-*d*<sub>4</sub>) and compared with (*rac*)-7k (See <sup>1</sup>H and <sup>13</sup>C NMR spectra Section S9, p. S198). The enantiopurity of (-)-(P)-7k was determined by capillary electrophoresis (Section S4, Figure S10, p. S82). For ECD and UV/Vis absorption spectra for pH-switching with dye (-)-(P)-7k, see Figures S31-33 (pp. S119-121).

**(+)-(M)-4,15-bis((E)-4-hydroxy-3,5-dimethoxystyryl)-6,7,8,11,12,13-hexahydrodipyrido[1,2-a:1',2'-a']benzo[2,1-c:3,4-c']bisazepindium trifluoromethanesulfonate, (+)-(M)-7k**



Compound (+)-(M)-7k was isolated as dark-green flakes (10 mg, 0.010 mmol, 67% yield,  $[\alpha]_D^{20} = +2078$  (c  $3 \times 10^{-4}$ , MeOH), 99% *ee*) from (+)-(M)-7 (10 mg, 0.016 mmol, 98% *ee*) following the procedure described

above. Progress of the reaction was monitored by TLC (mobile phase Stoddart's magic mixture, starting material (+)-(M)-7  $R_f = 0.31$ , product (+)-(M)-7k  $R_f = 0.76$ ). Chemical structure of the product was verified by <sup>1</sup>H NMR (400 MHz, DMSO-*d*<sub>6</sub> + 2 drops of 0.1 M solution of TfOH in methanol-*d*<sub>4</sub>) and compared with (*rac*)-7k (See <sup>1</sup>H and <sup>13</sup>C NMR spectra Section S9, p.S198). The enantiopurity of (+)-(M)-7k was determined by capillary electrophoresis (Section S4, Figure S10, p. S82). For ECD and UV/Vis absorption spectra for pH-switching with dye (+)-(M)-7k, see Figures S31-33 (pp. S119-121).

#### 4) Capillary electrophoresis (CE)

Chiral analysis of helical dyes was carried out by capillary electrophoresis using a novel protocol described below. This novel protocol was developed on a basis of a published work<sup>4</sup> and features fine-tuned composition of background electrolytes (BGE) including the judicious choice of a suitable chiral selector. The Beckman-Coulter MDQ apparatus used here was equipped with a photodiode array (PDA) module. Zones of analytes were detected by UV absorbance at 200 nm. The data was acquired by Beckman-Coulter Karat 32 system and further treated with Clarity data station (DataApex, Prague, Czech Republic).

Background electrolytes comprised a 22 mM sodium cation + 35 mM phosphate buffer, pH 2.4, 0 - 40% v/v ACN or MeOH, and a chiral selector, which was sulfated  $\gamma$ -cyclodextrin (S- $\gamma$ -CD, Beckman-Coulter, cat. no. A50924) or sulfobutyl- $\beta$ -cyclodextrin (SBE- $\beta$ -CD, Cyclodextrin-Shop, Budel, The Netherlands, cat. no. CDexB-080). For BGE compositions and preparation details, see Tables S1 and S2 below.

Separation capillaries were fused silica 50/370  $\mu\text{m}$  id/od and of 29.5/39.5 cm effective/total length (Polymicro Technologies, Phoenix, AZ, USA). The inner surface was coated with hydroxypropylcellulose (HPC) as described elsewhere.<sup>5,6</sup> Capillary cartridge was held at constant temperature (22°C). Capillary conditioning consisted of rinsing with the BGE between runs at 2 bar for 30 s. Sample solutions in DMSO were injected by pressure of 0.7 kPa for 10 s. Negative polarity separation voltage (*i.e.* cathode at the injection capillary end) and corresponding current are summarized in Table S1.

**Table S1.** Conditions for chiral analysis of helical dyes

Compound	Chiral selector	Solvent	Voltage (kV)	Current ( $\mu\text{A}$ )
3, 3a, 7	1.5% S- $\gamma$ -CD	0/100 v/v ACN/H <sub>2</sub> O	-11.4	37
3i	3.0% S- $\gamma$ -CD	25/75 v/v ACN/H <sub>2</sub> O	-11.4	41
3j	2.0% SBE- $\beta$ -CD	40/60 v/v ACN/H <sub>2</sub> O	-11.4	23
3k, 7a	1.5% S- $\gamma$ -CD	25/75 v/v ACN/H <sub>2</sub> O	-11.4	26
7i	1.5% S- $\gamma$ -CD	40/60 v/v ACN/H <sub>2</sub> O	-11.4	19
7j	3.0% S- $\gamma$ -CD	40/60 v/v ACN/H <sub>2</sub> O	-11.4	31
7k	4.0% SBE- $\beta$ -CD	40/60 v/v MeOH/H <sub>2</sub> O	-15.0	29

ACN = acetonitrile, v/v = volume ratio of binary solvent mixture

**Table S2.** Preparation of background electrolytes from stock solutions

<b>BGE<sup>a</sup></b>	<b>S-<math>\gamma</math>-CD<sup>b</sup></b> ( $\mu$ L)	<b>SBE-<math>\beta</math>-CD<sup>c</sup></b> (mg)	<b>Buffer<sup>d</sup></b> ( $\mu$ L)	<b>ACN/MeOH</b> ( $\mu$ L)	<b>Water</b> ( $\mu$ L)
1.5% S- $\gamma$ -CD in H <sub>2</sub> O	75	-	333	0	592
3.0% S- $\gamma$ -CD in 25% ACN	150	-	333	250	267
2.0% SBE- $\beta$ -CD 40% ACN	-	20	333	400	267
1.5% S- $\gamma$ -CD in 25% ACN	75	-	333	250	342
1.5% S- $\gamma$ -CD in 40% ACN	75	-	333	400	192
3.0% S- $\gamma$ -CD in 40% ACN	150	-	333	400	117
4.0% SBE- $\beta$ -CD in 40% MeOH	-	40	333	400	267

ACN = acetonitrile

<sup>a</sup> - values in the table refer to preparation of 1 mL of BGE<sup>b</sup> - volumes correspond to 20% w/v aqueous solution of sulfated  $\gamma$ -cyclodextrin obtained from commercial supplier<sup>c</sup> - sulfobutyl- $\beta$ -cyclodextrin was purchased as a solid<sup>d</sup> - volumes given correspond to stock solution of 66 mM NaOH + 105 mM H<sub>3</sub>PO<sub>4</sub> in water

CE charts from the individual enantiomeric composition analyses of helquats **3** and **7**, and dyes **3a**, **3i-k**, **7a** and **7i-k** are summarized in the next Section (Figures S1 – S10, pp. S78-S82).

**1. Determination of enantiopurity of non-racemic helquats **3** and **7**, and non-racemic dyes **3a**, **3i-k**, **7a** and **7i-k**:**

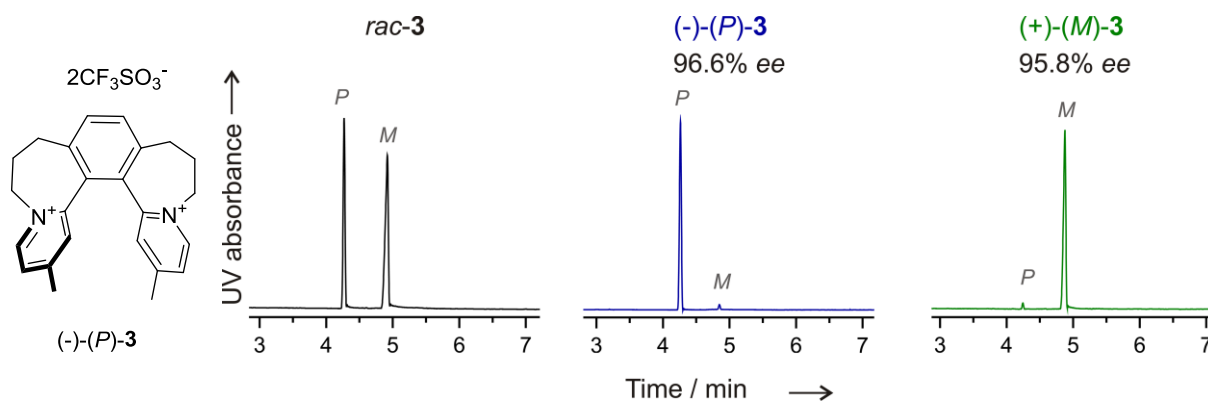


**Figure S1.** CE charts from the individual enantiomeric composition analyses of (*rac*)-**3** (left chart), (*-*)-(*P*)-**3** (central chart), and (*+*)-(*M*)-**3** (right chart). The samples as water solutions were analyzed in the presence of 1.5% of sulfated  $\gamma$ -cyclodextrin selector, H<sub>2</sub>O, 22 mM / 35 mM Na<sup>+</sup> / phosphate (pH 2.4).

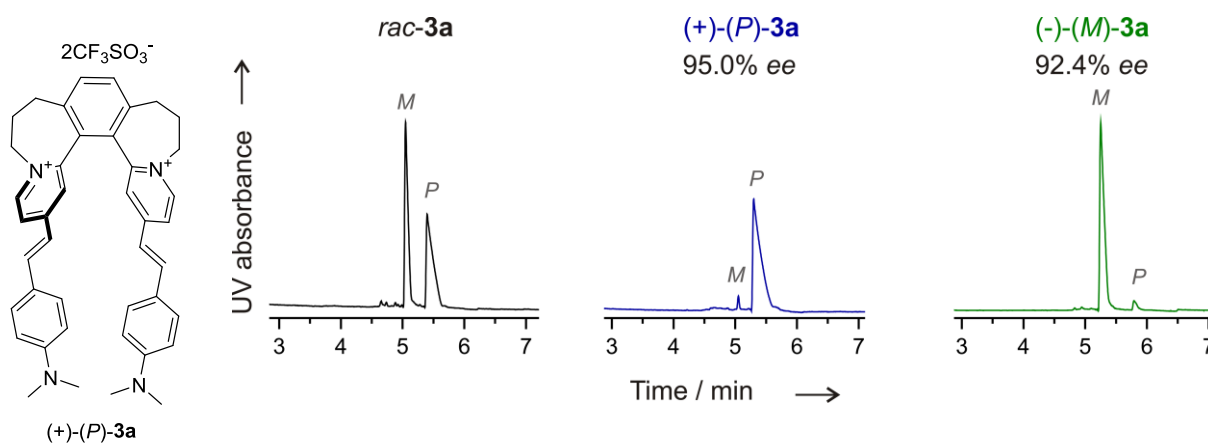


**Figure S2.** CE charts from the individual enantiomeric composition analyses of (*rac*)-**3a** (left chart), (*+*)-(*P*)-**3a** (central chart), and (*-*)-(*M*)-**3a** (right chart). The samples as DMSO solutions were analyzed in the presence of 1.5% of sulfated  $\gamma$ -cyclodextrin selector, H<sub>2</sub>O, 22 mM / 35 mM Na<sup>+</sup> / phosphate (pH 2.4).

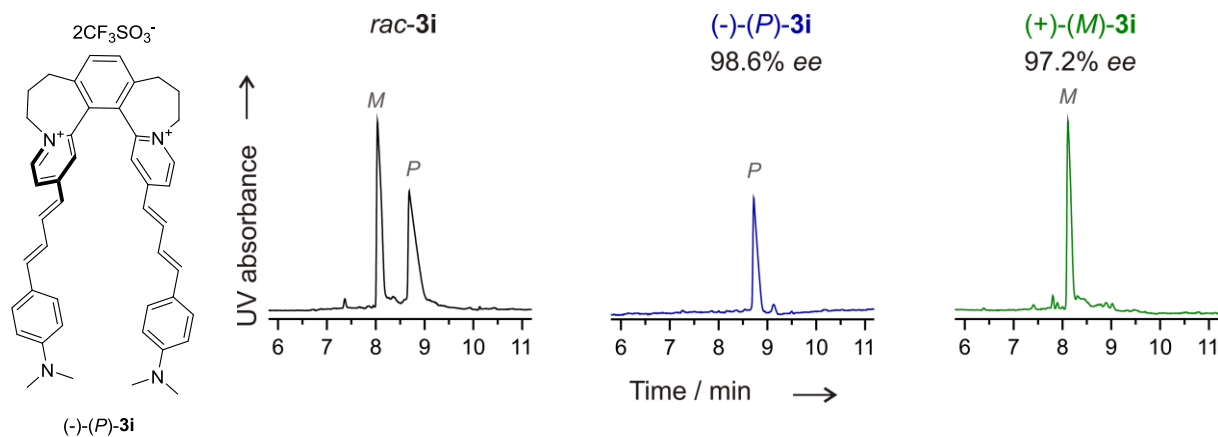


**Figure S3.** CE charts from the individual enantiomeric composition analyses of (*rac*)-**3i** (left chart), (-)-(*P*)-**3i** (central chart), and (+)-(*M*)-**3i** (right chart). The samples as DMSO solutions were analyzed in the presence of 3.0% of sulfated  $\gamma$ -cyclodextrin selector, 25% acetonitrile, 22 mM / 35 mM  $\text{Na}^+$  / phosphate (pH 2.4).

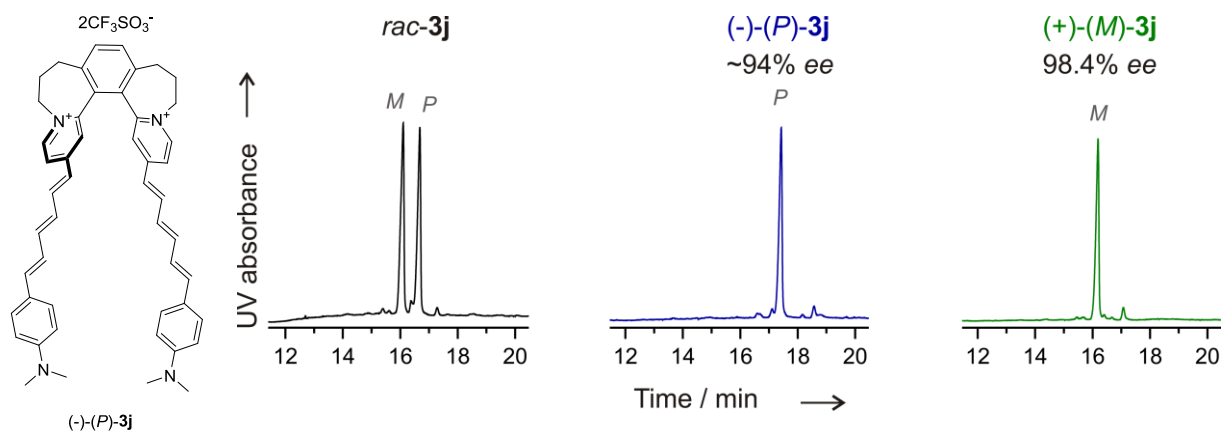


**Figure S4.** CE charts from the individual enantiomeric composition analyses of (*rac*)-**3j** (left chart), (-)-(*P*)-**3j** (central chart), and (+)-(*M*)-**3j** (right chart). The samples as DMSO solutions were analyzed in the presence of 2.0% of sulfobutyl ether  $\beta$ -cyclodextrin selector, 40% acetonitrile, 22 mM / 35 mM  $\text{Na}^+$  / phosphate (pH 2.4).

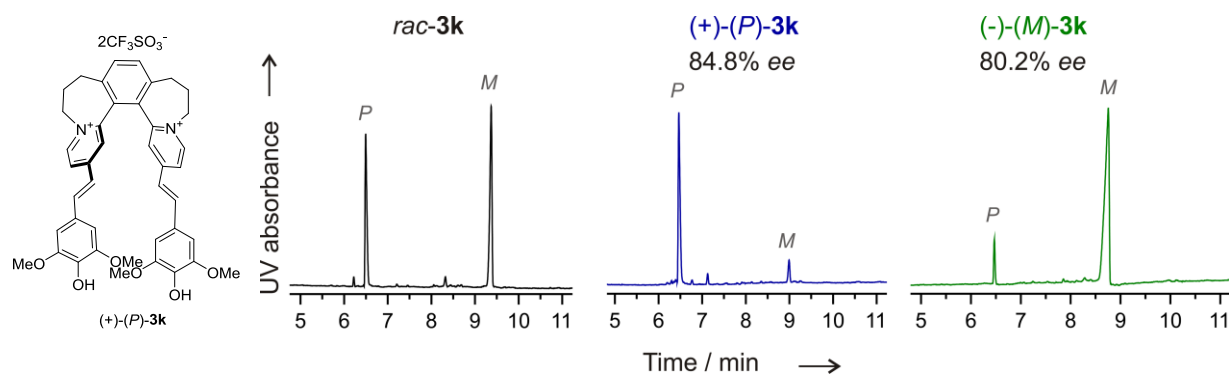


**Figure S5.** CE charts from the individual enantiomeric composition analyses of (*rac*)-**3k** (left chart), (+)-(*P*)-**3k** (central chart), and (-)-(*M*)-**3k** (right chart). The samples as DMSO solutions were analyzed in the presence of 1.5% of sulfated  $\gamma$ -cyclodextrin selector, 25% acetonitrile, 22 mM / 35 mM Na<sup>+</sup> / phosphate (pH 2.4).

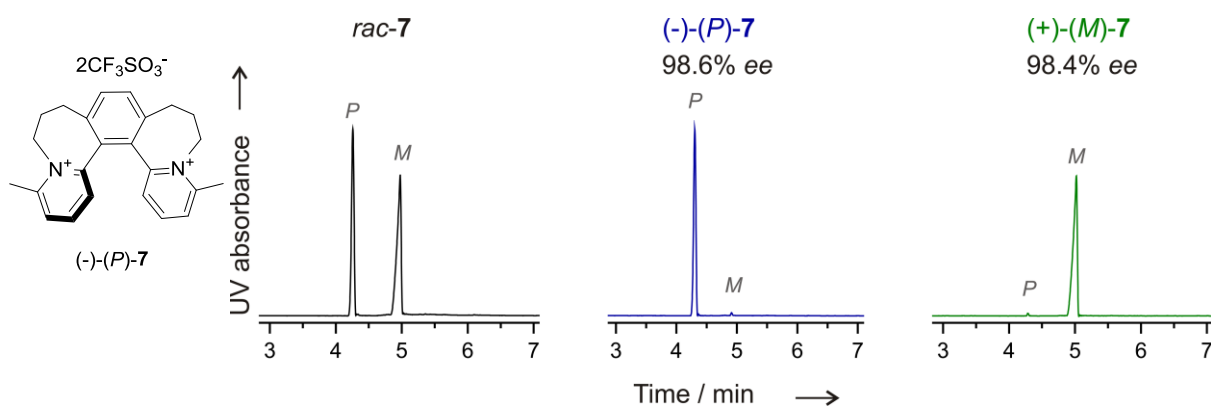


**Figure S6.** CE charts from the individual enantiomeric composition analyses of (*rac*)-**7** (left chart), (-)-(*P*)-**7** (central chart), and (+)-(*M*)-**7** (right chart). The samples as DMSO solutions were analyzed in the presence of 1.5% of sulfated  $\gamma$ -cyclodextrin selector, H<sub>2</sub>O, 22 mM / 35 mM Na<sup>+</sup> / phosphate (pH 2.4).



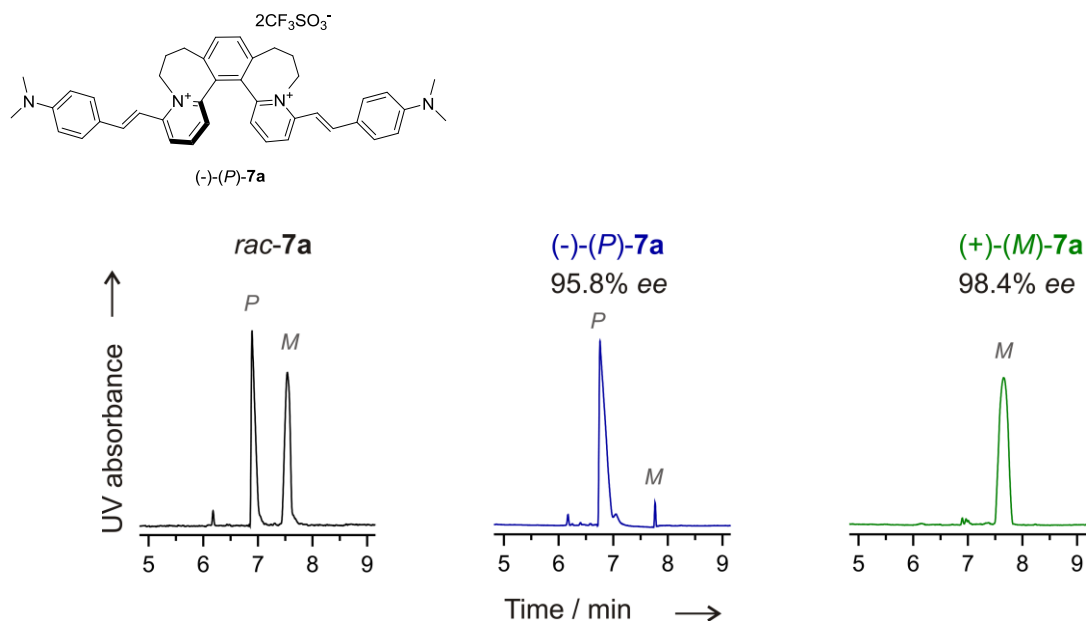


**Figure S7.** CE charts from the individual enantiomeric composition analyses of **(rac)-7a** (left chart), **(-)-(P)-7a** (central chart), and **(+)-(M)-7a** (right chart). The samples as DMSO solutions were analyzed in the presence of 1.5% of sulfated  $\gamma$ -cyclodextrin selector, 25% of acetonitrile, 22 mM / 35 mM  $Na^+$  / phosphate (pH 2.4).

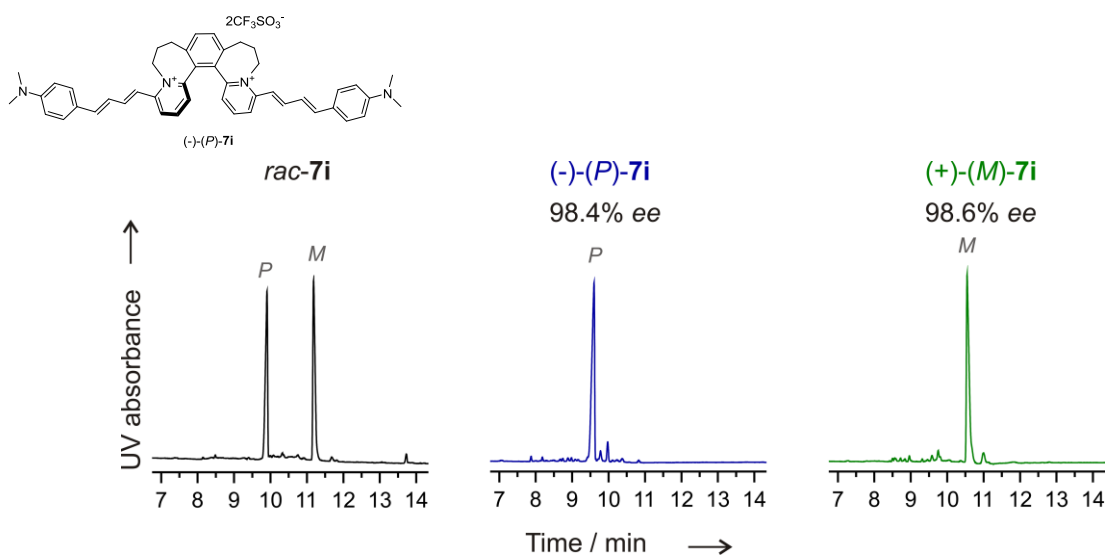


**Figure S8.** CE charts from the individual enantiomeric composition analyses of **(rac)-7i** (left chart), **(-)-(P)-7i** (central chart), and **(+)-(M)-7i** (right chart). The samples as DMSO solutions were analyzed in the presence of 1.5% of sulfated  $\gamma$ -cyclodextrin selector, 40% of acetonitrile, 22 mM / 35 mM  $Na^+$  / phosphate (pH 2.4).

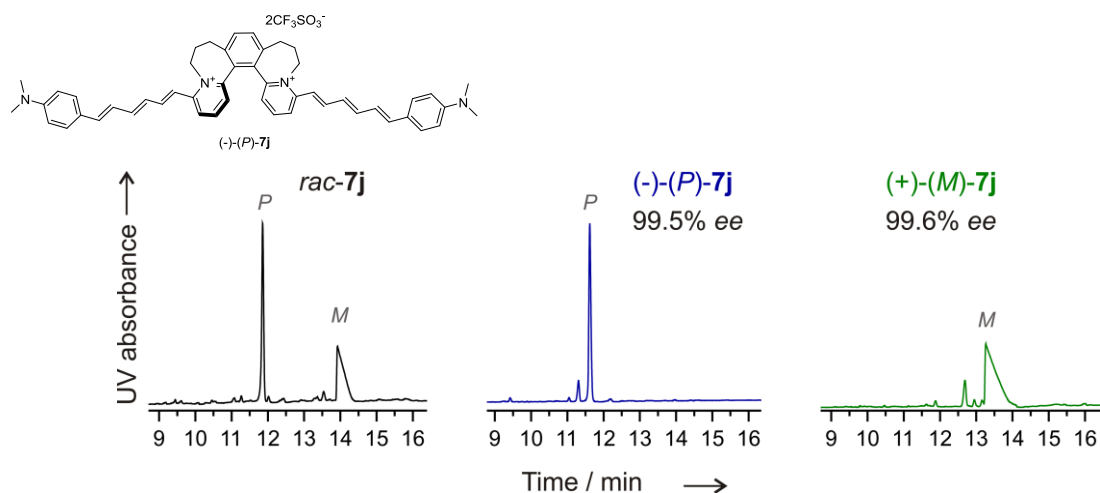


**Figure S9.** CE charts from the individual enantiomeric composition analyses of  $(rac)-7j$  (left chart),  $(-)-(P)-7j$  (central chart), and  $(+)-(M)-7j$  (right chart). The samples as DMSO solutions were analyzed in the presence of 3.0% of sulfated  $\gamma$ -cyclodextrin selector, 40% of acetonitrile, 22 mM / 35 mM  $Na^+$  / phosphate (pH 2.4).

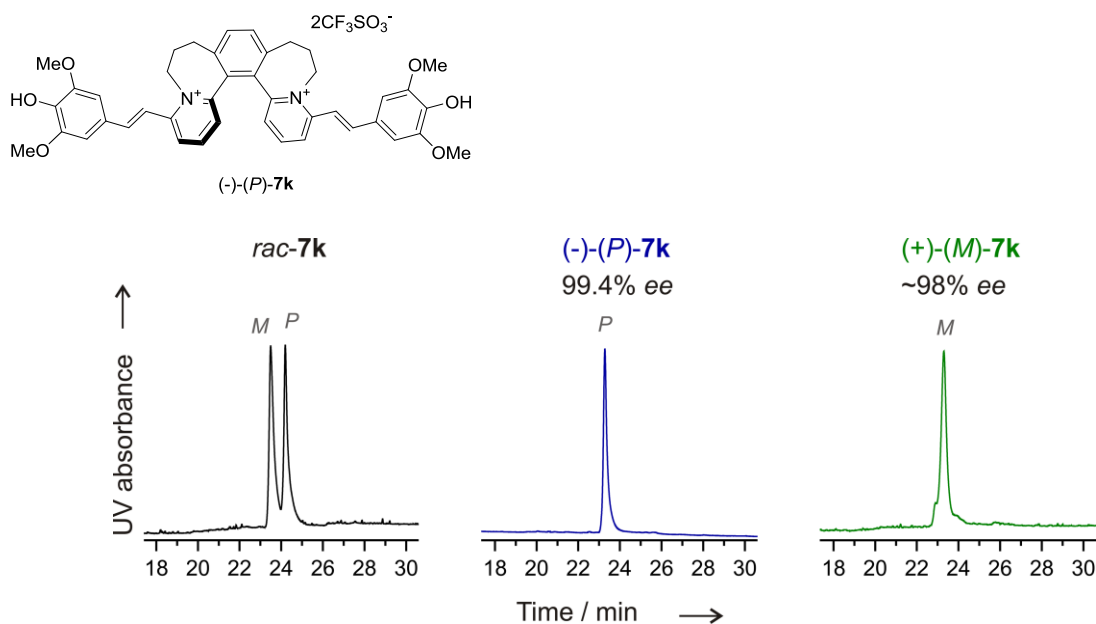
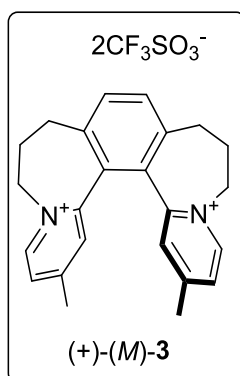


**Figure S10.** CE charts from the individual enantiomeric composition analyses of  $(rac)-7k$  (left chart),  $(-)-(P)-7k$  (central chart), and  $(+)-(M)-7k$  (right chart). The samples as DMSO solutions were analyzed in the presence of 4.0% of sulfobutyl ether  $\beta$ -cyclodextrin selector, 40% methanol, 22 mM / 35 mM  $Na^+$  / phosphate (pH 2.4).

## 2. Racemization barrier determination of (+)-(*M*)-**3**:



Determination of racemization barrier was performed in a block-heater with the actual temperature in the reaction vessel set to 61°C. (+)-(*M*)-**3** (0.9 mg, 1.4  $\mu\text{mol}$ ) was dissolved in DMSO (0.5 mL) and transferred to an NMR tube. The tube was placed into one of the holes of the block-heater filled with Rotitherm heating medium. The racemization experiment was run at 61°C. Before starting the heating, a sample for CE analysis (ca 10  $\mu\text{L}$ ) was taken with a capillary. Then, the NMR tube was immersed in the block with the Rotitherm medium equilibrated to 61°C. The samples for CE analysis (ca 10  $\mu\text{L}$ ) were taken every 20 min with a capillary (for illustrative CE charts, see Figure S11). The experiment was stopped after 240 min. The decreasing amount of (+)-(*M*)-**3** in the NMR tube monitored by CE (Figure S11) is listed in Table S3 and plotted in Figure S12.

**Table S3.** Racemization of (+)-(*M*)-**3** monitored by CE (DMSO at 61°C). For illustrative CE charts, see Figure S11.

time (min)	(-)-( <i>P</i> )- <b>3</b> (%)	(+)-( <i>M</i> )- <b>3</b> (%)	<i>ee</i> <sub>(+)-(<i>M</i>)-<b>3</b></sub>	<i>lnee</i> <sub>(+)-(<i>M</i>)-<b>3</b></sub>
0	2.23	97.77	95.54	4.560
20	12.09	87.91	75.82	4.328
40	19.03	80.97	61.94	4.126
60	25.75	74.25	48.50	3.882
80	31.21	68.79	37.58	3.626
100	34.59	65.41	30.82	3.428
120	37.48	62.52	25.04	3.220
140	40.41	59.59	19.18	2.954
160	43.25	56.75	13.50	2.603
180	44.33	55.67	11.34	2.428
200	45.92	54.08	8.16	2.099
220	46.67	53.33	6.66	1.896
240	47.61	52.39	4.78	1.564

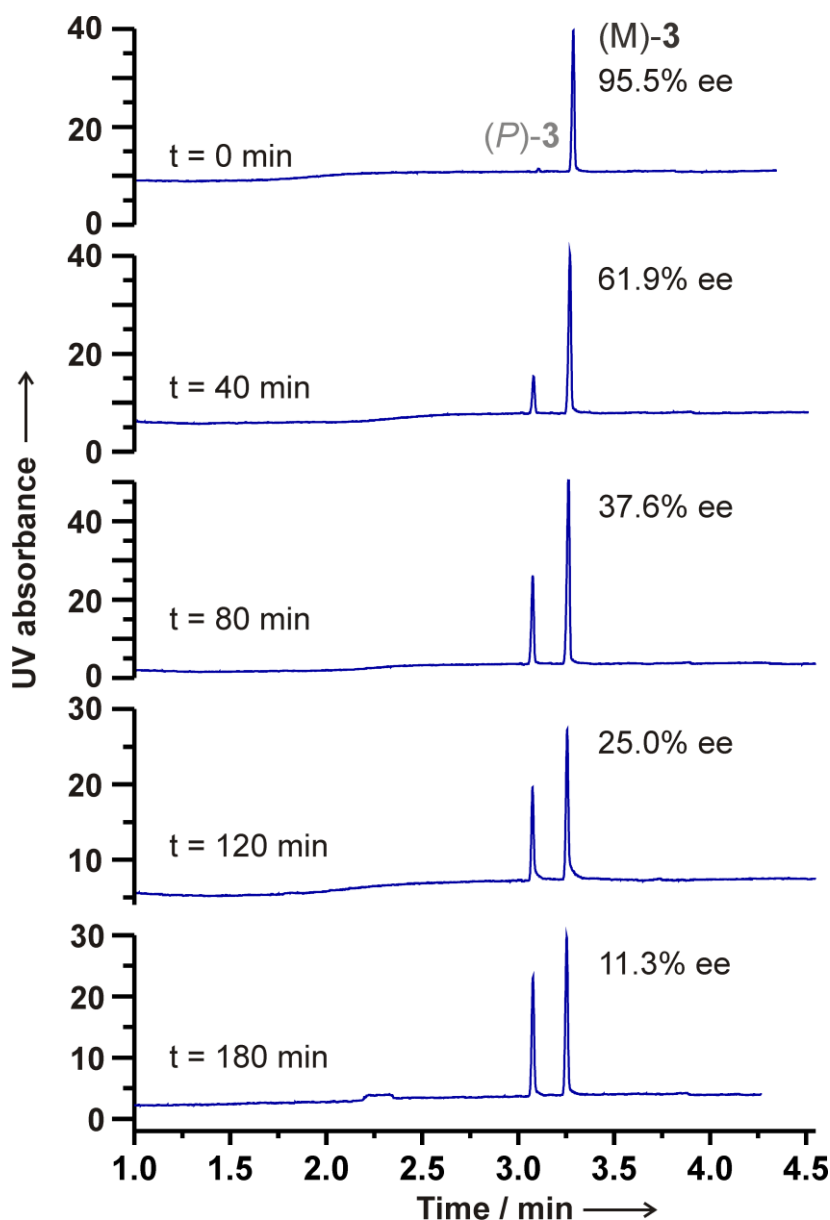


**Figure S11.** CE charts from the individual composition analyses during the racemization of (+)-(*M*)-**3** at 61°C in DMSO starting from mixture (-)-(*P*)-**3** : (+)-(*M*)-**3** = 2 : 98. The samples were analyzed in defined intervals (every 20 min) and only selected traces are shown here. For full data see Table S3 and plot in Figure S12.

Racemization process is a combination of two elemental processes: (*M*)-enantiomer converts to (*P*)-enantiomer with rate constant  $k$  and (*P*)-enantiomer converts to (*M*)-enantiomer with the same rate constant  $k$ . When these two processes are combined, the enantiomeric excess ( $ee$ ) of one enantiomer (or optical rotation of the sample) decays by first order kinetics with rate constant  $2k$  (Eq. 1, decay of enantiomeric excess  $ee_{(+)-(M)-3}$  according to first-order kinetics)

$$ee_{(+)-(M)-3} = ee_{(+)-(M)-3} \cdot e^{-2kt} \text{ (Eq. 1)}$$

where  $ee_{M-3}$  is the initial enantiomeric excess of (+)-(M)-3.

$ee_{(+)-(M)-3}$  determined by CE experiment thus decays according to the first order kinetics. The natural logarithm of  $ee_{(+)-(M)-3}$  was plotted against time and a trendline was calculated as a straight line. This trendline in the form  $y = -2kx + a$  gave the kinetic constant  $2k$ . From this value, half-life ( $T_{1/2}$ ) of racemization can be calculated (Eq. 2, half-life expressed using rate constant  $k$ ):

$$T_{1/2} = \frac{\ln 2}{2k} \text{ (Eq. 2)}$$

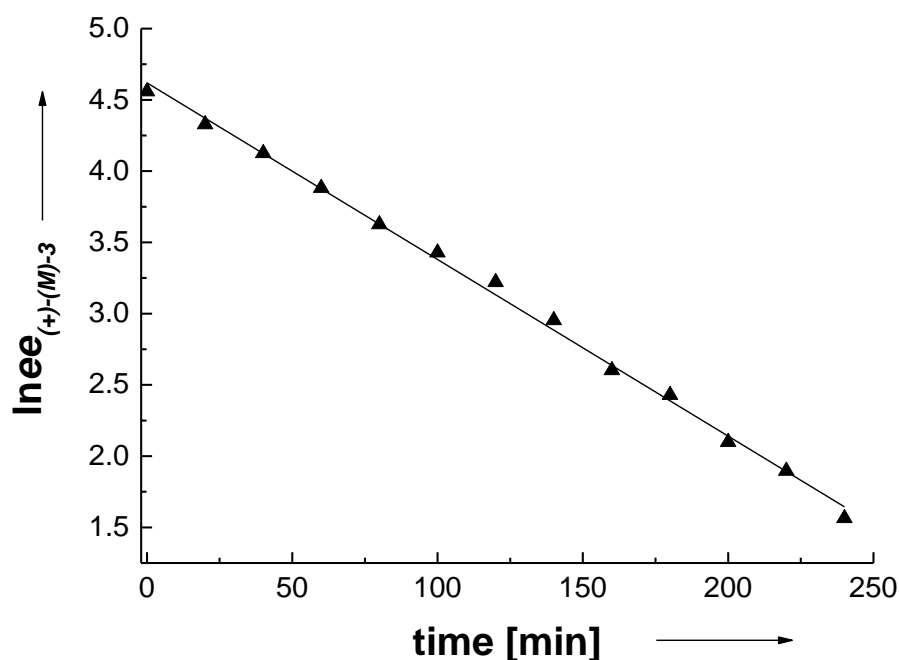


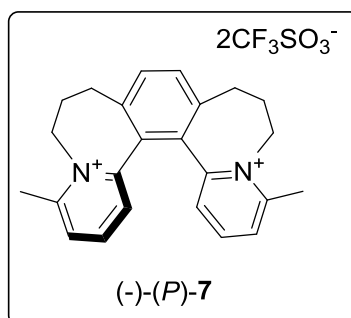
**Figure S12.** Racemization of (+)-(M)-3 in DMSO at 61°C. Dependence of natural logarithm of the enantiomeric excess  $\ln ee_{(+)-(M)-3}$  on time as determined by CE.

According to the theory of transition state, rate constant  $k$  can be transformed into activation Gibbs energy. This is the barrier of interconversion of one enantiomer into the other. The Gibbs free energy was calculated using Eq. 3 (Gibbs free energy calculation), where  $R = 8.314472 \text{ J}\cdot\text{K}^{-1}\cdot\text{mol}^{-1}$  is the gas constant,  $T$  is the thermodynamic temperature (in K),  $k$  is a kinetic constant obtained from the measurement,  $h = 6.62606896 \times 10^{-34} \text{ J}\cdot\text{s}$  is Planck's constant,  $k_B = 1.3806504 \times 10^{-23} \text{ J}\cdot\text{K}^{-1}$  is Boltzmann constant.

$$\Delta G^\ddagger = -RT \ln \frac{kh}{k_B T} \quad (\text{Eq. 3})$$

The experimental value for (+)-(*M*)-**3** enantiomer was  $\Delta G^\ddagger = 107.7 \text{ kJ}\cdot\text{mol}^{-1}$  (measured at 61°C) determining the racemization half-life to be 56 min at 61°C.

### 3. Racemization barrier determination of (-)-(*P*)-**7**:



Determination of racemization barrier was performed in a block-heater with the actual temperature in the reaction vessel set to 66°C. (-)-(*P*)-**7** (1.0 mg, 1.6  $\mu\text{mol}$ ) was dissolved in DMSO (0.5 mL) and transferred to an NMR tube. The tube was placed into one of the holes of the block-heater filled with Rotitherm heating medium. The racemization experiment was run at 66°C. Before starting the heating, a sample for CE analysis (ca 10  $\mu\text{L}$ ) was taken with a capillary. Then, the NMR tube was immersed in the block with the Rotitherm medium equilibrated to 66°C. Samples for CE analysis (ca 10  $\mu\text{L}$ ) were taken every 40 min with a capillary (for illustrative CE charts, see Figure S13). The experiment was stopped after 240 min. The decreasing amount of (-)-(*P*)-**7** in the NMR tube monitored by CE (Figure S13) is listed in Table S4 and plotted in Figure S14.

**Table S4.** Racemization of (-)-*(P)*-**7** monitored by CE (DMSO at 66°C). For illustrative CE charts, see Figure S13.

time (min)	(-)- <i>(P)</i> - <b>7</b> (%)	(+)- <i>(M)</i> - <b>7</b> (%)	<i>ee</i> <sub>(-)-<i>(P)</i>-<b>7</b></sub>	<i>ln</i> <i>ee</i> <sub>(-)-<i>(P)</i>-<b>7</b></sub>
0	99.31	0.69	98.62	4.591
40	97.00	3.00	94.00	4.543
80	95.2	4.80	90.40	4.504
120	92.75	7.25	85.50	4.449
160	90.97	9.03	81.94	4.406
200	88.04	11.96	76.08	4.332
240	86.46	13.54	72.92	4.289



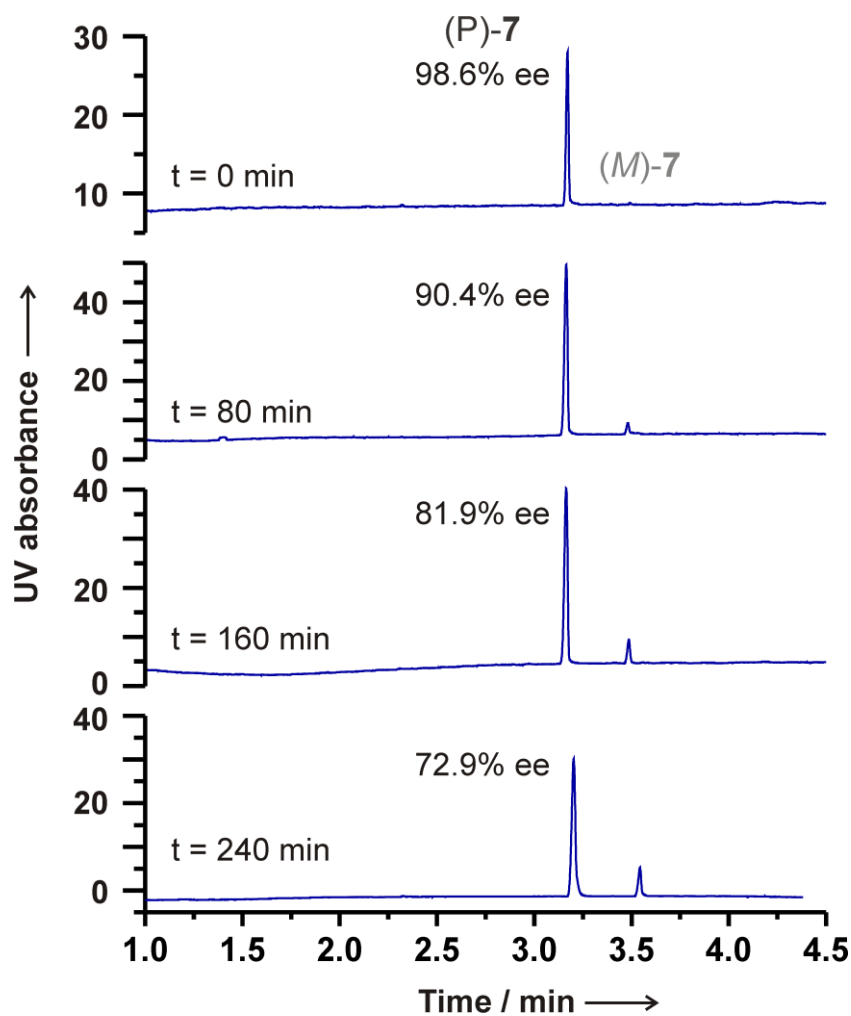


**Figure S13.** CE charts from the individual composition analyses during the racemization of (-)-(P)-7 at 66°C in DMSO starting from mixture (-)-(P)-7 : (+)-(M)-7 = 99 : 1. The samples were analyzed in defined intervals (every 20 min) and only selected traces are shown here. For full data see Table S4 and plot in Figure S14.

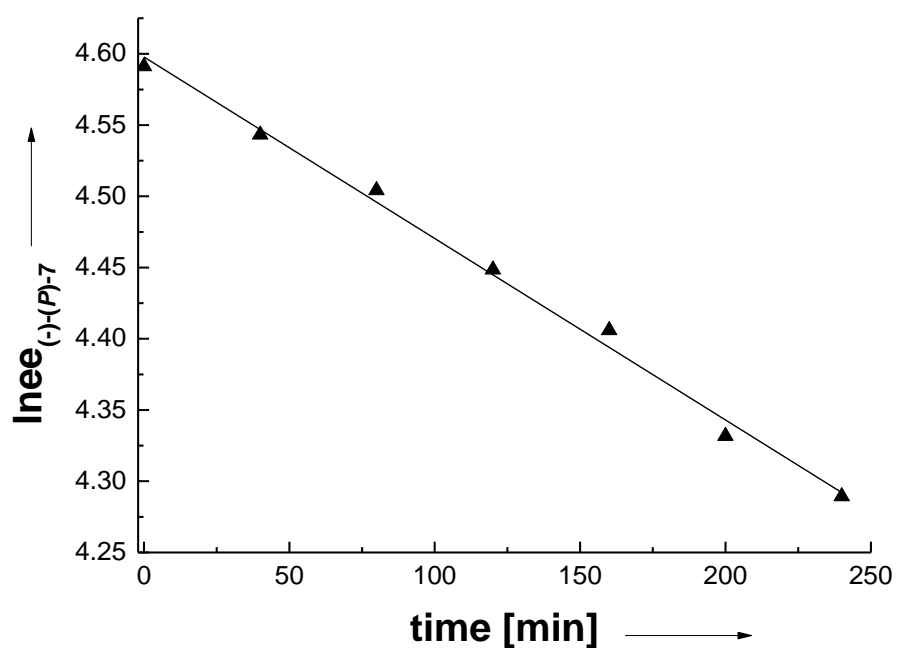
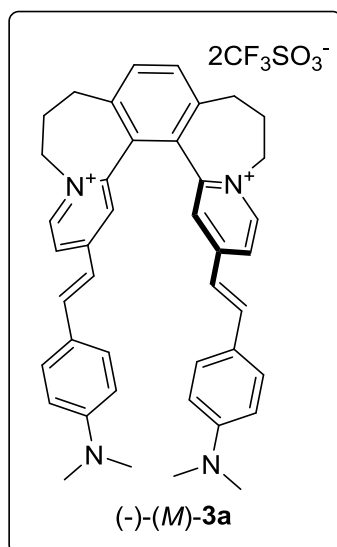


**Figure S14.** Racemization of (-)-(*P*)-**7** in DMSO at 66°C. Dependence of natural logarithm of the enantiomeric excess  $\ln ee_{(-)-(P)-7}$  on time as determined by CE.

According to the equations showed for the racemization of (+)-(*M*)-**3**, the experimental value for (-)-(*P*)-**7** is  $\Delta G^\ddagger = 115.7 \text{ kJ}\cdot\text{mol}^{-1}$  (measured at 66°C) determining the half-life to be 9 h at 66°C.

#### 4. Racemization barrier determination of (-)-(M)-3a:



The racemization barrier determination was performed in a block-heater with the actual temperature in the reaction vessel set to 62°C. (-)-(M)-**3a** (1.0 mg, 1.1 μmol) was dissolved in DMSO (0.5 mL) and transferred to an NMR tube. The tube was placed into one of the holes of the block-heater filled with Rotitherm heating medium. The racemization experiment was run at 62°C. Before starting the heating, a sample for CE analysis (ca 10 μL) was taken with a capillary. Then, the NMR tube was immersed in the block with the Rotitherm medium equilibrated to 62°C. Samples for CE analysis (ca 10 μL) were taken every 20 min with a capillary (for illustrative CE charts, see Figure S15). The experiment was stopped after 240 min. The decreasing amount of (-)-(M)-**3a** in the NMR tube monitored by CE (Figure S15) is listed in Table S5 and plotted in Figure S16.

**Table S5.** Racemization of (-)-(*M*)-**3a** monitored by CE (DMSO at 62°C). For illustrative CE charts, see Figure S15.

time (min)	(+)-( <i>P</i> )- <b>3a</b> (%)	(-)-( <i>M</i> )- <b>3a</b> (%)	<i>ee</i> <sub>(-)-(<i>M</i>)-<b>3a</b></sub>	<i>ln</i> <i>ee</i> <sub>(-)-(<i>M</i>)-<b>3a</b></sub>
0	3.80	96.20	92.40	4.526
20	10.19	89.81	79.62	4.377
40	14.64	85.36	70.72	4.259
60	20.21	79.79	59.58	4.087
80	25.05	74.95	49.90	3.910
100	28.35	71.65	43.30	3.768
120	32.27	67.73	35.46	3.568
140	33.07	66.93	33.86	3.522
160	35.27	64.73	29.46	3.383
180	38.84	61.16	22.32	3.105
200	39.96	60.04	20.08	3.000
220	41.21	58.79	17.58	2.867
240	42.50	57.50	15.00	2.708

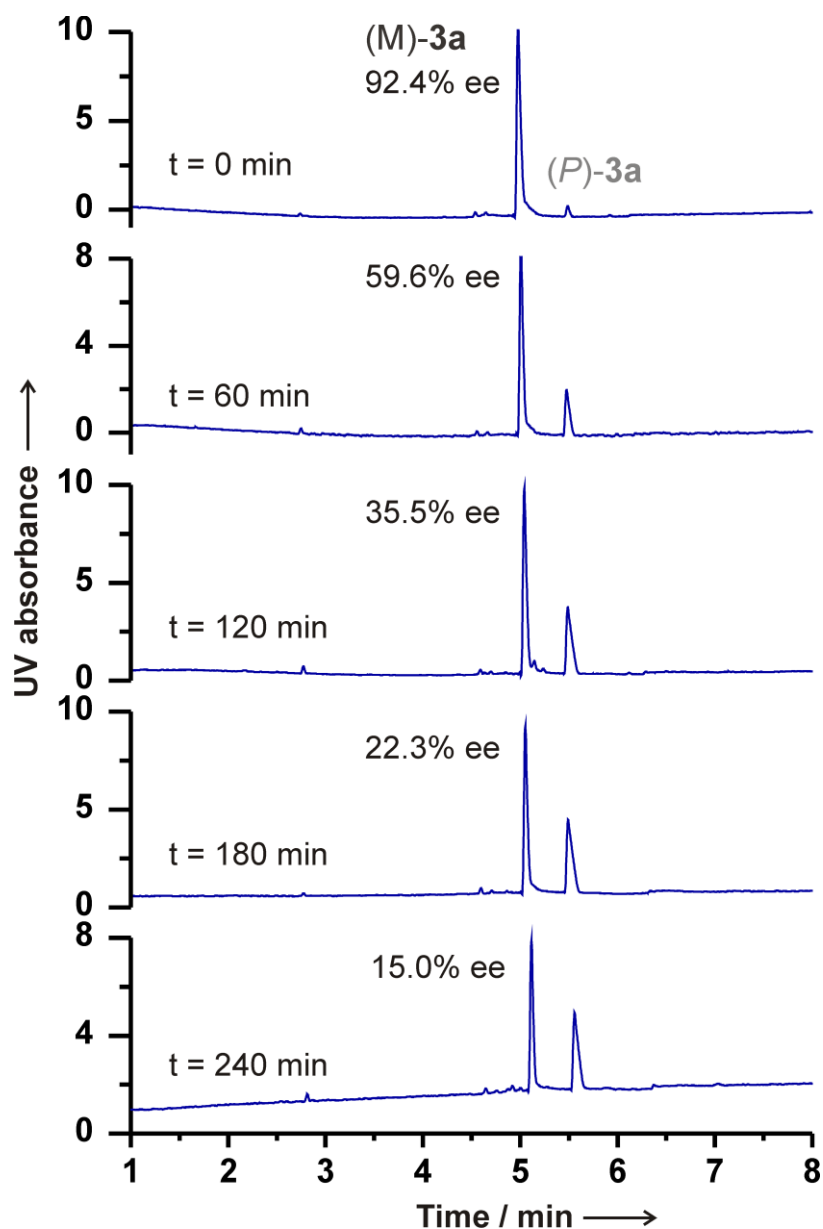


**Figure S15.** CE charts from the individual composition analyses during the racemization of (-)-**3a** at 62°C in DMSO starting from mixture (+)-**3a** : (-)-**3a** = 4 : 96. The samples were analyzed in defined intervals (every 20 min) and only selected traces are shown here. For full data see Table S5 and plot in Figure S16.

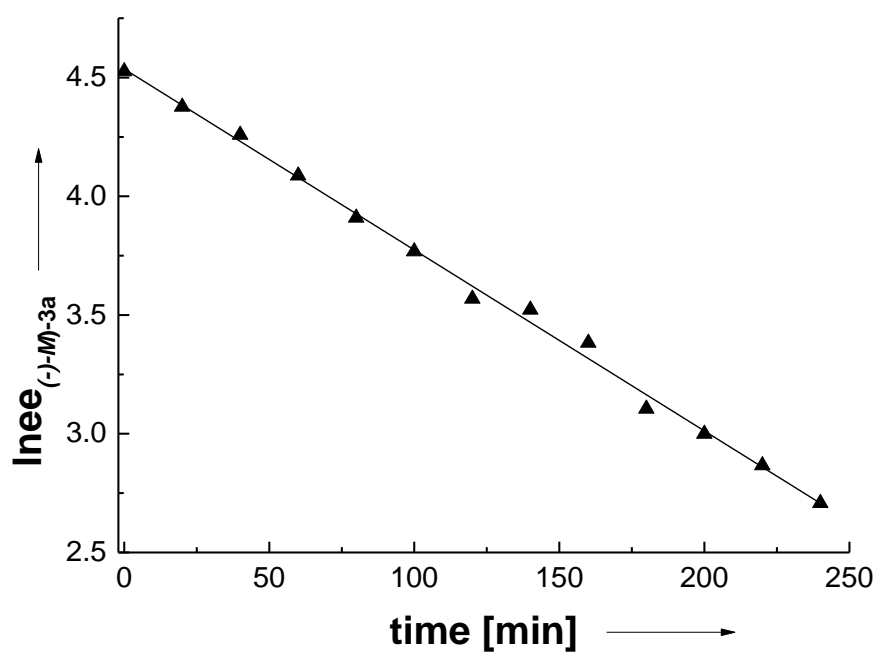
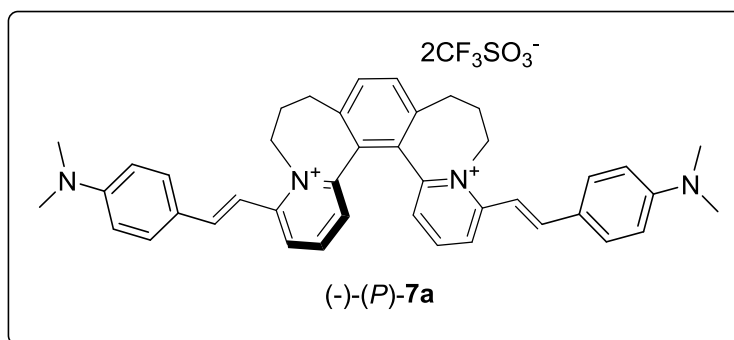


**Figure S16.** Racemization of (-)-(*M*)-**3a** in DMSO at 62°C. Dependence of natural logarithm of the enantiomeric excess  $\ln ee_{(-)-M-3a}$  on time as determined by CE.

According to the equations showed for the racemization of (-)-(*M*)-**3**, the experimental value for (-)-(*M*)-**3a** was determined to be  $\Delta G^\ddagger = 109.25 \text{ kJ}\cdot\text{mol}^{-1}$  (measured at 62°C) determining the half-life to be 1 h and 30 min at 62°C.

## 5. Racemization barrier determination of (-)-*(P)*-7a:



The racemization barrier determination was performed in a block-heater with the actual temperature in the reaction vessel set to 66°C. (-)-*(P)*-7a (1.0 mg, 1.1 μmol) was dissolved in DMSO (0.5 mL) and transferred to an NMR tube. The tube was placed into one of the holes of the block-heater filled with Rotitherm heating medium. The racemization experiment was run at 66°C. Before starting the heating, a sample for CE analysis (ca 10 μL) was taken with a capillary. Then, the NMR tube was immersed in the block with the Rotitherm medium equilibrated to 66°C. Samples for CE analysis (ca 10 μL) were taken every 20 min with a capillary (for illustrative CE charts, see Figure S17). The experiment was stopped after 240 min. The decreasing amount of (-)-*(P)*-7a in the NMR tube monitored by CE (Figure S17) is listed in Table S6 and plotted in Figure S18.

**Table S6.** Racemization of (-)-(*P*)-**7a** monitored by CE (DMSO at 66°C). For illustrative CE charts, see Figure S17.

time (min)	(-)-( <i>P</i> )- <b>7a</b> (%)	(+)-( <i>M</i> )- <b>7a</b> (%)	<i>ee</i> <sub>(-)-(<i>P</i>)-<b>7a</b></sub>	<i>lnee</i> <sub>(-)-(<i>P</i>)-<b>7a</b></sub>
0	99.28	0.72	98.56	4.591
20	98.005	1.995	96.01	4.564
40	96.8	3.2	93.60	4.539
60	95.625	4.375	91.25	4.514
80	94.46	5.54	88.92	4.488
100	93.57	6.43	87.14	4.468
120	92.09	7.91	84.18	4.433
140	91.19	8.81	82.38	4.411
160	88.98	11.02	77.96	4.356
180	88.95	11.05	77.90	4.355
200	87.875	12.125	75.75	4.327
220	87.26	12.74	74.52	4.311
240	86.205	13.795	72.41	4.282



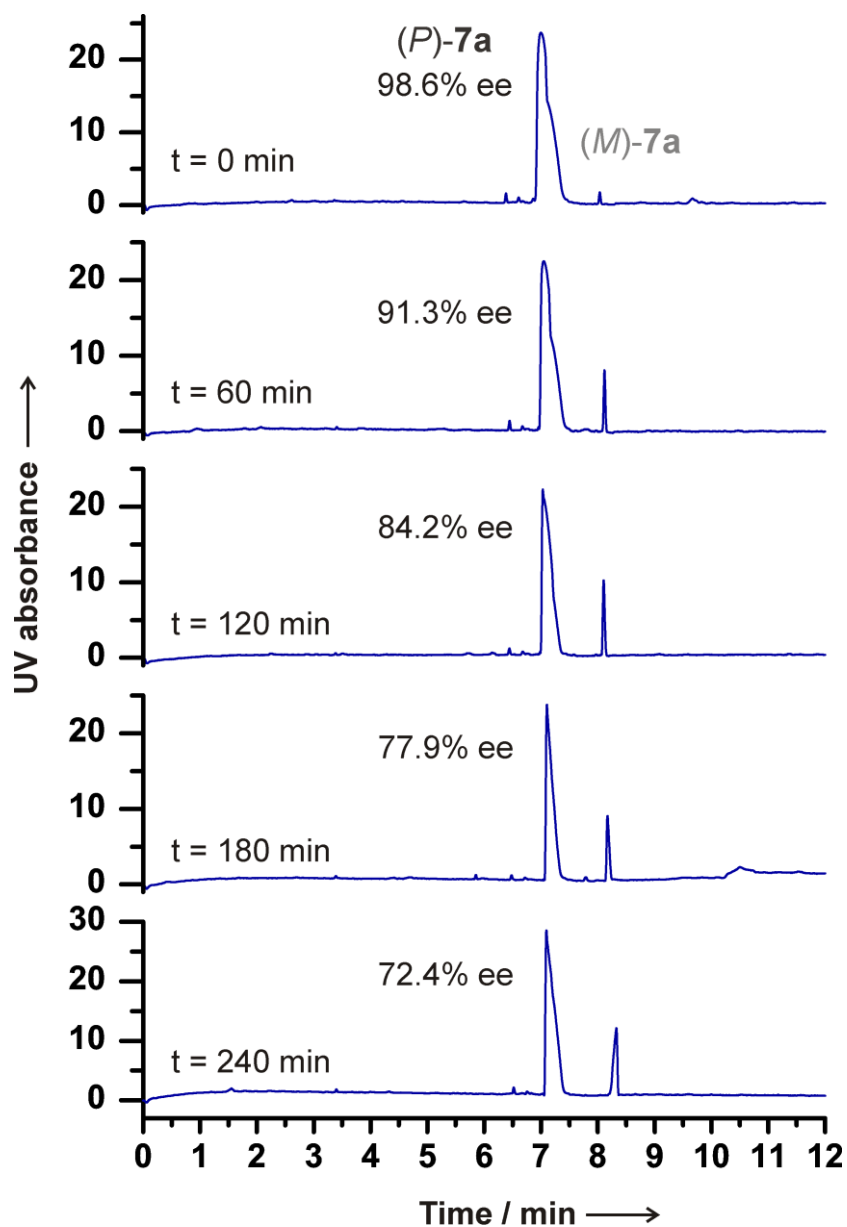


**Figure S17.** CE charts from the individual composition analyses during the racemization of (-)-(P)-7a at 66°C in DMSO starting from mixture (-)-(P)-7a : (+)-(M)-7a = 99 : 1. The samples were analyzed in defined intervals (every 20 min) and only selected traces are shown here. For full data see Table S6 and plot in Figure S18.

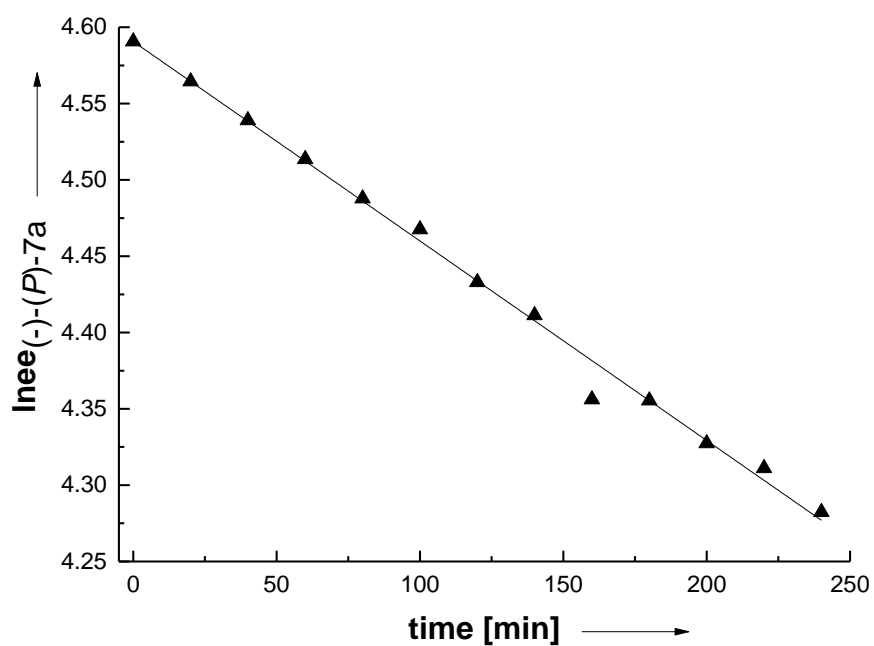


**Figure S18.** Racemization of (-)-(P)-**7a** in DMSO at 66°C. Dependence of natural logarithm of the enantiomeric excess  $\ln ee_{(-)-(P)-7a}$  on time as determined by CE.

According to the equations showed for the racemization of (+)-(M)-**3**, the experimental value for (-)-(P)-**7a** was  $\Delta G^\ddagger = 115.5 \text{ kJ}\cdot\text{mol}^{-1}$  (measured at 66°C) determining the half-life to be 8 h and 50 min at 66°C.

## 5) Experimental UV-Vis absorption and ECD spectra

### 1. UV-Vis absorption spectra for (*rac*)-**6** and (*rac*)-**6a-h**

**Table S7.** UV/Vis molar absorption coefficient ( $\epsilon$ ) and corresponding absorption wavelength maximum ( $\lambda_{\max}$ ) for (*rac*)-**6** and (*rac*)-**6a-h**.

Entry	Compound	UV/Vis	
		$\lambda_{\max}$ [nm]	$\epsilon$ [ $M^{-1}cm^{-1}$ ]
1	<b>(<i>rac</i>)-6</b>	374	13666
2	<b>(<i>rac</i>)-6a</b>	525	29466
3	<b>(<i>rac</i>)-6b</b>	375	42069
4	<b>(<i>rac</i>)-6c</b>	577	30035
5	<b>(<i>rac</i>)-6d</b>	438	25406
6	<b>(<i>rac</i>)-6e</b>	491	27302
7	<b>(<i>rac</i>)-6f</b>	367	29073
8	<b>(<i>rac</i>)-6g</b>	374	35650
9	<b>(<i>rac</i>)-6h</b>	470	6410

### 2. ECD and UV-Vis absorption spectra for (-)-(*P*)-**3**, and (+)-(*M*)-**3**

The ECD and UV-Vis absorption spectra for (-)-(*P*)-**3**, and (+)-(*M*)-**3** were measured in a quartz cuvette with an optical path length of 1 mm (Helma, Germany) using a J-810 spectrometer (Jasco, Japan) equipped with a thermostat controlled cell holder attached to a Jasco Peltier temperature control system PTC-423S with an accuracy of  $\pm 0.2^\circ C$ . The conditions of the measurements were as follows: a spectral region of 200–800 nm, a scanning speed of 100 nm/min, a response time of 1 s, a resolution of 1 nm, a bandwidth of 1 nm, a sensitivity of 1000 mdeg and controlled temperature of  $25^\circ C$ . The measurements were done at the 0.1 mM concentration of the compound. The solutions were prepared by diluting the appropriate amount of the compound in MeOH. The final spectra were obtained as an average of 3 accumulations. The spectra were corrected for a baseline by subtracting the spectrum of the solvent. For data plots, see Figure S19.

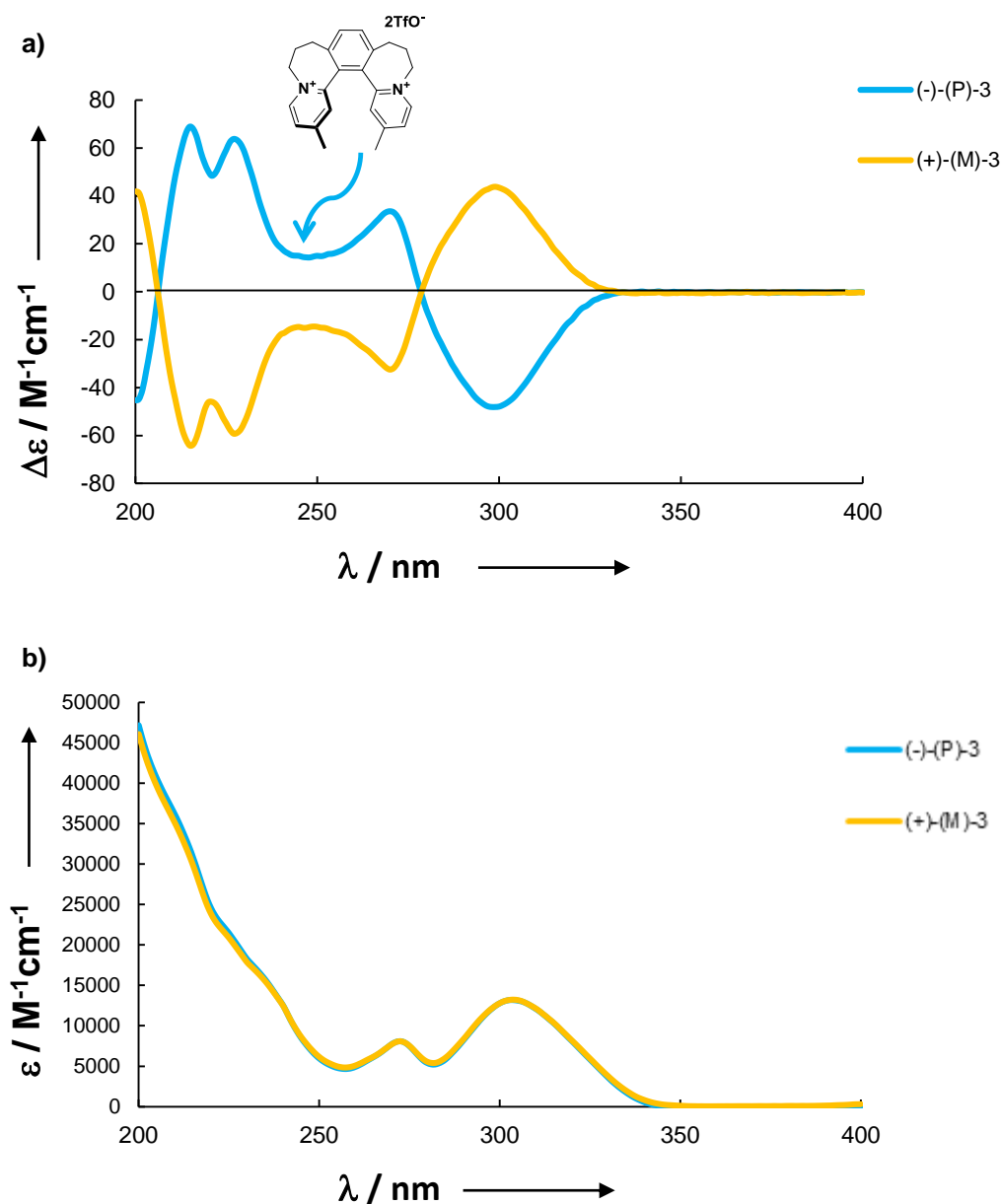


**Figure S19.** a) ECD spectra of (-)-(P)-3 (blue line) and (+)-(M)-3 (yellow line). b) UV/Vis spectra of (-)-(P)-3 and (+)-(M)-3. MeOH solutions (0.1 mM).

### 3. ECD and UV-Vis absorption spectra for (+)-(P)-3a, (-)-(P)-3i, (-)-(P)-3j, (-)-(M)-3a, (+)-(M)-3i, and (+)-(M)-3j

The ECD and UV-Vis absorption spectra for (+)-(P)-3a, (-)-(P)-3i, (-)-(P)-3j, (-)-(M)-3a, (+)-(M)-3i, and (+)-(M)-3j were measured in a quartz cuvette with an optical path length of 1 mm (Helma, Germany) using a J-810 spectrometer (Jasco, Japan) equipped with a thermostat controlled cell holder attached to a Jasco Peltier temperature control system PTC-

423S with an accuracy of  $\pm 0.2^\circ\text{C}$ . The conditions of the measurements were as follows: a spectral region of 200–800 nm, a scanning speed of 100 nm/min, a response time of 1 s, a resolution of 1 nm, a bandwidth of 1 nm, a sensitivity of 1000 mdeg and controlled temperature of  $25^\circ\text{C}$ . The measurements were done at the 0.1 mM concentration of the compound with the exception of (-)-**(M)-3a** and (+)-**(M)-3i** which were measured at 0.25 mM concentration. The solutions were prepared by diluting the appropriate amount of the compound in MeOH. The final spectra were obtained as an average of 3 accumulations. The spectra were corrected for a baseline by subtracting the spectrum of the solvent. For summary overlay of ECD curves, see Figure S20a. The individual data plots, see Figures S21-23. ECD molar circular dichroism ( $\Delta\varepsilon$ ) and the corresponding wavelength ( $\lambda_{\text{max}}$ ), and UV/Vis molar absorption coefficient ( $\varepsilon$ ) and the corresponding absorption wavelength ( $\lambda_{\text{max}}$ ) are shown in Table S8.

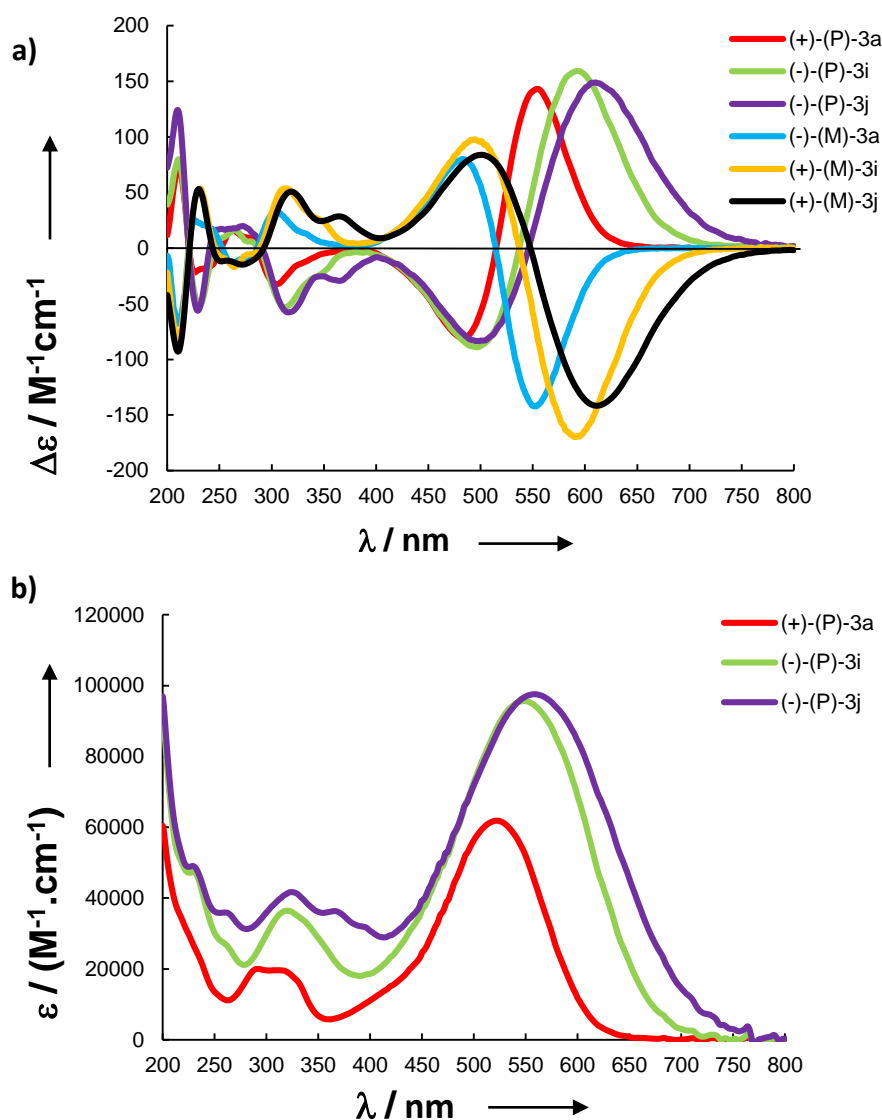


**Figure S20.** a) ECD spectra of (+)-(P)-**3a**, (-)-(P)-**3i**, and (-)-(P)-**3j** with positive Cotton effects in the visible region and their respective enantiomers (-)-(M)-**3a**, (+)-(M)-**3i**, and (+)-(M)-**3j** with negative Cotton effects in the visible region. MeOH solutions were used (0.1 mM concentration for all compounds, except for (-)-(M)-**3a** and (+)-(M)-**3i** which were measured at 0.25 mM concentration). b) UV/Vis spectra of (+)-(P)-**3a**, (-)-(P)-**3i**, and (-)-(P)-**3j**. UV/Vis spectra of (-)-(M)-**3a**, (+)-(M)-**3i**, and (+)-(M)-**3j** are not shown here. They are essentially identical to the UV/Vis spectra of the respective enantiomers (+)-(P)-**3a**, (-)-(P)-**3i**, and (-)-(P)-**3j** as shown in Figures S21-23.

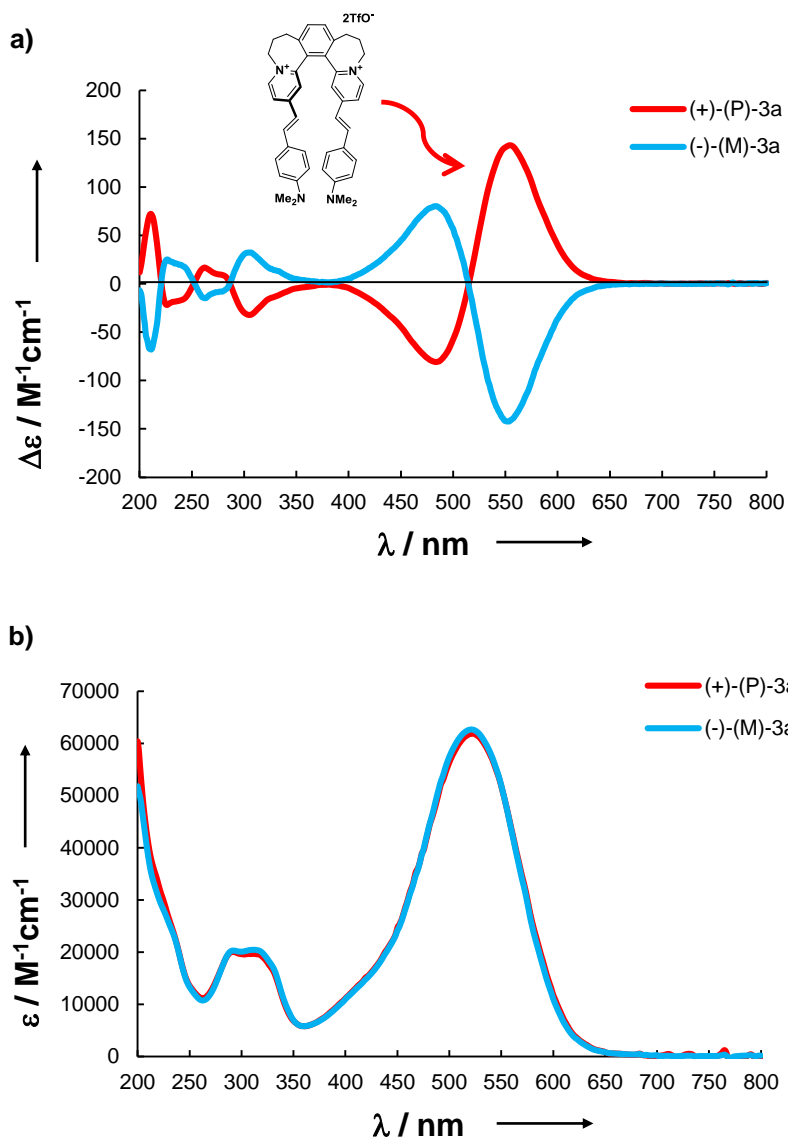


**Figure S21.** a) ECD spectra of (+)-(*P*)-**3a** (red line, positive Cotton effect in the visible region) and (-)-(*M*)-**3a** (blue line, negative Cotton effect in the visible region). b) UV/Vis spectra of (+)-(*P*)-**3a** and (-)-(*M*)-**3a**.

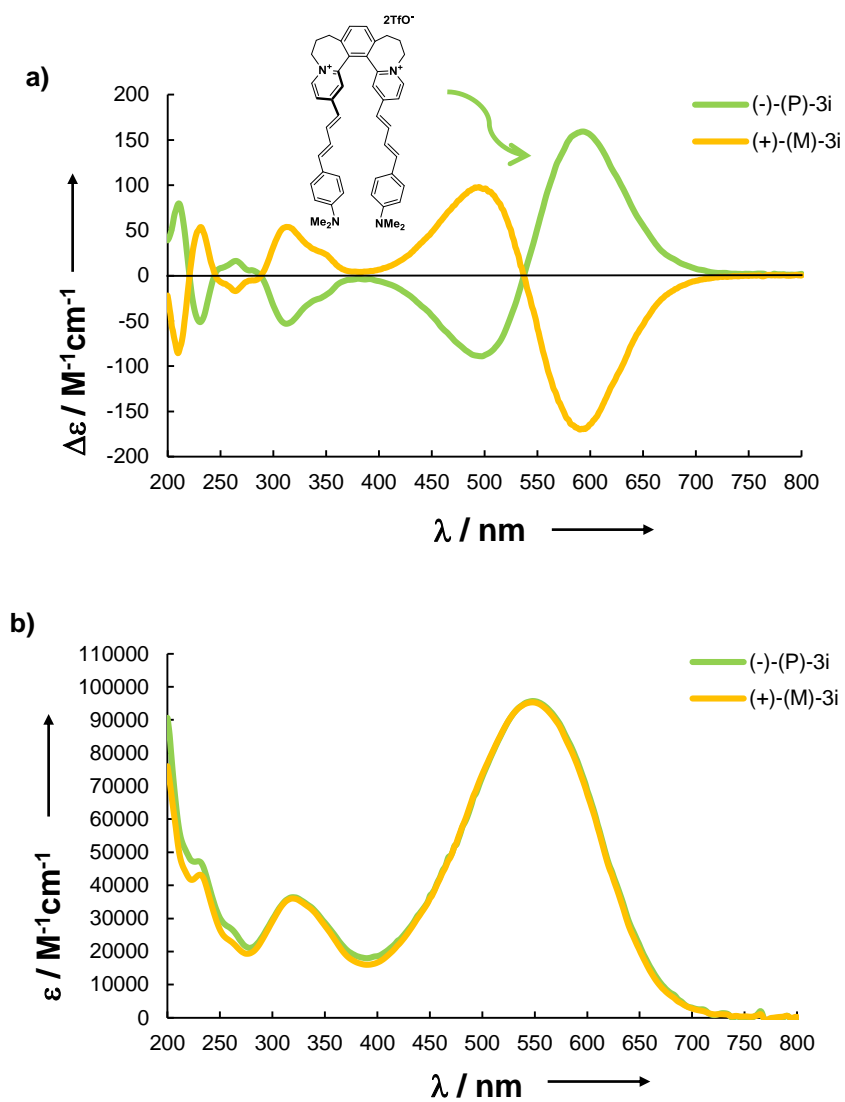


**Figure S22.** a) ECD spectra of (-)-(P)-3i (green line, positive Cotton effect in the visible region) and (+)-(M)-3i (yellow line, negative Cotton effect in the visible region). b) UV/Vis spectra of (-)-(P)-3i and (+)-(M)-3i.



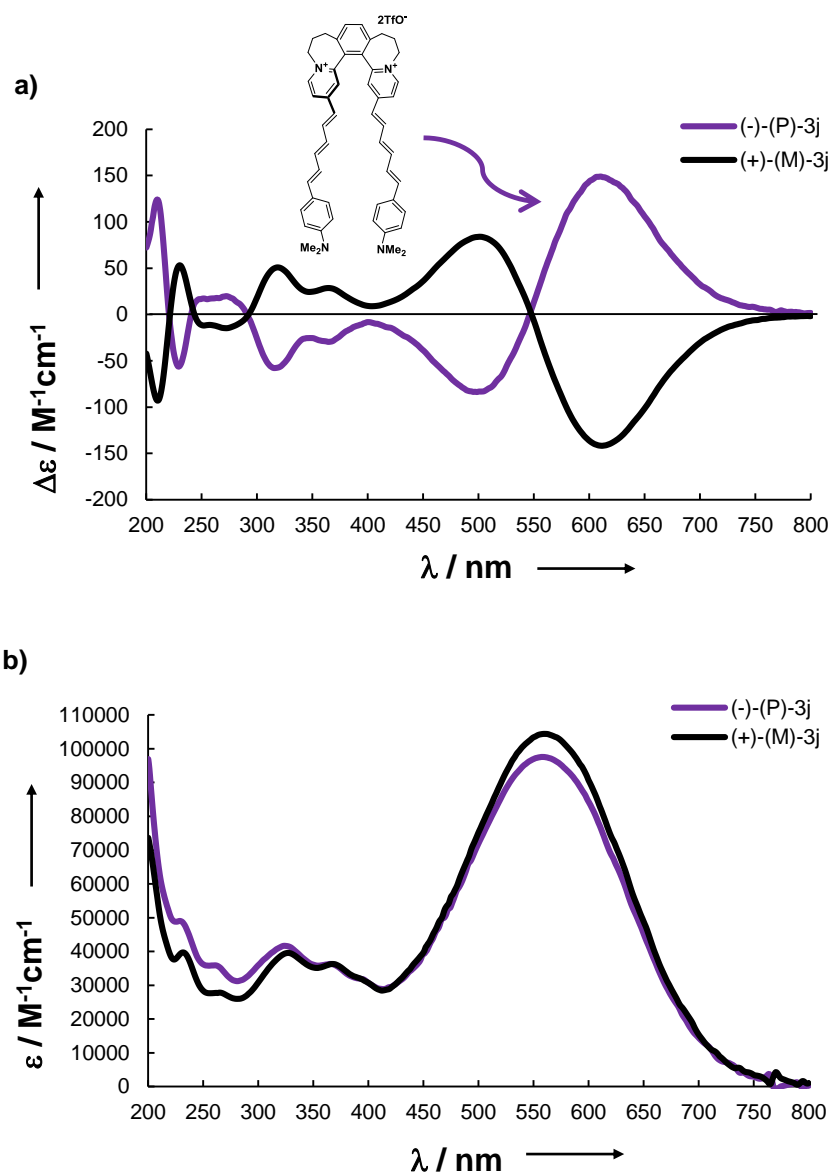


**Figure S23.** a) ECD spectra of (-)-(P)-**3j** (violet line, positive Cotton effect in visible region) and (+)-(M)-**3j** (black line, negative Cotton effect in visible region). b) UV/Vis spectra of (-)-(P)-**3j** and (+)-(M)-**3j**.

**Table S8.** ECD molar circular dichroism ( $\Delta\varepsilon$ ) and corresponding wavelength ( $\lambda_{\max}$ ) and UV/Vis molar absorption coefficient ( $\varepsilon$ ) and corresponding absorption wavelength ( $\lambda_{\max}$ ).

Entry	Compound	ECD		UV/Vis	
		$\lambda_{\max}$ [nm]	$\Delta\varepsilon$ [ $M^{-1}cm^{-1}$ ]	$\lambda_{\max}$ [nm]	$\varepsilon$ [ $M^{-1}cm^{-1}$ ]
1	(-)-(P)- <b>3</b>	298	-48.1	303	13200
2	(+)-(M)- <b>3</b>	299	43.8	304	13233
3	(+)-(P)- <b>3a</b>	555	143.2	522	61883
4	(-)-(M)- <b>3a</b>	552	-142.2	521	62702
5	(-)-(P)- <b>3i</b>	593	159.3	548	95702
6	(+)-(M)- <b>3i</b>	590	-169.8	548	95257
7	(-)-(P)- <b>3j</b>	610	149.0	558	97543
8	(+)-(M)- <b>3j</b>	611	-141.7	560	104362

#### 4. ECD and UV-Vis absorption spectra for (-)-(P)-**7** and (+)-(M)-**7**

The ECD and UV-Vis absorption spectra for (-)-(P)-**7**, and (+)-(M)-**7** were measured in a quartz cuvette with an optical path length of 1 mm (Helma, Germany) using a J-810 spectrometer (Jasco, Japan) equipped with a thermostat controlled cell holder attached to a Jasco Peltier temperature control system PTC-423S with an accuracy of  $\pm 0.2^{\circ}C$ . The conditions of the measurements were as follows: a spectral region of 200–800 nm, a scanning speed of 100 nm/min, a response time of 1 s, a resolution of 1 nm, a bandwidth of 1 nm, a sensitivity of 1000 mdeg and controlled temperature of  $25^{\circ}C$ . The measurements were done at the 0.1 mM concentration of the compound. The solutions were prepared by diluting the appropriate amount of the compound in MeOH. The final spectra were obtained as an average of 3 accumulations. The spectra were corrected for a baseline by subtracting the spectrum of the solvent. For data plots, see Figure S24.

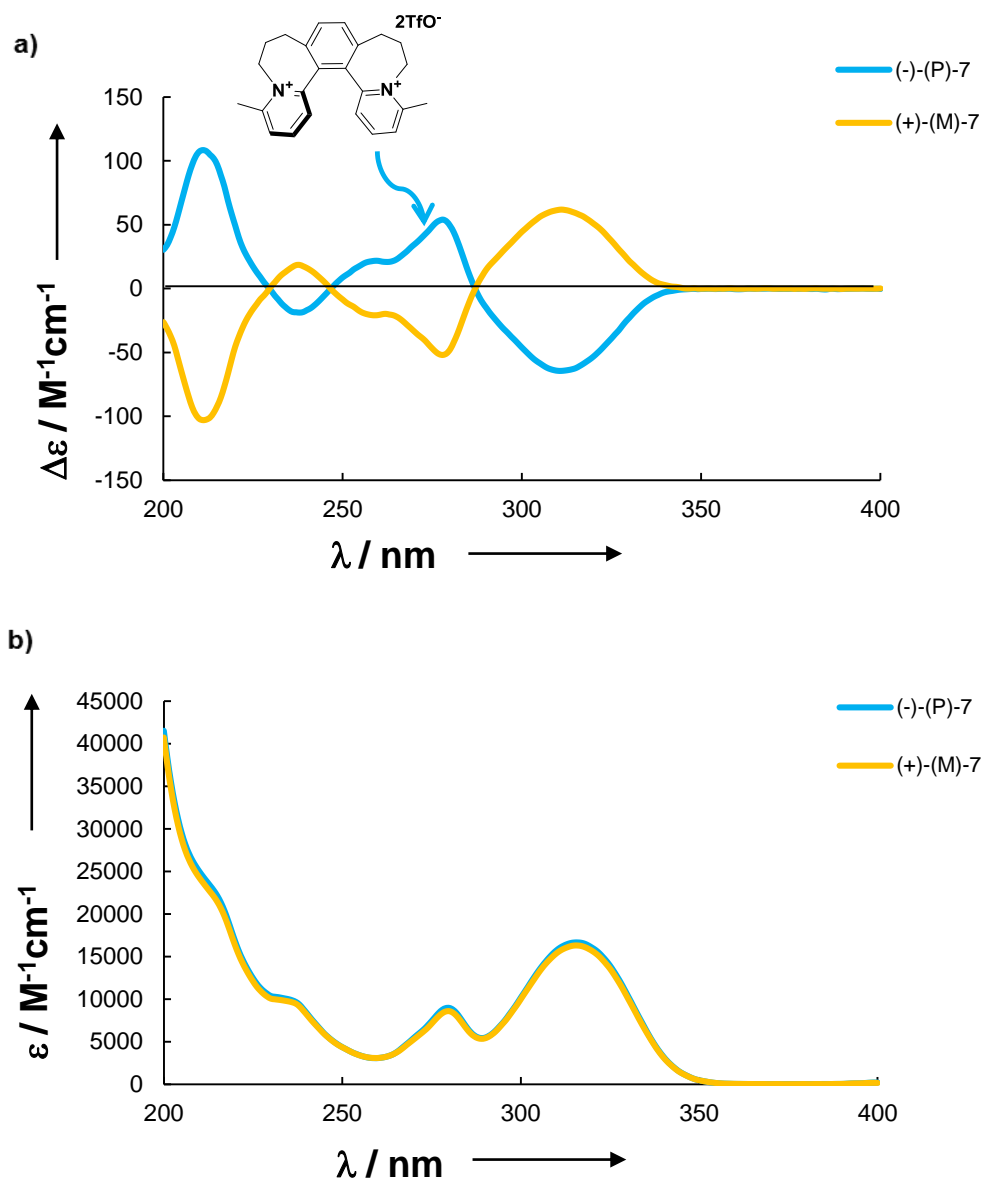


**Figure S24.** a) ECD spectra of (-)-(P)-7 (blue line) and (+)-(M)-7 (yellow line). b) UV/Vis spectra of (-)-(P)-7 and (+)-(M)-7. MeOH solutions (0.1 mM).

### 5. ECD and UV-Vis absorption spectra for (-)-(P)-7a, (-)-(P)-7i, (-)-(P)-7j, (+)-(M)-7a, (+)-(M)-7i, and (+)-(M)-7j

The ECD and UV-Vis absorption spectra for (-)-(P)-7a, (-)-(P)-7i, (-)-(P)-7j, (+)-(M)-7a, (+)-(M)-7i, and (+)-(M)-7j were measured in a quartz cuvette with an optical path length of 1 mm (Helma, Germany) using a J-810 spectrometer (Jasco, Japan) equipped with a thermostat controlled cell holder attached to a Jasco Peltier temperature control system PTC-423S with

an accuracy of  $\pm 0.2^\circ\text{C}$ . The conditions of the measurements were as follows: a spectral region of 200–800 nm, a scanning speed of 100 nm/min, a response time of 1 s, a resolution of 1 nm, a bandwidth of 1 nm, a sensitivity of 1000 mdeg and controlled temperature of  $25^\circ\text{C}$ . The measurements were done at the 0.1 mM concentration of the compound. The solutions were prepared by diluting the appropriate amount of the compound in MeOH. The final spectra were obtained as an average of 3 accumulations. The spectra were corrected for a baseline by subtracting the spectrum of the solvent. For summary overlay of ECD curves, see Figure S25a. For individual data plots, see Figures S26-28. ECD molar circular dichroism ( $\Delta\epsilon$ ) and corresponding wavelength ( $\lambda_{\text{max}}$ ), and UV/Vis molar absorption coefficient ( $\epsilon$ ) and corresponding absorption wavelength ( $\lambda_{\text{max}}$ ) are shown in Table S9.

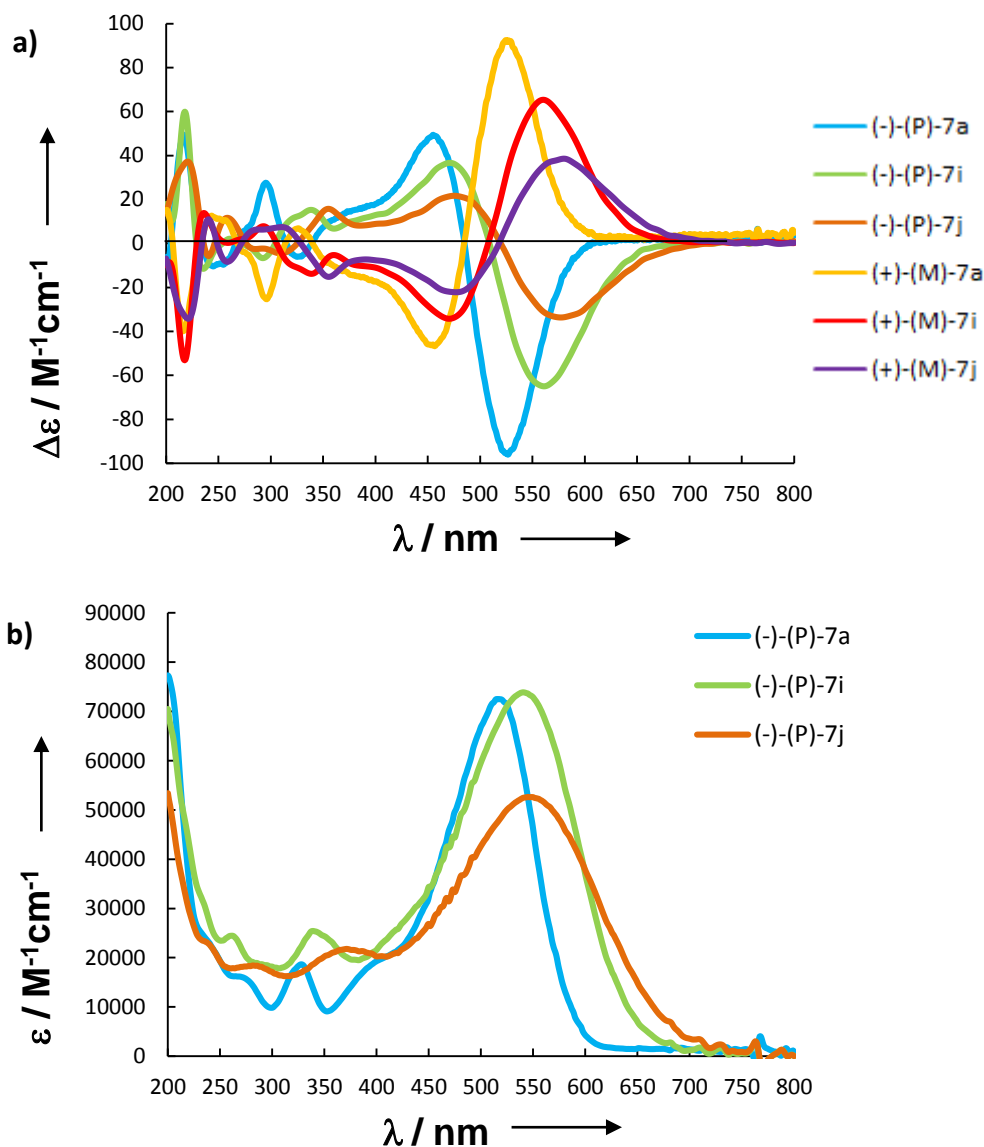


**Figure S25.** ECD spectra of (-)-(P)-**7a**, (-)-(P)-**7i**, and (-)-(P)-**7j** with negative Cotton effects in the visible region and their respective enantiomers (+)-(M)-**7a**, (+)-(M)-**7i**, and (+)-(M)-**7j** with positive Cotton effects in the visible region. MeOH solutions were used (0.1 mM concentration for all compounds). b) UV/Vis spectra of (-)-(P)-**7a**, (-)-(P)-**7i**, and (-)-(P)-**7j**. UV/Vis spectra of (+)-(M)-**7a**, (+)-(M)-**7i**, and (+)-(M)-**7j** are not shown here. They are essentially identical to the UV/Vis spectra of the respective enantiomers (-)-(P)-**7a**, (-)-(P)-**7i**, and (-)-(P)-**7j** as shown in Figures S26-28.

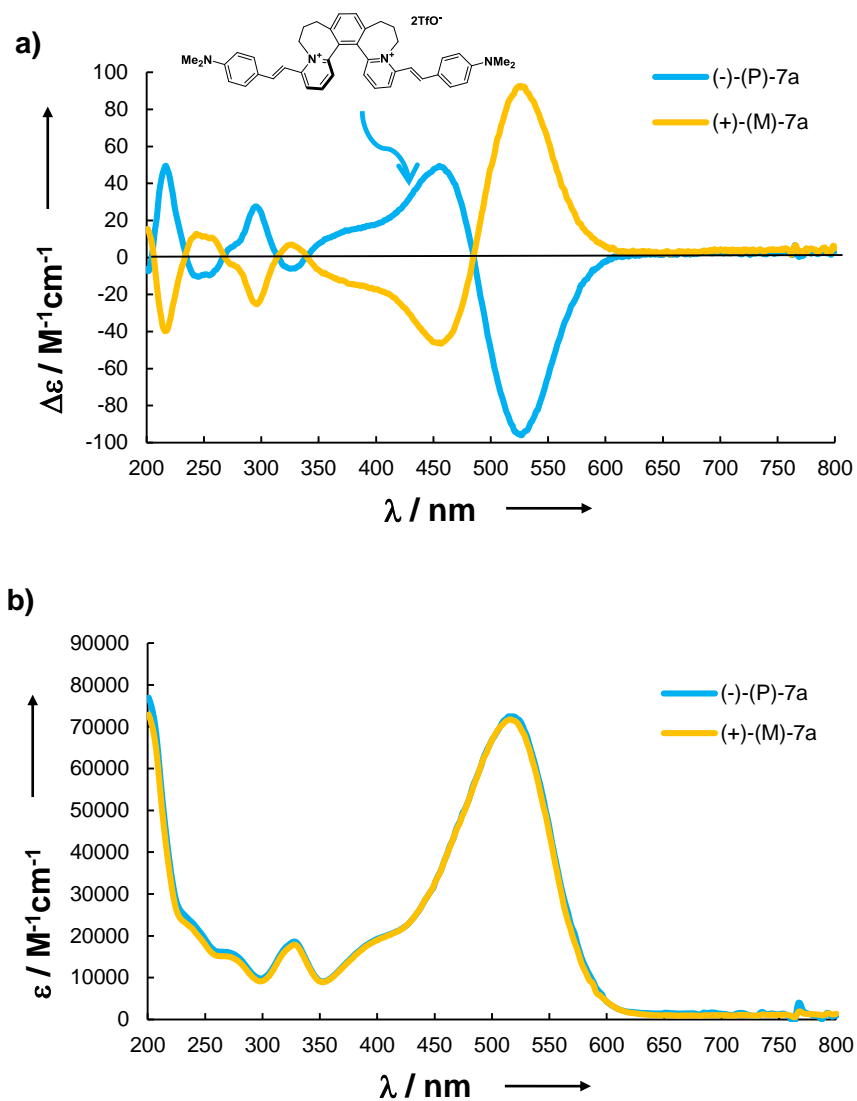


**Figure S26.** a) ECD spectra of (-)-(P)-7a (blue line, negative Cotton effect in the visible region) and (+)-(M)-7a (yellow line, positive Cotton effect in the visible region). b) UV/Vis spectra of (-)-(P)-7a and (+)-(M)-7a.

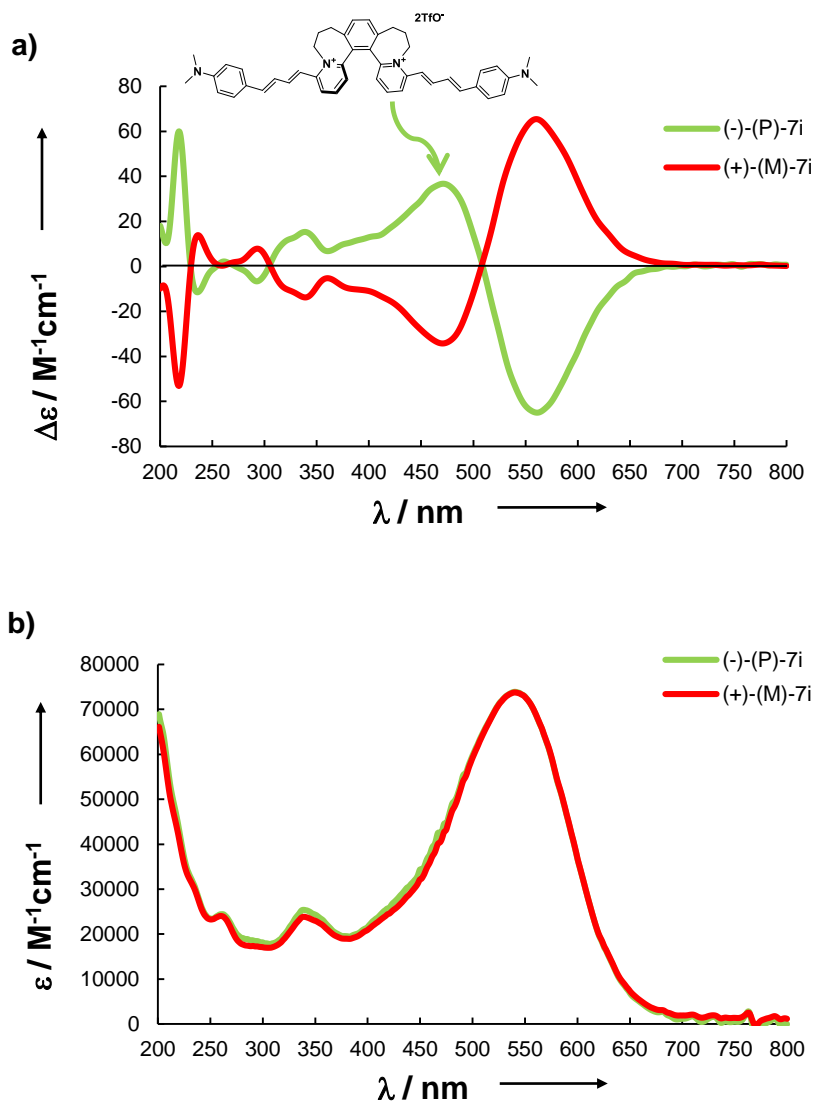


**Figure S27.** a) ECD spectra of (-)-(P)-7i (green line, negative Cotton effect in the visible region) and (+)-(M)-7i (orange line, positive Cotton effect in the visible region). b) UV/Vis spectra of (-)-(P)-7i and (+)-(M)-7i.

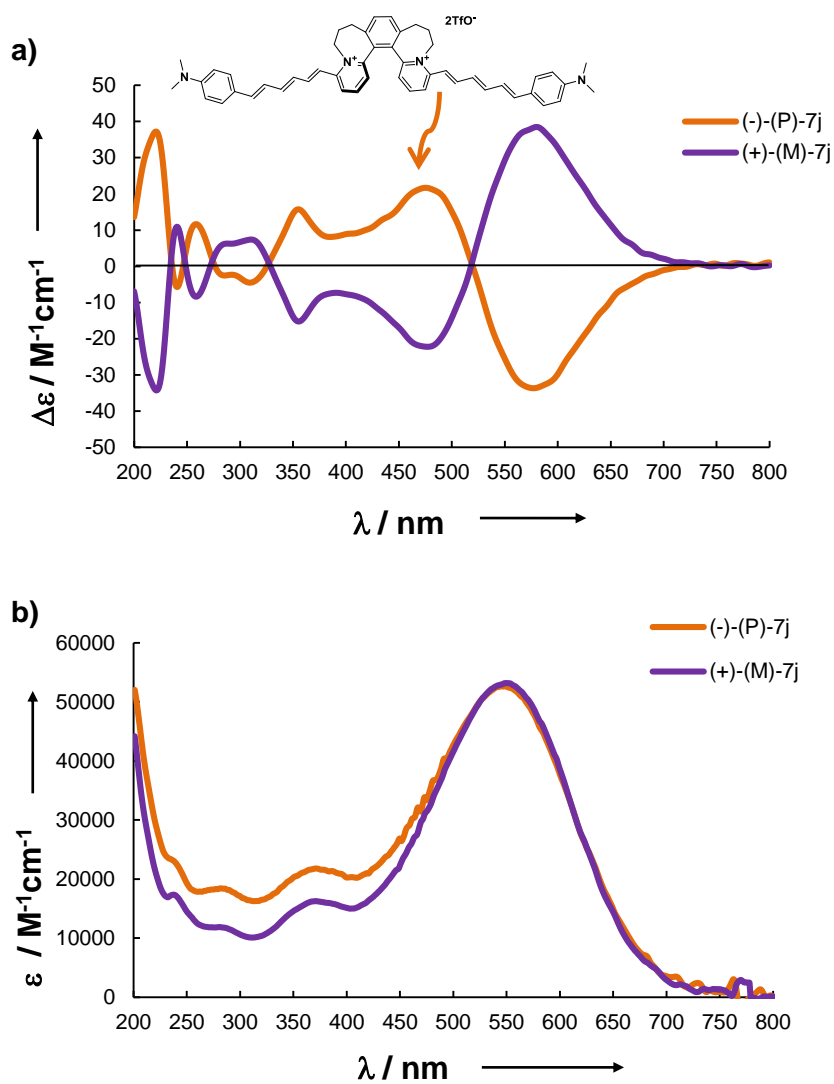


**Figure S28.** a) ECD spectra of (-)-(P)-7j (orange line, negative Cotton effect in the visible region) and (+)-(M)-7j (violet line, positive Cotton effect in the visible region). b) UV/Vis spectra of (-)-(P)-7j and (+)-(M)-7j.



**Table S9.** ECD molar circular dichroism ( $\Delta\varepsilon$ ) and corresponding wavelength ( $\lambda_{\max}$ ), and UV/Vis molar absorption coefficient ( $\varepsilon$ ) and corresponding absorption wavelength ( $\lambda_{\max}$ ).

Entry	Compound	ECD		UV/Vis	
		$\lambda_{\max}$ [nm]	$\Delta\varepsilon$ [ $\text{M}^{-1}\text{cm}^{-1}$ ]	$\lambda_{\max}$ [nm]	$\varepsilon$ [ $\text{M}^{-1}\text{cm}^{-1}$ ]
1	(-)-(P)- <b>7</b>	311	-64.5	316	16648
2	(+)-(M)- <b>7</b>	311	61.8	316	16289
3	(-)-(P)- <b>7a</b>	527	-96.0	517	72512
4	(+)-(M)- <b>7a</b>	527	92.5	516	71754
5	(-)-(P)- <b>7i</b>	561	-65.0	540	73883
6	(+)-(M)- <b>7i</b>	560	65.4	540	73720
7	(-)-(P)- <b>7j</b>	577	-33.7	548	52611
8	(+)-(M)- <b>7j</b>	580	38.5	550	53170

### 6. ECD and UV/Vis absorption spectra for pH-switchable dyes (+)-(P)-**3k** and (-)-(M)-**3k**

The ECD and UV/Vis absorption spectra for (+)-(P)-**3k** and (-)-(M)-**3k** were measured in a quartz cuvette with an optical path length of 1 mm (Helma, Germany) using a J-810 spectrometer (Jasco, Japan) equipped with a thermostat controlled cell holder attached to a Jasco Peltier temperature control system PTC-423S with an accuracy of  $\pm 0.2^\circ\text{C}$ . The conditions of the measurements were as follows: a spectral region of 200–800 nm, a scanning speed of 100 nm/min, a response time of 1 s, a resolution of 1 nm, a bandwidth of 1 nm, a sensitivity of 1000 mdeg and controlled temperature  $25^\circ\text{C}$ . The solutions were prepared by diluting the appropriate amount of the compound in MeOH (0.1 mM). The final spectra were obtained as an average of 3 accumulations. The spectra were corrected for a baseline by subtracting the spectrum of the solvent. ECD molar circular dichroism ( $\Delta\varepsilon$ ) and corresponding wavelength ( $\lambda_{\max}$ ), and UV/Vis molar absorption coefficient ( $\varepsilon$ ) and corresponding absorption wavelength ( $\lambda_{\max}$ ) are shown in Table S10.

The initial spectrum of each compound alone was measured in the concentration of 0.1 mM and solution of this concentration was also used as a stock solution for pH-switching experiments.

1) **ECD and UV/Vis spectra of (+)-(P)-3k and (-)-(M)-3k under basic conditions**

10  $\mu\text{L}$  of 0.1 M pyrrolidine solution in methanol was added to a 0.1 mM stock solutions (300  $\mu\text{L}$ ) of (+)-(P)-3k (blue curve, Figure S29) and (-)-(M)-3k (violet curve) in methanol. ECD and UV/Vis spectra were measured.

2) **ECD and UV/Vis spectra of (+)-(P)-3k and (-)-(M)-3k under acidic conditions**

10  $\mu\text{L}$  of 0.1 M TfOH solution in methanol was added to a 0.1 mM stock solutions (300  $\mu\text{L}$ ) of (+)-(P)-3k (yellow curve, Figure S29) and (-)-(M)-3k (orange curve) in methanol. ECD and UV/Vis spectra were measured.

**pH-switching with (-)-(M)-3k starting with acidic conditions**

**(switching sequence: acidic  $\rightarrow$  basic  $\rightarrow$  acidic pH)**

For pH-switching experiment with (-)-(M)-3k starting with acidic conditions, 10  $\mu\text{L}$  of 0.1 M TfOH solution in methanol was added to a 0.1 mM (-)-(M)-3k in methanol (Solution 1, orange curve, Figure S30). Next, 20  $\mu\text{L}$  of 0.1 M pyrrolidine solution in methanol was added to switch to basic conditions (Solution 2, violet curve). Finally, 20  $\mu\text{L}$  of 0.1 M TfOH solution in methanol was added to switch to acidic conditions (Solution 3, green curve). ECD and UV/Vis spectra were measured after each addition.

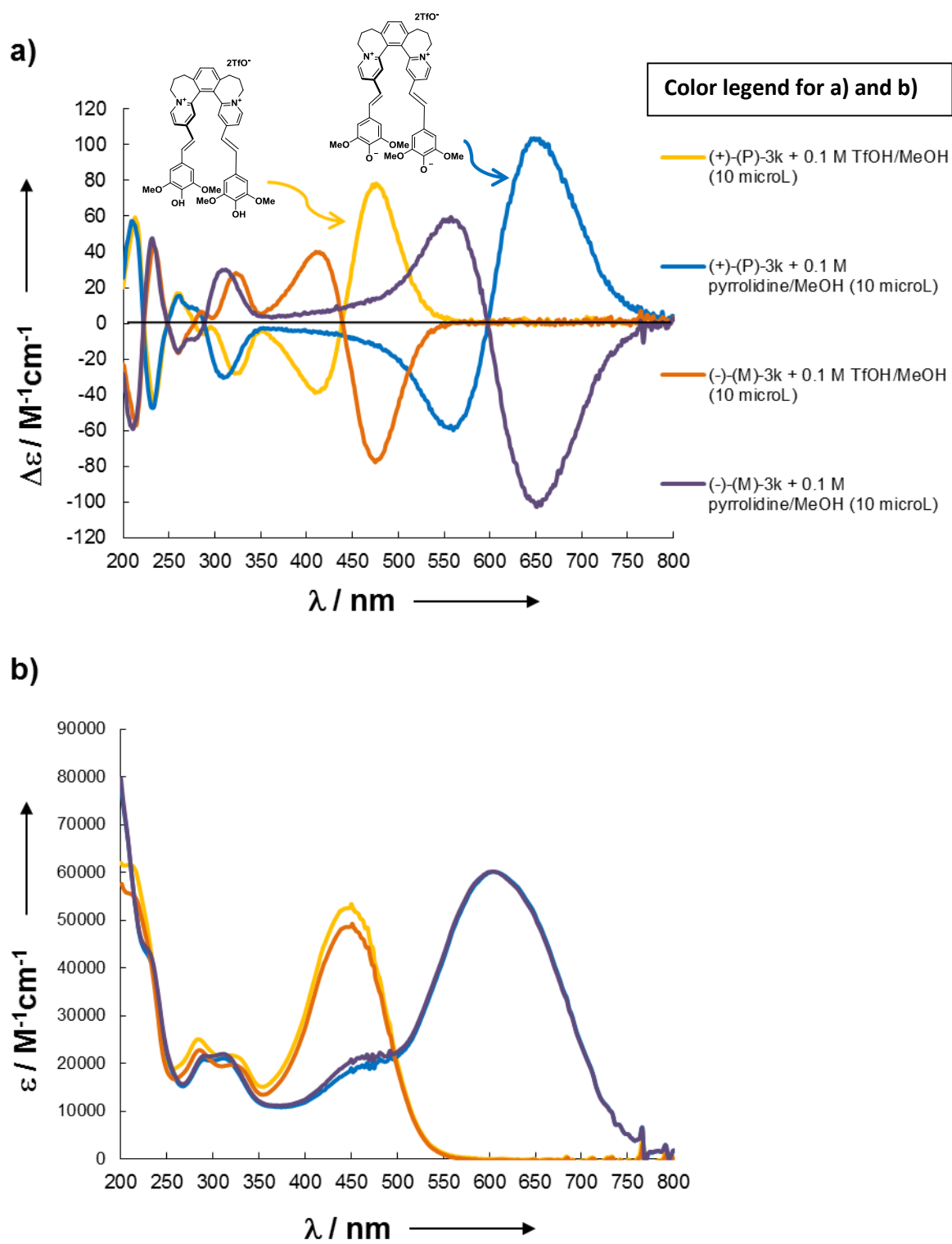


**Figure S29.** a) ECD spectra and b) UV/Vis spectra of (+)-(P)-**3k** under acidic (yellow curves) and basic conditions (blue curves) and of (-)-(M)-**3k** under acidic (orange curves) and basic conditions (violet curves).

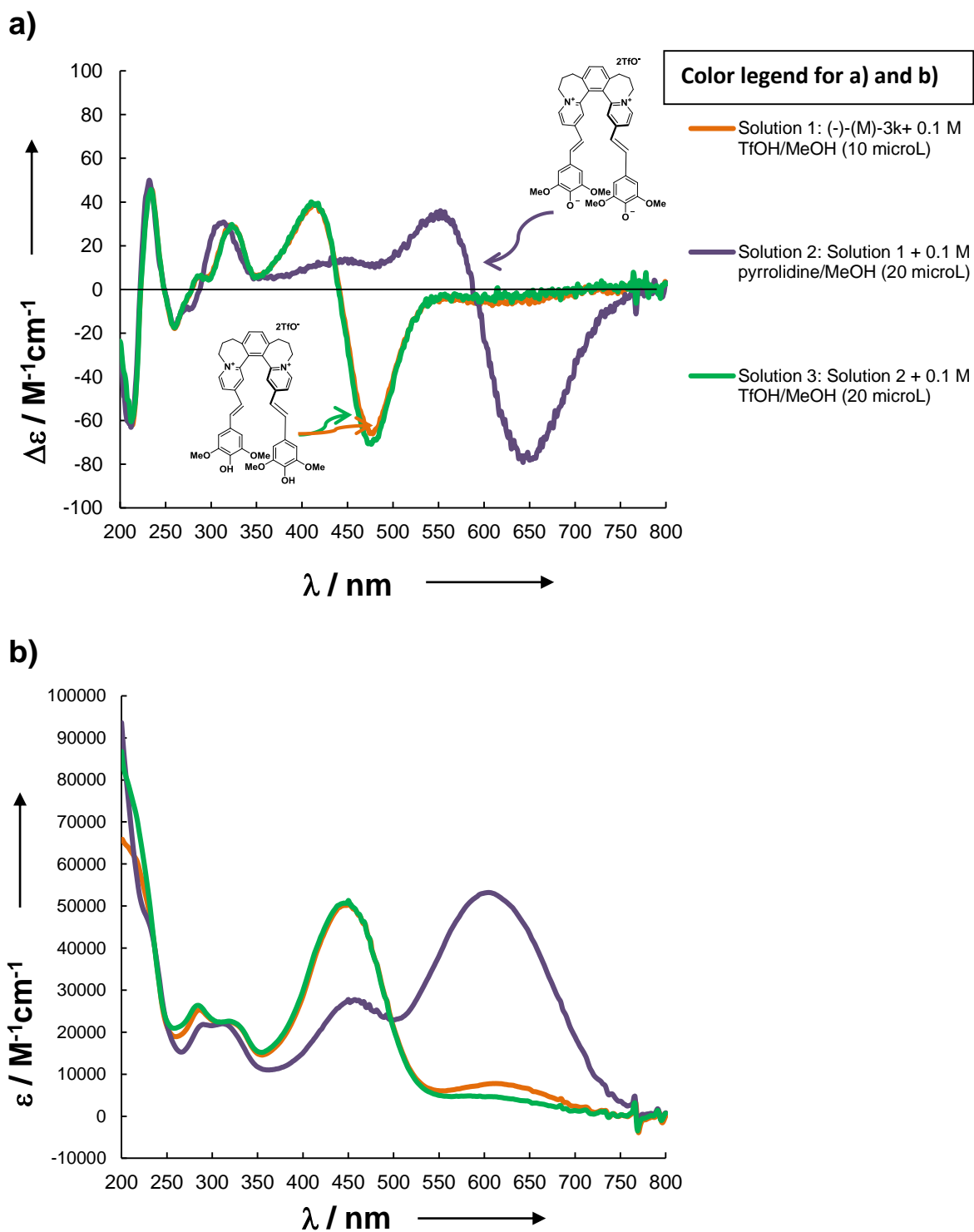


**Figure S30.** a) ECD spectra; b) UV/Vis spectra recorded in the course of pH-switching experiments starting with (-)-(M)-**3k** under acidic conditions. pH-switching sequence: acidic  $\rightarrow$  basic  $\rightarrow$  acidic corresponds to spectral changes in ECD and UV/Vis (orange  $\rightarrow$  violet  $\rightarrow$  green curves).

**Table S10.** ECD molar circular dichroism ( $\Delta\varepsilon$ ) and corresponding wavelength ( $\lambda_{\max}$ ), and UV/Vis molar absorption coefficient ( $\varepsilon$ ) and corresponding absorption wavelength ( $\lambda_{\max}$ ).

Entry	Compound	ECD		UV/Vis	
		$\lambda_{\max}$ [nm]	$\Delta\varepsilon$ [ $M^{-1}cm^{-1}$ ]	$\lambda_{\max}$ [nm]	$\varepsilon$ [ $M^{-1}cm^{-1}$ ]
1	(+)-(P)- <b>3k</b> <sub>basic pH</sub>	648	103.7	605	60118
2	(-)-(M)- <b>3k</b> <sub>basic pH</sub>	651	-102.7	604	60190
3	(+)-(P)- <b>3k</b> <sub>acidic pH</sub>	476	78.4	449	52743
4	(-)-(M)- <b>3k</b> <sub>acidic pH</sub>	475	-77.8	445	48619

### 7. ECD and UV/Vis absorption spectra for pH-switchable dyes (-)-(P)-**7k** and (+)-(M)-**7k**

The ECD and UV-Vis absorption spectra for compounds (-)-(P)-**7k** and (+)-(M)-**7k** were measured in a quartz cuvette with an optical path length of 1 mm (Helma, Germany) using a J-810 spectrometer (Jasco, Japan) equipped with a thermostat controlled cell holder attached to a Jasco Peltier temperature control system PTC-423S with an accuracy of  $\pm 0.2^\circ C$ . The conditions of the measurements were as follows: a spectral region of 200–800 nm, a scanning speed of 100 nm/min, a response time of 1 s, a resolution of 1 nm, a bandwidth of 1 nm, a sensitivity of 1000 mdeg and controlled temperature  $25^\circ C$ . The solutions were prepared by diluting the appropriate amount of the compound in MeOH (0.1 mM). The final spectrum was obtained as an average of 3 accumulations. The spectra were corrected for a baseline by subtracting the spectra of the solvent. ECD molar circular dichroism ( $\Delta\varepsilon$ ) and corresponding wavelength ( $\lambda_{\max}$ ), and UV/Vis molar absorption coefficient ( $\varepsilon$ ) and corresponding absorption wavelength ( $\lambda_{\max}$ ) are shown in Table S11.

The spectrum of the compound alone was measured for the concentration of 0.1 mM and solution of this concentration was also used as a stock solution.

1) **ECD and UV/Vis spectra of (-)-(P)-7k and (+)-(M)-7k under basic condition**

3.33  $\mu\text{L}$  of 0.1 M pyrrolidine solution in methanol was added to 0.1 mM stock solutions (300  $\mu\text{L}$ ) of (-)-(P)-7k (blue curve, Figure S31) and (+)-(M)-7k (violet curve) in methanol. ECD and UV/Vis spectra were measured.

2) **ECD and UV/Vis spectra of (-)-(P)-7k and (+)-(M)-7k under acidic condition**

4  $\mu\text{L}$  of 0.1 M TfOH solution in methanol was added to 0.1 mM stock solutions (300  $\mu\text{L}$ ) of (-)-(P)-7k (yellow curve, Figure S31) and (+)-(M)-7k (orange curve) in methanol. ECD and UV/Vis spectra were measured.

**pH-switching with (-)-(P)-7k and (+)-(M)-7k starting with basic conditions**

For pH-switching experiment from basic to acidic pH with (-)-(P)-7k or (+)-(M)-7k, 3.3  $\mu\text{L}$  of 0.1 M pyrrolidine solution in methanol was added to 0.1 mM solution of (-)-(P)-7k (Solution 1-(P), blue curve, Figure S32) or 0.1 mM solution of (+)-(M)-7k (Solution 1-(M), violet curve) in methanol. Next, 4  $\mu\text{L}$  of 0.1 M TfOH solution in methanol was added to switch to acidic conditions (Solution 2-(P), yellow curve or Solution 2-(M), orange curve). ECD and UV/Vis spectra were measured after each addition.

**pH-switching with (-)-(P)-7k and (+)-(M)-7k starting with acidic conditions**

For pH-switching experiment from acidic to basic pH with (-)-(P)-7k or (+)-(M)-7k, 4.0  $\mu\text{L}$  of 0.1 M TfOH solution in methanol was added to 0.1 mM solution of (-)-(P)-7k (Solution 1-(P), yellow curve, Figure S33) or 0.1 mM solution of (+)-(M)-7k (Solution 1-(M), orange curve) in methanol. Next, 15  $\mu\text{L}$  of 0.1 M pyrrolidine solution in methanol was added to switch to basic conditions (Solution 2-(P), blue curve or Solution 2-(M), violet curve). ECD and UV/Vis spectra were measured after each addition.

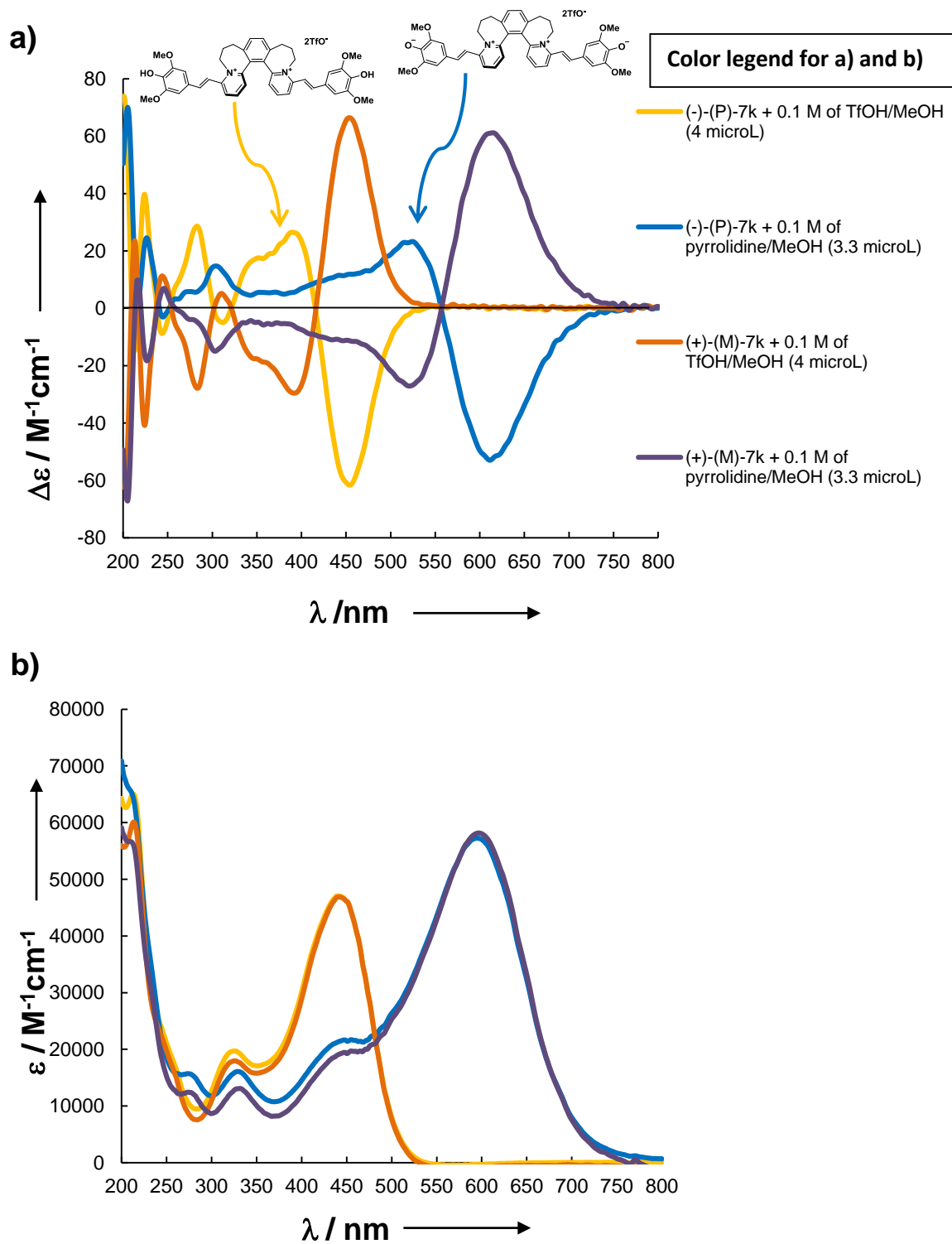


**Figure S31.** a) ECD spectra and b) UV/Vis spectra of (-)-(P)-7k under acidic (yellow curves) and basic conditions (blue curves) and of (+)-(M)-7k under acidic (orange curves) and basic conditions (violet curves).

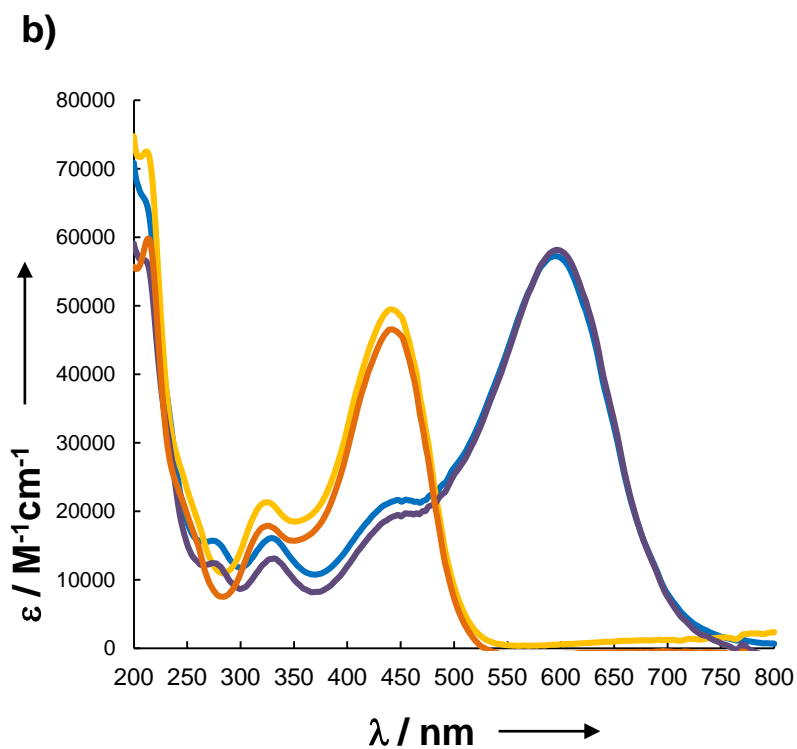
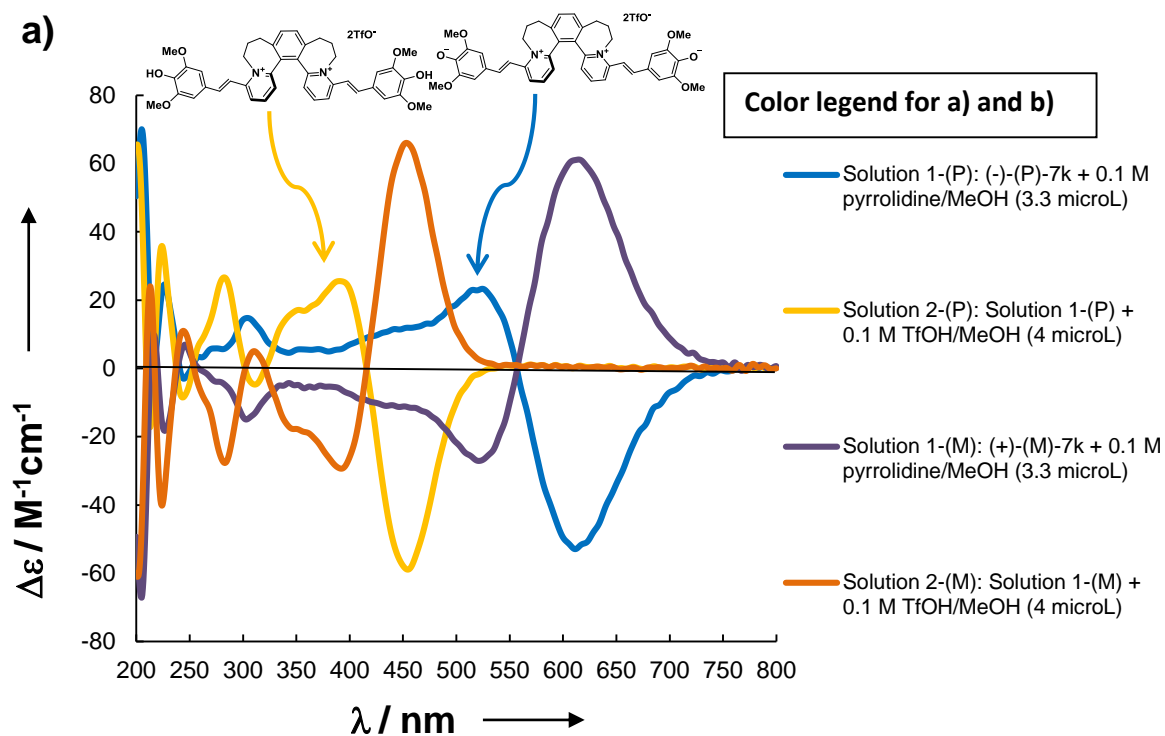


**Figure S32.** a) ECD spectra; b) UV/Vis spectra recorded in the course of pH-switching experiments starting with (-)-(P)-7k or (+)-(M)-7k under basic conditions. pH-switching sequence: basic  $\rightarrow$  acidic corresponds to spectral changes in ECD and UV/Vis for (-)-(P)-7k: blue  $\rightarrow$  yellow curves or for (+)-(M)-7k: violet  $\rightarrow$  orange curves.



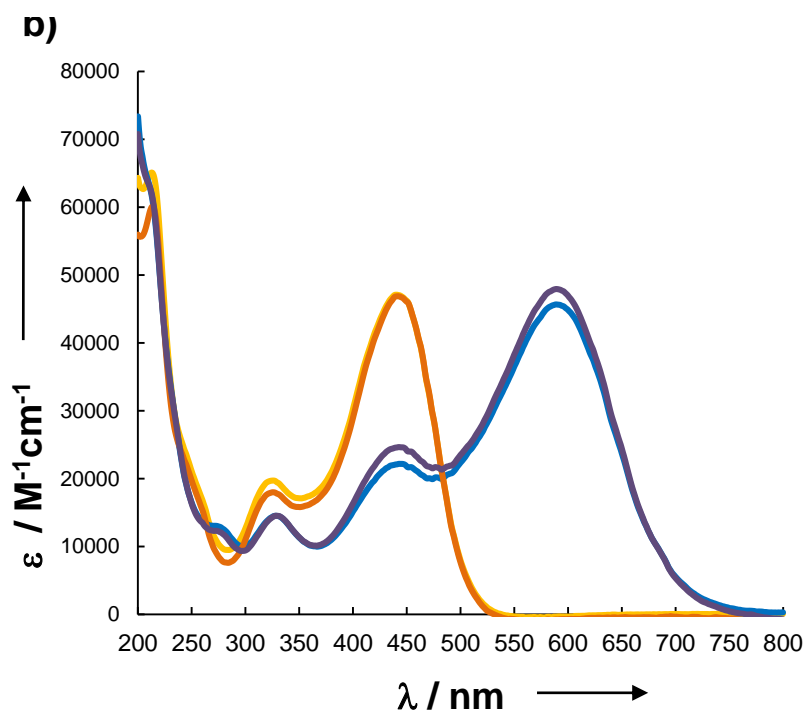
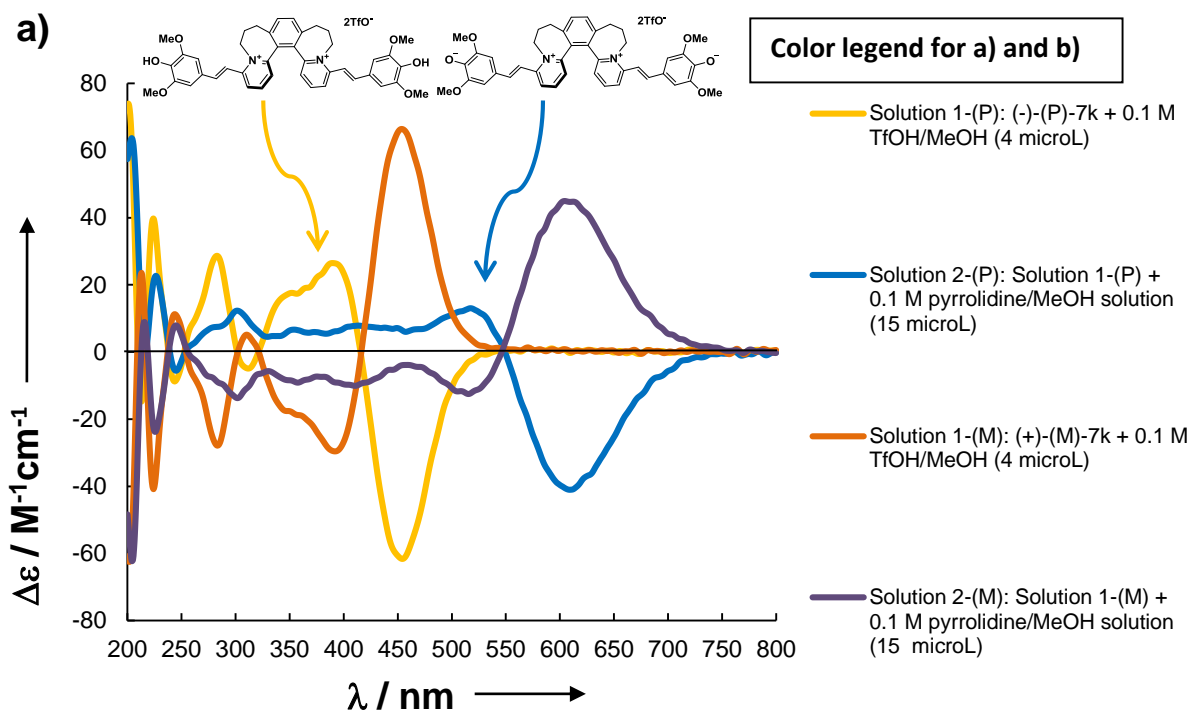


**Figure S33.** a) ECD spectra; b) UV/Vis spectra recorded in the course of pH-switching experiments starting with (-)-(P)-7k or (+)-(M)-7k under acidic conditions. pH-switching sequence: acidic  $\rightarrow$  basic corresponds to spectral changes in ECD and UV/Vis for (-)-(P)-7k: yellow  $\rightarrow$  blue curves or for (+)-(M)-7k: orange  $\rightarrow$  violet curves.

**Table S11.** ECD molar circular dichroism ( $\Delta\epsilon$ ) and corresponding wavelength ( $\lambda_{\max}$ ), and UV/Vis molar absorption coefficient ( $\epsilon$ ) and corresponding absorption wavelength ( $\lambda_{\max}$ ).

Entry	Compound	ECD		UV/Vis	
		$\lambda_{\max}$ [nm]	$\Delta\epsilon$ [ $M^{-1}cm^{-1}$ ]	$\lambda_{\max}$ [nm]	$\epsilon$ [ $M^{-1}cm^{-1}$ ]
1	(-)-(P)- <b>7k</b> <sub>basic pH</sub>	611	-52.9	596	57250
2	(+)-(M)- <b>7k</b> <sub>basic pH</sub>	615	61.2	596	58196
3	(-)-(P)- <b>7k</b> <sub>acidic pH</sub>	454	-61.6	440	47090
4	(+)-(M)- <b>7k</b> <sub>acidic pH</sub>	454	66.4	442	46876

## 6) Calculated UV-Vis absorption and ECD spectra

The quantum chemical calculations were performed using Turbomole 6.5 program package<sup>7,8</sup> (geometry optimizations and frequency calculations) and Gaussian 09 program package (Revision A.02, TDDFT calculations).<sup>9</sup> The starting geometries for geometry optimization of both dications, (*P*)-**3a** and (*P*)-**7a** were taken from X-ray crystal structures. The geometry optimizations of these structures were performed in Turbomole 6.5 program package using PBE<sup>10</sup> functional with RI<sup>11</sup> (resolution of identity) approximation, def2-SVP basis set<sup>12</sup> and DFT-D3 Grimme's empirical dispersion correction<sup>13</sup> (\$disp3 keyword in control file). Optimized structures were confirmed to be minima by harmonic frequency calculations at the same level of theory. Optimization of other rotamers, different from X-ray structures, gave higher energy structures (after geometry optimization). Geometry of the lowest minimum for each dication was taken as a starting point for further geometry optimization at the same level of theory mentioned above with addition of solvation model for MeOH. For this purpose the conductor-like screening model (COSMO<sup>14</sup>) method was utilized with dielectric permittivity constant corresponding to MeOH ( $\epsilon_r = 32.613$ ). This procedure was used as it is not possible to perform frequency calculation in Turbomole 6.5 program package with COSMO switched on.

Geometry from the previous procedure for dications (*P*)-**3a** and (*P*)-**7a** was directly used for TDDFT excited state calculation in Gaussian 09 program package (Revision A.02).<sup>9</sup> Polarizable continuum model (PCM<sup>15</sup>) was used for the description of solvent in all calculations (MeOH,  $\epsilon_r = 32.613$ ). For the spectrum, 120 excited states were calculated. Functionals, that were used to calculate excited states, can be divided into 2 groups, functionals in each group give similar theoretical UV-VIS and ECD spectra. The first group is represented by functionals BMK,<sup>16</sup> CAM-B3LYP,<sup>17</sup> and M062X.<sup>18</sup> The second group contains functionals B3LYP,<sup>19</sup> PBE1PBE,<sup>20</sup> and M06.<sup>18</sup> For all TDDFT calculations, 6-31+G\* basis set was used.

The protocol for simulation of both UV-VIS and ECD spectra within the overlapping Gaussian scheme is as follows.<sup>21</sup> To transform the calculated quantities (dimensionless oscillator strength  $f$  and rotatory strength  $R$  in cgs units) to the ones directly measured (decadic molar extinction coefficient  $\varepsilon$  and molar circular dichroism  $\Delta\varepsilon$ , both in  $\text{dm}^3\text{mol}^{-1}\text{cm}^{-1}$ ), the following equations were employed

$$f = 4.319 \times 10^{-9} \int_{\bar{\nu}_1}^{\bar{\nu}_2} \varepsilon(\bar{\nu}) d\bar{\nu} \quad (\text{Eq. 1})$$

$$R = 2.296 \times 10^{-39} \int_{\lambda_1}^{\lambda_2} \frac{\Delta\varepsilon(\lambda)}{\lambda} d\lambda \quad (\text{Eq. 2})$$

where  $\bar{\nu}$  represent wavenumbers in  $\text{cm}^{-1}$ ,  $\lambda$  is wavelength in arbitrary units.

We have assumed the Gaussian shape of the absorption peaks with the normalized Gaussian  $G$  in the form:

$$G(E) = \frac{1}{\sqrt{2\pi} \sigma} \exp\left(-\frac{(E - \Delta E_{0i})^2}{2\sigma^2}\right) \quad (\text{Eq. 3})$$

where  $\sigma$  is the standard deviation and  $\Delta E_{0i}$  central position of the peak (excitation energy peak). After transformation from wavenumber (Eq. 1) and wavelength (Eq. 2) into the energy scale  $E$ , we get following expressions for molar extinction coefficient  $\varepsilon$  and molar circular dichroism  $\Delta\varepsilon$  (factor of 8065.54 is introduced as a conversion from  $\text{cm}^{-1}$  to eV):

$$\varepsilon(E) = \frac{1}{4.319 \times 10^{-9} \times 8065.54 \sqrt{2\pi} \sigma} \sum_{i=1}^{nstates} f_{0i} \exp\left(-\frac{(E - \Delta E_{0i})^2}{2\sigma^2}\right) \quad (\text{Eq. 4})$$

$$\Delta\varepsilon(E) = \frac{1}{2.296 \times 10^{-39} \sqrt{2\pi} \sigma} \sum_{i=1}^{nstates} \Delta E_{0i} R_{0i} \exp\left(-\frac{(E - \Delta E_{0i})^2}{2\sigma^2}\right) \quad (\text{Eq. 5})$$

In the equations above, summation over all electronically excited states  $i$  is performed, with respective excitation energies  $\Delta E_{0i}$ , oscillator strengths  $f_{0i}$  and rotatory strengths  $R_{0i}$ . The  $\varepsilon$  and  $\Delta\varepsilon$  coefficients are given in the usual units of  $\text{dm}^3\text{mol}^{-1}\text{cm}^{-1}$ . In Eq. 4, conversion factors were chosen so that  $\sigma$  parameter is given in eV, rotatory strengths  $R_{0i}$  in Eq. 5 should be substituted in cgs units ( $\text{erg esu cm gauss}^{-1}$ ). These are the units directly provided by Gaussian quantum

chemistry package. Note that the excitation wavelength was kept constant during integration in Eq. 2.

To convert energy units ( $E$  in eV) to wavelength ( $\lambda$  in nm), the following equation was used:

$$\lambda = 1239.84 / E$$

Note that all the simulated ECD and UV-VIS spectra were generated by broadening the calculated transition intensities by Gaussian curve with standard deviation  $\sigma = 0.25$  eV. No scaling of the wavelengths and intensities was employed.<sup>22</sup>

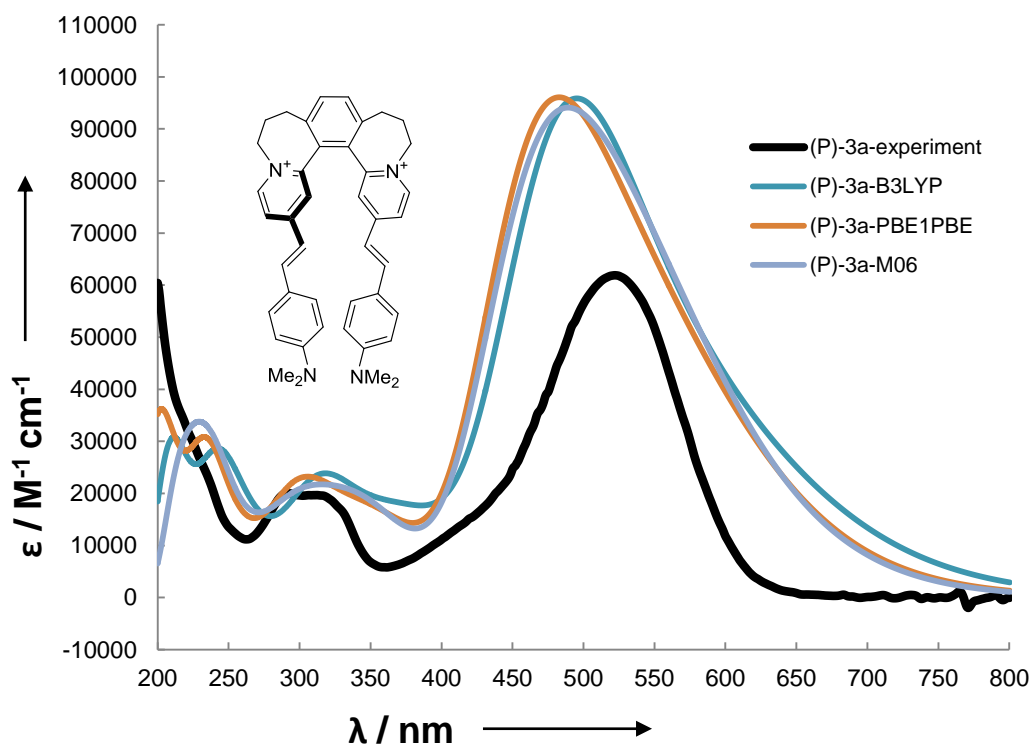
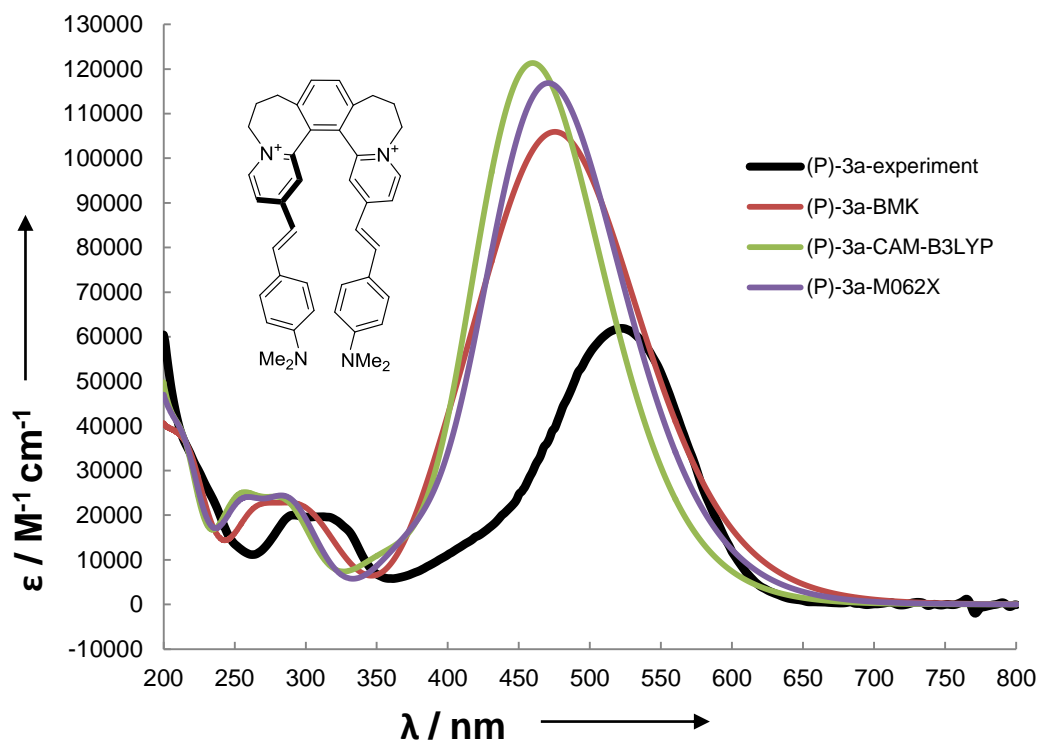


**Figure S34.** Comparison of experimental UV-VIS spectrum of (P)-3a (in MeOH,  $c = 0.1 \text{ mM}$ , black line) with simulated spectra. All calculations were performed using 6-31+G\* basis set and PCM model (MeOH).

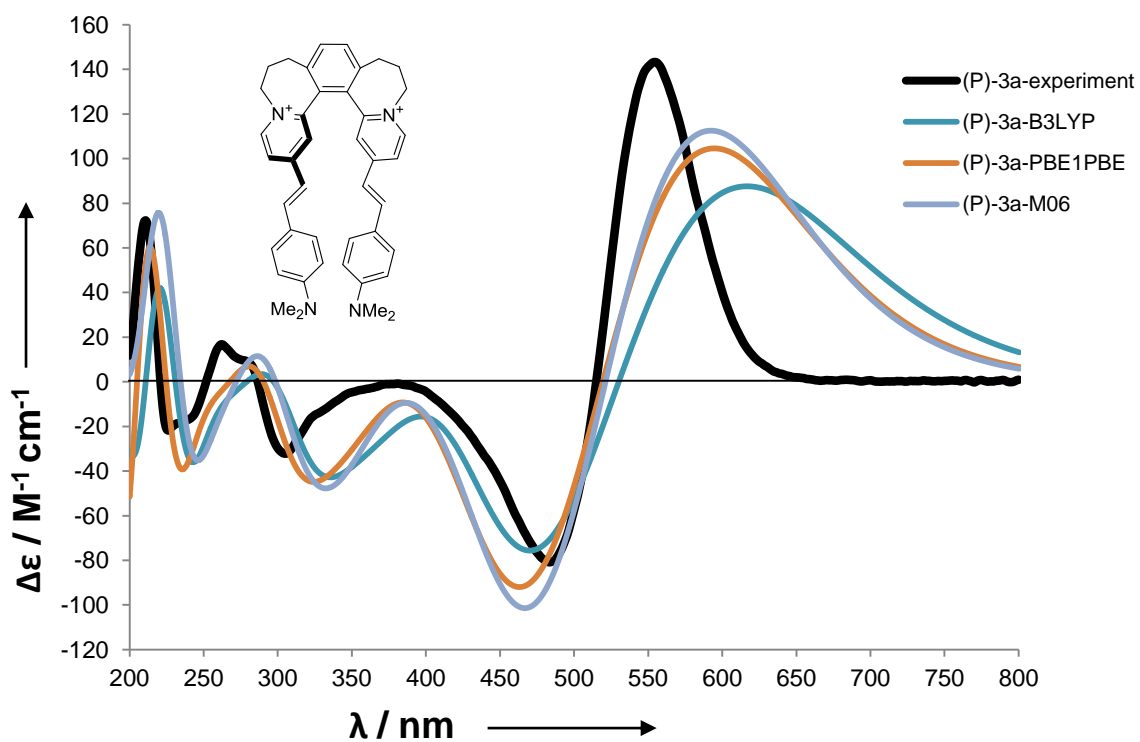
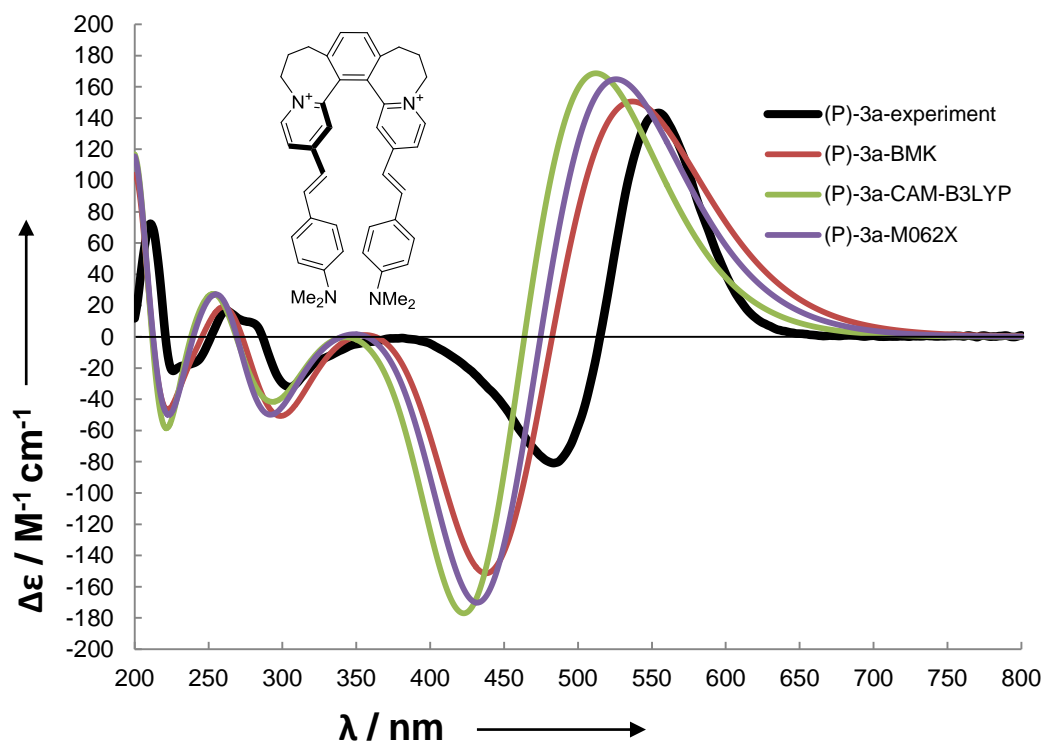


**Figure S35.** Comparison of experimental ECD spectrum of (*P*)-**3a** (in MeOH,  $c = 0.1 \text{ mM}$ , black line) with simulated spectra. All calculations were performed using 6-31+G\* basis set and PCM model (MeOH).

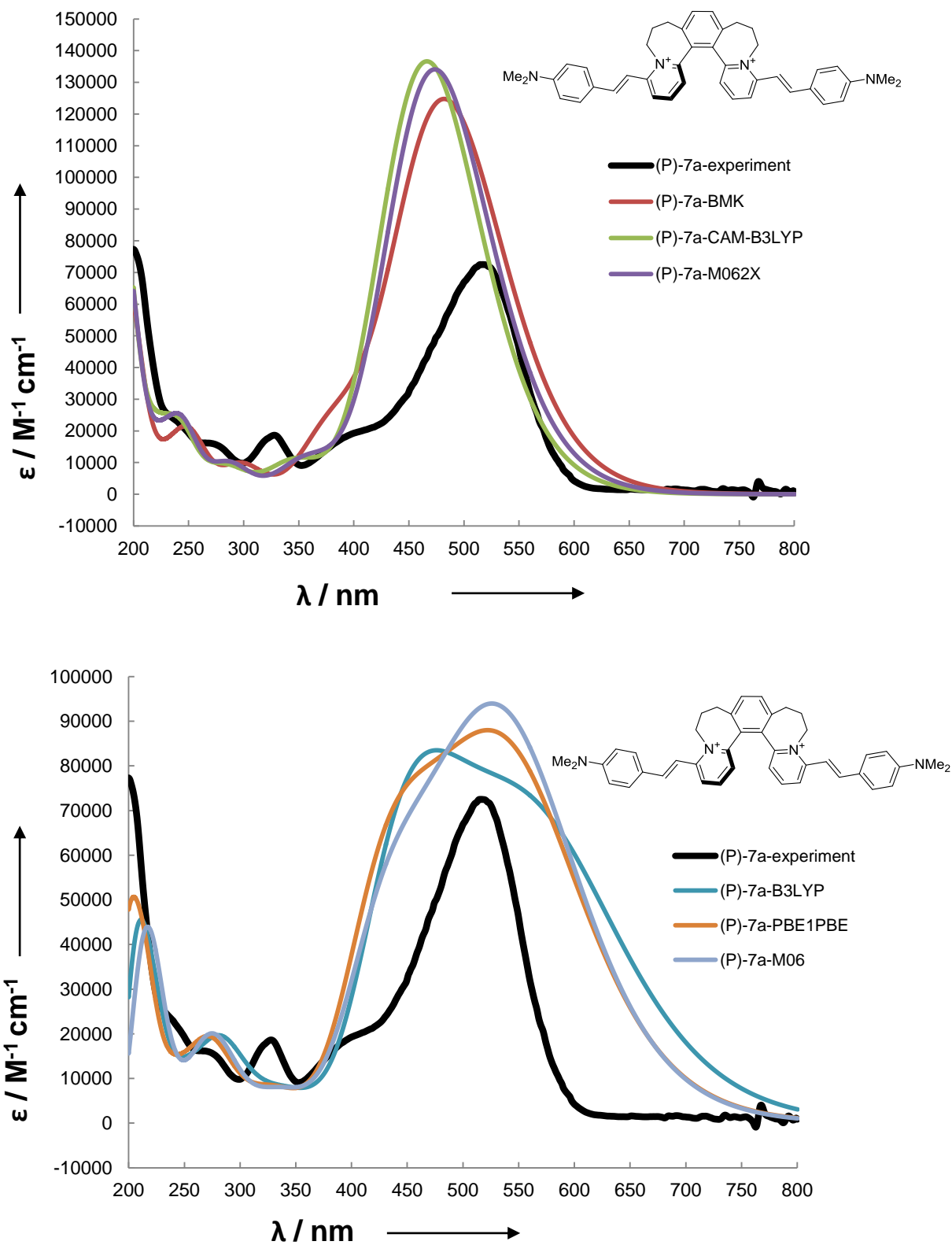


**Figure S36.** Comparison of experimental UV-VIS spectrum of (P)-7a (in MeOH,  $c = 0.1$  mM, black line) with simulated spectra. All calculations were performed using 6-31+G\* basis set and PCM model (MeOH).



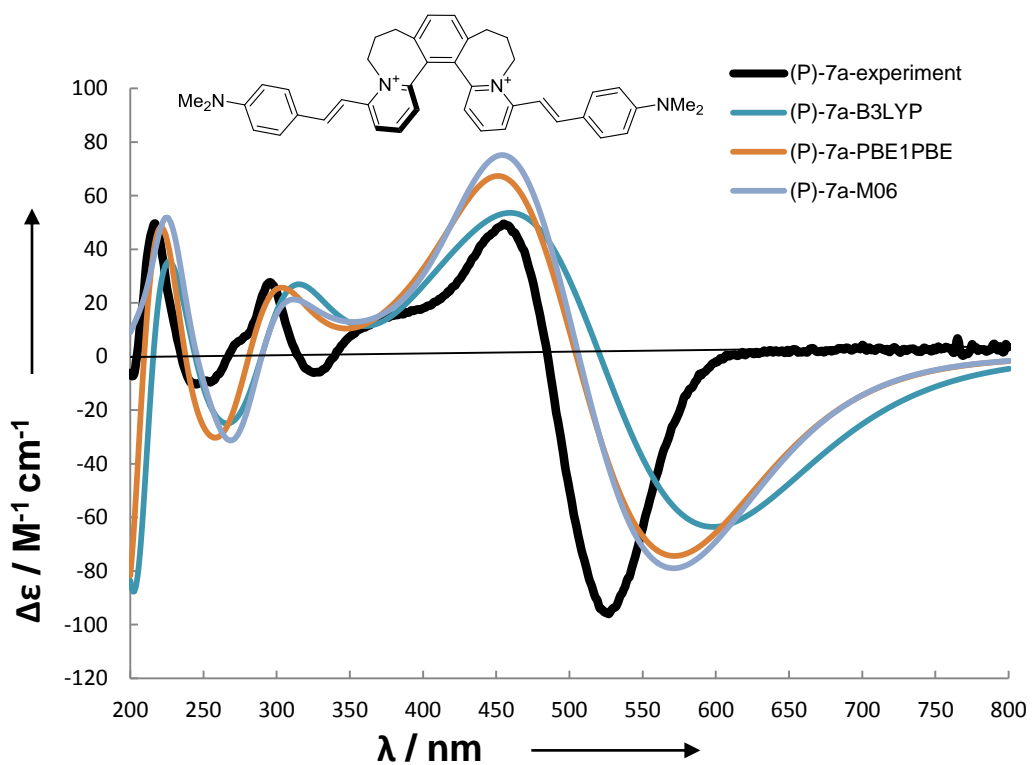
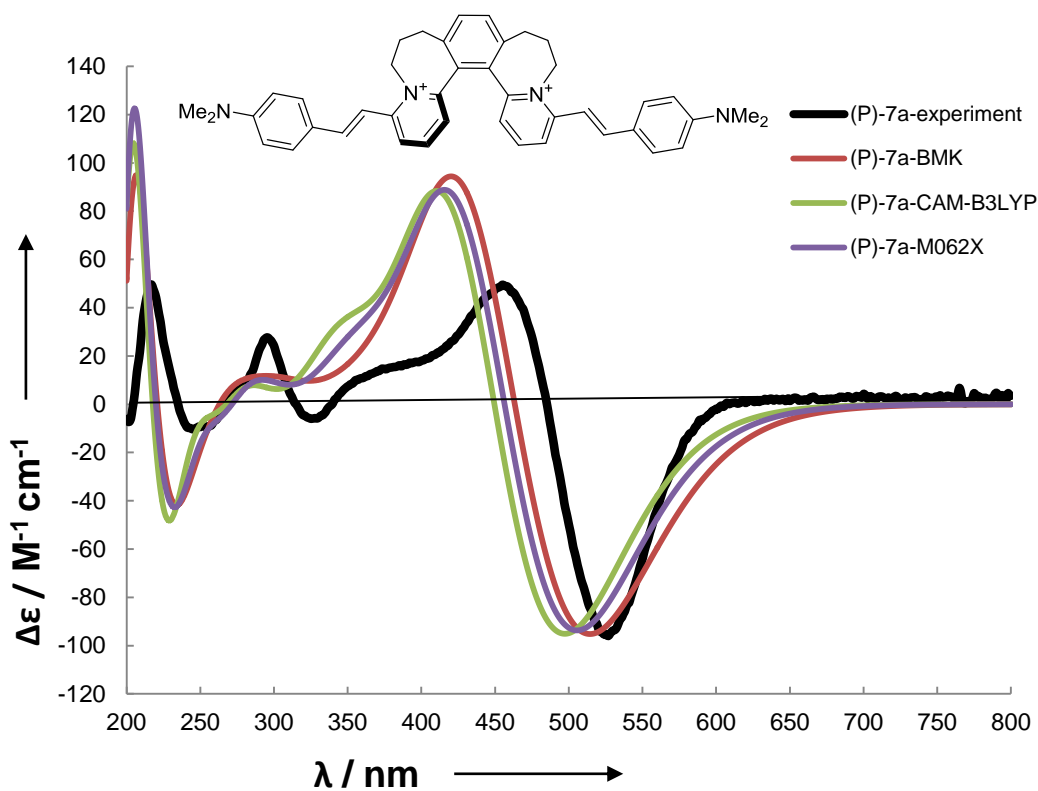


**Figure S37.** Comparison of experimental ECD spectrum of (*P*)-7a (in MeOH, *c* = 0.1 mM, black line) with simulated spectra. All calculations were performed using 6-31+G\* basis set and PCM model (MeOH).

## Relevant molecular orbitals and electronic transitions in the long-wavelength region for dyes (*P*)-3a and (*P*)-7a

**Table S12.** Relative contributions of individual molecular orbital (MO) pairs to selected excited states of (*P*)-3a calculated on B3LYP/6-31+G\*/PCM level of theory. Only transitions at wavelengths longer than 400 nm and contributions greater than 5% are reported.

Transition	$\lambda$ / nm	$R \cdot 10^{-40}$ (erg-esu-cm/Gauss)	MO from $\rightarrow$ to	%
1	602	843	161 $\rightarrow$ 162	97
2	576	-233	160 $\rightarrow$ 162	84
			161 $\rightarrow$ 163	16
3	493	1264	160 $\rightarrow$ 163	97
4	487	-1672	160 $\rightarrow$ 162	16
			161 $\rightarrow$ 163	84

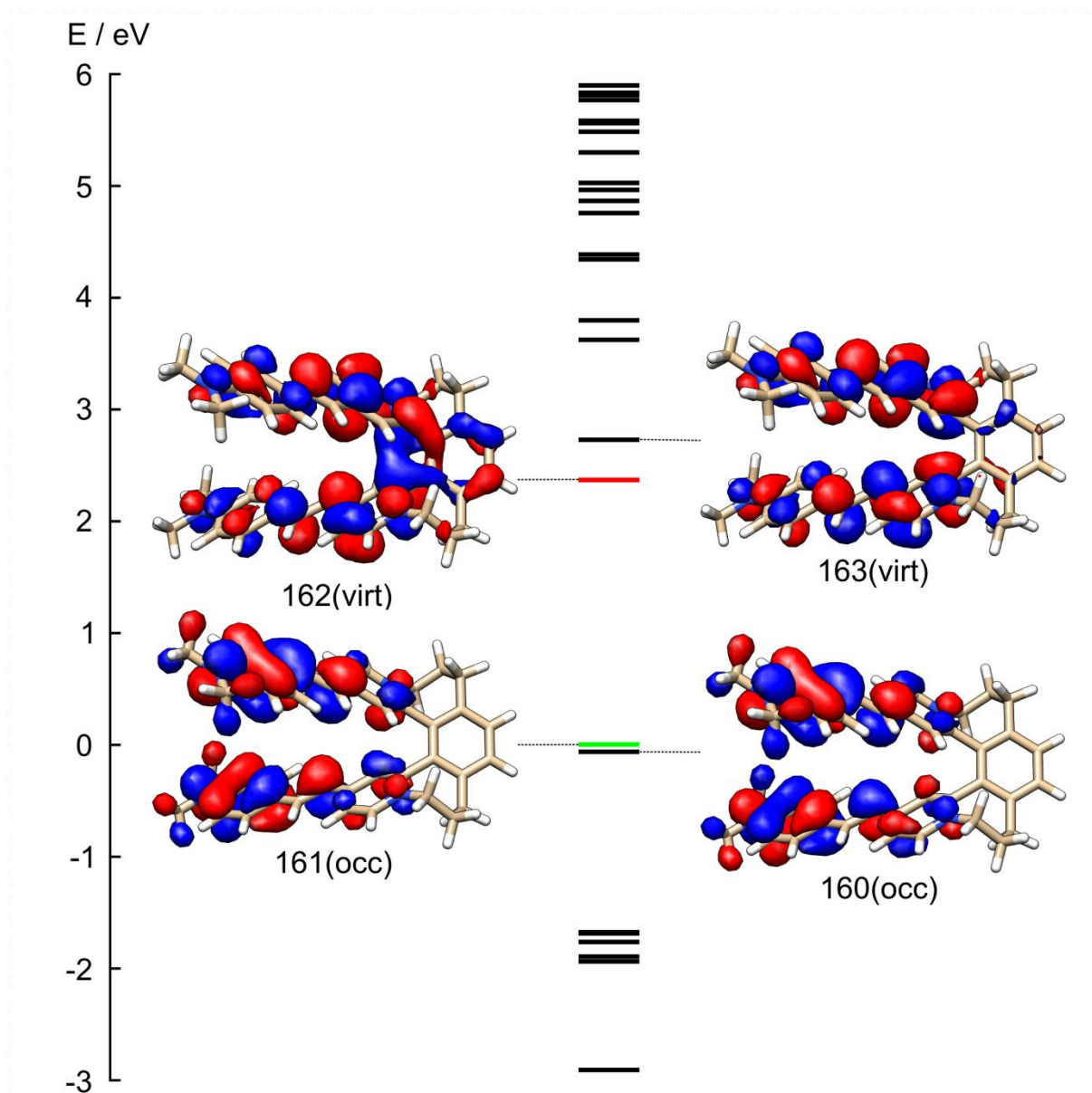


**Figure S38.** Selected molecular orbital isodensity surfaces (plotted for 0.02 a.u.) and relative orbital energies for species (*P*)-**3a** calculated on B3LYP/6-31+G\*/PCM level of theory. Molecular orbital occupation is indicated for clarity. Zero energy is arbitrarily set to the energy of the highest occupied orbital.

**Table S13.** Relative contributions of individual molecular orbital (MO) pairs to selected excited states of (*P*)-**3a** calculated on BMK/6-31+G\*/PCM level of theory. Only transitions at wavelengths longer than 400 nm and contributions greater than 5% are reported.

Transition	$\lambda$ / nm	$R \cdot 10^{-40}$ (erg-esu-cm/Gauss)	MO	%
			from $\rightarrow$ to	
1	503	1974	160 $\rightarrow$ 163	10
			161 $\rightarrow$ 162	87
2	469	-1703	160 $\rightarrow$ 162	89
			161 $\rightarrow$ 163	9
3	413	-561	160 $\rightarrow$ 162	10
			161 $\rightarrow$ 163	89
4	407	438	160 $\rightarrow$ 163	87
			161 $\rightarrow$ 162	11

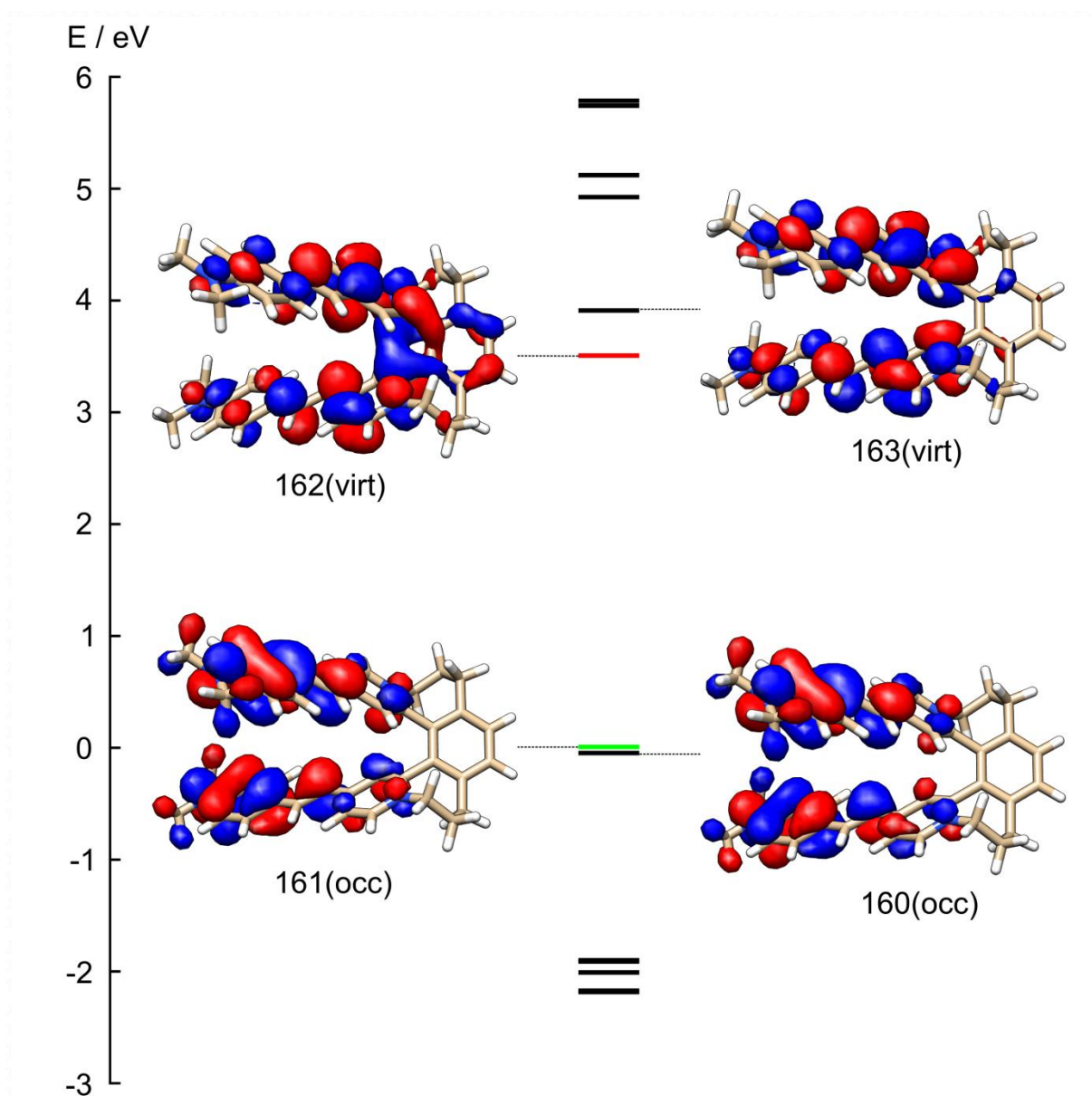


**Figure S39.** Selected molecular orbital isodensity surfaces (plotted for 0.02 a.u.) and relative orbital energies for species (*P*)-**3a** calculated on BMK/6-31+G\*/PCM level of theory. Molecular orbital occupation is indicated for clarity. Zero energy is arbitrarily set to the energy of the highest occupied orbital.

**Table S14.** Relative contributions of individual molecular orbital (MO) pairs to selected excited states of (*P*)-**7a** calculated on B3LYP/6-31+G\*/PCM level of theory. Only transitions at wavelengths longer than 400 nm and contributions greater than 5% are reported.

Transition	$\lambda$ / nm	$R \cdot 10^{-40}$ (erg-esu-cm/Gauss)	MO from $\rightarrow$ to	%
1	576	-601	161 $\rightarrow$ 162	98
2	536	153	160 $\rightarrow$ 162	91
			161 $\rightarrow$ 163	7
3	478	540	161 $\rightarrow$ 163	91
			160 $\rightarrow$ 162	6
4	473	-287	160 $\rightarrow$ 163	97
5	438	-19	161 $\rightarrow$ 164	95
6	424	131	160 $\rightarrow$ 164	94

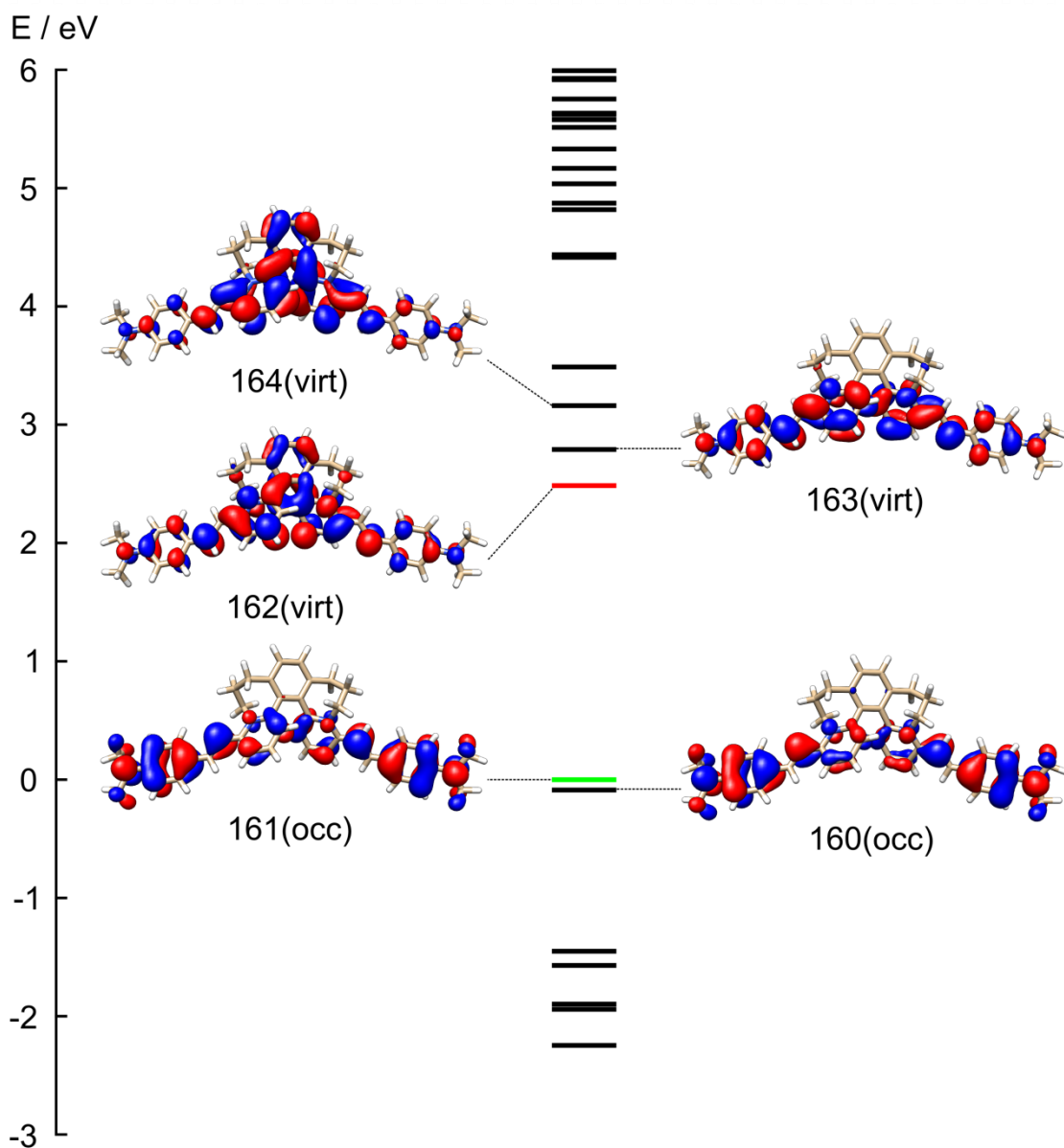


**Figure S40.** Selected molecular orbital isodensity surfaces (plotted for 0.02 a.u.) and relative orbital energies for species (*P*)-**7a** calculated on B3LYP/6-31+G\*/PCM level of theory. Molecular orbital occupation is indicated for clarity. Zero energy is arbitrarily set to the energy of the highest occupied orbital.

**Table S15.** Relative contributions of individual molecular orbital (MO) pairs to selected excited states of (*P*)-**7a** calculated on BMK/6-31+G\*/PCM level of theory. Only transitions at wavelengths longer than 400 nm and contributions greater than 5% are reported.

Transition	$\lambda$ / nm	$R \cdot 10^{-40}$ (erg-esu-cm/Gauss)	MO	%
			from $\rightarrow$ to	
1	487	-985	160 $\rightarrow$ 163	18
			161 $\rightarrow$ 162	77
2	446	847	160 $\rightarrow$ 162	66
			161 $\rightarrow$ 163	30



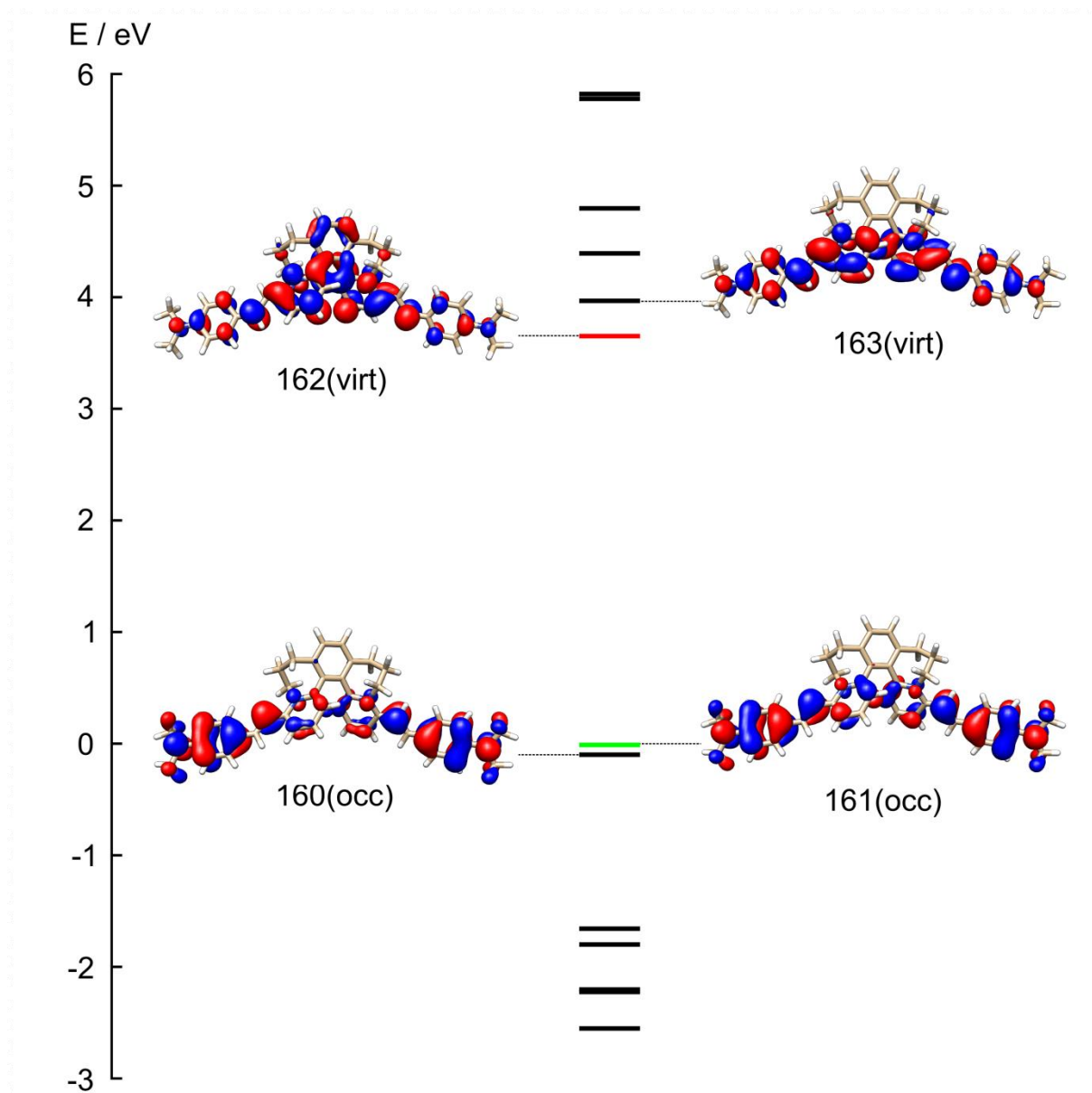


**Figure S41.** Selected molecular orbital isodensity surfaces (plotted for 0.02 a.u.) and relative orbital energies for species (*P*)-**7a** calculated on BMK/6-31+G\*/PCM level of theory. Molecular orbital occupation is indicated for clarity. Zero energy is arbitrarily set to the energy of the highest occupied orbital.

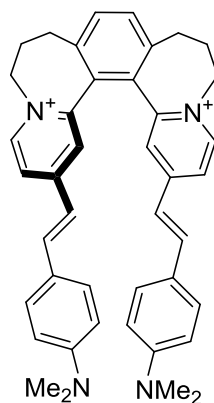
Coordinates of dications calculated in Turbomole 6.5 – DFT-D3, ri-PBE/def2-SVP +  $\$disp3$  + COSMO (MeOH,  $\epsilon_r = 32.613$ ).

(*P*)-**3a**:

90

Energy = -1842.101763678

C	4.7556788	12.4007408	38.4595241
H	4.2941189	12.1440289	37.4953457
C	4.4436362	13.6458850	39.0771424
C	5.0593011	13.8735111	40.3482098
H	4.8834429	14.7959579	40.9172768
C	5.8968141	12.9285768	40.8997304
H	6.3825463	13.0754378	41.8741496
N	6.1877498	11.7529537	40.2612222
C	7.0901164	10.7682545	40.8938959
H	7.6709829	11.2968354	41.6707029
H	7.8040234	10.4341966	40.1150445
C	6.3269014	9.5744153	41.4804901
H	5.8514225	9.8606985	42.4404635
H	7.0796559	8.7929766	41.7095369
C	5.2457183	9.0240499	40.5242768
H	4.9284725	8.0193305	40.8629478
H	4.3454500	9.6728138	40.5874769
C	5.7031143	8.9685147	39.0852088
C	5.9031614	7.7509266	38.4134194
H	5.7215338	6.8073151	38.9507000
C	6.3089239	7.7195914	37.0714178
H	6.4483456	6.7515744	36.5658564
C	6.5616570	8.9041341	36.3595645
C	7.0183430	8.8923445	34.9193716
H	7.2919787	7.8644526	34.6133393
H	7.9451207	9.4998872	34.8343720
C	5.9593291	9.4565244	33.9463421
H	6.4444838	9.6908860	32.9770721
H	5.1740884	8.7002895	33.7429990
C	5.2478656	10.7001470	34.4938150
H	4.6879963	11.2264675	33.7002563
H	4.5227545	10.4221811	35.2838885
N	6.1921469	11.6665998	35.0923043
C	6.5290033	12.8078028	34.4152129
H	6.0447305	12.9440482	33.4385534
C	7.4090271	13.7330961	34.9324823
H	7.6207684	14.6284545	34.3331926
C	8.0228381	13.5194397	36.2068794
C	7.6599511	12.3100556	36.8665802
H	8.1151950	12.0647781	37.8368847
C	6.7533879	11.4041199	36.3262455
C	6.3827047	10.1454198	37.0275525
C	5.9359669	10.1778401	38.3762739
C	5.6196931	11.4743687	39.0339031
C	3.5630247	14.5671795	38.4159588
H	3.1746853	14.2324872	37.4406346
C	3.1888254	15.8039729	38.9038424
H	3.5883806	16.1194412	39.8832817
C	2.3175495	16.7600525	38.2773908
C	1.6966691	16.5571317	37.0079517
H	1.8774323	15.6254167	36.4506829



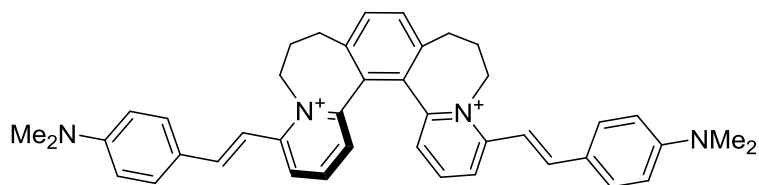
C	0.8607234	17.5063060	36.4422449
H	0.4112172	17.2948582	35.4637112
C	0.5805604	18.7446778	37.1141982
C	1.2021276	18.9550870	38.3887783
H	1.0252627	19.8826112	38.9477574
C	2.0367532	17.9923388	38.9381769
H	2.4982940	18.1855853	39.9200792
C	-0.8653984	19.4438992	35.2617597
H	-0.1053388	19.3040553	34.4635589
H	-1.4877637	20.3149029	34.9946915
H	-1.5181239	18.5449243	35.2781576
C	-0.5164143	20.9297539	37.2599470
H	-0.9966900	20.7497993	38.2457630
H	-1.2012693	21.5447233	36.6513277
H	0.4134113	21.5136361	37.4307011
C	8.9493018	14.4212380	36.8311845
H	9.3335302	14.0998759	37.8125719
C	9.3713841	15.6247570	36.3008004
H	8.9726195	15.9279362	35.3171531
C	10.2930287	16.5596433	36.8855401
C	10.9268977	16.3658861	38.1499706
H	10.7160924	15.4590491	38.7369285
C	11.8135440	17.2929942	38.6734828
H	12.2715787	17.0895809	39.6498169
C	12.1350757	18.4982637	37.9610791
C	11.5003130	18.6996206	36.6915352
H	11.7071622	19.6022460	36.1029355
C	10.6152152	17.7591009	36.1844238
H	10.1446968	17.9444153	35.2052689
C	13.6438512	19.1855982	39.7673849
H	12.8933924	19.1032402	40.5826779
H	14.3090906	20.0351436	39.9975104
H	14.2553434	18.2580611	39.7663923
C	13.3217748	20.6287150	37.7337350
H	13.7752880	20.4007880	36.7451728
H	14.0436120	21.2301609	38.3123728
H	12.4147341	21.2472059	37.5625410
N	-0.2440605	19.6802443	36.5597050
N	13.0095173	19.4120054	38.4739465

(P)-7a:

90

Energy = -1842.088447406

C	8.7112181	11.7385667	2.0794072
H	8.2188937	10.9437626	1.5044799
C	9.7740162	12.4820819	1.5301734
H	10.1496812	12.2480300	0.5236763
C	10.3111034	13.5398435	2.2480337
H	11.0990238	14.1598102	1.8024490
C	9.8221153	13.8835252	3.5369687
N	8.8339415	13.0648676	4.0783074
C	8.3475380	13.2732183	5.4622067
H	9.1504294	13.7429235	6.0543347
H	8.1908538	12.2653699	5.8923517
C	7.0431743	14.0756846	5.4984688
H	7.2365095	15.1534652	5.3201661
H	6.6322845	13.9846951	6.5246427
C	6.0279154	13.5610859	4.4539499
H	5.0253890	13.9776142	4.6691232
H	6.3178580	13.9434361	3.4512552
C	5.9675003	12.0520831	4.4083214
C	4.8247226	11.3474935	4.8201428
H	3.9478871	11.9115606	5.1736982
C	4.7753207	9.9473616	4.7674643
H	3.8600980	9.4213987	5.0803024
C	5.8818764	9.1954594	4.3408059
C	5.8413789	7.6863665	4.2814129
H	4.9276143	7.3077422	4.7778129
H	6.7015260	7.2764995	4.8536906
C	5.9064374	7.1563578	2.8315868
H	6.1315872	6.0702318	2.8491373
H	4.9279043	7.2769940	2.3235485
C	6.9434609	7.9143062	1.9973676
H	7.1403272	7.4314599	1.0256159
H	6.5811124	8.9349819	1.7697817
N	8.2252056	8.0789840	2.7218520
C	9.2953595	7.2174001	2.4914651
C	10.5170301	7.5142543	3.1535589
H	11.3807914	6.8605295	2.9798058
C	10.6185220	8.5718747	4.0439146
H	11.5672000	8.7696555	4.5632718
C	9.4856484	9.3646542	4.3123676
H	9.5184956	10.1645897	5.0634383
C	8.2912488	9.1090525	3.6431624
C	7.0593967	9.8884312	3.9436659
C	7.0921514	11.3106066	3.9494061
C	8.2486448	12.0379568	3.3588247
C	10.2829155	15.0337132	4.2679337
H	9.6969117	15.3509359	5.1411140
C	11.3910400	15.7842467	3.9250785
H	12.0096537	15.4528746	3.0732332
C	11.8621656	16.9758851	4.5745731
C	13.0533366	17.6037399	4.1040833
H	13.5882514	17.1544566	3.2522698
C	13.5593772	18.7596193	4.6814211
H	14.4793968	19.1956748	4.2731165
C	12.8925451	19.3775868	5.7903345
C	11.6911335	18.7506422	6.2679546
H	11.1403751	19.1844985	7.1118624



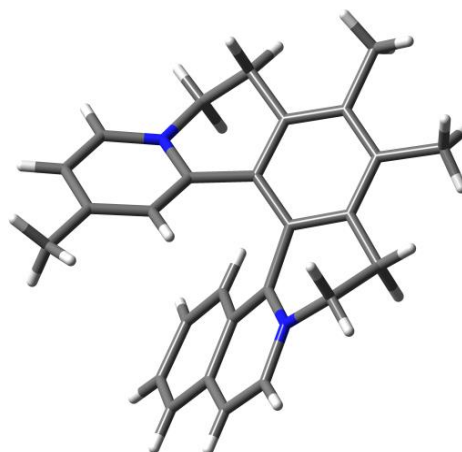
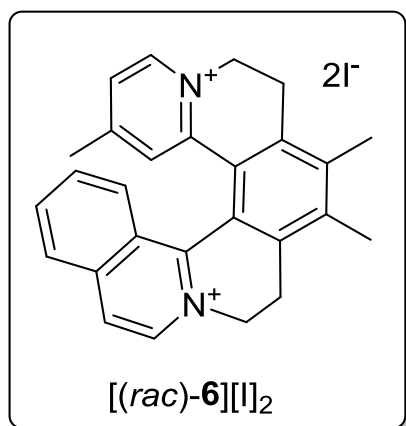
C	11.2029772	17.5956194	5.6788133
H	10.2769868	17.1592396	6.0824234
C	14.5940414	21.1378121	5.8661288
H	15.4602347	20.4452252	5.9275350
H	14.8235618	22.0295280	6.4743768
H	14.4830590	21.4588983	4.8081291
C	12.6708201	21.1342223	7.4870222
H	11.6416717	21.4414670	7.2030327
H	13.2222351	22.0343385	7.8076322
H	12.5988053	20.4459470	8.3559034
C	9.1282128	6.0749282	1.6334046
H	8.1075620	5.8134611	1.3256082
C	10.1609305	5.2671401	1.1970573
H	11.1941363	5.5322898	1.4783791
C	10.0513707	4.0900765	0.3812203
C	11.2336669	3.3811732	0.0150093
H	12.2080624	3.7562602	0.3670030
C	11.1982522	2.2354957	-0.7663334
H	12.1421243	1.7332247	-1.0120612
C	9.9518619	1.7121575	-1.2437013
C	8.7572437	2.4227906	-0.8800038
H	7.7769505	2.0669289	-1.2212049
C	8.8139599	3.5648379	-0.0981200
H	7.8684773	4.0698458	0.1513265
C	11.1259454	-0.1104630	-2.3827821
H	11.8138886	0.5500687	-2.9523377
H	10.8733233	-0.9745686	-3.0206143
H	11.6689029	-0.4863642	-1.4890056
C	8.6187059	0.0641855	-2.4761381
H	7.9447643	-0.1769269	-1.6268516
H	8.7920956	-0.8624393	-3.0494673
H	8.0960490	0.7879212	-3.1378474
N	13.3748967	20.5154750	6.3690716
N	9.8995309	0.5862672	-2.0126601

## 7) X-ray analysis

Crystallographic data for all compounds were collected on Nonius KappaCCD diffractometer equipped with a Bruker APEX-II CCD detector by monochromatized MoK $\alpha$  radiation ( $\lambda = 0.71073 \text{ \AA}$ ) at a temperature of 150(2) K. The structures were solved by direct methods (SHELXS)<sup>23</sup> and refined by full matrix least squares based on  $F^2$  (SHELXL97).<sup>23</sup> The hydrogen atoms on carbons were fixed into idealised positions (riding model) and assigned temperature factors either  $H_{\text{iso}}(\text{H}) = 1.2 U_{\text{eq}}(\text{pivot atom})$  or  $H_{\text{iso}}(\text{H}) = 1.5 U_{\text{eq}}$  for methyl moiety. For crystals grown from racemic material (see below), geometry of only one example helical scaffold with (*P*)-helicity is displayed. Anions are omitted for clarity.

[(*rac*)-**6**][I]<sub>2</sub>

CCDC 925828:



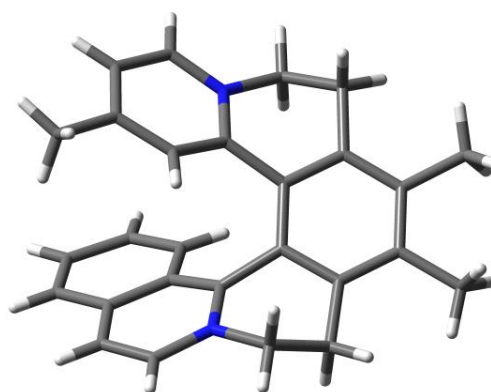
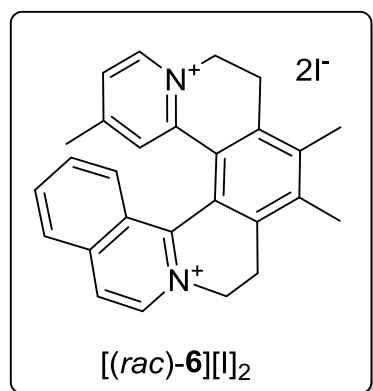
[(*rac*)-**6**][TfO]<sub>2</sub> (15 mg, 22  $\mu\text{mol}$ , 1 equiv) was dissolved in a minimum amount of acetone (approximately 0.5 mL). NaI (17 mg, 110  $\mu\text{mol}$ , 5 equiv) was dissolved in a minimum amount of acetone (approximately 0.5 mL). The two solutions were mixed and a yellow precipitate resulted. The resulting suspension was centrifuged, the solids were separated and then sonicated with acetone (0.5 mL). The suspension was again centrifuged and the solid pellet was separated and dried in vacuo. [(*rac*)-**6**][I]<sub>2</sub> was obtained as a pale yellow solid in 59% yield (8.2 mg, 13  $\mu\text{mol}$ ).

The solids (2 mg) were dissolved in MeOH (0.2 mL). Single crystals of [(*rac*)-**6**][I]<sub>2</sub>·MeOH suitable for X-ray analysis were grown via a slow diffusion of *i*-Pr<sub>2</sub>O into the MeOH solution in the fridge (7°C) within 7 days.

Crystal data for [(*rac*)-**6**][I]<sub>2</sub>: C<sub>27</sub>H<sub>26</sub>N<sub>2</sub>·CH<sub>4</sub>O·2(I), *M<sub>r</sub>* = 664.34; Triclinic, *P*-1 (No 2), *a* = 9.5036 (4) Å, *b* = 11.1664 (4) Å, *c* = 12.3553 (5) Å,  $\alpha$  = 87.908 (1)°,  $\beta$  = 83.391 (1)°,  $\gamma$  = 82.468 (1)°, *V* = 1290.90 (9) Å<sup>3</sup>, *Z* = 2, *D<sub>x</sub>* = 1.709 Mg m<sup>-3</sup>, orange prism of dimensions 0.60 × 0.23 × 0.18 mm, numerical absorption correction ( $\mu$  = 2.46 mm<sup>-1</sup>) *T<sub>min</sub>* = 0.318, *T<sub>max</sub>* = 0.671; a total of 28212 measured reflections ( $\theta_{\max}$  = 26°), from which 5067 were unique (*R<sub>int</sub>* = 0.021) and 4614 observed according to the *I* > 2σ(*I*) criterion. The refinement converged ( $\Delta/\sigma_{\max}$  = 0.002) to *R* = 0.016 for observed reflections and *wR*(*F*<sup>2</sup>) = 0.038, *GOF* = 1.11 for 302 parameters and all 5067 reflections. The final difference Fourier map displayed no peaks of chemical significance ( $\Delta\rho_{\max}$  = 0.63,  $\Delta\rho_{\min}$  = -0.59 e.Å<sup>-3</sup>).

[(*rac*)-**6**][I]<sub>2</sub>

CCDC 925829:



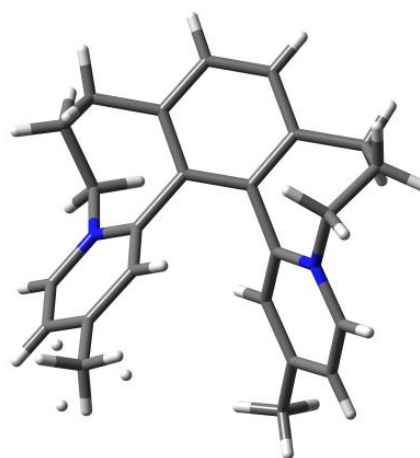
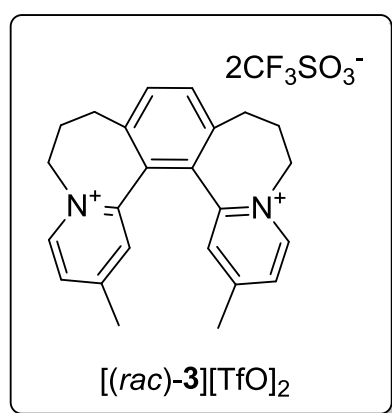
[(*rac*)-**6**][TfO]<sub>2</sub> (15 mg, 22 μmol, 1 equiv) was dissolved in a minimum amount of acetone (approximately 0.5 mL). NaI (17 mg, 0.110 μmol, 5 equiv) was dissolved in a minimum amount of acetone (approximately 0.5 mL). The two solutions were mixed and a yellow precipitate resulted. The resulting suspension was centrifuged, the solids were separated and then sonicated with acetone (0.5 mL). The suspension was again centrifuged and the solid pellet was dried in vacuo. [(*rac*)-**6**][I]<sub>2</sub> was obtained as a pale yellow solid in 59% yield (8.2 mg, 13 μmol).

The solids (2 mg) were dissolved in MeNO<sub>2</sub> (0.2 mL). Single crystals of [(*rac*)-**6**][I]<sub>2</sub> suitable for X-ray analysis were grown via a slow diffusion of *i*-Pr<sub>2</sub>O into the MeNO<sub>2</sub> solution in the fridge (7°C) within 5 days.

Crystal data for [(*rac*)-**6**][I]<sub>2</sub>: C<sub>27</sub>H<sub>26</sub>N<sub>2</sub>•2(I), *M<sub>r</sub>* = 632.30; Monoclinic, space group *P*2<sub>1</sub>/*n* (No 14), *a* = 7.8813 (2) Å, *b* = 16.2049 (4) Å, *c* = 19.5829 (5) Å, β = 99.067 (1)°; *V* = 2469.79 (11) Å<sup>3</sup>, *Z* = 4, *D<sub>x</sub>* = 1.700 Mg m<sup>-3</sup>; dimensions of yellow bar 0.44 × 0.12 × 0.11 mm, θ<sub>max</sub> = 27.5°; numerical absorption correction (μ = 2.56 mm<sup>-1</sup>) *T*<sub>min</sub> = 0.401, *T*<sub>max</sub> = 0.769; 31665 diffractions collected, 5678 independent (*R*<sub>int</sub> = 0.025) and 5069 observed according to the *I* > 2σ(*I*) criterion. The refinement converged (Δ/σ<sub>max</sub> = 0.002) to *R* = 0.022 for observed reflections and *wR*(*F*<sup>2</sup>) = 0.047, *GOF* = 1.02 for 283 parameters and all 5678 reflections. The final difference map displayed no peaks of chemical significance (Δρ<sub>max</sub> = 1.02, Δρ<sub>min</sub> = -0.83 e.Å<sup>-3</sup>).

### [(*rac*)-**3**][TfO]<sub>2</sub>

CCDC 1004339:



Single crystals of [(*rac*)-**3**][TfO]<sub>2</sub> suitable for X-ray analysis were grown via a slow diffusion of *t*-BuOMe into a solution of [(*rac*)-**3**][TfO]<sub>2</sub> in acetone.

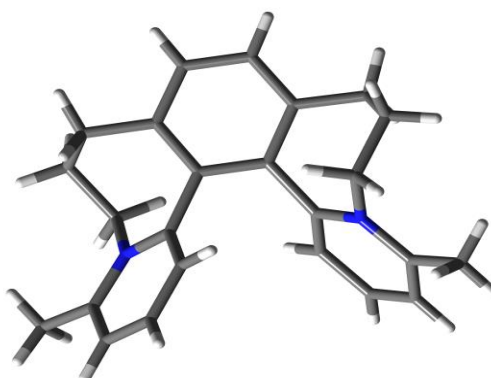
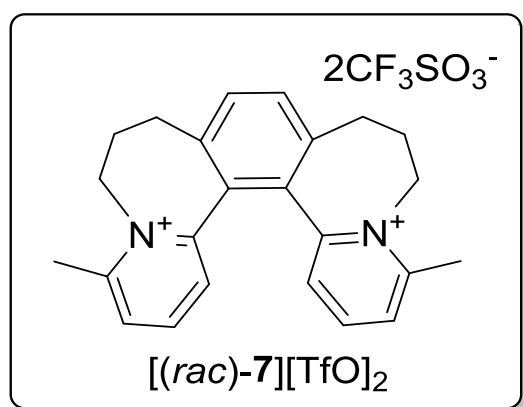
Crystal data for [(*rac*)-**3**][TfO]<sub>2</sub>: C<sub>24</sub>H<sub>26</sub>N<sub>2</sub>•2(CF<sub>3</sub>O<sub>3</sub>S), *M<sub>r</sub>* = 640.61; Monoclinic, space group *P*2<sub>1</sub>/*c* (No 14), *a* = 14.2532 (9) Å, *b* = 8.9518 (5) Å, *c* = 21.2552 (12) Å, β = 92.286 (2)°; *V* = 2709.8 (3) Å<sup>3</sup>, *Z* = 4, *D<sub>x</sub>* = 1.570 Mg m<sup>-3</sup>; dimensions of colorless prism 0.41 × 0.23 × 0.18 mm, θ<sub>max</sub> = 27.5°; multi-scan absorption correction (μ = 0.28 mm<sup>-1</sup>) *T*<sub>min</sub> = 0.892, *T*<sub>max</sub> = 0.950; 43735 diffractions collected, 6221 independent (*R*<sub>int</sub> = 0.025) and 5347 observed



according to the  $I > 2\sigma(I)$  criterion. The refinement converged ( $\Delta/\sigma_{\max} = 0.001$ ) to  $R = 0.034$  for observed reflections and  $wR(F^2) = 0.093$ ,  $GOF = 1.03$  for 380 parameters and all 6221 reflections. The final difference map displayed no peaks of chemical significance ( $\Delta\rho_{\max} = 0.34$ ,  $\Delta\rho_{\min} = -0.40 \text{ e.}\text{\AA}^{-3}$ ).

**[(*rac*)-7][TfO]<sub>2</sub>**

**CCDC 1004340:**

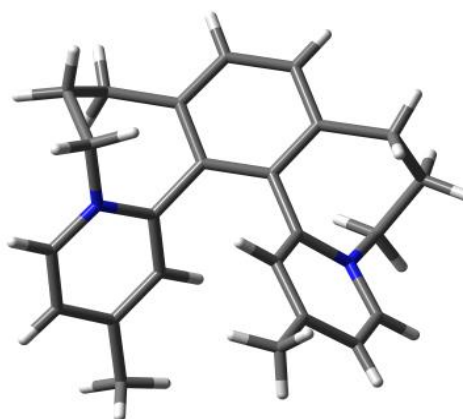
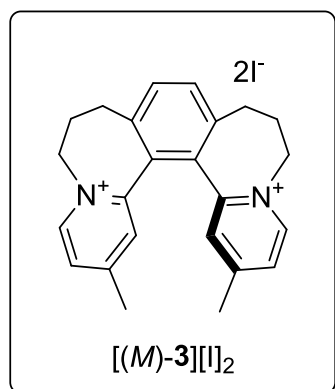


Single crystals of [(*rac*)-7][TfO]<sub>2</sub> suitable for X-ray analysis were grown via a slow diffusion of *t*-BuOMe into a solution of [(*rac*)-7][TfO]<sub>2</sub> in acetone.

Crystal data for [(*rac*)-7][TfO]<sub>2</sub>: C<sub>24</sub>H<sub>26</sub>N<sub>2</sub>•2(CF<sub>3</sub>O<sub>3</sub>S)•0.5(C<sub>3</sub>H<sub>6</sub>O), M<sub>r</sub> = 669.65; Triclinic, *P*-1 (No 2),  $a = 9.0232(4) \text{ \AA}$ ,  $b = 12.5214(6) \text{ \AA}$ ,  $c = 14.3223(6) \text{ \AA}$ ,  $\alpha = 101.780(2)^\circ$ ,  $\beta = 106.423(1)^\circ$ ,  $\gamma = 101.248(2)^\circ$ ,  $V = 1463.37(11) \text{ \AA}^3$ ,  $Z = 2$ ,  $D_x = 1.520 \text{ Mg m}^{-3}$ ; dimensions of colorless plate  $0.66 \times 0.59 \times 0.42 \text{ mm}$ ,  $\theta_{\max} = 27.5^\circ$ ; multi-scan absorption correction ( $\mu = 0.27 \text{ mm}^{-1}$ )  $T_{\min} = 0.765$ ,  $T_{\max} = 0.896$ ; 32985 diffractions collected, 6718 independent ( $R_{\text{int}} = 0.013$ ) and 6101 observed according to the  $I > 2\sigma(I)$  criterion. The refinement converged ( $\Delta/\sigma_{\max} = 0.001$ ) to  $R = 0.036$  for observed reflections and  $wR(F^2) = 0.096$ ,  $GOF = 1.02$  for 408 parameters and all 6718 reflections. The final difference map displayed no peaks of chemical significance ( $\Delta\rho_{\max} = 0.42$ ,  $\Delta\rho_{\min} = -0.41 \text{ e.}\text{\AA}^{-3}$ ). The solvating acetone molecule is disordered into two positions, being placed on crystallographic inversion center.

[(*M*)-3][I]<sub>2</sub>

CCDC 1004341:

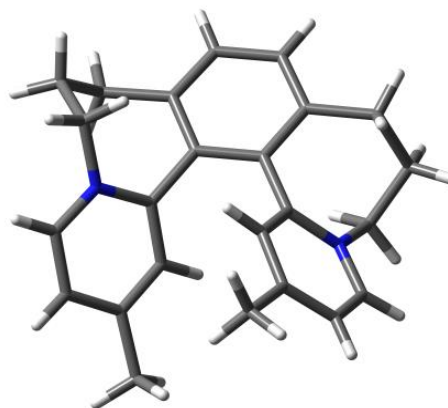
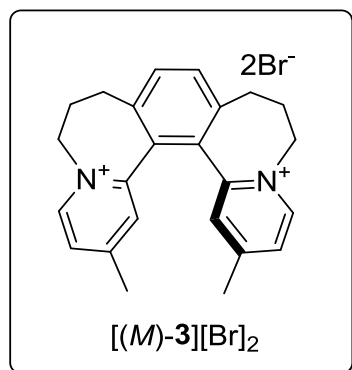


Solution of [(*M*)-3][TfO]<sub>2</sub> (13.2 mg, 20.6 μmol) in 0.5 mL acetone was mixed with 0.5 mL of acetone solution of NaI (32.6 mg, 217.5 μmol, 10 equiv). A yellow precipitate resulted. The suspension was centrifuged and the supernatant was removed. The solids were next sonicated with 1 mL of acetone, and the suspension was then centrifuged and supernatant was removed. The solid pellet was dissolved in 1 mL MeCN and three parallel diffusion crystallizations were set up from this solution. Single crystals of [(*M*)-3][I]<sub>2</sub> suitable for X-ray analysis (and assignment of absolute configuration of the helical dicationic scaffold) were grown via a slow diffusion of toluene into a MeCN solution of [(*M*)-3][I]<sub>2</sub>.

Crystal data for [(*M*)-3][I]<sub>2</sub>: C<sub>24</sub>H<sub>26</sub>N<sub>2</sub>•2(I), *M<sub>r</sub>* = 596.27; Orthorhombic, space group *P*2<sub>1</sub>2<sub>1</sub>2<sub>1</sub> (No 19), *a* = 8.7530 (2) Å, *b* = 13.2791 (4) Å, *c* = 19.7500 (6) Å; *V* = 2295.58 (11) Å<sup>3</sup>, *Z* = 4, *D<sub>x</sub>* = 1.725 Mg m<sup>-3</sup>; dimensions of yellow prism 0.39 × 0.32 × 0.17 mm, *θ*<sub>max</sub> = 27.5°; numerical absorption correction (*μ* = 2.75 mm<sup>-1</sup>) *T*<sub>min</sub> = 0.413, *T*<sub>max</sub> = 0.646; 14692 diffractions collected, 5263 independent (*R*<sub>int</sub> = 0.022) and 4990 observed according to the *I* > 2σ(*I*) criterion. The refinement converged (*Δ*/σ<sub>max</sub> = 0.003) to *R* = 0.020 for observed reflections and *wR*(*F*<sup>2</sup>) = 0.045, *GOF* = 1.04 for 255 parameters and all 5263 reflections. Absolute structure: Flack parameter -0.030 (15). The final difference map displayed no peaks of chemical significance (*Δρ*<sub>max</sub> = 0.89, *Δρ*<sub>min</sub> = -0.43 e.Å<sup>-3</sup>).

**[(*M*)-3][Br]<sub>2</sub>**

**CCDC 1004342:**



The triflate anion of [(*M*)-3][TfO]<sub>2</sub> was exchanged to Br<sup>-</sup> anion via passing a methanolic solution (5 mL) of [(*M*)-3][TfO]<sub>2</sub> (10.5 mg, 16.4 μmol) through strongly basic anion exchange resin in Br<sup>-</sup> cycle.

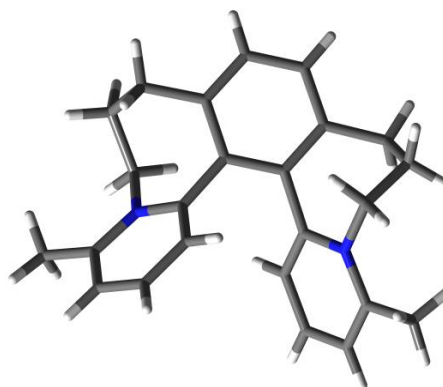
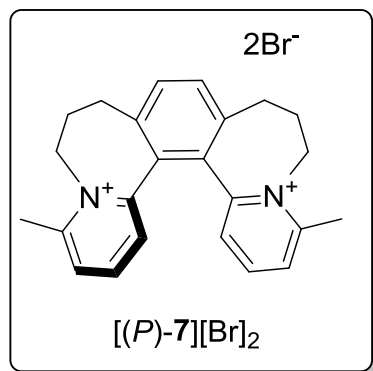
The resin was prepared as follows: 3 mL bed volume of commercially available strongly basic anion exchange resin in water (in Cl<sup>-</sup> cycle) was prepared in a column equipped with a sinter S1. The resin was switched from Cl<sup>-</sup> to OH<sup>-</sup> cycle by passing 120 mL of 2M aq. solution of NaOH. The complete exchange to OH<sup>-</sup> anions was proved by a negative test for Cl<sup>-</sup> anions in an outcoming solution (a few drops of 0.1M aq. solution of AgNO<sub>3</sub> were added to a sample acidified by 1:1 HNO<sub>3</sub>). Then, water was passed through the resin bed until the outcoming solution gave neutral reaction (30 mL of water). Then, the resin was switched to Br<sup>-</sup> cycle by passing 15 mL of 0.25M aq. solution of HBr. Then, 30 mL of water was passed through to remove all free acid (until the outcoming solution was neutral). Finally, water in the resin bed was exchanged for MeOH.

After passing the helquat sample, resin was washed with 20 mL of MeOH and the outcoming liquids were collected to a 50 mL rbf. The volatiles from the resulting methanolic solution of [(*M*)-3][Br]<sub>2</sub> were removed on a rotary evaporator and the residue was dissolved in 1 mL of MeCN and three parallel diffusion crystallizations were set up from the resulting solution. Single crystals of [(*M*)-3][Br]<sub>2</sub> suitable for X-ray analysis (and assignment of absolute configuration of the helical dicationic scaffold) were grown via a slow diffusion of toluene into a MeCN solution of [(*M*)-3][Br]<sub>2</sub>.

Crystal data for [(*M*)-**3**][Br]<sub>2</sub>: C<sub>24</sub>H<sub>26</sub>N<sub>2</sub>•2(Br), *M<sub>r</sub>* = 502.29; Orthorhombic, space group *P*2<sub>1</sub>2<sub>1</sub>2 (No 18), *a* = 27.6754 (9) Å, *b* = 10.0575 (3) Å, *c* = 14.6734 (6) Å; *V* = 4084.3 (2) Å<sup>3</sup>, *Z* = 6, *D<sub>x</sub>* = 1.225 Mg m<sup>-3</sup>; dimensions of colorless needle 0.55 × 0.19 × 0.08 mm, *θ*<sub>max</sub> = 26°; numerical absorption correction (*μ* = 2.99 mm<sup>-1</sup>) *T*<sub>min</sub> = 0.292, *T*<sub>max</sub> = 0.792; 20906 diffractions collected, 8032 independent (*R*<sub>int</sub> = 0.049) and 6052 observed according to the *I* > 2σ(*I*) criterion. The refinement converged (*Δ*/σ<sub>max</sub> = 0.001) to *R* = 0.041 for observed reflections and *wR*(*F*<sup>2</sup>) = 0.077, *GOF* = 0.94 for 382 parameters and all 8032 reflections. Absolute structure: Flack parameter -0.006 (8). The final difference map displayed no peaks of chemical significance (*Δρ*<sub>max</sub> = 0.65, *Δρ*<sub>min</sub> = -0.47 e.Å<sup>-3</sup>). PLATON/ SQUEEZE<sup>24</sup> procedure was used to correct the diffraction data for the presence of the disordered mixture of solvents (acetonitrile and toluene). One of two symmetrically independent helquat cations is placed on two-fold axis of the space group *P*2<sub>1</sub>2<sub>1</sub>2, however both molecules fit to each other, differing slightly (< 0.6 Å) in positions of methyl moieties.

### [(*P*)-**7**][Br]<sub>2</sub>

CCDC 1004343:



The triflate anion of [(*P*)-**7**][TfO]<sub>2</sub> was exchanged for Br<sup>-</sup> anion via passing a methanolic solution (5 mL) of [(*P*)-**7**][TfO]<sub>2</sub> (10.1 mg, 15.8 μmol) through strongly basic anion exchange resin in Br<sup>-</sup> cycle.

The resin was prepared as follows: 3 mL bed volume of commercially available strongly basic anion exchange resin in water (in Cl<sup>-</sup> cycle) was prepared in a column equipped with a sinter S1. The resin was switched from Cl<sup>-</sup> to OH<sup>-</sup> cycle by passing 120 mL of 2M aq. solution of NaOH. The complete exchange to OH<sup>-</sup> anions was proved by negative test of outgoing solution for chlorides (a few drops of 0.1M aq. solution of AgNO<sub>3</sub> were added to a

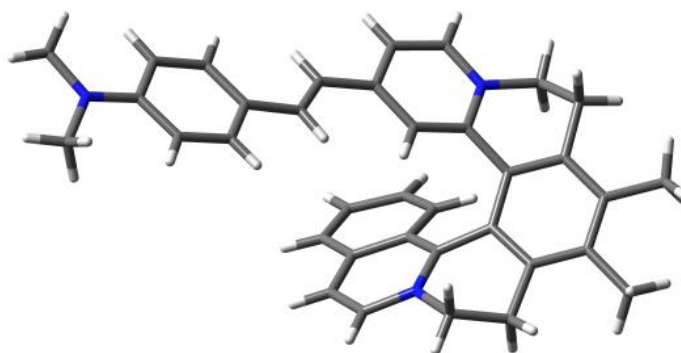
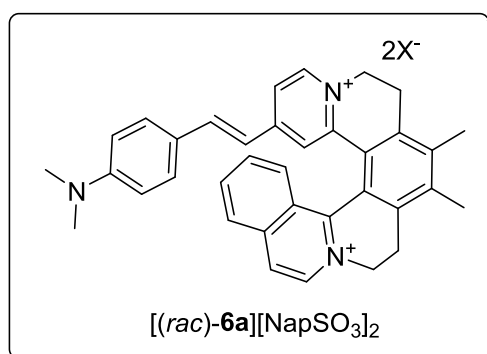
sample acidified by 1:1 HNO<sub>3</sub>). Then, water was passed through the resin until the outcoming solution was neutral (30 mL). Then, resin was switched to Br<sup>-</sup> cycle by passing 15 mL of 0.22M aq. solution of HBr. Then, 30 mL of water was passed through to remove all free acid (until the outcoming solution was neutral). Finally, water in the resin bed was exchanged for MeOH.

After passing the helquat, resin was washed with 20 mL of MeOH and the outcoming liquids were collected to a 50 mL rbf. The volatiles from the methanolic solution of [(*P*)-7][Br]<sub>2</sub> were removed on a rotary evaporator, the residue was dissolved in 1 mL MeCN and two parallel diffusion crystallizations were set up from the resulting solution. Single crystals of [(*P*)-7][Br]<sub>2</sub> suitable for X-ray analysis (and assignment of absolute configuration of the helical dicationic scaffold) were grown via a slow diffusion of *i*-Pr<sub>2</sub>O into a MeCN solution of [(*P*)-7][Br]<sub>2</sub>.

Crystal data for [(*P*)-7][Br]<sub>2</sub>: C<sub>24</sub>H<sub>26</sub>N<sub>2</sub>•2(Br)•3(H<sub>2</sub>O) *M*<sub>r</sub> = 556.34; Orthorhombic, space group *P*2<sub>1</sub>2<sub>1</sub>2<sub>1</sub> (No 19), *a* = 12.7303 (4) Å, *b* = 12.7933 (5) Å, *c* = 14.8125 (6) Å; *V* = 2412.40 (16) Å<sup>3</sup>, *Z* = 4, *D*<sub>x</sub> = 1.532 Mg m<sup>-3</sup>; dimensions of colorless prism 0.35 × 0.26 × 0.17 mm, *θ*<sub>max</sub> = 27.5°; numerical absorption correction (*μ* = 3.39 mm<sup>-1</sup>) *T*<sub>min</sub> = 0.384, *T*<sub>max</sub> = 0.590; 13720 diffractions collected, 5525 independent (*R*<sub>int</sub> = 0.023) and 4905 observed according to the *I* > 2σ(*I*) criterion. The refinement converged (*Δ*/σ<sub>max</sub> = 0.001) to *R* = 0.027 for observed reflections and *wR*(*F*<sup>2</sup>) = 0.055, *GOF* = 1.03 for 282 parameters and all 5525 reflections. Absolute structure: Flack parameter -0.022 (6). The final difference map displayed no peaks of chemical significance (*Δρ*<sub>max</sub> = 0.57, *Δρ*<sub>min</sub> -0.38 e.Å<sup>-3</sup>).

### [(*rac*)-6a][NapSO<sub>3</sub>]<sub>2</sub>

CCDC 925830:



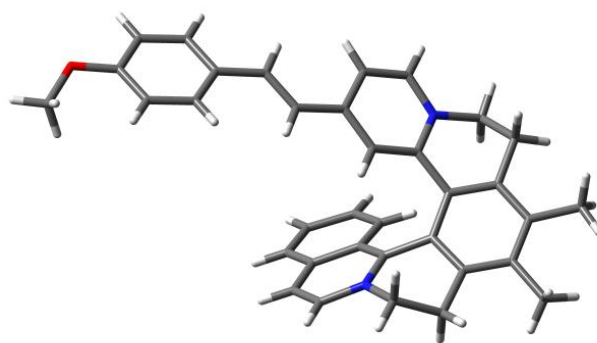
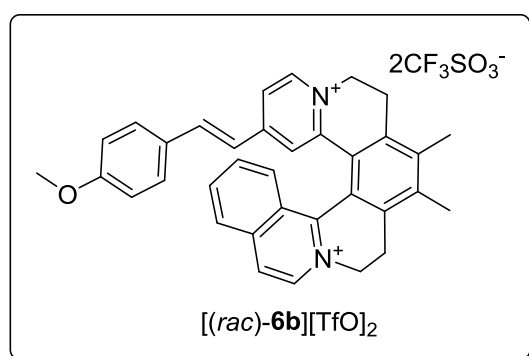
[(*rac*)-**6a**][TfO]<sub>2</sub> (15 mg, 19 μmol, 1 equiv) was dissolved in a minimum amount of acetone (approximately 0.5 mL). Tetrabutylammonium 2-naphthylsulphonate (41.8 mg, 93 μmol, 5 equiv) was dissolved in a minimum amount of acetone (approximately 1 mL). Tetrabutylammonium 2-naphthylsulphonate was prepared according to literature.<sup>25</sup> The two solutions were mixed and a dark precipitate resulted. The suspension was then centrifuged, and the solid pellet was separated and then sonicated with acetone (1 mL). The mixture was again centrifuged and the solid pellet was dried in vacuo. [(*rac*)-**6a**][NapSO<sub>3</sub>]<sub>2</sub> was obtained as a dark powder in 45% yield (7.7 mg, 8 μmol).

[(*rac*)-**6a**][NapSO<sub>3</sub>]<sub>2</sub> (2 mg) was dissolved in MeNO<sub>2</sub> (0.2 mL). Single crystals of [(*rac*)-**6a**][NapSO<sub>3</sub>]<sub>2</sub>·MeNO<sub>2</sub> suitable for X-ray analysis were grown via a slow diffusion of *i*-Pr<sub>2</sub>O into the MeNO<sub>2</sub> solution in the fridge (7°C) within 4 days.

Crystal data for [(*rac*)-**6a**][NapSO<sub>3</sub>]<sub>2</sub>: C<sub>36</sub>H<sub>35</sub>N<sub>3</sub>•2(C<sub>10</sub>H<sub>7</sub>O<sub>3</sub>S)•CH<sub>3</sub>NO<sub>2</sub>, M<sub>r</sub> = 985.15; Triclinic, *P*-1 (No 2), *a* = 8.2074 (6) Å, *b* = 16.4498 (11) Å, *c* = 19.3506 (12) Å, α = 70.455 (2), β = 86.370 (2)°, γ = 77.900 (2)°; *V* = 2407.2 (3) Å<sup>3</sup>, *Z* = 2, *D<sub>x</sub>* = 1.359 Mg m<sup>-3</sup>; dimensions of violet bar 0.59 × 0.45 × 0.10 mm, θ<sub>max</sub> = 25°; multi-scan absorption correction (μ = 0.17 mm<sup>-1</sup>) *T*<sub>min</sub> = 0.875, *T*<sub>max</sub> = 0.984; 16715 diffractions collected, 8251 independent (*R*<sub>int</sub> = 0.030) and 5700 observed according to the *I* > 2σ(*I*) criterion. The refinement converged (Δ/σ<sub>max</sub> = 0.004) to *R* = 0.053 for observed reflections and *wR*(*F*<sup>2</sup>) = 0.141, *GOF* = 1.03 for 648 parameters and all 8251 reflections. The final difference map displayed no peaks of chemical significance (Δρ<sub>max</sub> = 0.54, Δρ<sub>min</sub> = -0.58 e.Å<sup>-3</sup>).

### [(*rac*)-**6b**][TfO]<sub>2</sub>

CCDC 925831:

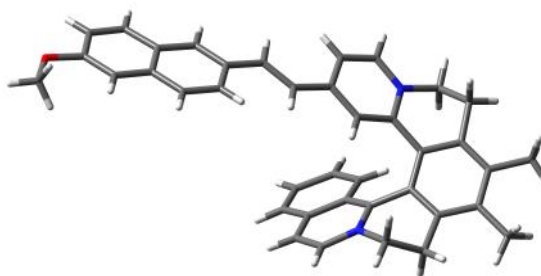
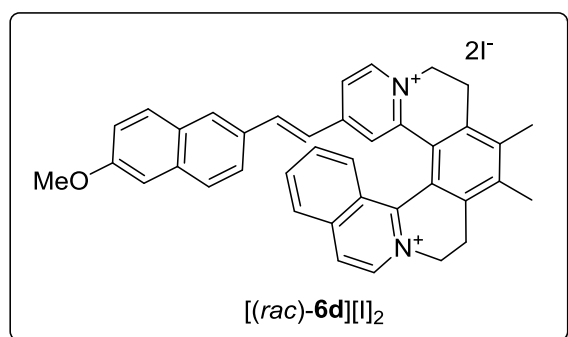


Single crystals of [(*rac*)-**6b**][TfO]<sub>2</sub>•0.5MeNO<sub>2</sub> suitable for X-ray analysis were grown via a slow diffusion of *i*-Pr<sub>2</sub>O into a solution of [(*rac*)-**6b**][TfO]<sub>2</sub> (2 mg) in MeNO<sub>2</sub> (0.2 mL) in the fridge (7°C) within 4 days.

Crystal data for [(*rac*)-**6b**][TfO]<sub>2</sub>: 2(C<sub>35</sub>H<sub>32</sub>N<sub>2</sub>O)•4(CF<sub>3</sub>O<sub>3</sub>S)•CH<sub>3</sub>NO<sub>2</sub>, M<sub>r</sub> = 1650.58; Triclinic, *P*-1 (No 2), *a* = 12.8456 (3) Å, *b* = 13.7518 (3) Å, *c* = 21.7960 (4) Å, α = 75.143 (1)°, β = 84.454 (1)°, γ = 87.583 (1)°; *V* = 3703.52 (14) Å<sup>3</sup>, *Z* = 2, *D<sub>x</sub>* = 1.480 Mg m<sup>-3</sup>; dimensions of orange prism 0.37 × 0.28 × 0.17 mm, θ<sub>max</sub> = 27.5°; multi-scan absorption correction (μ = 0.23 mm<sup>-1</sup>) *T*<sub>min</sub> = 0.919, *T*<sub>max</sub> = 0.962; 47477 diffractions collected, 16927 independent (*R*<sub>int</sub> = 0.028) and 12139 observed according to the *I* > 2σ(*I*) criterion. The refinement converged (Δ/σ<sub>max</sub> = 0.001) to *R* = 0.046 for observed reflections and *wR*(*F*<sup>2</sup>) = 0.116, *GOF* = 1.02 for 1016 parameters and all 16927 reflections. The final difference map displayed no peaks of chemical significance (Δρ<sub>max</sub> = 0.38, Δρ<sub>min</sub> = -0.49 e.Å<sup>-3</sup>).

#### [(*rac*)-**6d**][I]<sub>2</sub>

CCDC 1004883:



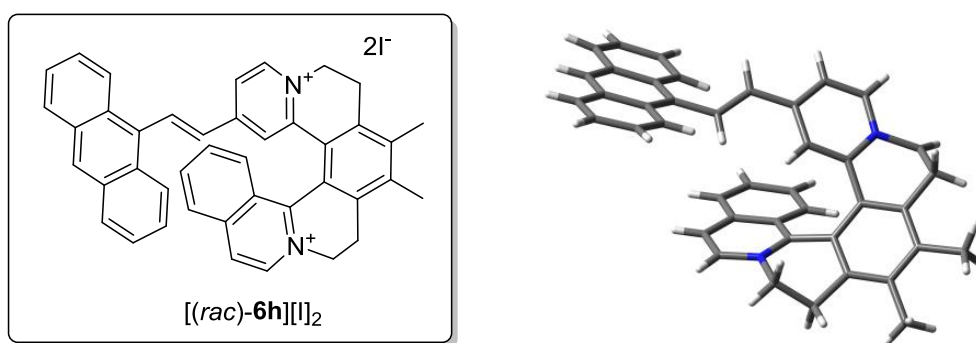
[(*rac*)-**6d**][TfO]<sub>2</sub> (10 mg, 11.8 μmol) was dissolved in acetone (0.5 mL). NaI (18 mg, 120 μmol, 10 equiv) was dissolved in acetone (0.5 mL). The two solutions were mixed and an orange precipitate resulted. The suspension was centrifuged, the precipitate was separated as the solid pellet and then sonicated with acetone (0.5 mL). The mixture was again centrifuged and the solid pellet was dried in vacuo. [(*rac*)-**6d**][I]<sub>2</sub> was obtained as an orange solid in 74% yield (7 mg, 8.7 μmol).

Single crystals of [(*rac*)-**6d**][I]<sub>2</sub> suitable for X-ray analysis were grown via a slow diffusion of *i*-Pr<sub>2</sub>O into a solution of [(*rac*)-**6d**][I]<sub>2</sub> (2 mg) in mixture of MeNO<sub>2</sub> (0.2 mL) and MeOH (drop, approximately 0.05 mL) in the fridge (7°C) within 5 days.

Crystal data for [(*rac*)-**6d**][I]<sub>2</sub>: C<sub>39</sub>H<sub>34</sub>N<sub>2</sub>O•2(I), M<sub>r</sub> = 800.48; Triclinic, *P*-1 (No 2), *a* = 13.5867 (4) Å, *b* = 14.1603 (4) Å, *c* = 19.3953 (6) Å,  $\alpha$  = 87.9609 (10)°,  $\beta$  = 76.1122 (10)°,  $\gamma$  = 86.1412 (11)° *V* = 3613.48 (19) Å<sup>3</sup>, *Z* = 4, *D*<sub>x</sub> = 1.471 g m<sup>-3</sup>; dimensions of red plate 0.28 × 0.14 × 0.09 mm,  $\theta_{max}$  = 26°; numerical absorption correction ( $\mu$  = 1.77 mm<sup>-1</sup>) *T*<sub>min</sub> = 0.633, *T*<sub>max</sub> = 0.857; 33318 diffractions collected, 14184 independent (*R*<sub>int</sub> = 0.039) and 9525 observed according to the *I* > 2σ(*I*) criterion. The refinement converged ( $\Delta/\sigma_{max}$  = 0.001) to *R* = 0.044 for observed reflections and *wR*(*F*<sup>2</sup>) = 0.081, *GOF* = 0.94 for 799 parameters and all 14184 reflections. The final difference map displayed no peaks of chemical significance ( $\Delta\rho_{max}$  = 0.86,  $\Delta\rho_{min}$  = -0.62 e.Å<sup>-3</sup>). PLATON/SQUEEZE<sup>24</sup> procedure was used to correct the data for the presence of large number of the disordered methanol molecules.

### [(*rac*)-**6h**][I]<sub>2</sub>

CCDC 1004884:



[(*rac*)-**6h**][TfO]<sub>2</sub> (10 mg, 11.5 μmol) was dissolved in acetone (0.5 mL). NaI (17 mg, 120 μmol, 10 equiv) was dissolved in acetone (0.5 mL). The two solutions were mixed and an orange precipitate resulted. The suspension was centrifuged, the solid precipitate was separated as a pellet and then sonicated with acetone (0.5 mL). The mixture was again centrifuged and the pellet was dried in vacuo. [(*rac*)-**6h**][I]<sub>2</sub> was obtained as an orange solid in 63% yield (6 mg, 7.3 μmol).

Single crystals of [(*rac*)-**6h**][I]<sub>2</sub> suitable for X-ray analysis were grown via a slow diffusion of *i*-Pr<sub>2</sub>O into a solution of [(*rac*)-**6h**][I]<sub>2</sub> (2 mg) in mixture of MeNO<sub>2</sub> (0.1 mL) and MeOH (0.1 mL) in the fridge (7°C) within 5 days.

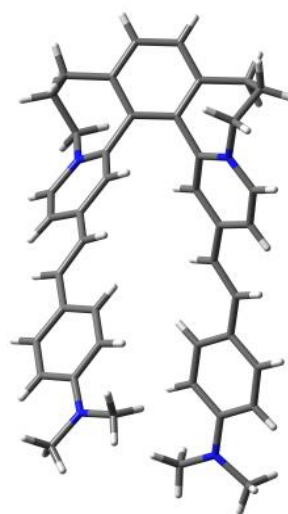
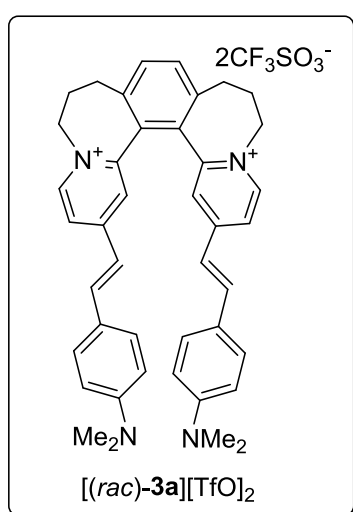
Crystal data for [(*rac*)-**6h**][I]<sub>2</sub>: C<sub>42</sub>H<sub>34</sub>N<sub>2</sub>•2(I), M<sub>r</sub> = 820.51; Orthorhombic, *Pbca* (No 61), *a* = 7.7728 (2) Å, *b* = 23.8635 (6) Å, *c* = 36.1252 (8) Å; *V* = 6700.7 (3) Å<sup>3</sup>, *Z* = 8, *D*<sub>x</sub> = 1.627 Mg



$\text{m}^{-3}$ ; dimensions of red bar  $0.41 \times 0.13 \times 0.11 \text{ mm}$ ,  $\theta_{\text{max}} = 26^\circ$ ; numerical absorption correction ( $\mu = 1.91 \text{ mm}^{-1}$ )  $T_{\text{min}} = 0.508$ ,  $T_{\text{max}} = 0.823$ ; 43985 diffractions collected, 6591 independent ( $R_{\text{int}} = 0.043$ ) and 5580 observed according to the  $I > 2\sigma(I)$  criterion. The refinement converged ( $\Delta/\sigma_{\text{max}} = 0.001$ ) to  $R = 0.061$  for observed reflections and  $wR(F^2) = 0.133$ ,  $GOF = 1.27$  for 417 parameters and all 6591 reflections. The final difference map displayed no peaks of chemical significance ( $\Delta\rho_{\text{max}} = 1.61$ ,  $\Delta\rho_{\text{min}} = -1.38 \text{ e.}\text{\AA}^{-3}$ ).

### [(*rac*)-**3a**][TfO]<sub>2</sub>

CCDC 1004344:



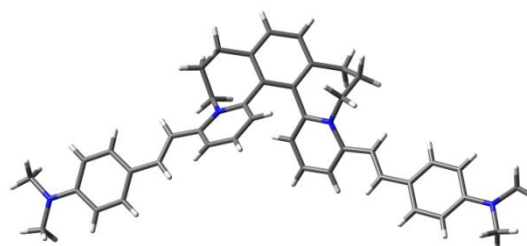
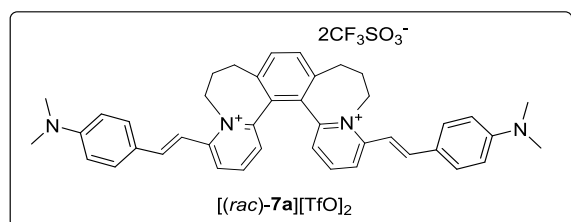
Single crystals of [(*rac*)-**3a**][TfO]<sub>2</sub> suitable for X-ray analysis were grown via a slow diffusion of *i*-Pr<sub>2</sub>O into a solution of [(*rac*)-**3a**][TfO]<sub>2</sub> in MeCN.

Crystal data for [(*rac*)-**3a**][TfO]<sub>2</sub>: C<sub>42</sub>H<sub>44</sub>N<sub>4</sub>•2(CF<sub>3</sub>O<sub>3</sub>S),  $M_r = 902.95$ ; Orthorhombic, space group *Pbca* (No 61),  $a = 25.3083 (18) \text{ \AA}$ ,  $b = 17.1165 (12) \text{ \AA}$ ,  $c = 42.198 (3) \text{ \AA}$ ;  $V = 18280 (2) \text{ \AA}^3$ ,  $Z = 16$ ,  $D_x = 1.312 \text{ Mg m}^{-3}$ ; dimensions of violet plate  $0.55 \times 0.23 \times 0.08 \text{ mm}$ ,  $\theta_{\text{max}} = 26^\circ$ ; multi-scan absorption correction ( $\mu = 0.19 \text{ mm}^{-1}$ )  $T_{\text{min}} = 0.902$ ,  $T_{\text{max}} = 0.984$ ; 96260 diffractions collected, 17955 independent ( $R_{\text{int}} = 0.095$ ) and 8822 observed according to the  $I > 2\sigma(I)$  criterion. The refinement converged ( $\Delta/\sigma_{\text{max}} = 0.001$ ) to  $R = 0.106$  for observed reflections and  $wR(F^2) = 0.295$ ,  $GOF = 1.05$  for 1105 parameters and all 17955 reflections. The final difference map displayed no peaks of chemical significance ( $\Delta\rho_{\text{max}} = 1.07$ ,  $\Delta\rho_{\text{min}} = -0.88 \text{ e.}\text{\AA}^{-3}$ ). The precision of the structure determination is hampered by severe disorder of triflate anions and even more disordered solvent molecules. PLATON/ SQUEEZE<sup>24</sup>

procedure had to be used to correct the diffraction data for the presence of the disordered solvates to improve the precision of structural parameters of dicationic helquat scaffolds, which appears to be well resolved.

**[(*rac*)-7a][TfO]<sub>2</sub>**

**CCDC 1004345:**

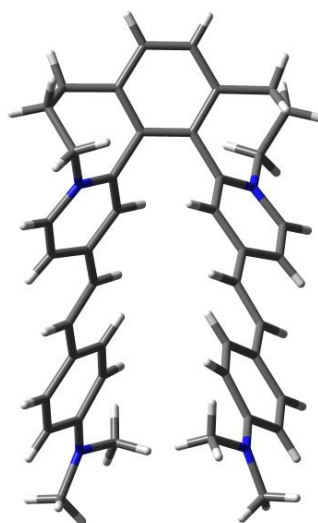
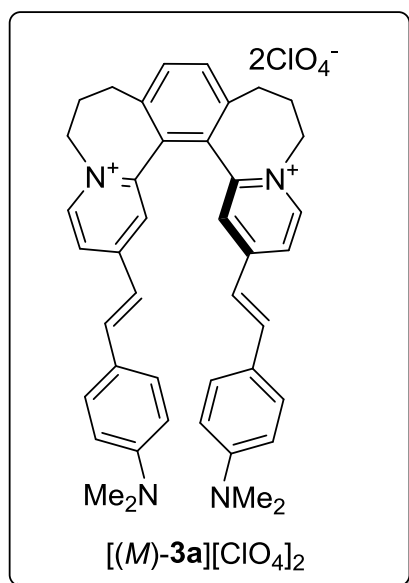


Single crystals of [(*rac*)-7a][TfO]<sub>2</sub> suitable for X-ray analysis were grown via a slow diffusion of Et<sub>2</sub>O into a solution of [(*rac*)-7a][TfO]<sub>2</sub> in MeNO<sub>2</sub>.

Crystal data for [(*rac*)-7a][TfO]<sub>2</sub>: C<sub>42</sub>H<sub>44</sub>N<sub>4</sub>•2(CF<sub>3</sub>O<sub>3</sub>S), M<sub>r</sub> = 902.95; Triclinic, *P*-1 (No 2), *a* = 10.9183 (3) Å, *b* = 13.1838 (3) Å, *c* = 15.8627 (3) Å, α = 69.603 (1)°, β = 77.874 (1)°, γ = 78.155 (1)°; *V* = 2070.60 (8) Å<sup>3</sup>, *Z* = 2, *D<sub>x</sub>* = 1.448 Mg m<sup>-3</sup>; dimensions of red plate 0.58 × 0.38 × 0.31 mm, θ<sub>max</sub> = 27.5°; multi-scan absorption correction (μ = 0.21 mm<sup>-1</sup>) *T*<sub>min</sub> = 0.888, *T*<sub>max</sub> = 0.938; 34575 diffractions collected, 9476 independent (*R*<sub>int</sub> = 0.024) and 7847 observed according to the *I* > 2σ(*I*) criterion. The refinement converged (Δ/σ<sub>max</sub> = 0.002) to *R* = 0.041 for observed reflections and *wR*(*F*<sup>2</sup>) = 0.113, *GOF* = 1.03 for 563 parameters and all 9476 reflections. The final difference map displayed no peaks of chemical significance (Δρ<sub>max</sub> = 0.47, Δρ<sub>min</sub> -0.39 e.Å<sup>-3</sup>).

**[(M)-3a][ClO<sub>4</sub>]<sub>2</sub>**

**CCDC 1008162:**



Triflate anion of [(M)-3a][TfO]<sub>2</sub> was exchanged to ClO<sub>4</sub><sup>-</sup> anion via passing a methanolic solution (10 mL) of [(M)-3a][TfO]<sub>2</sub> (10.4 mg, 11.5 μmol) through a strongly basic anion exchange resin in ClO<sub>4</sub><sup>-</sup> cycle.

The resin was prepared as follows: 2 mL bed volume of commercially available strongly basic anion exchange resin in water (in Cl<sup>-</sup> cycle) was prepared in a column equipped with a sinter S1. The resin was switched from Cl<sup>-</sup> to OH<sup>-</sup> cycle by passing 100 mL of a 2M aq. solution of NaOH. The complete exchange to OH<sup>-</sup> anions was proved by a negative test for Cl<sup>-</sup> anions in the outcoming solution (a few drops of 0.1M aq. solution of AgNO<sub>3</sub> were added to a sample acidified by 1:1 HNO<sub>3</sub>). Then, water was passed through the resin until the outcoming solution was neutral (50 mL of water). Then, the resin was switched to ClO<sub>4</sub><sup>-</sup> cycle by passing 12 mL of 0.2M aq. solution of HClO<sub>4</sub>. Then, 50 mL of water was passed through to remove all free acid (until the outcoming solution gave neutral reaction). Finally, water in the resin bed was exchanged for MeOH.

After passing the helquat solution, the resin was washed with 5 mL of MeOH and the outcoming liquids were collected to a 25 mL rbf. The volatiles from the methanolic solution of [(M)-3a][ClO<sub>4</sub>]<sub>2</sub> were removed on a rotary evaporator.

Single crystals of [(M)-3a][ClO<sub>4</sub>]<sub>2</sub> suitable for X-ray analysis (and assignment of absolute configuration of the helical dicationic scaffold) were grown via a slow diffusion of *i*-Pr<sub>2</sub>O into a MeOH:MeNO<sub>2</sub> (1:1) solution of [(M)-3a][ClO<sub>4</sub>]<sub>2</sub>.

Crystal data for [(*M*)-**3a**][ClO<sub>4</sub>]<sub>2</sub>: C<sub>42</sub>H<sub>44</sub>N<sub>4</sub>•2(ClO<sub>4</sub>), M<sub>r</sub> = 803.71; Tetragonal, space group *P*4<sub>2</sub>2<sub>1</sub>2 (No 94), *a* = 13.3242 (4) Å, *c* = 24.3016 (9) Å; *V* = 4314.4 (2) Å<sup>3</sup>, *Z* = 4, *D*<sub>x</sub> = 1.237 Mg m<sup>-3</sup>; dimensions of dark red plate 0.44 × 0.20 × 0.13 mm, *θ*<sub>max</sub> = 26°; multi-scan absorption correction (*μ* = 0.20mm<sup>-1</sup>) *T*<sub>min</sub> = 0.79, *T*<sub>max</sub> = 0.97; 24485 diffractions collected, 4285 independent (*R*<sub>int</sub> = 0.065) and 2512 observed according to the *I* > 2σ(*I*) criterion. The refinement converged ( $\Delta/\sigma_{\max} = 0.001$ ) to *R* = 0.122 for observed reflections and *wR*(*F*<sup>2</sup>) = 0.359, *GOF* = 1.27 for 263 parameters and all 4285 reflections. The final difference map displayed no peaks of chemical significance ( $\Delta\rho_{\max} = 1.13$ ,  $\Delta\rho_{\min} = -0.53$  e.Å<sup>-3</sup>). Absolute structure: Flack parameter 0.1(3), Parsons 0.07(4). The precision of the structure determination is strongly affected by a severe disorder of both ClO<sub>4</sub><sup>-</sup> anions, they are placed into more than two position forming almost a ball of electron density. The only reason for including this structure into the presented set of X-ray structures is the independent assignment of absolute configuration of the dicationic helquat scaffold. To this end, the presented structural data unambiguously confirm the helicity of this compound to be (*M*) as expected.

## 8) References

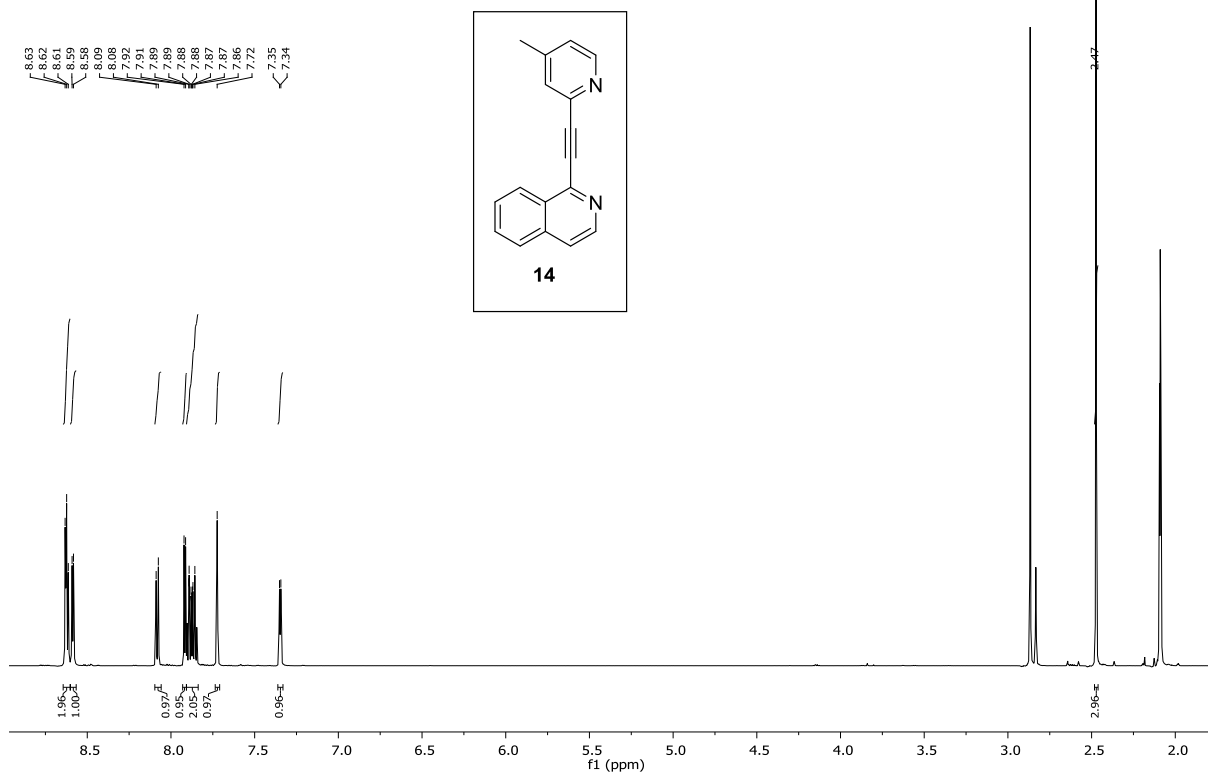
- <sup>1</sup> D. B. Amabilino, P. R. Ashton, A. S. Reder, N. Spencer, J. F. Stoddart, *Angew. Chem. Int. Ed. Engl.* **1994**, *33*, 1286.
- <sup>2</sup> L. Severa, L. Adriaenssens, J. Vávra, D. Šaman, I. Císařová, P. Fiedler, F. Teplý, *Tetrahedron* **2010**, *66*, 3537.
- <sup>3</sup> B. J. Coe, S. P. Foxon, E. C. Harper, J. A. Harris, M. Helliwell, J. Raftery, I. Asselberghs, K. Clays, E. Franz, B. S. Brunshwig, A. G. Fitch, *Dyes Pigments* **2009**, *82*, 171.
- <sup>4</sup> L. Severa, M. Ončák, D. Koval, R. Pohl, D. Šaman, I. Císařová, P. E. Reyes-Gutiérrez, P. Sázelová, V. Kašička, F. Teplý, P. Slaviček, *Angew. Chem. Int. Ed.* **2012**, *51*, 11972.
- <sup>5</sup> Y. F. Shen, R. D. Smith, *J. Microcolumn Sep.* **2000**, *12*, 135.
- <sup>6</sup> D. Koval, V. Kašička, H. Cottet, *Anal. Biochem.* **2011**, *413*, 8.
- <sup>7</sup> (a) R. Ahlrichs, M. Bär, M. Häser, H. Horn, C. Kölmel, *Chem. Phys. Lett.* **1989**, *162*, 165; (b) TURBOMOLE V6.5 2013, a development of University of Karlsruhe and Forschungszentrum Karlsruhe GmbH, 1989-2007, TURBOMOLE GmbH, since 2007; available from <http://www.turbomole.com>.
- <sup>8</sup> (a) P. Sehnal, Z. Krausová, F. Teplý, I. G. Stará, I. Starý, L. Rulišek, D. Šaman, I. Císařová, *J. Org. Chem.* **2008**, *73*, 2074; (b) A. Andronova, F. Szydło, F. Teplý, M. Tobrmanová, A. Volot, I. G. Stará, I. Starý, L. Rulišek, D. Šaman, J. Cvačka, P. Fiedler, P. Vojtíšek, *Collect. Czech. Chem. Commun.* **2009**, *74*, 189; (c) L. Adriaenssens, L. Severa, D. Koval, I. Císařová, M. Martínez Belmonte, E. C. Escudero-Adán, P. Novotná, P. Sázelová, J. Vávra, R. Pohl, D. Šaman, M. Urbanová, V. Kašička, F. Teplý, *Chem. Sci.* **2011**, *2*, 2314.

- <sup>9</sup> Gaussian 09, Revision A.02, M. J. Frisch, G. W. Trucks, H. B. Schlegel, G. E. Scuseria, M. A. Robb, J. R. Cheeseman, G. Scalmani, V. Barone, B. Mennucci, G. A. Petersson, H. Nakatsuji, M. Caricato, X. Li, H. P. Hratchian, A. F. Izmaylov, J. Bloino, G. Zheng, J. L. Sonnenberg, M. Hada, M. Ehara, K. Toyota, R. Fukuda, J. Hasegawa, M. Ishida, T. Nakajima, Y. Honda, O. Kitao, H. Nakai, T. Vreven, J. A. Montgomery, Jr., J. E. Peralta, F. Ogliaro, M. Bearpark, J. J. Heyd, E. Brothers, K. N. Kudin, V. N. Staroverov, R. Kobayashi, J. Normand, K. Raghavachari, A. Rendell, J. C. Burant, S. S. Iyengar, J. Tomasi, M. Cossi, N. Rega, J. M. Millam, M. Klene, J. E. Knox, J. B. Cross, V. Bakken, C. Adamo, J. Jaramillo, R. Gomperts, R. E. Stratmann, O. Yazyev, A. J. Austin, R. Cammi, C. Pomelli, J. W. Ochterski, R. L. Martin, K. Morokuma, V. G. Zakrzewski, G. A. Voth, P. Salvador, J. J. Dannenberg, S. Dapprich, A. D. Daniels, O. Farkas, J. B. Foresman, J. V. Ortiz, J. Cioslowski, D. J. Fox, Gaussian, Inc., Wallingford CT, 2009.
- <sup>10</sup> J. P. Perdew, K. Burke, M. Ernzerhof, *Phys. Rev. Lett.* **1996**, *77*, 3865.
- <sup>11</sup> (a) K. Eichkorn, O. Treutler, H. Öhm, M. Häser, R. Ahlrichs, *Chem. Phys. Lett.* **1995**, *240*, 283; (b) K. Eichkorn, F. Weigend, O. Treutler, R. Ahlrichs, *Theor. Chem. Acc.* **1997**, *97*, 119.
- <sup>12</sup> A. Schäfer, H. Horn, R. Ahlrichs, *J. Chem. Phys.* **1992**, *97*, 2571.
- <sup>13</sup> S. Grimme, J. Antony, S. Ehrlich, H. Krieg, *J. Chem. Phys.* **2010**, *132*, 154104.
- <sup>14</sup> (a) A. Klamt, G. Schüürmann, *J. Chem. Soc., Perkin Trans. 2* **1993**, 799; (b) A. Schäfer, A. Klamt, D. Sattel, J. C. W. Lohrenz, F. Eckert, *Phys. Chem. Chem. Phys.* **2000**, *2*, 2187.
- <sup>15</sup> (a) J. Tomasi, B. Mennucci, R. Cammi, *Chem. Rev.* **2005**, *105*, 2999; (b) G. Scalmani, M. J. Frisch, *J. Chem. Phys.* **2010**, *132*, 114110.
- <sup>16</sup> A. D. Boese, J. M. L. Martin, *J. Chem. Phys.* **2004**, *121*, 3405.
- <sup>17</sup> T. Yanai, D. Tew, N. Handy, *Chem. Phys. Lett.* **2004**, *393*, 51.

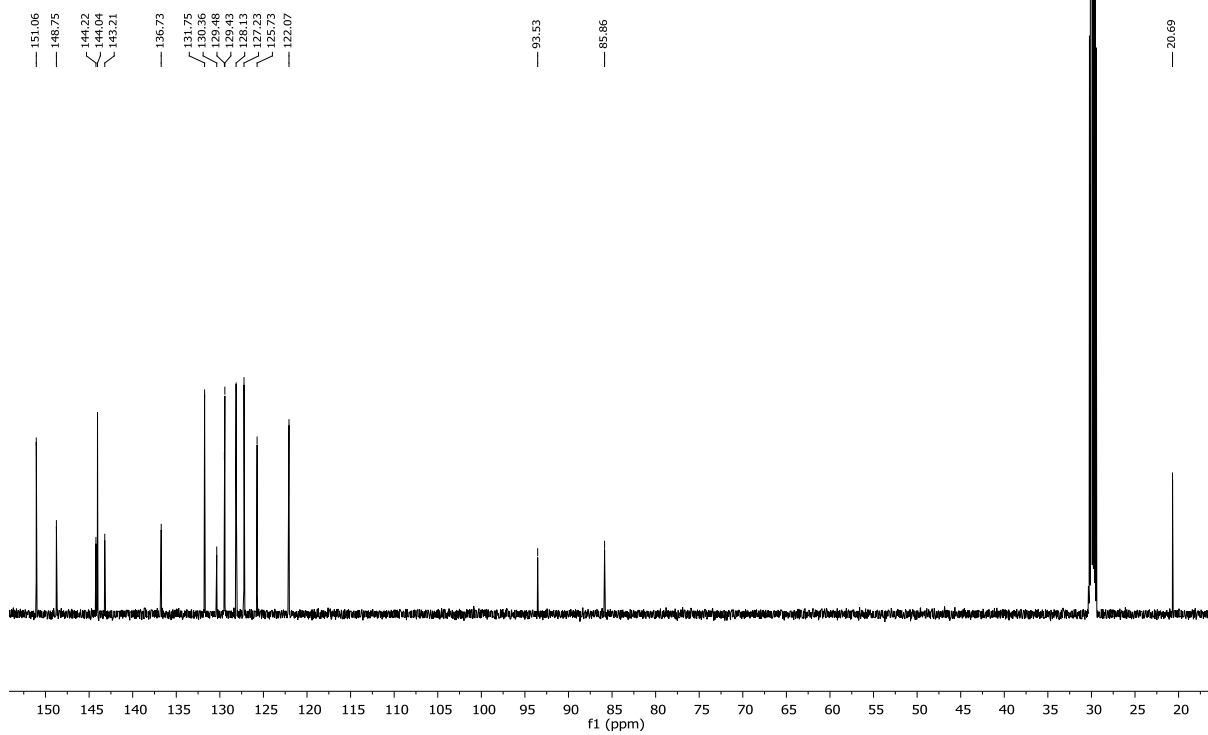
- <sup>18</sup> Y. Zhao, D. G. Truhlar, *Theor. Chem. Acc.* **2008**, *120*, 215.
- <sup>19</sup> (a) A. D. Becke, *J. Chem. Phys.* **1993**, *98*, 5648; (b) P. J. Stephens, F. J. Devlin, C. F. Chabalowski, M. J. Frisch, *J. Phys. Chem.* **1994**, *98*, 11623; (c) C. T. Lee, W. T. Yang, R. G. Parr, *Phys. Rev. B* **1988**, *37*, 785; (d) A. D. Becke, *Phys. Rev. A* **1988**, *38*, 3098.
- <sup>20</sup> C. Adamo, V. Barone, *J. Chem. Phys.* **1999**, *110*, 6158.
- <sup>21</sup> L. Severa, D. Koval, P. Novotná, M. Ončák, P. Sázelová, D. Šaman, P. Slavíček, M. Urbanová, V. Kašička, F. Teplý, *New J. Chem.* **2010**, *34*, 1063.
- <sup>22</sup> L. Pospíšil, L. Bednárová, P. Štěpánek, P. Slavíček, J. Vávra, M. Hromadová, H. Dlouhá, J. Tarábek, F. Teplý, *J. Am. Chem. Soc.* **2014**, *136*, 10826.
- <sup>23</sup> G. M. Sheldrick, *Acta Cryst.* **2008**, *A64*, 112.
- <sup>24</sup> A. L. Spek, *Acta Cryst.* **2009**, *D65*, 148.
- <sup>25</sup> B. J. Coe, J. Fielden, S. P. Foxon, J. A. Harris, M. Helliwell, B. S. Brunshwig, I. Asselberghs, K. Clays, J. Garín, J. Orduna, *J. Am. Chem. Soc.* **2010**, *132*, 10498.

## 9) $^1\text{H}$ and $^{13}\text{C}$ NMR spectra

Teply-MJ093.1.fid  
600 MHz, acetone-d<sub>6</sub>

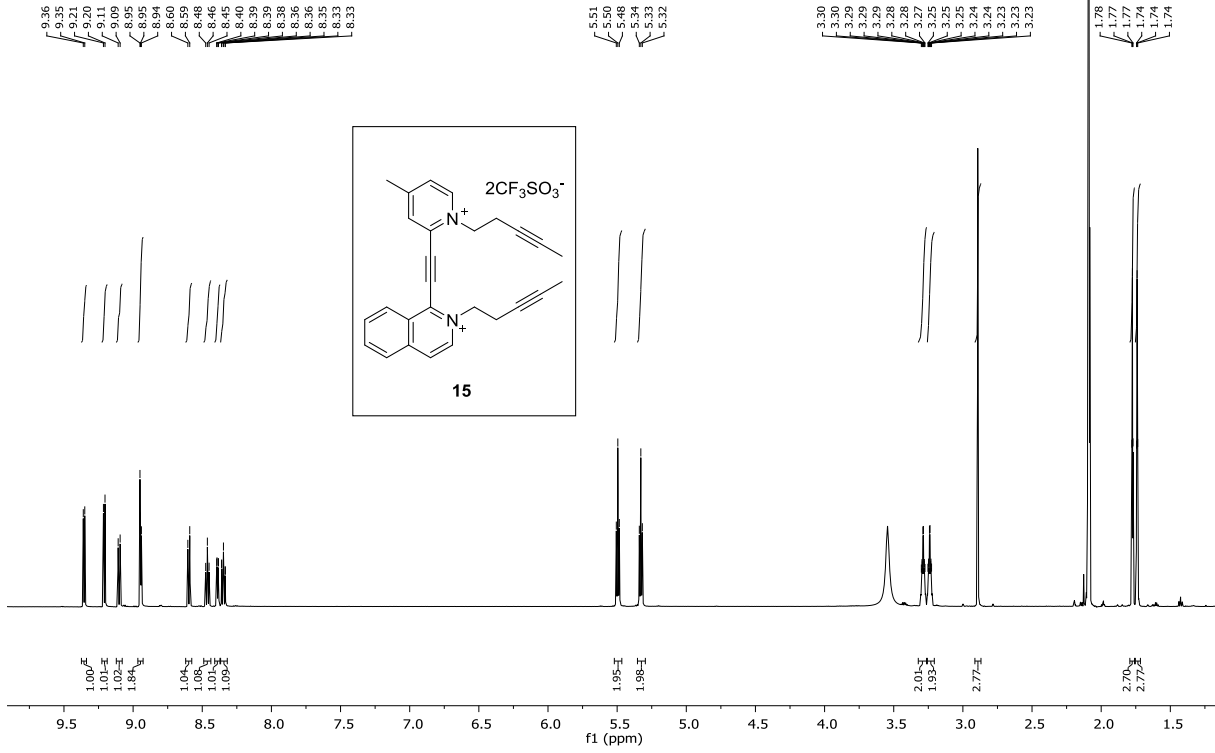


Teply-MJ093.2.fid  
151 MHz, acetone-d<sub>6</sub>

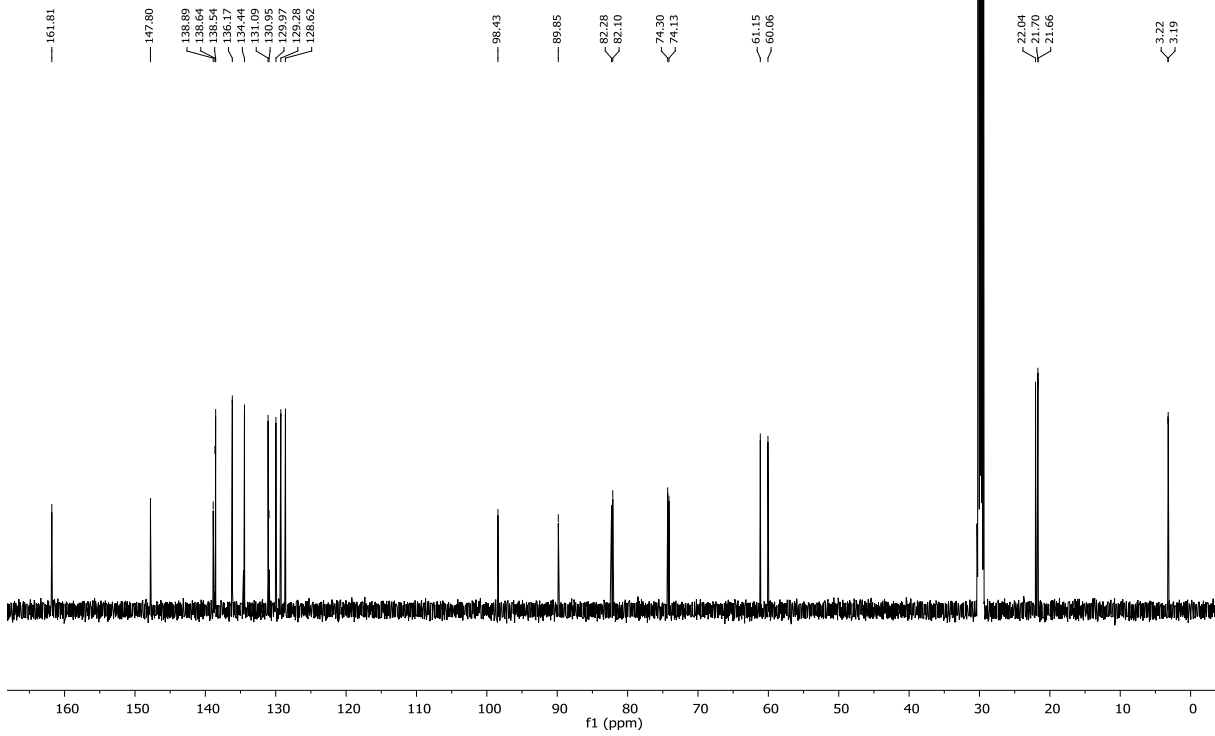




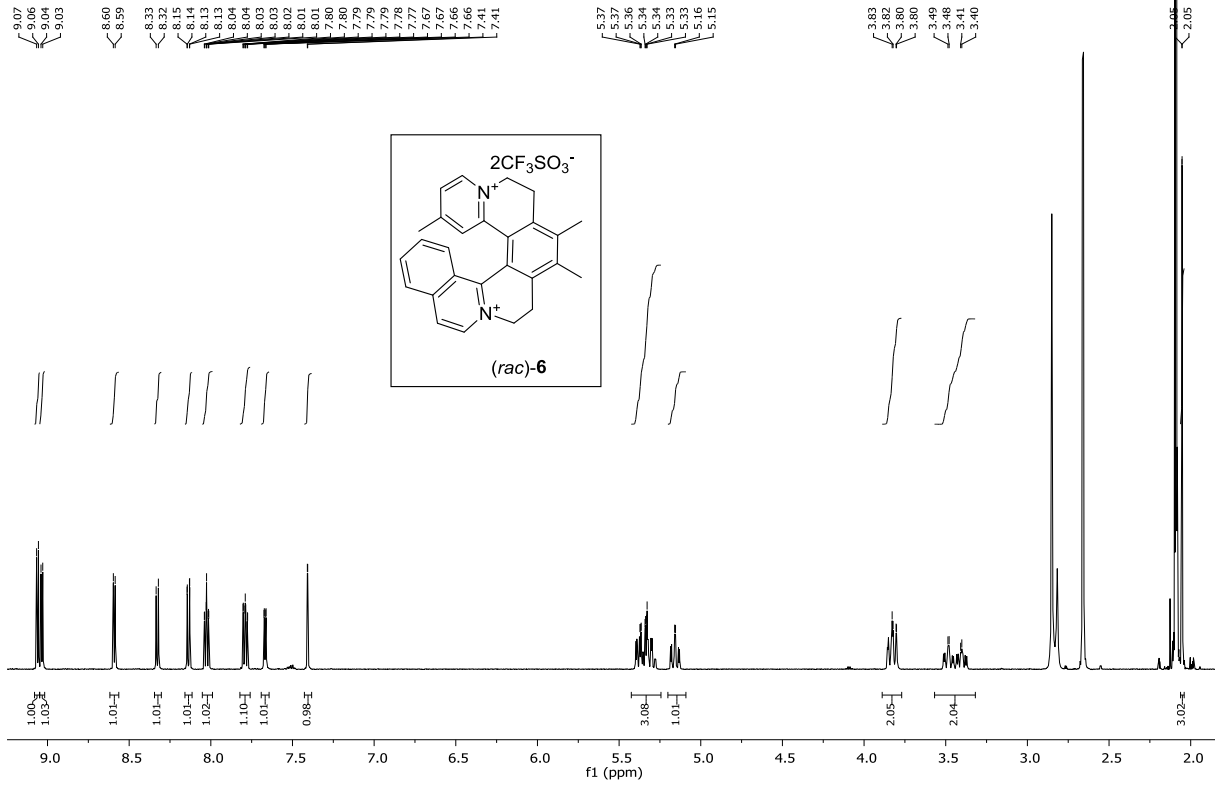
Teply-MJ096.1.fid  
600 MHz, acetone-d6



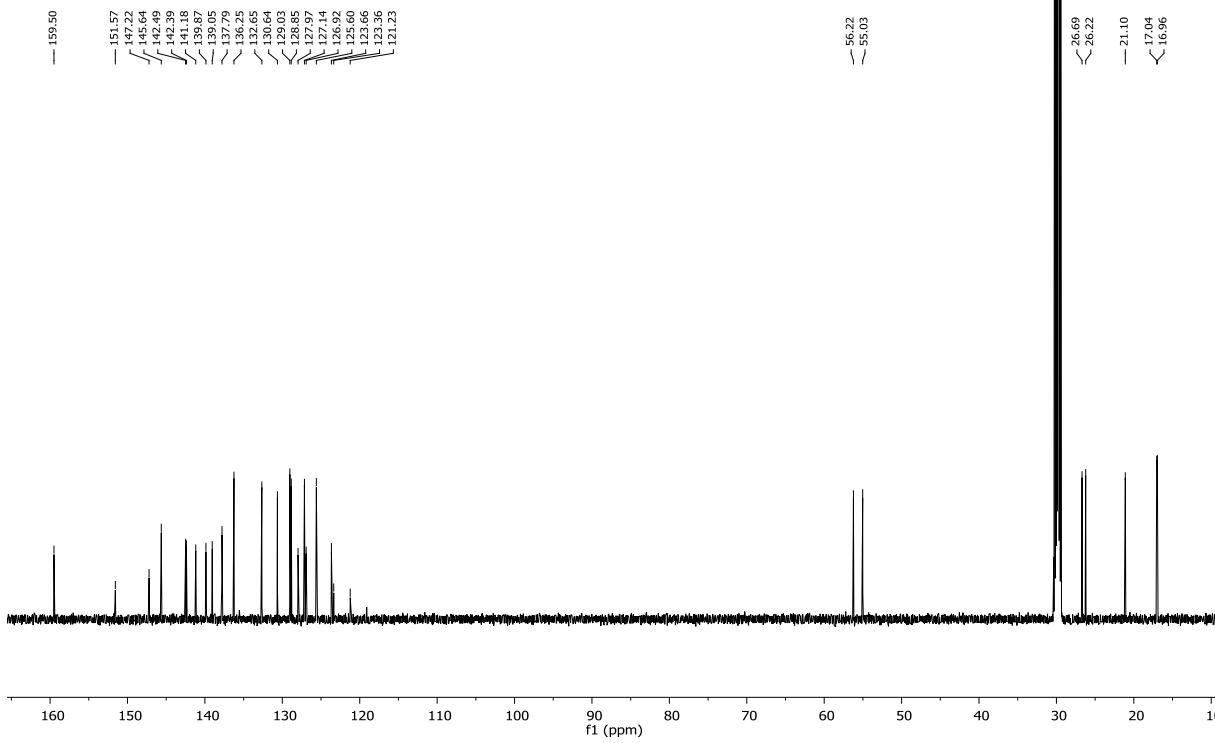
Teply-MJ096.2.fid  
151 MHz, acetone-d6



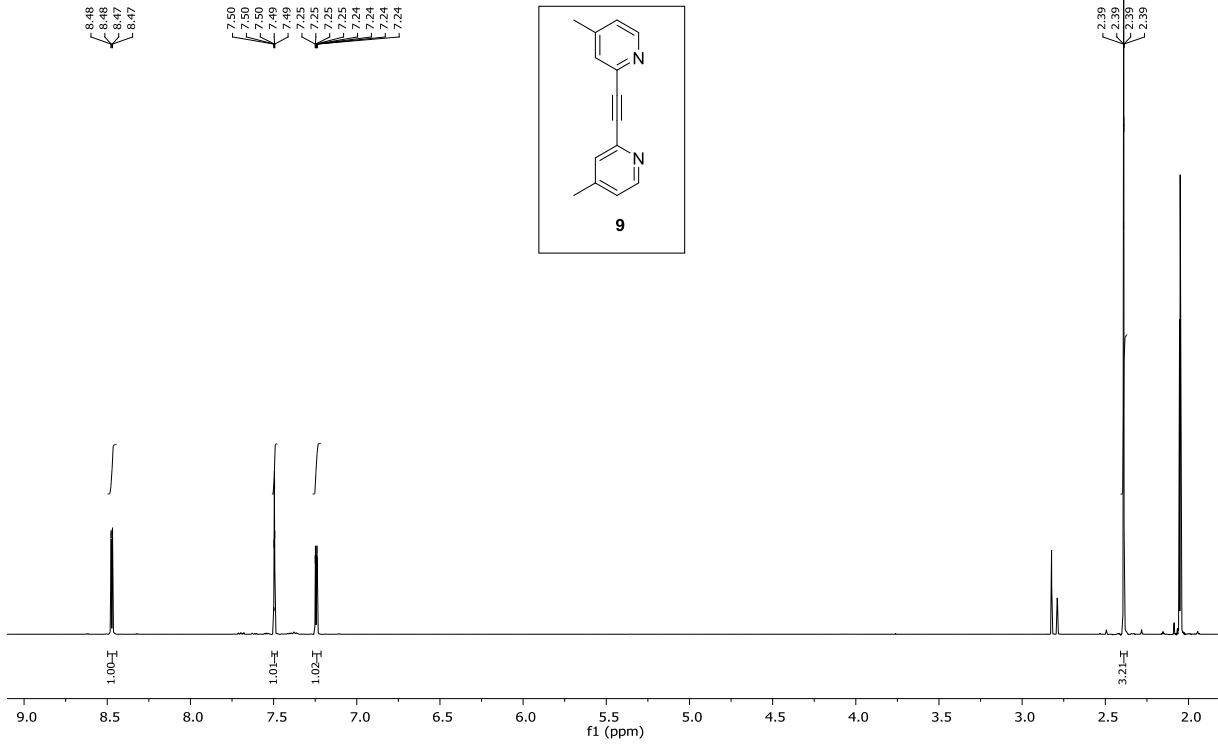
Teplý-MJ097.1.fid  
600 MHz, acetone-d6



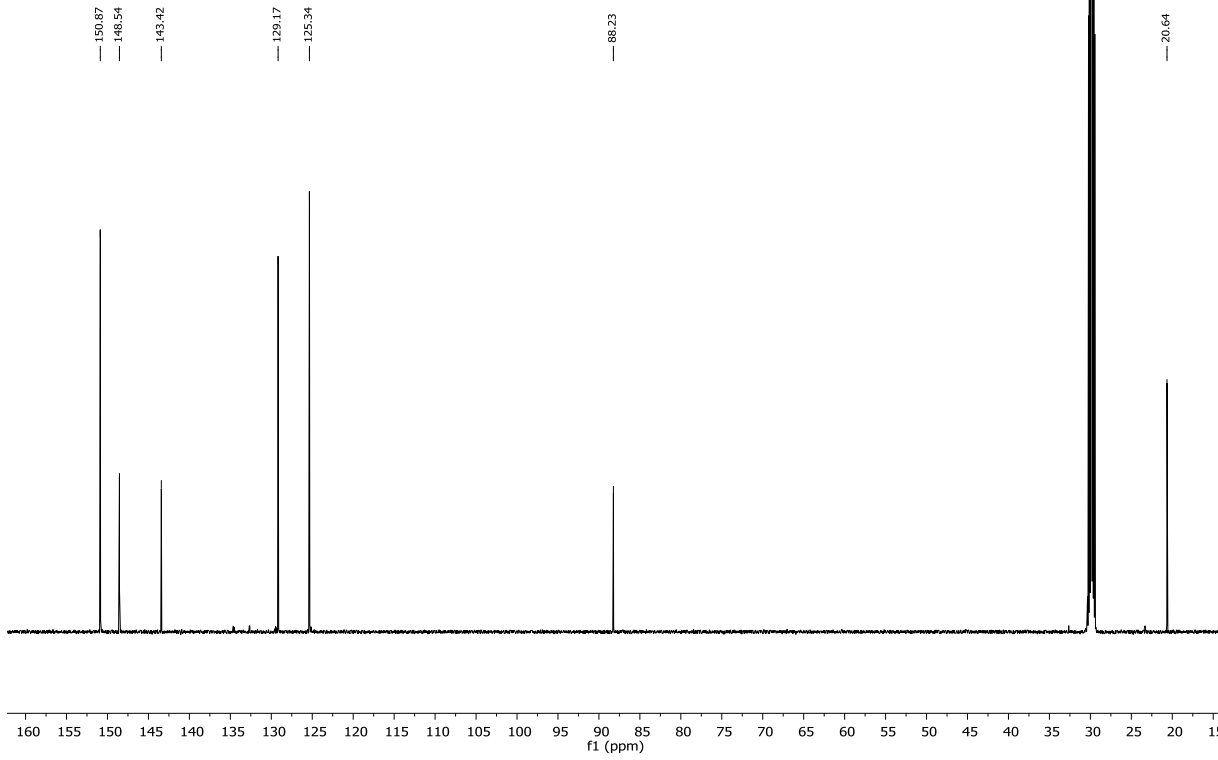
Teplý-MJ097.2.fid  
151 MHz, acetone-d6



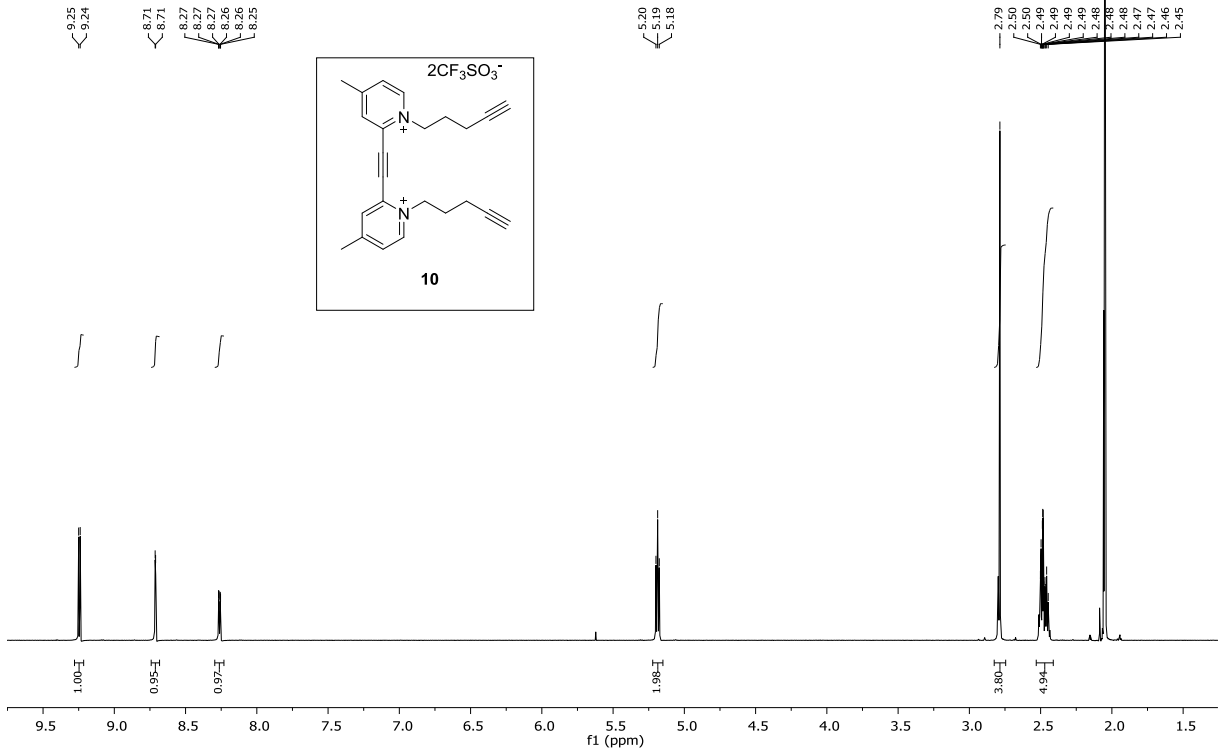
Reyes-PR261.1.fid  
600MHz, acetone-d6



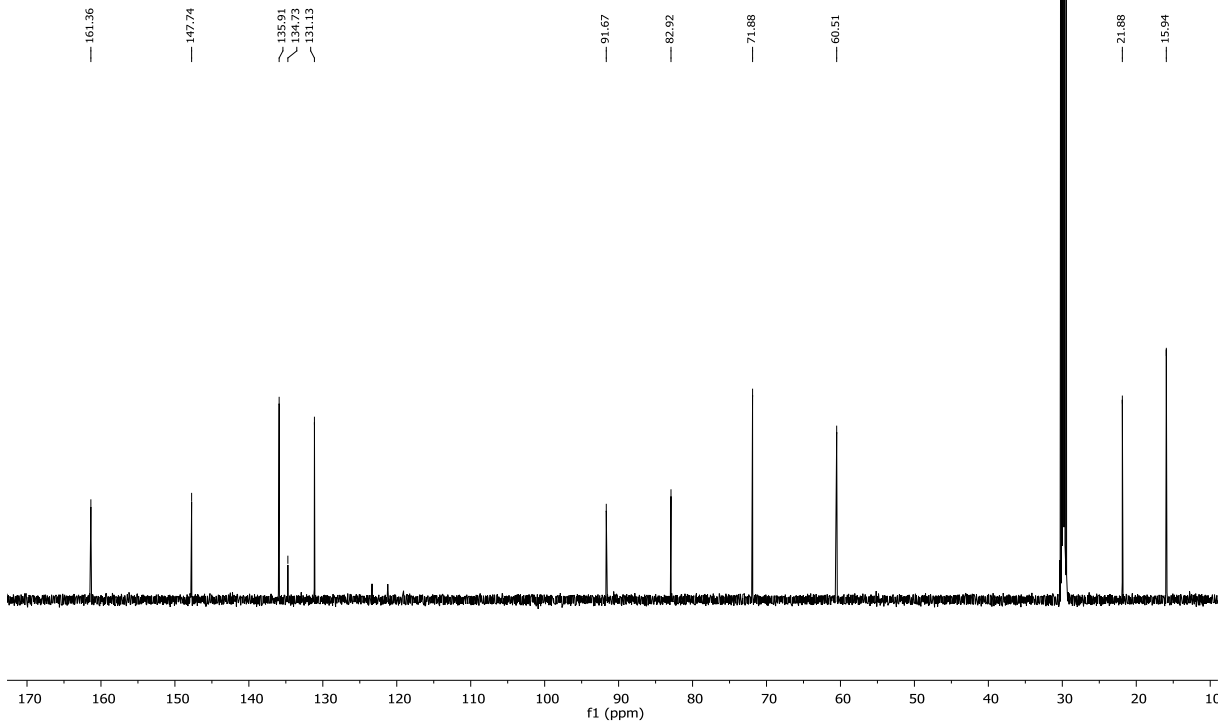
Reyes-PR261.2.fid  
151 MHz, acetone-d6



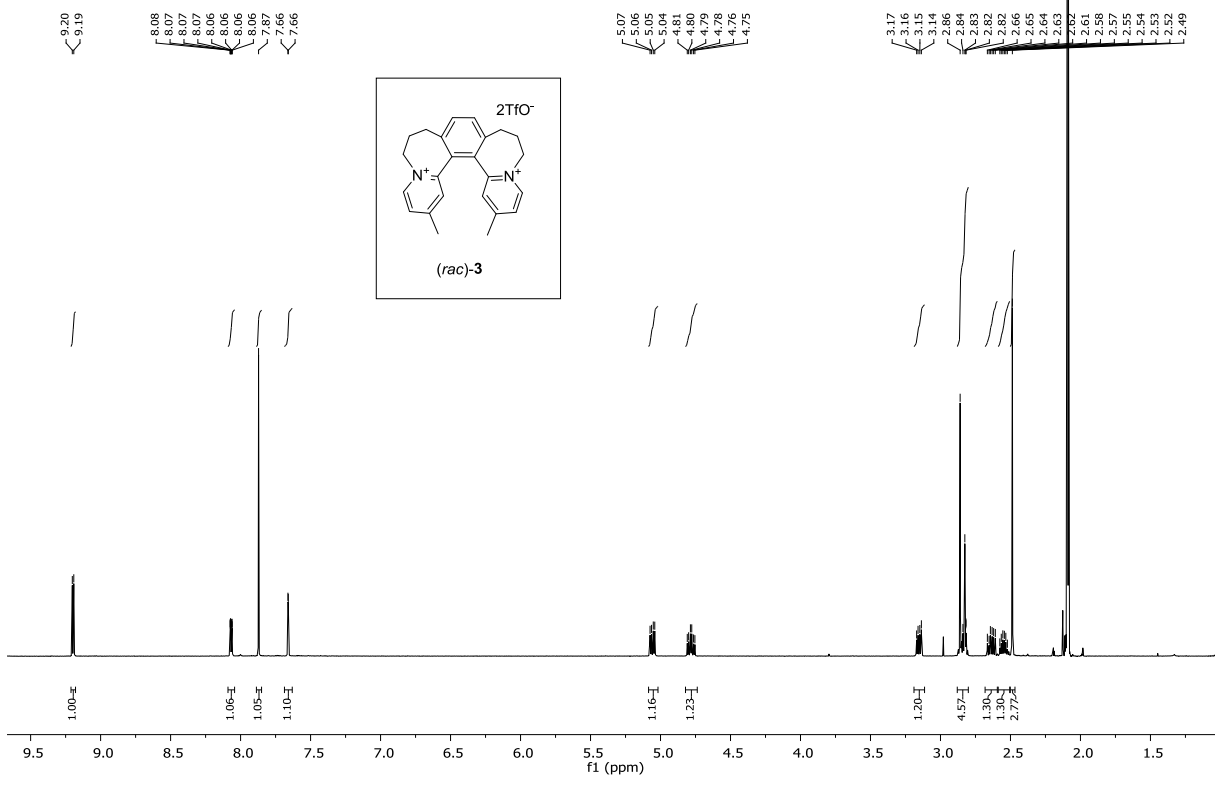
Reyes-PR268.1.fid  
600 MHz, acetone-d6



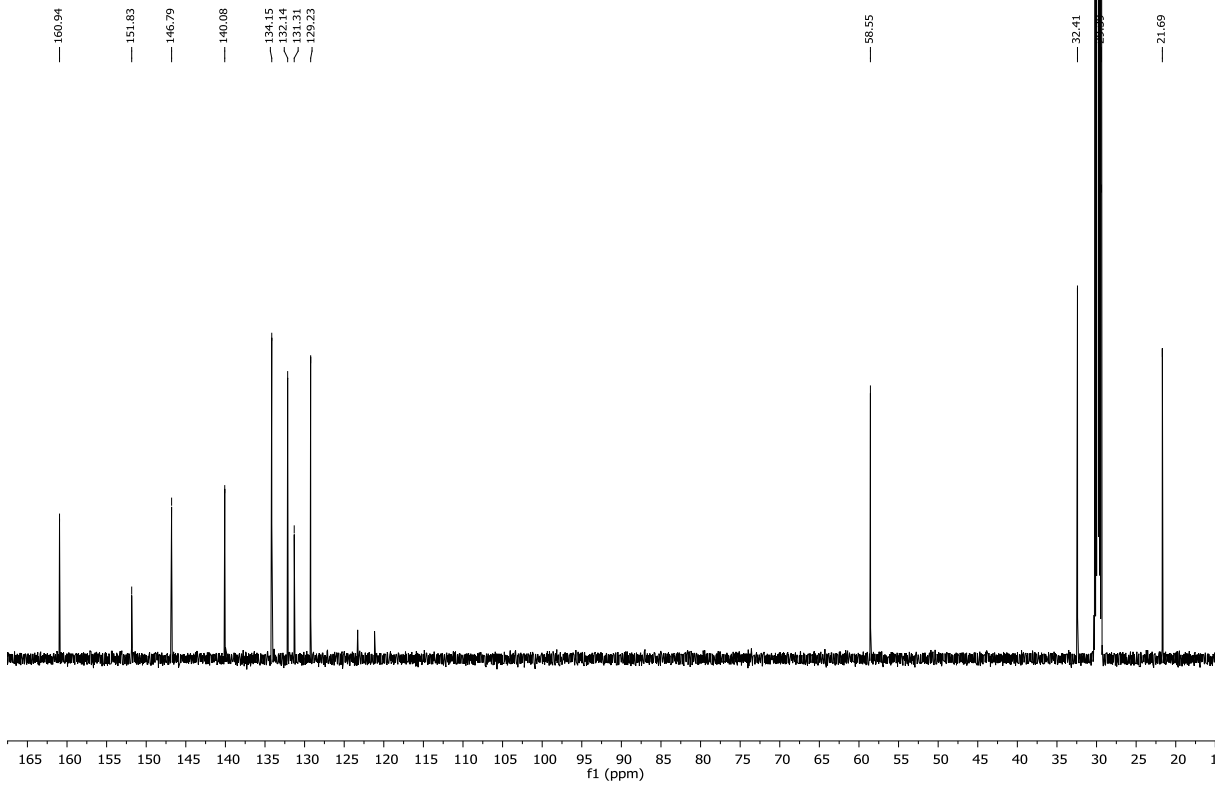
Reyes-PR268.2.fid  
151 MHz, acetone-d6



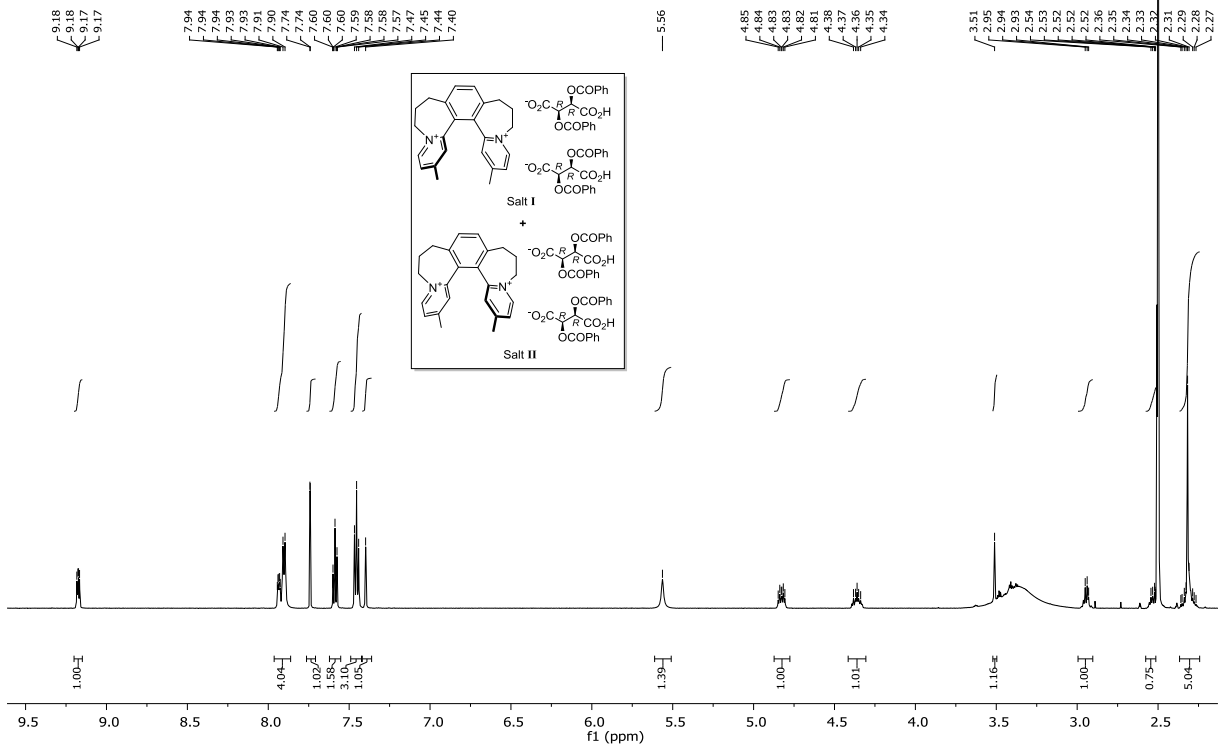
Reyes-PR272.1.fid  
600 MHz, acetone-d6



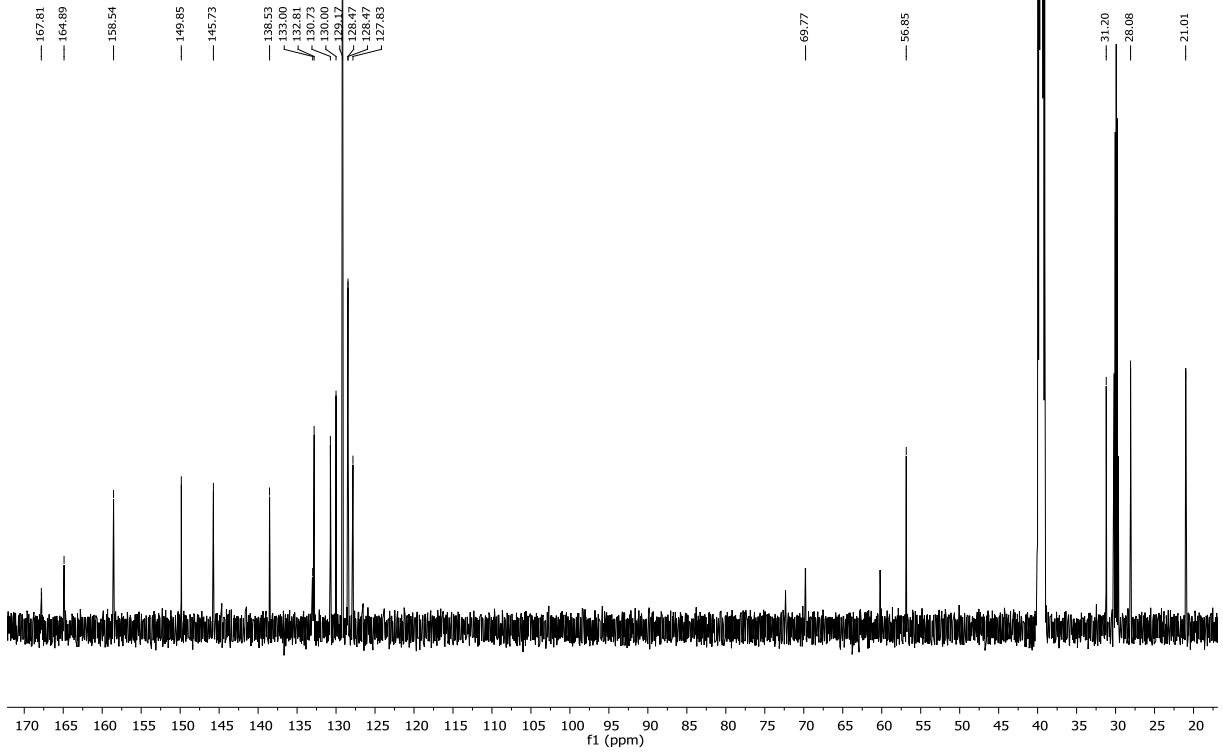
Reyes-PR272.12.fid  
151 MHz, acetone-d6



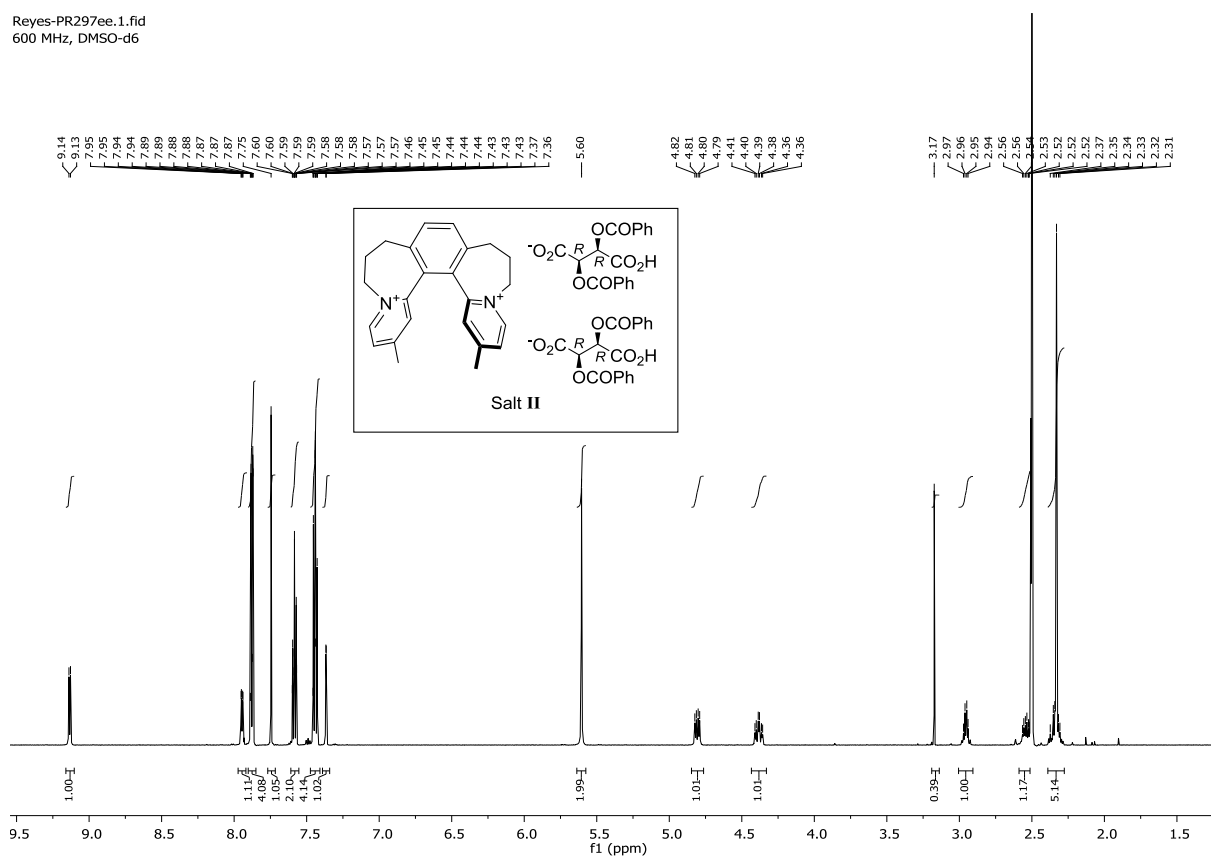
Reyes-PR275.1.fid  
600 MHz, DMSO-d6



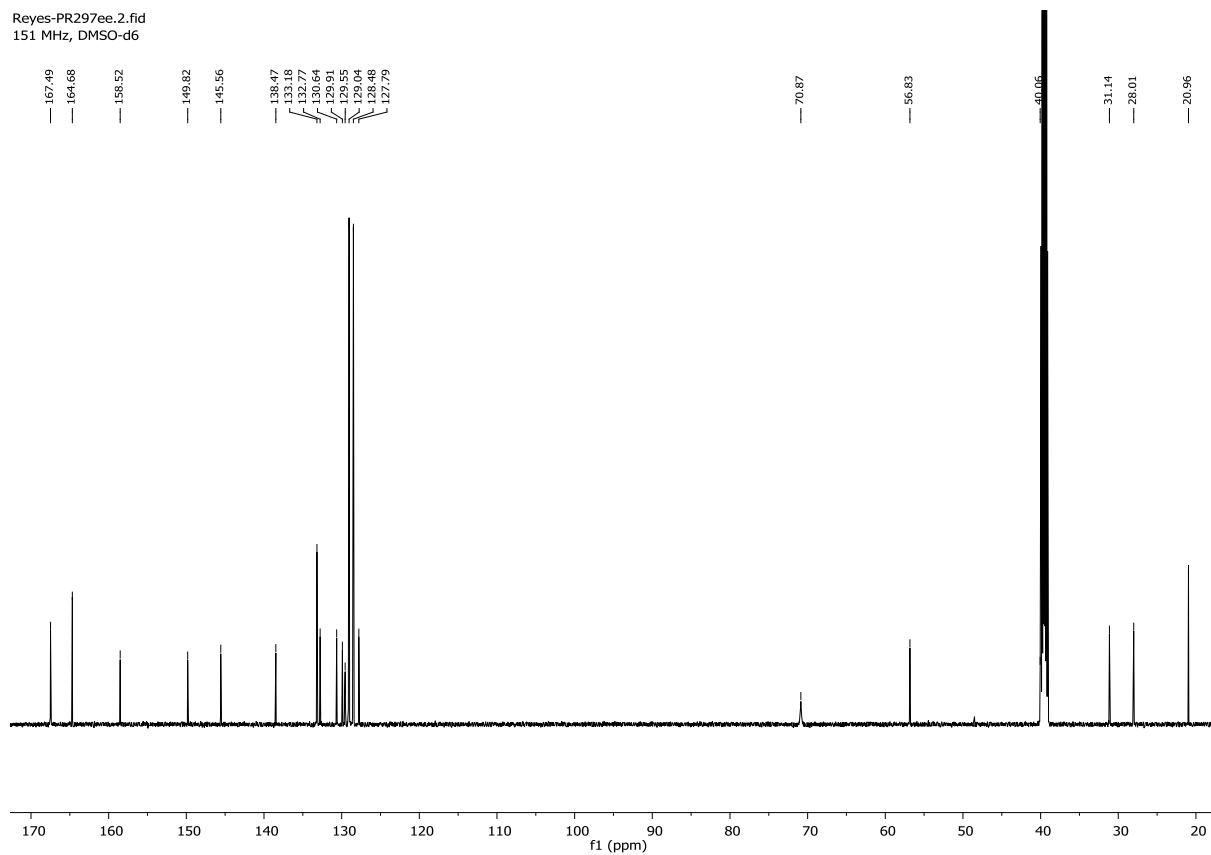
Reyes-PR275.2.fid  
151 MHz, DMSO-d6



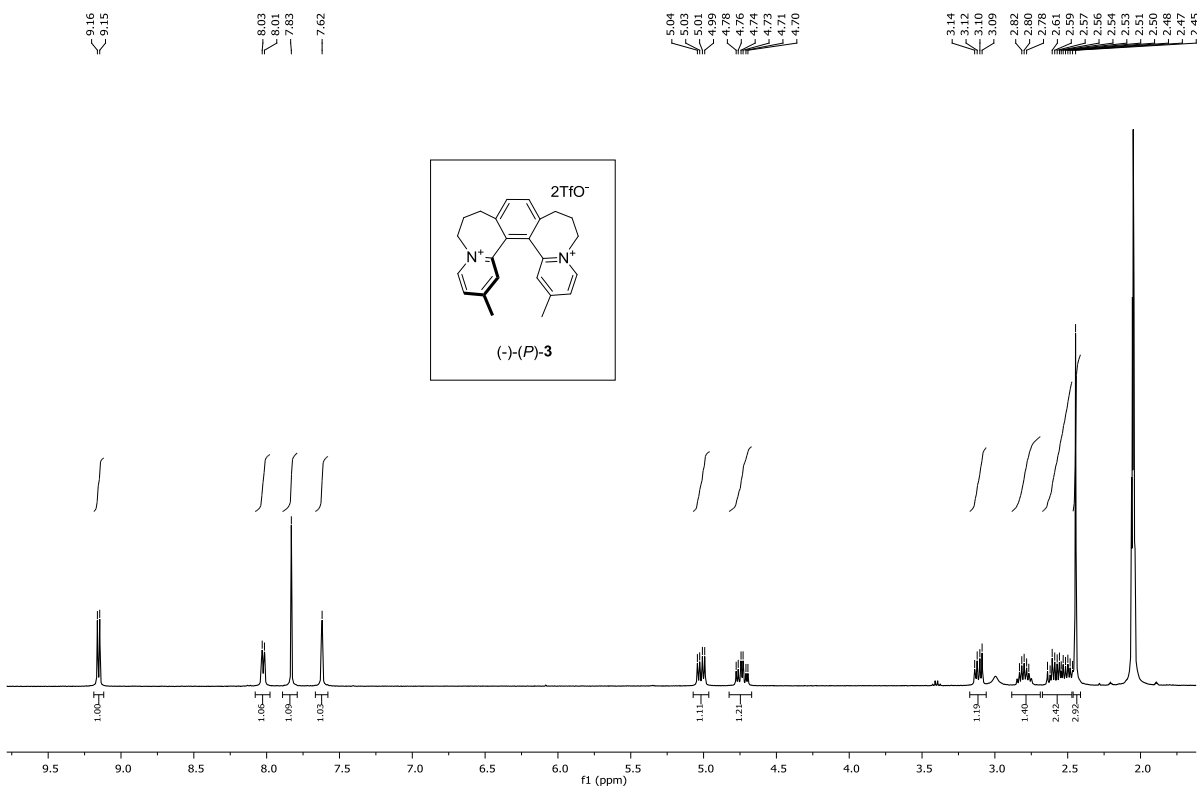
Reyes-PR297ee.1.fid  
600 MHz, DMSO-d6



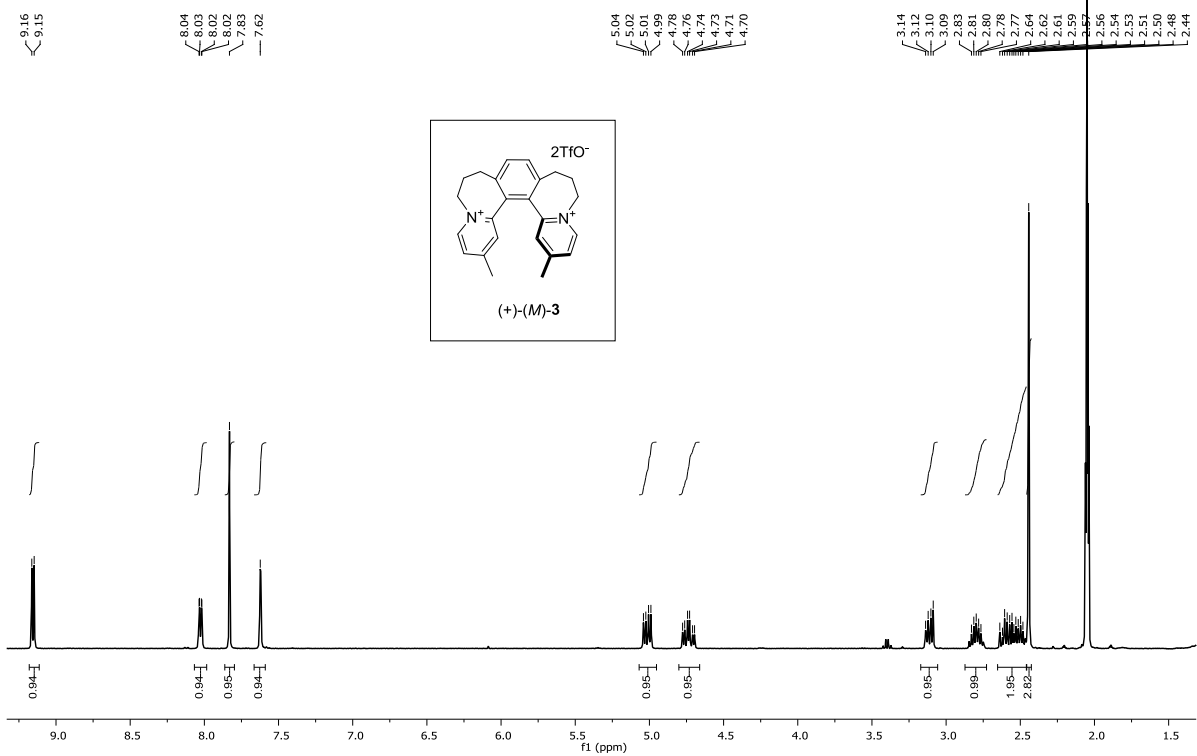
Reyes-PR297ee.2.fid  
151 MHz, DMSO-d6



(P)-PR364  
400 MHz, acetone-d6

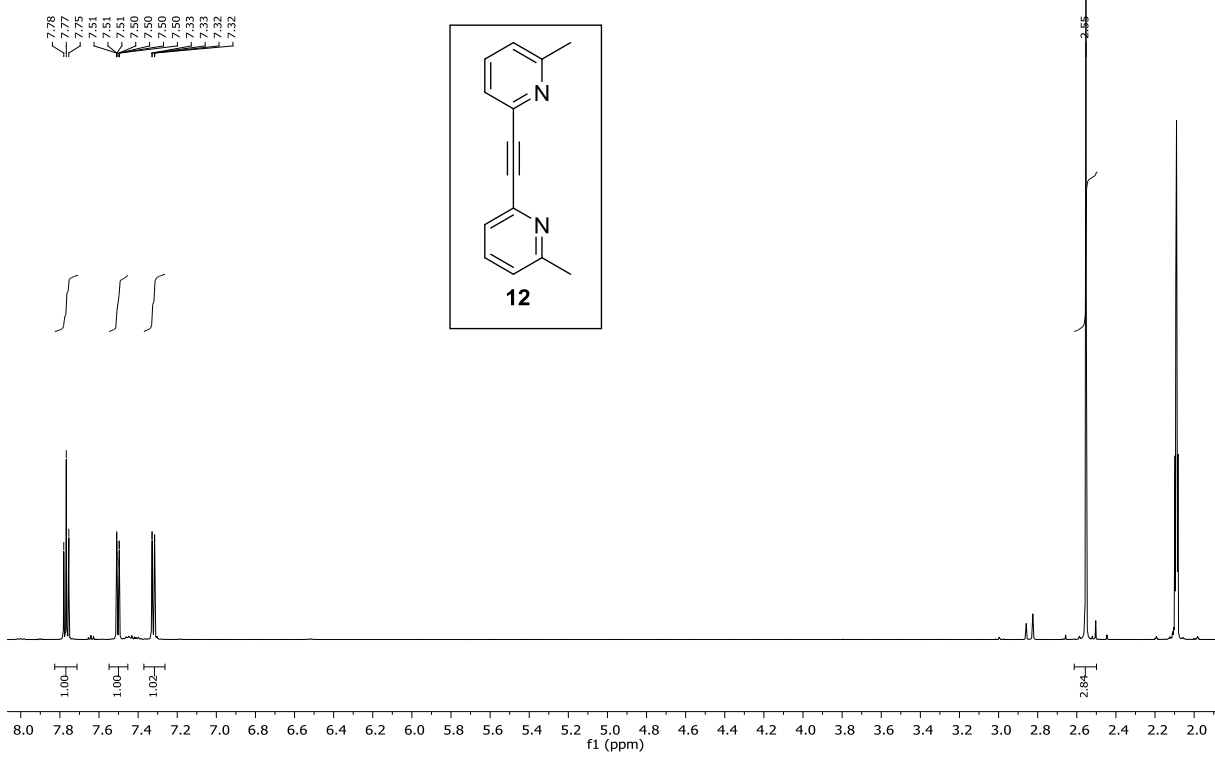


PR301/1  
400 MHz, acetone-d6

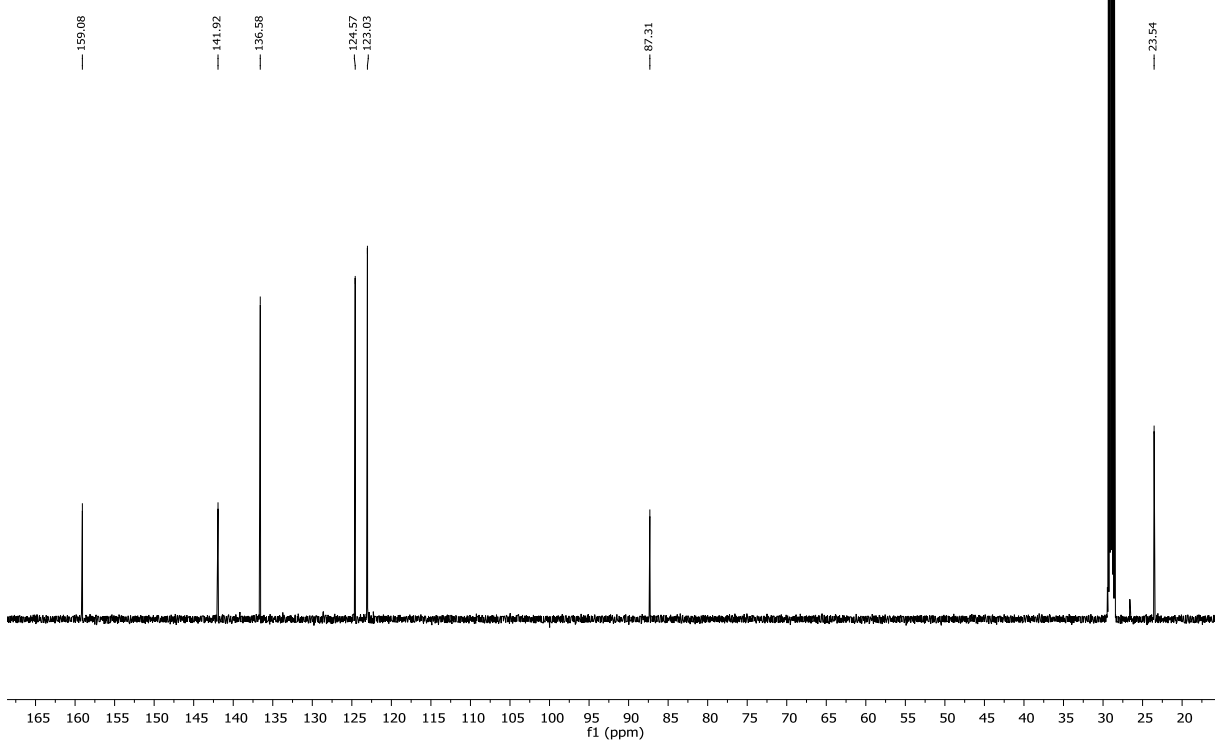




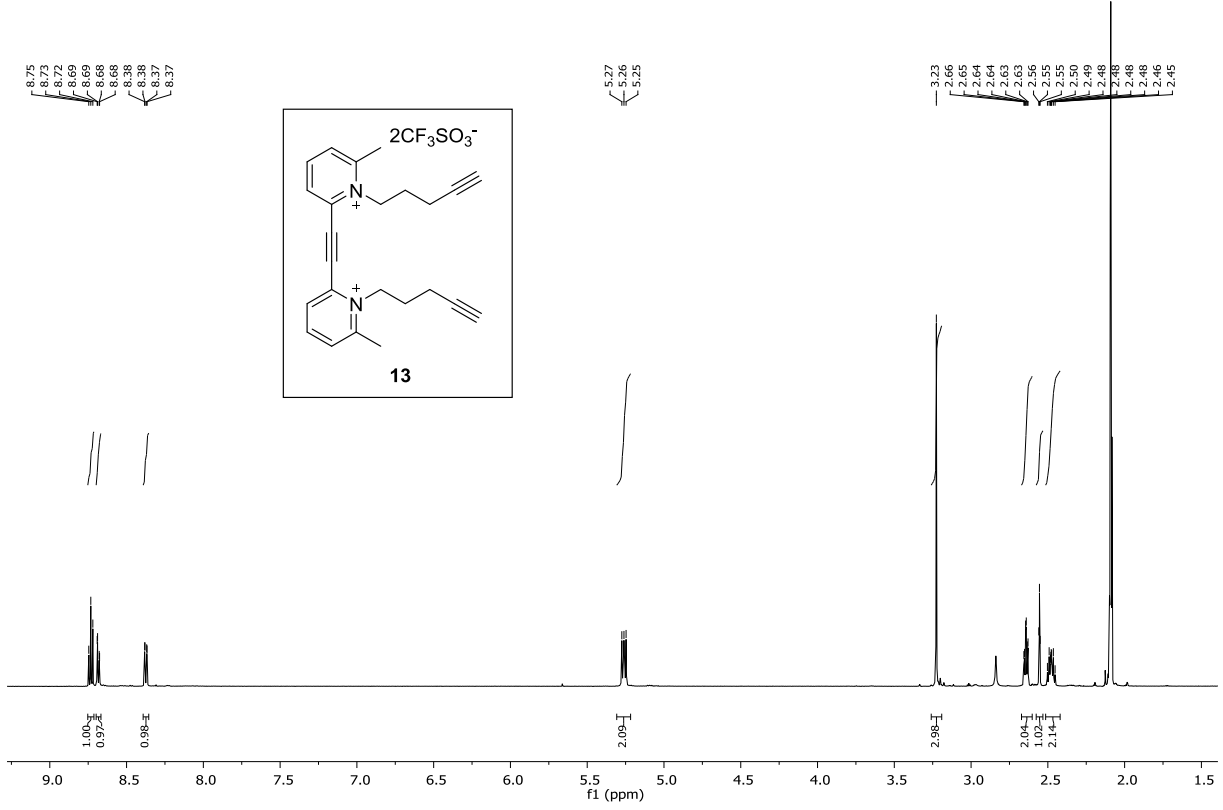
Teply-AM003.1.fid  
600 MHz, acetone-d6



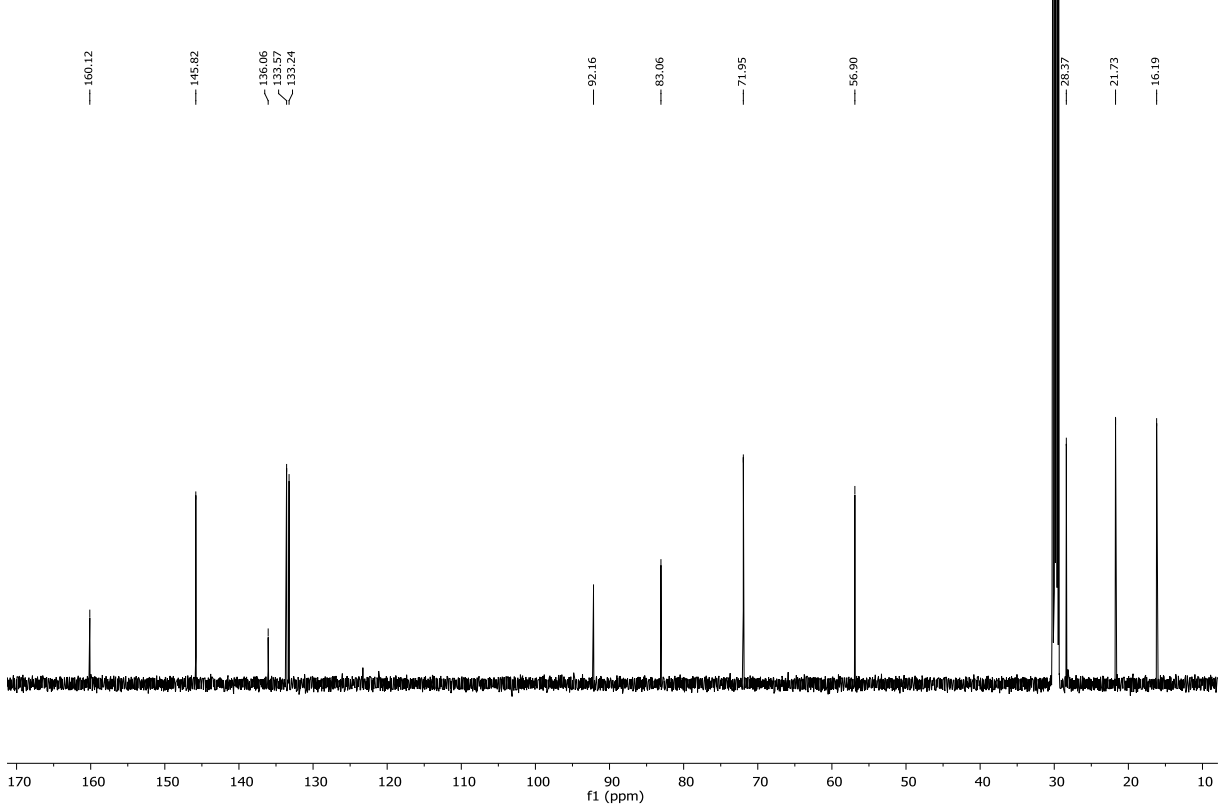
Teply-AM003.2.fid  
151 MHz, acetone-d6



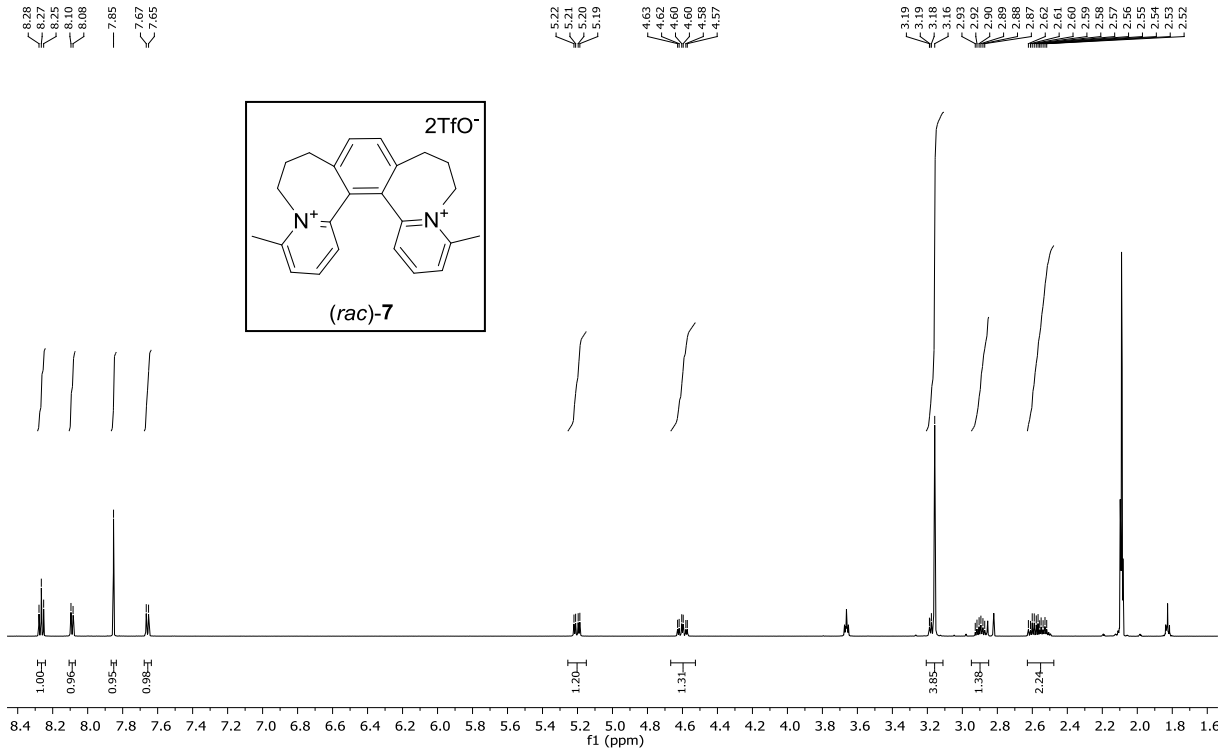
Teply-AM006.1.fid  
600 MHz, acetone-d6



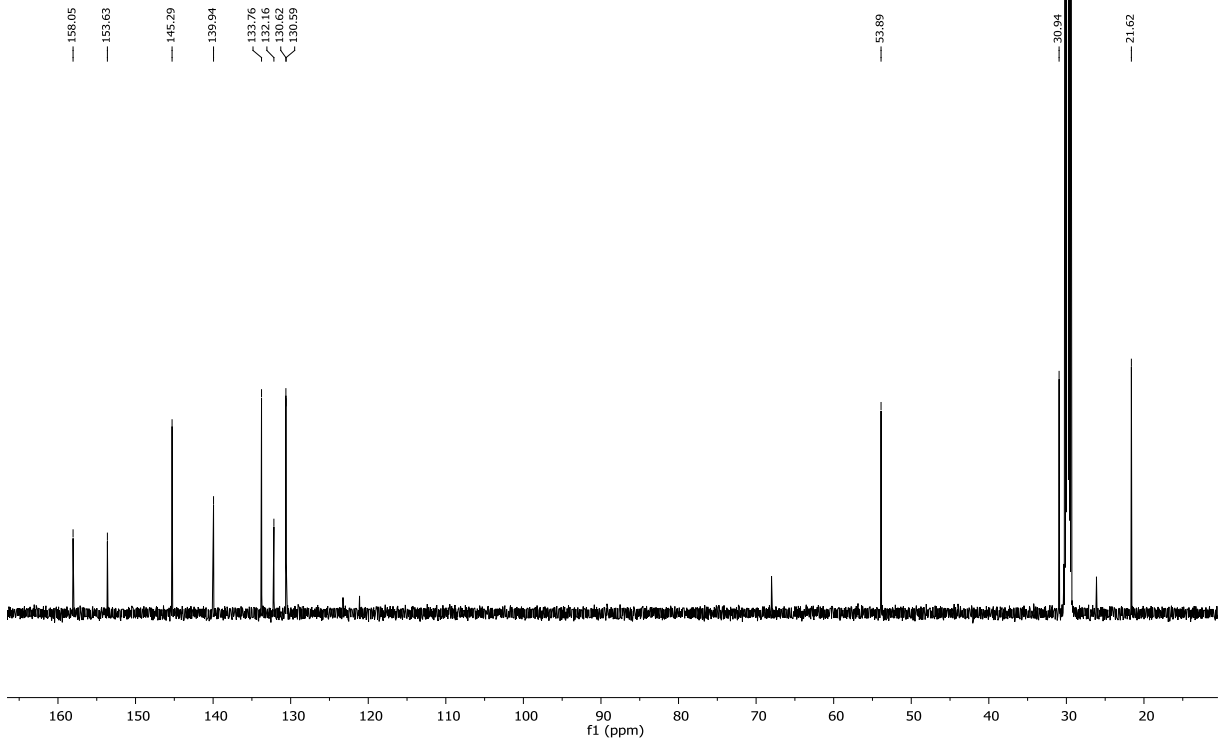
Teply-AM006.2.fid  
151 MHz, acetone-d6



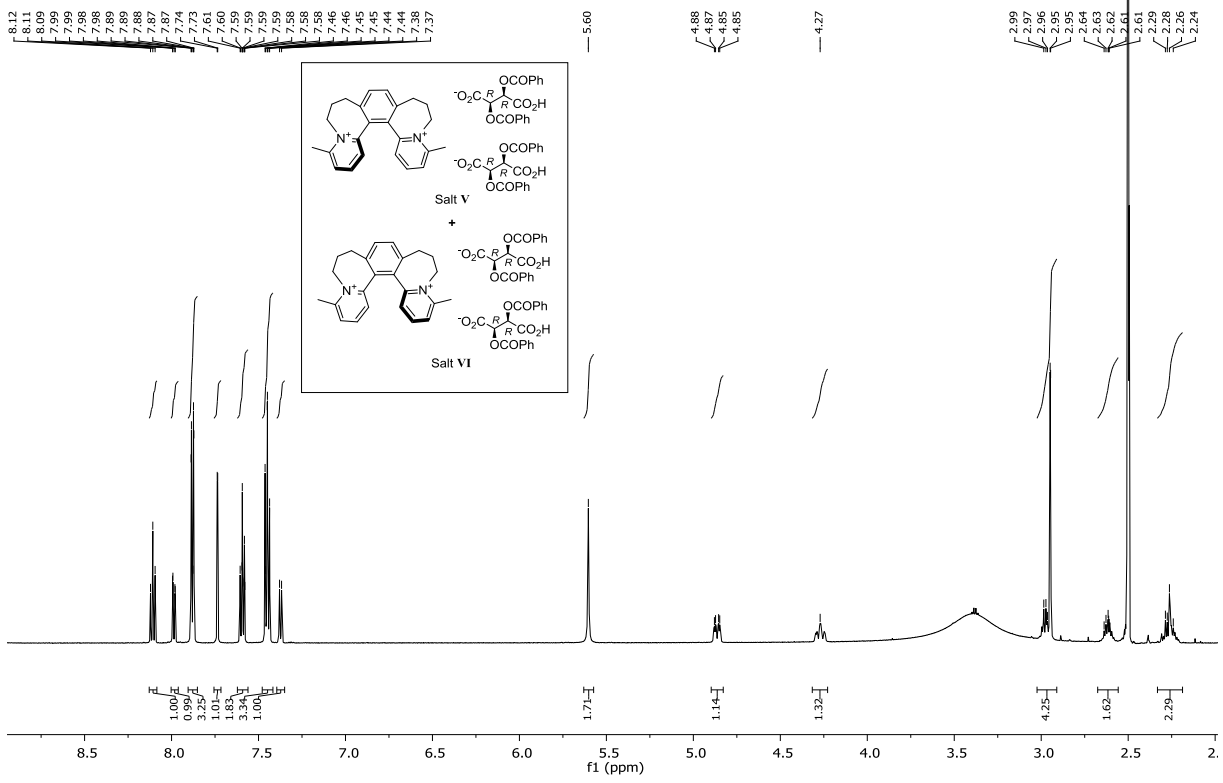
Teply-AM008.1.fid  
600 MHz, acetone-d6



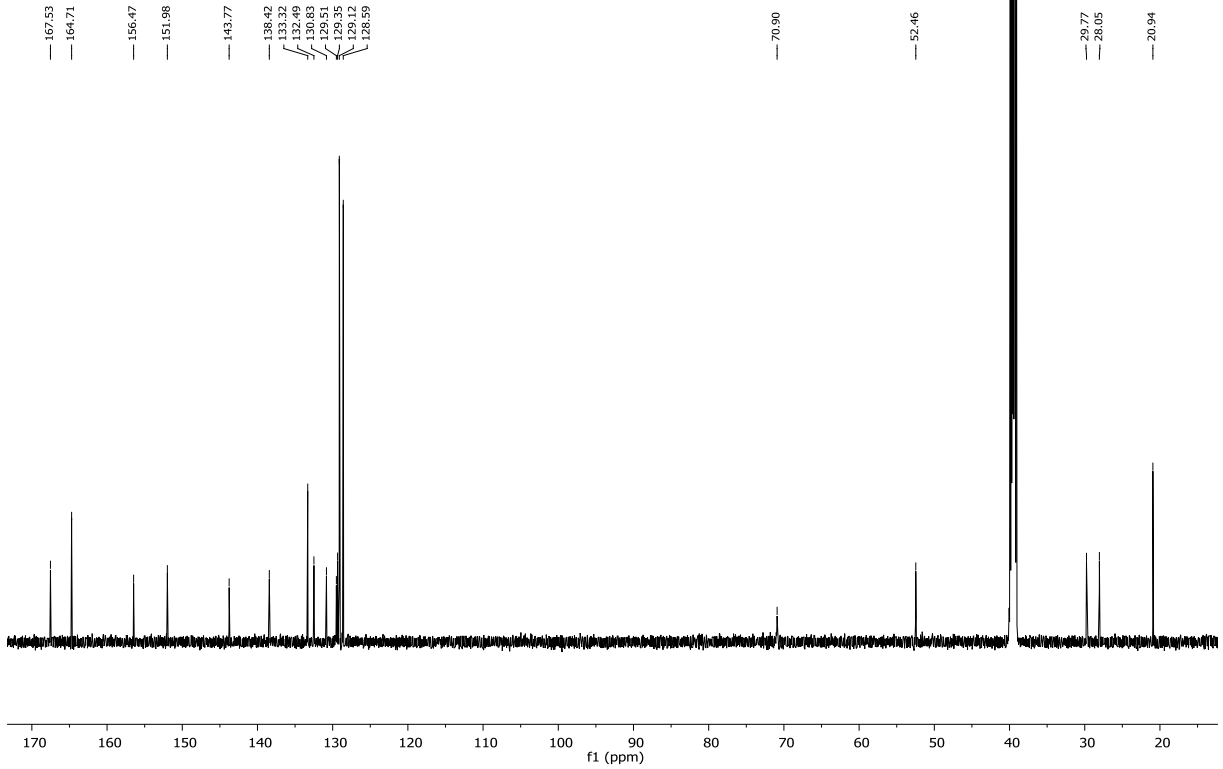
Teply-AM008.2.fid  
151 MHz, acetone-d6



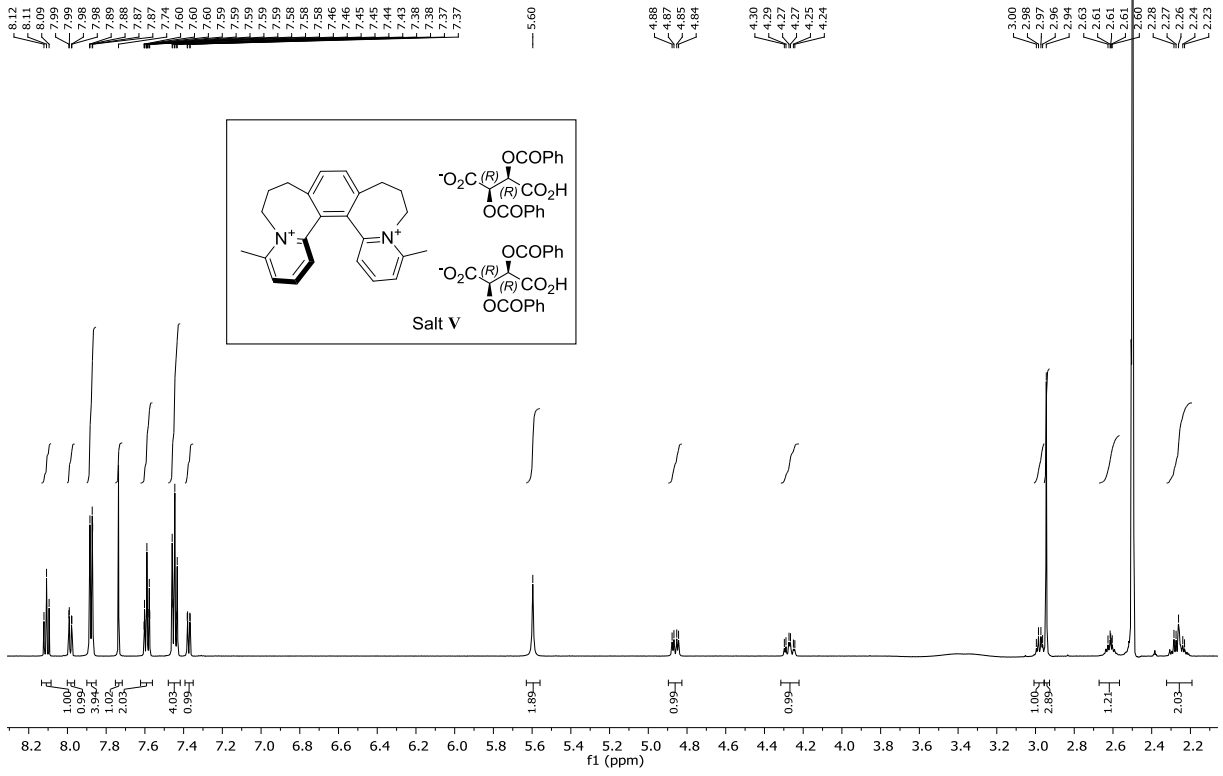
Reyes-PR273.1.fid  
600 MHz, DMSO-d6



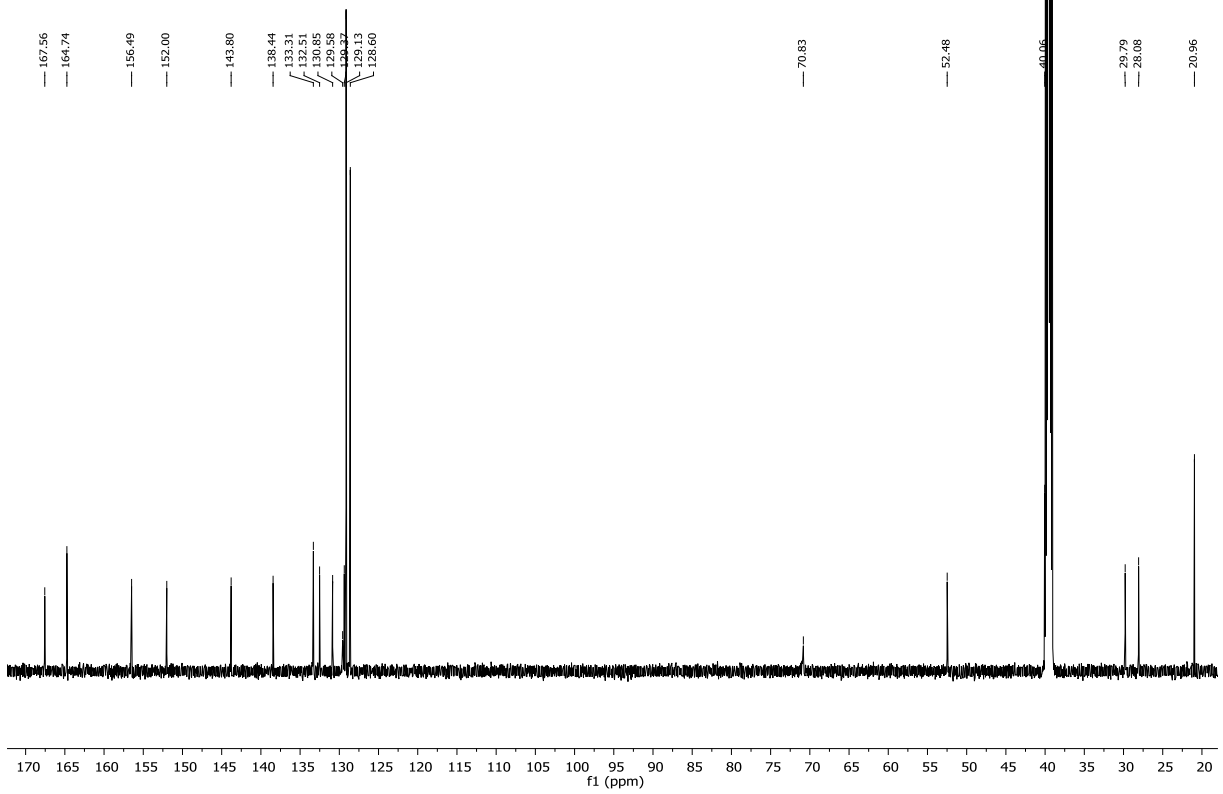
Reyes-PR273.2.fid  
151 MHz, DMSO-d6



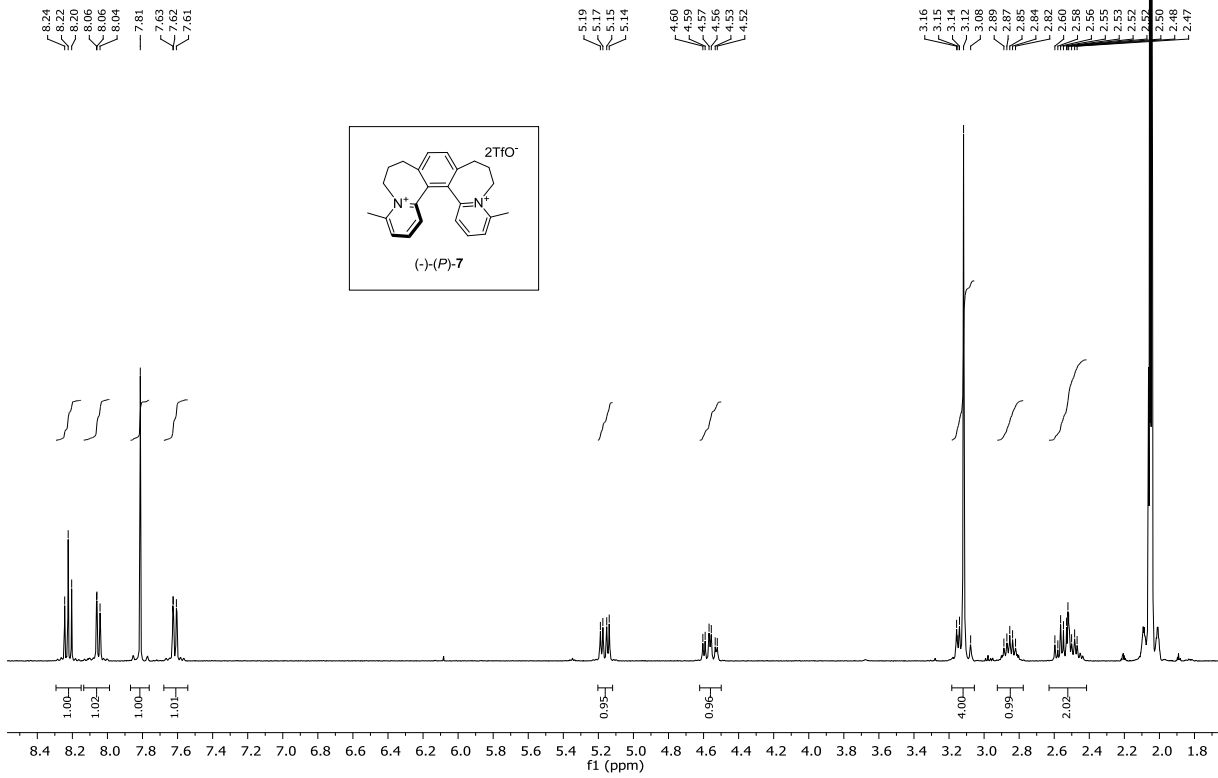
Severa-LS812\_01.1.fid  
600 MHz, DMSO-d6



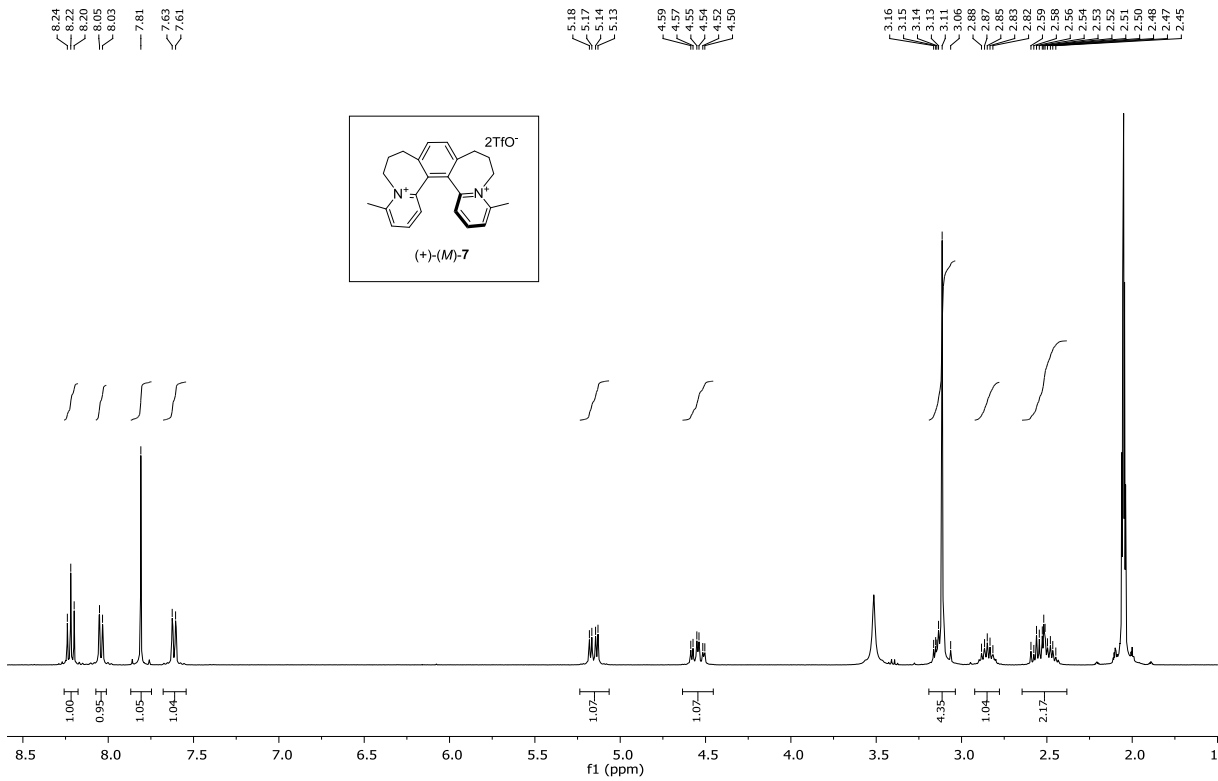
Severa-LS812\_01.2.fid  
151 MHz, DMSO-d6



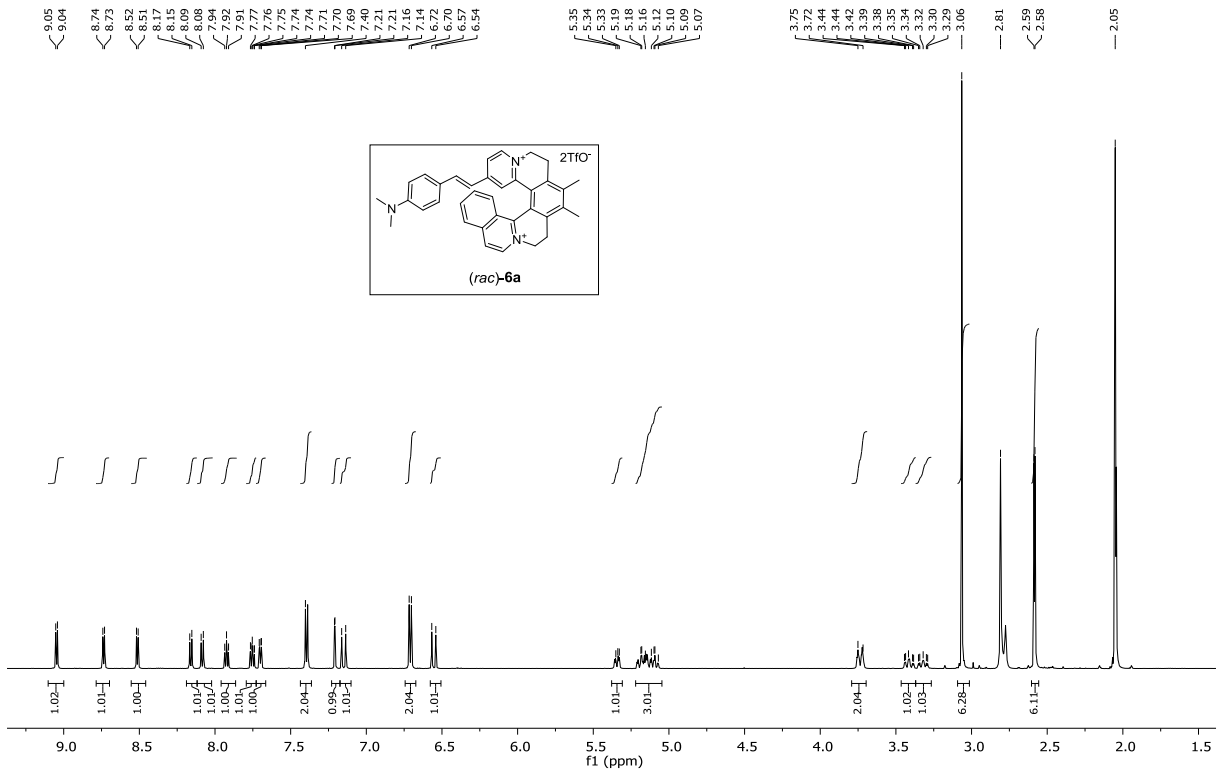
LS762-01  
400 MHz, acetone-d6



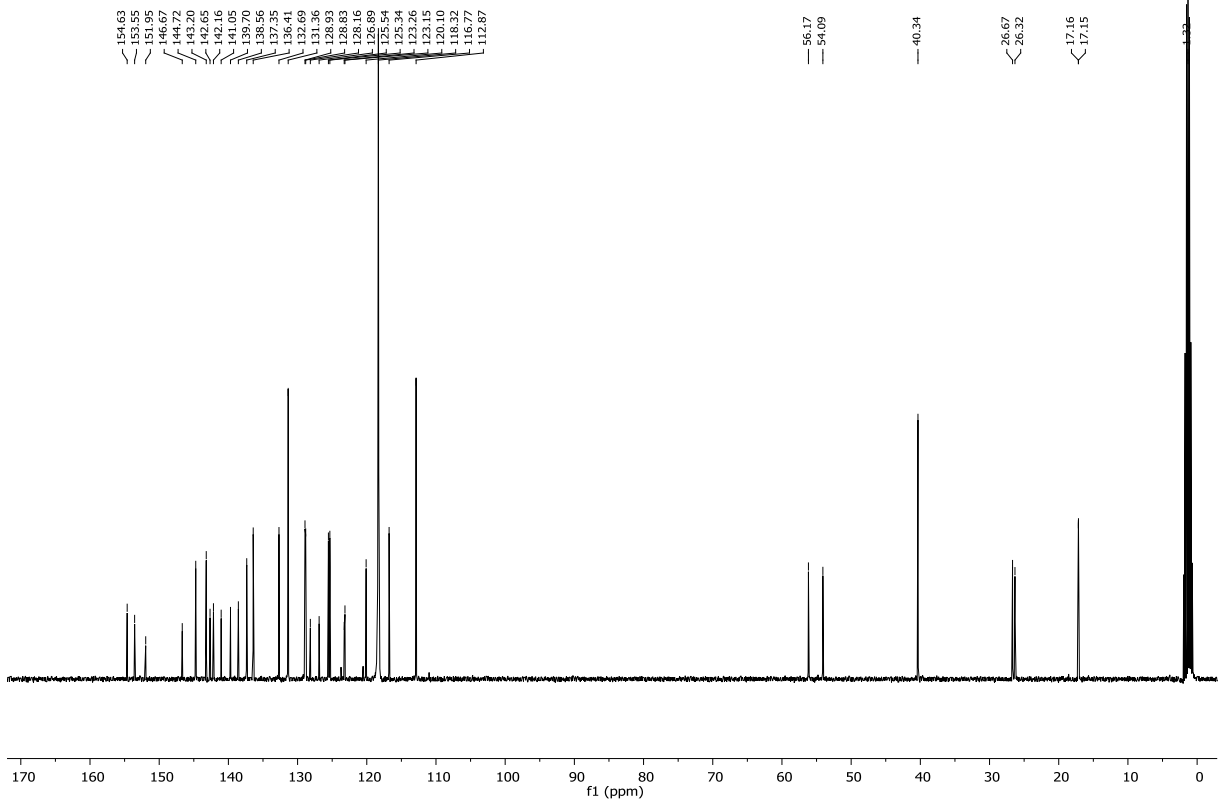
LS773-01.1.fid  
400 MHz, acetone-d6



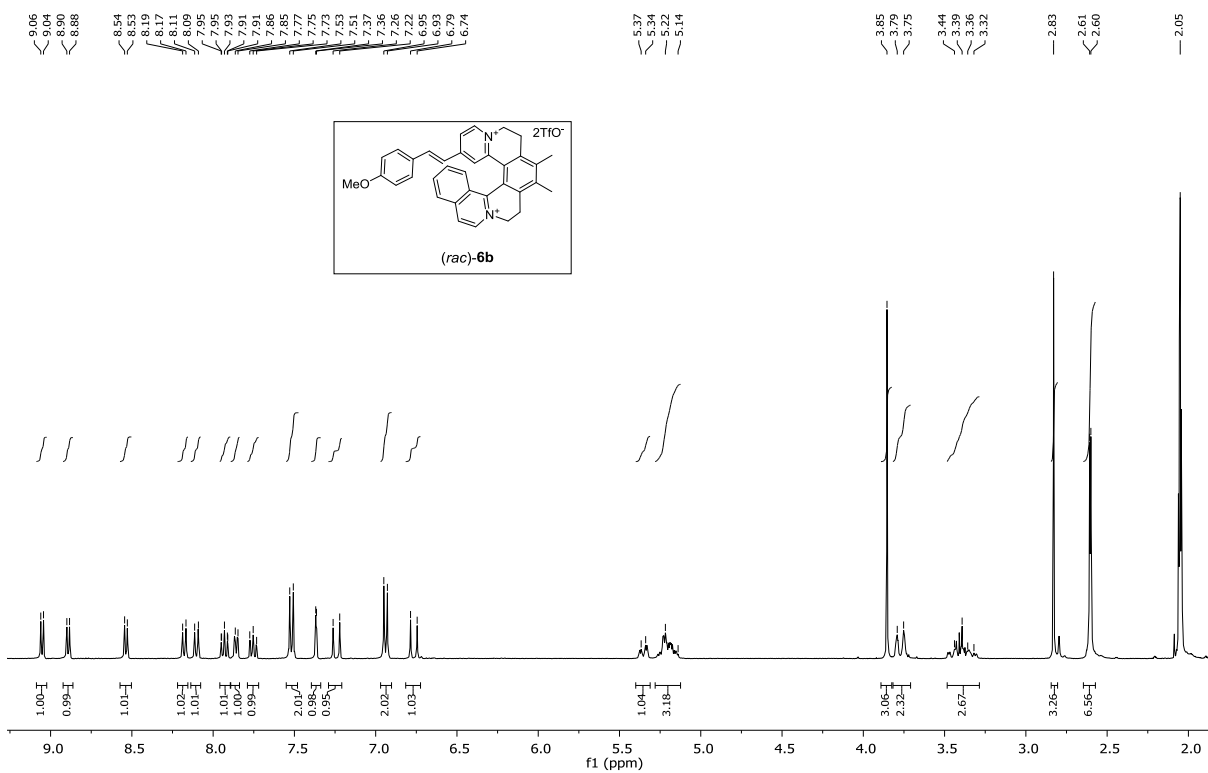
Teply-MJ125.1.fid  
600 MHz, acetone-d6



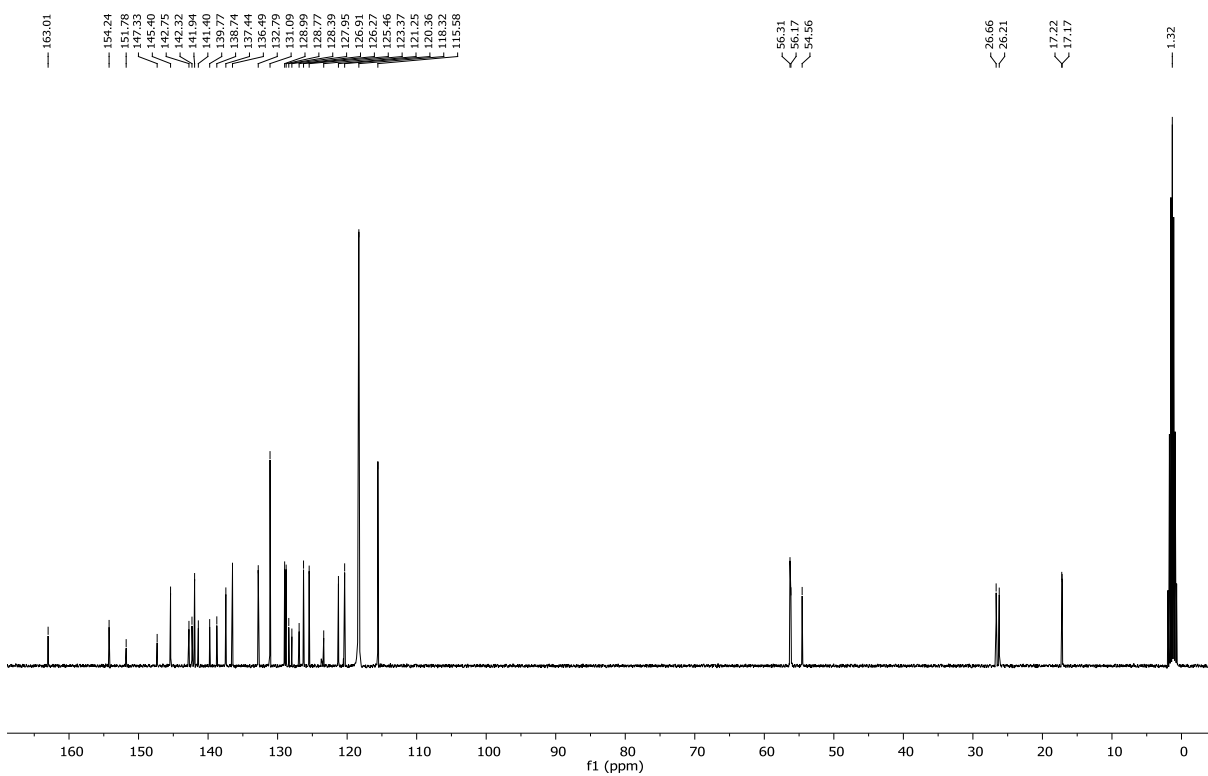
MJ1250.fid  
100 MHz, CD3CN



MJ264.1.fid  
600 MHz, Acetone

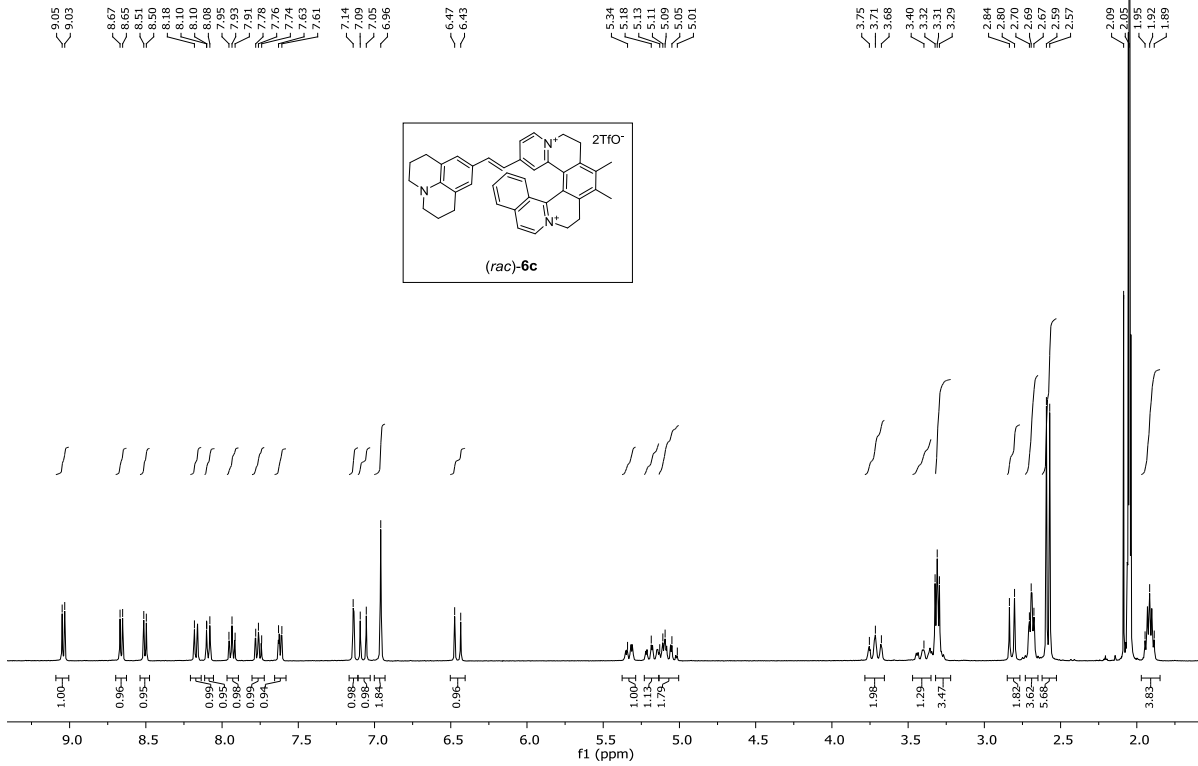


MJ264.fid  
100 MHz, CD<sub>3</sub>CN

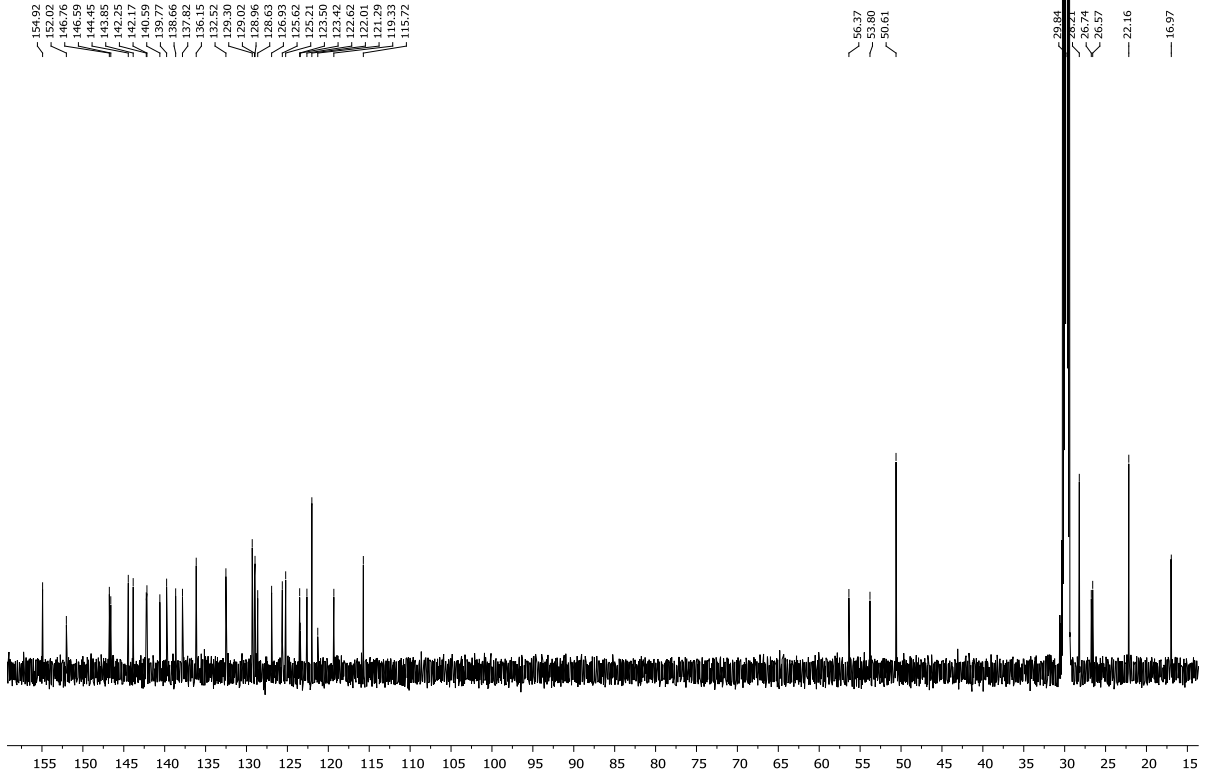




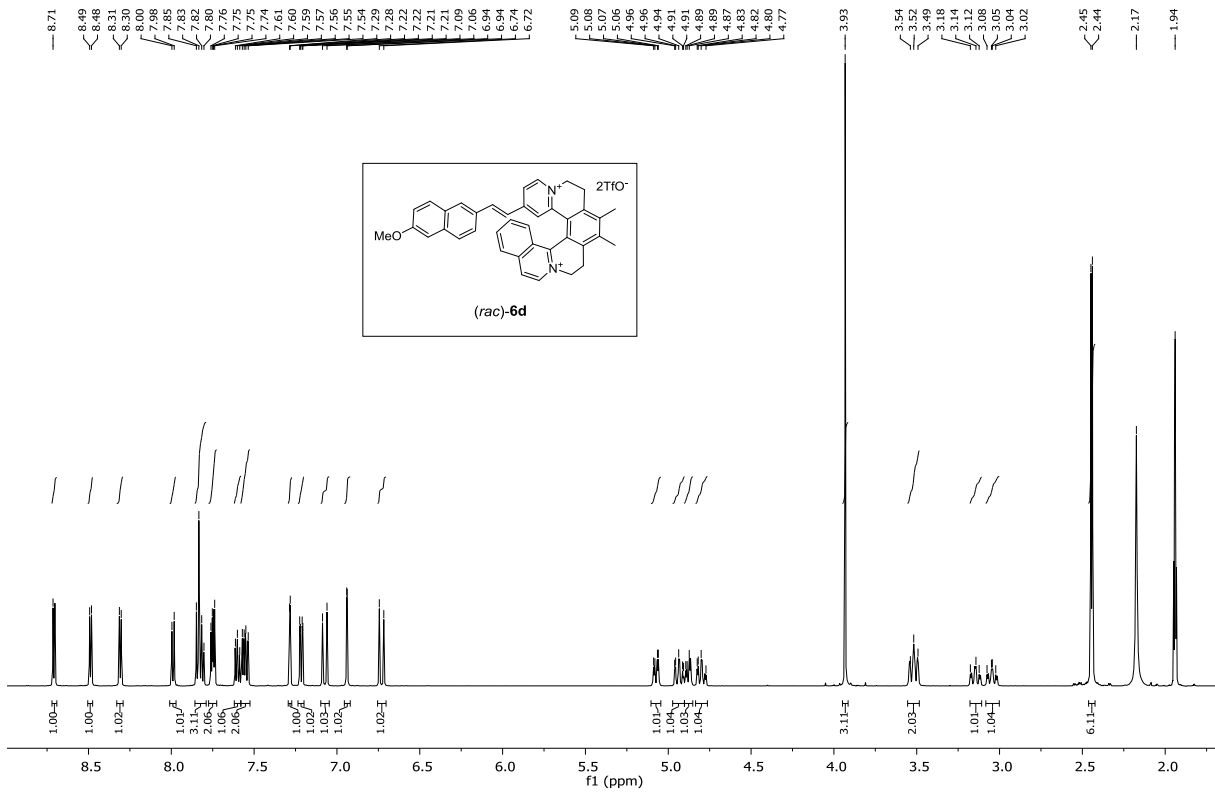
MJ173p1b.1.fid  
600 MHz, acetone-d6



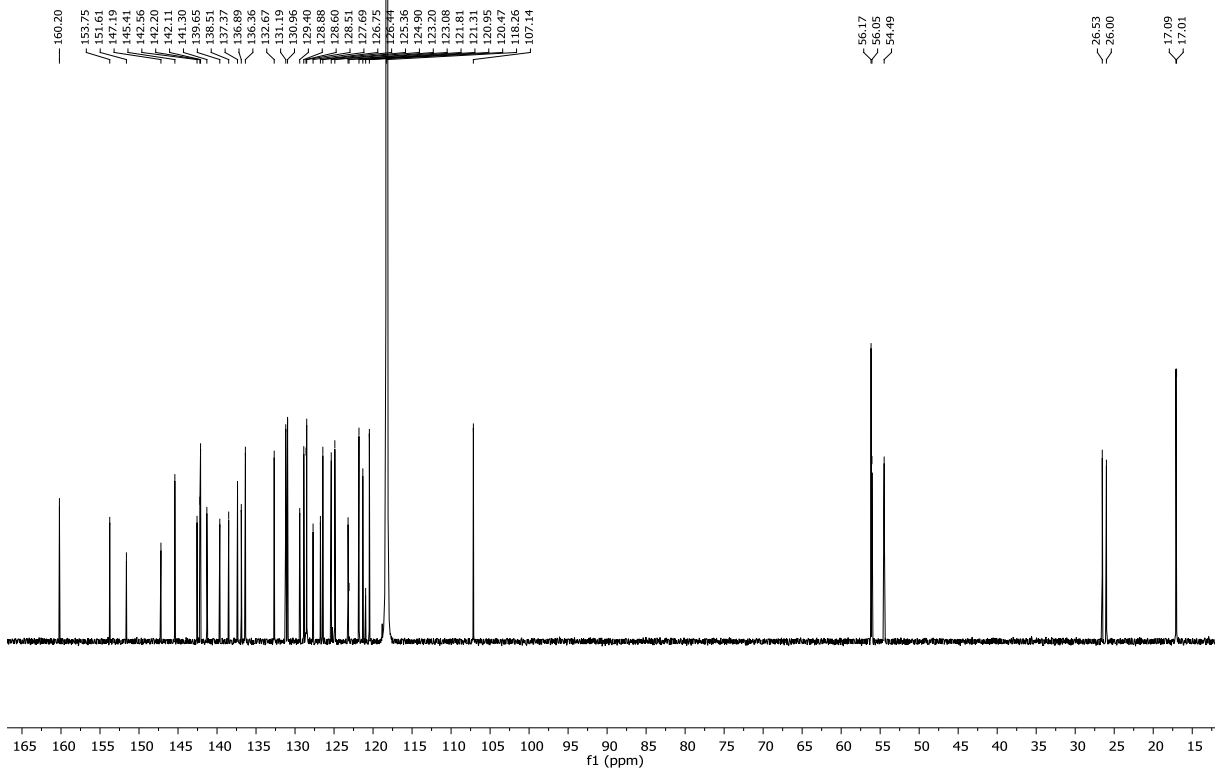
Teply-MJ123.2.fid  
151 MHz, acetone-d6



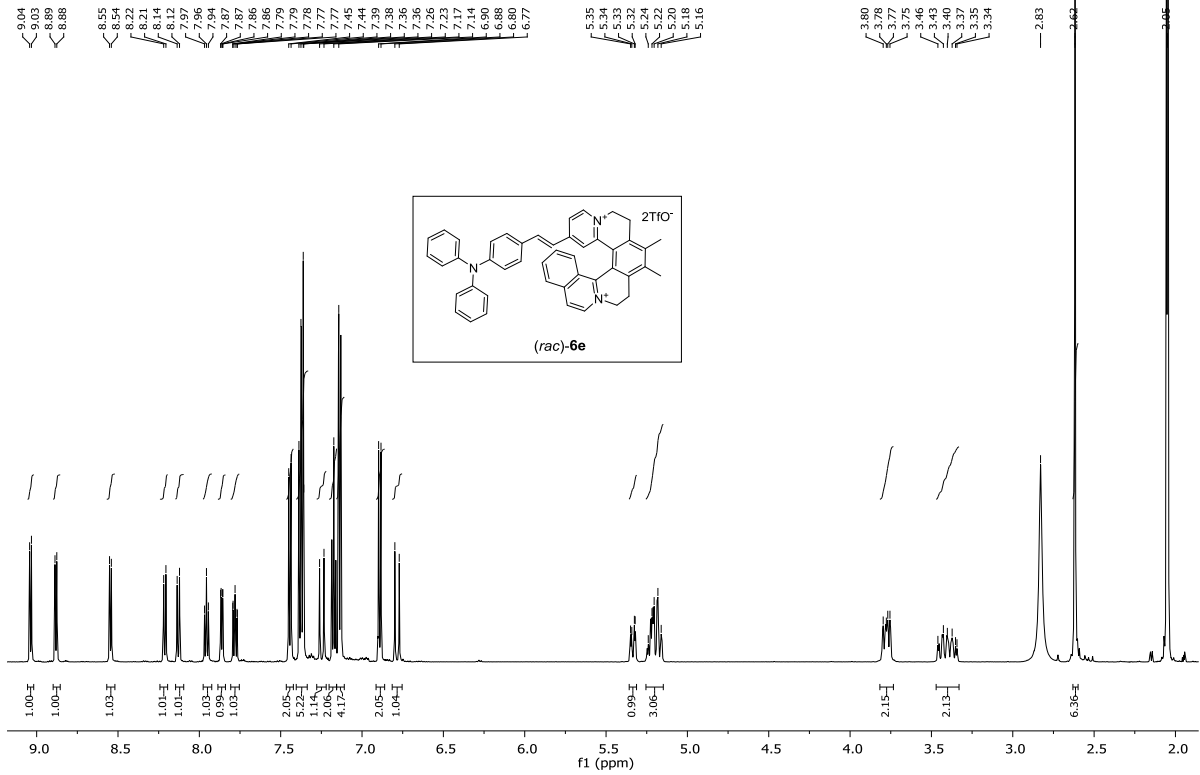
Teply-MJ127.1.fid  
600 MHz, CD3CN



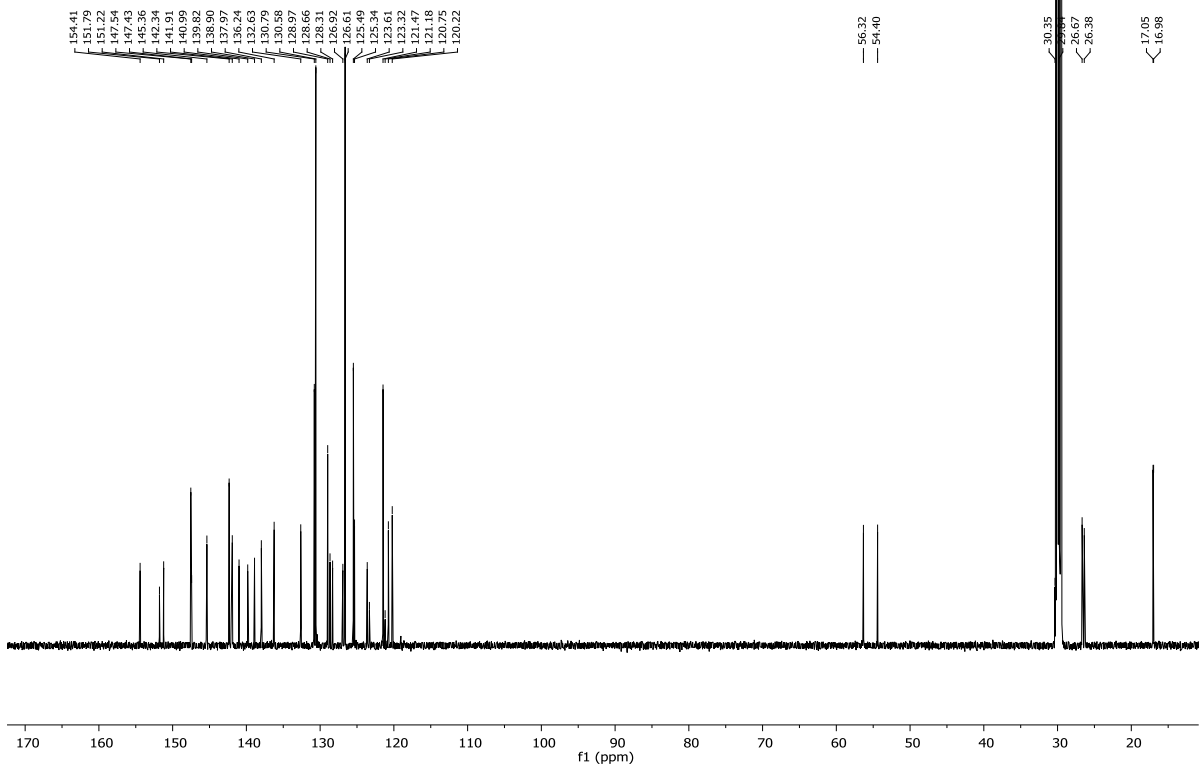
Teply-MJ127.2.fid  
151 MHz, CD3CN



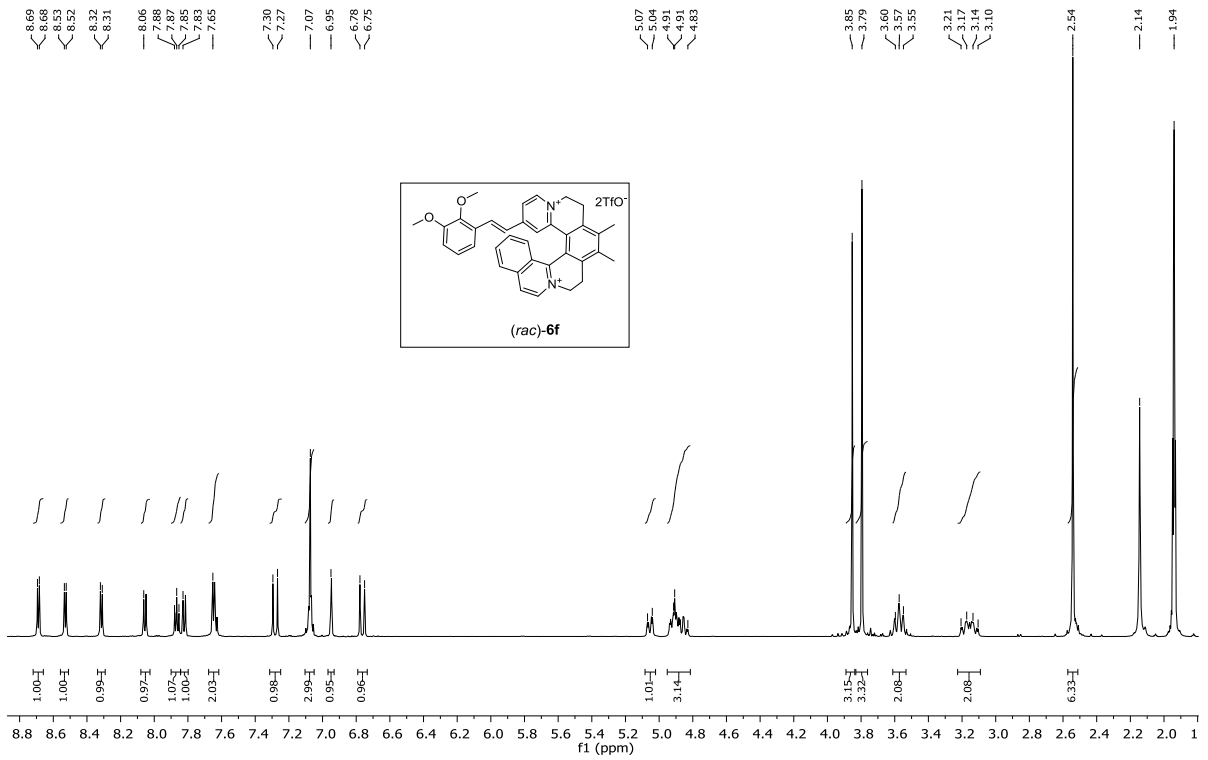
Teply-MJ239.1.fid  
600 MHz, acetone-d6



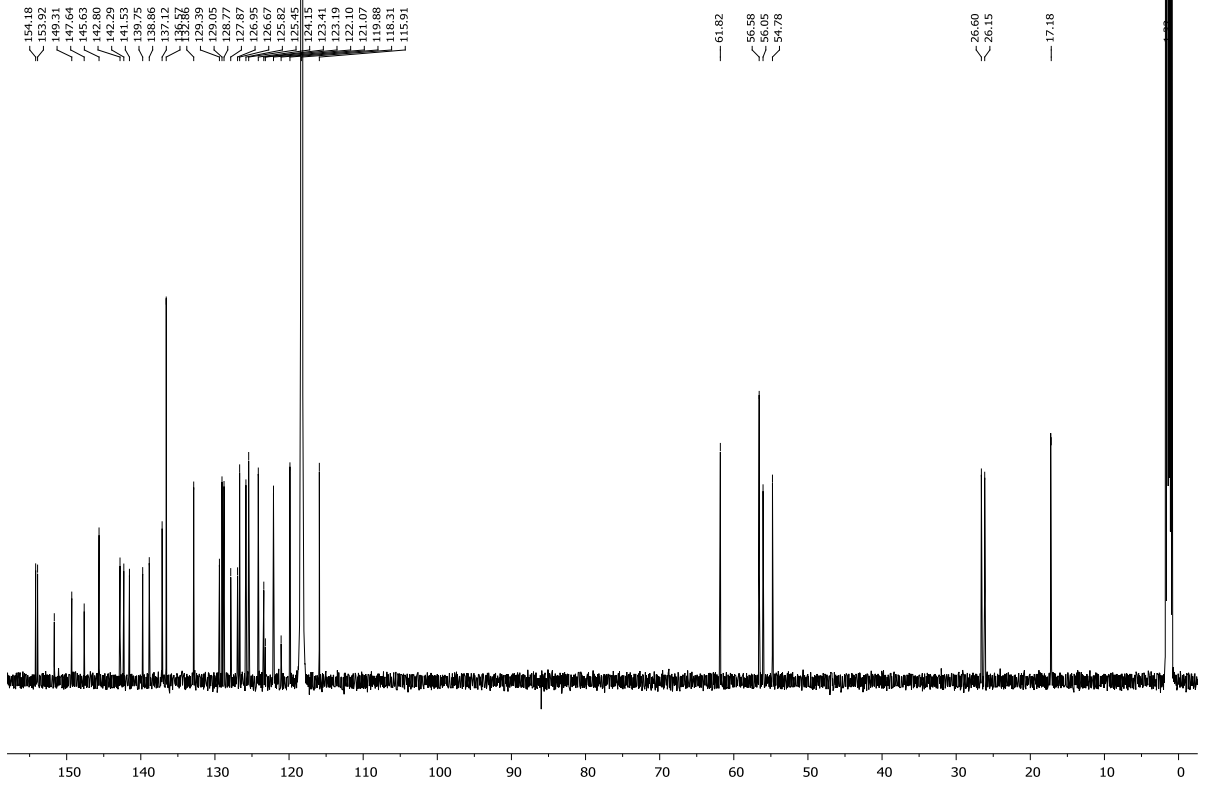
Teply-MJ239.2.fid  
151 MHz, acetone-d6



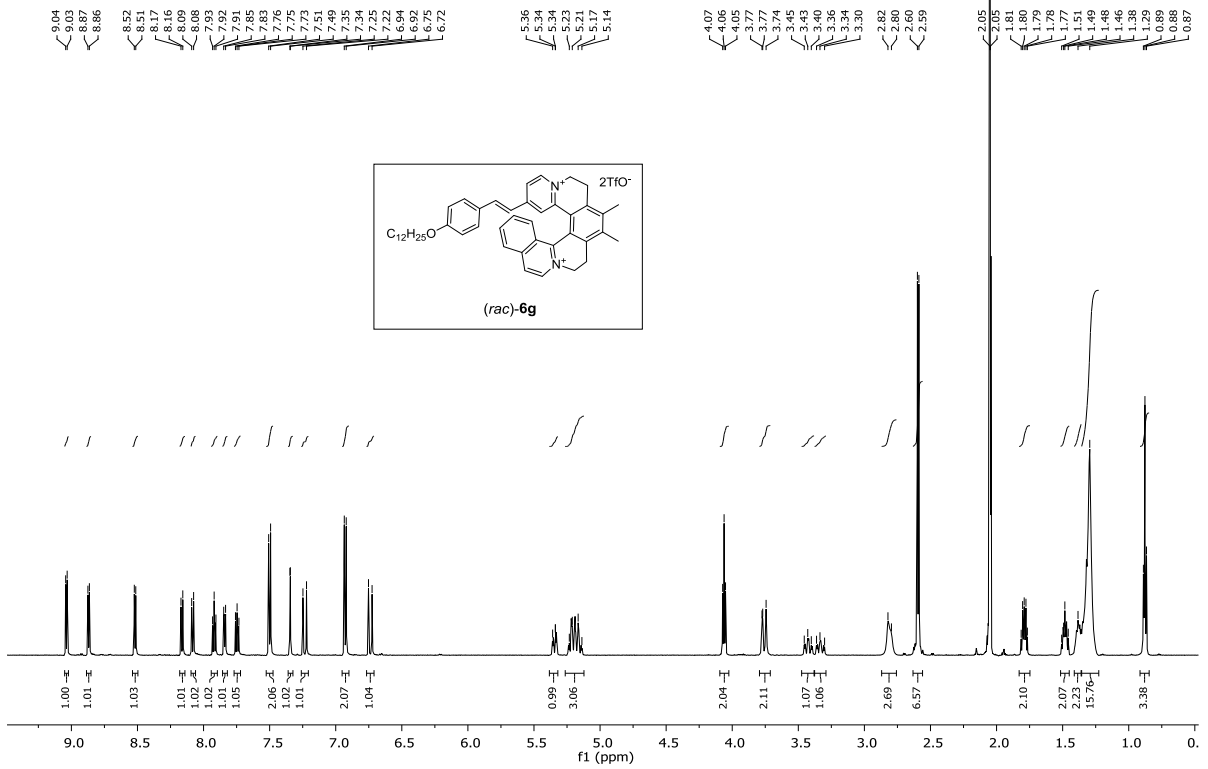
Teply-MJ370.1.fid  
600 MHz, CD3CN



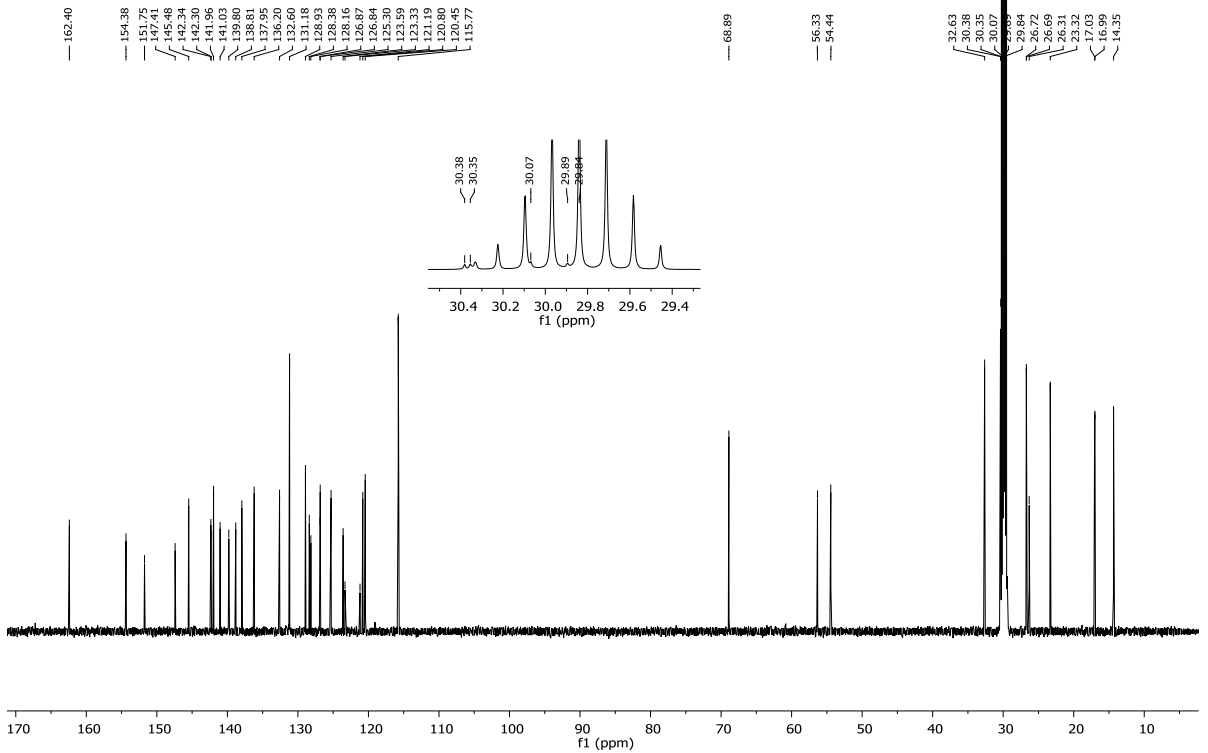
Teply-MJ370.2.fid  
151 MHz, CD3CN



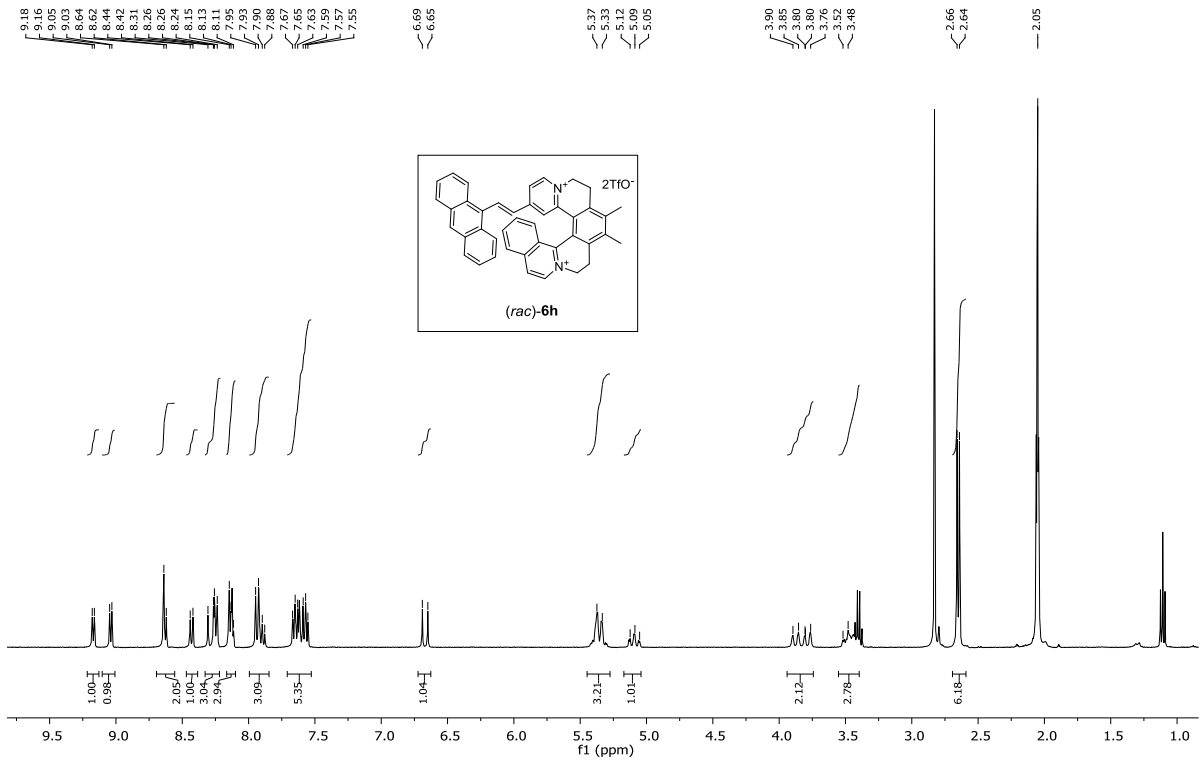
Teply-MJ244.1.fid  
600 MHz, acetone-d6



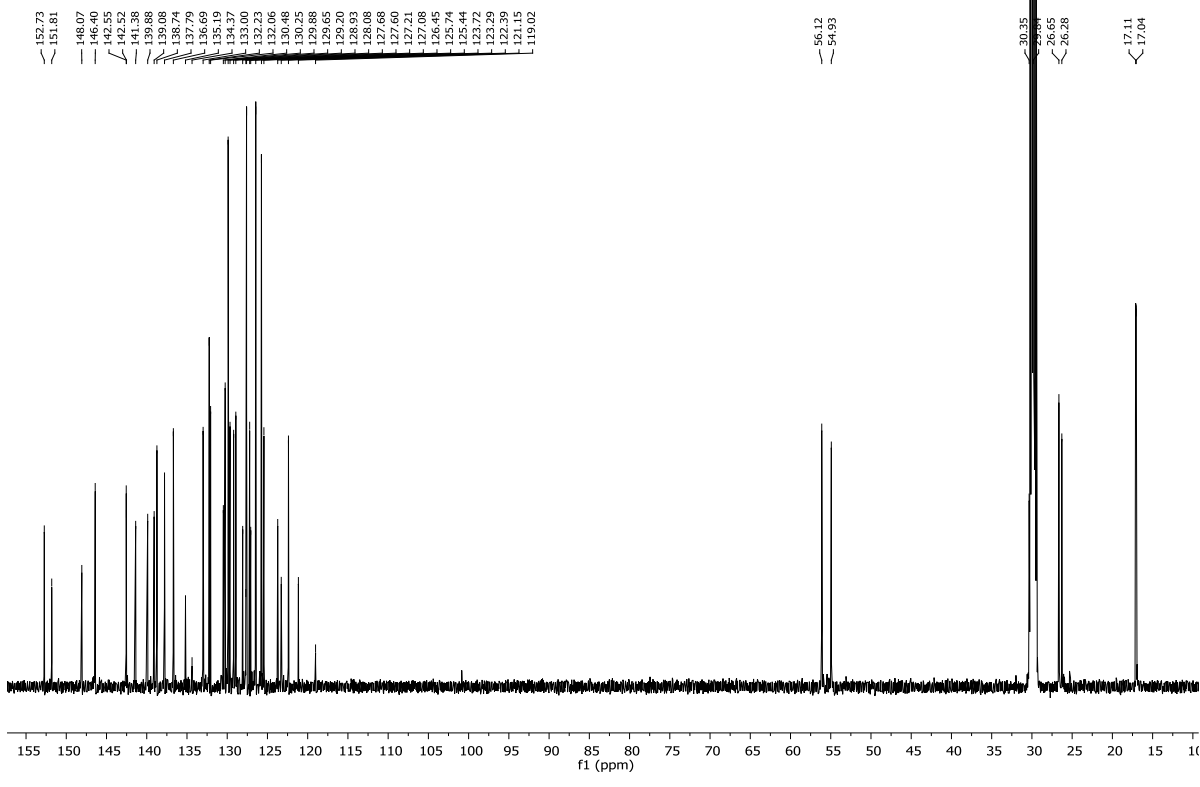
Teply-MJ244.2.fid  
151 MHz, acetone-d6



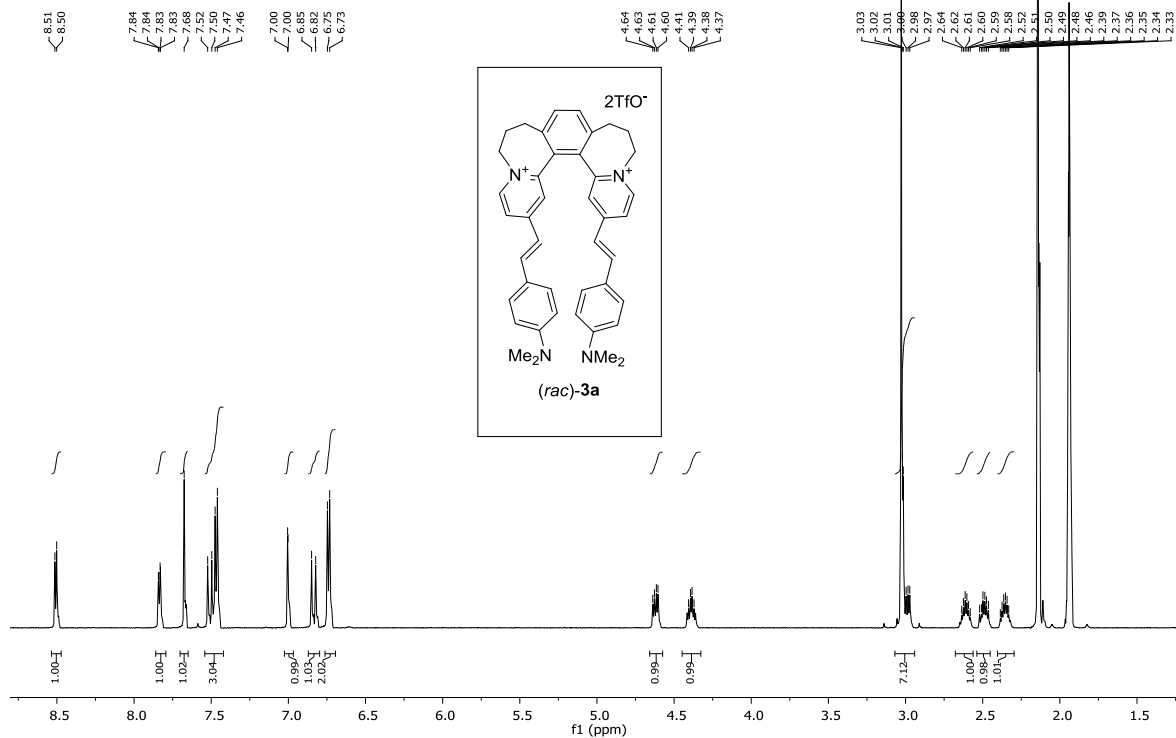
MJ256p.1.fid  
600 MHz, acetone-d6



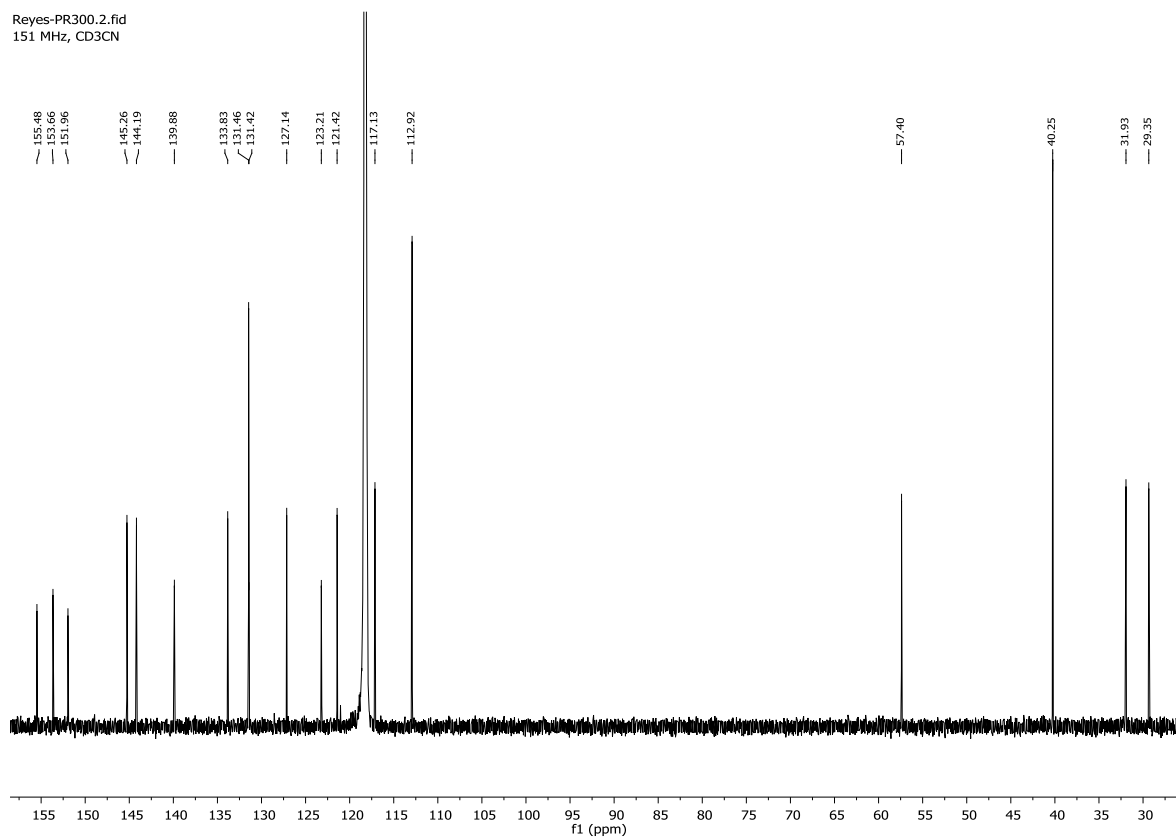
Teply-MJ131.2.fid  
151 MHz, acetone-d6



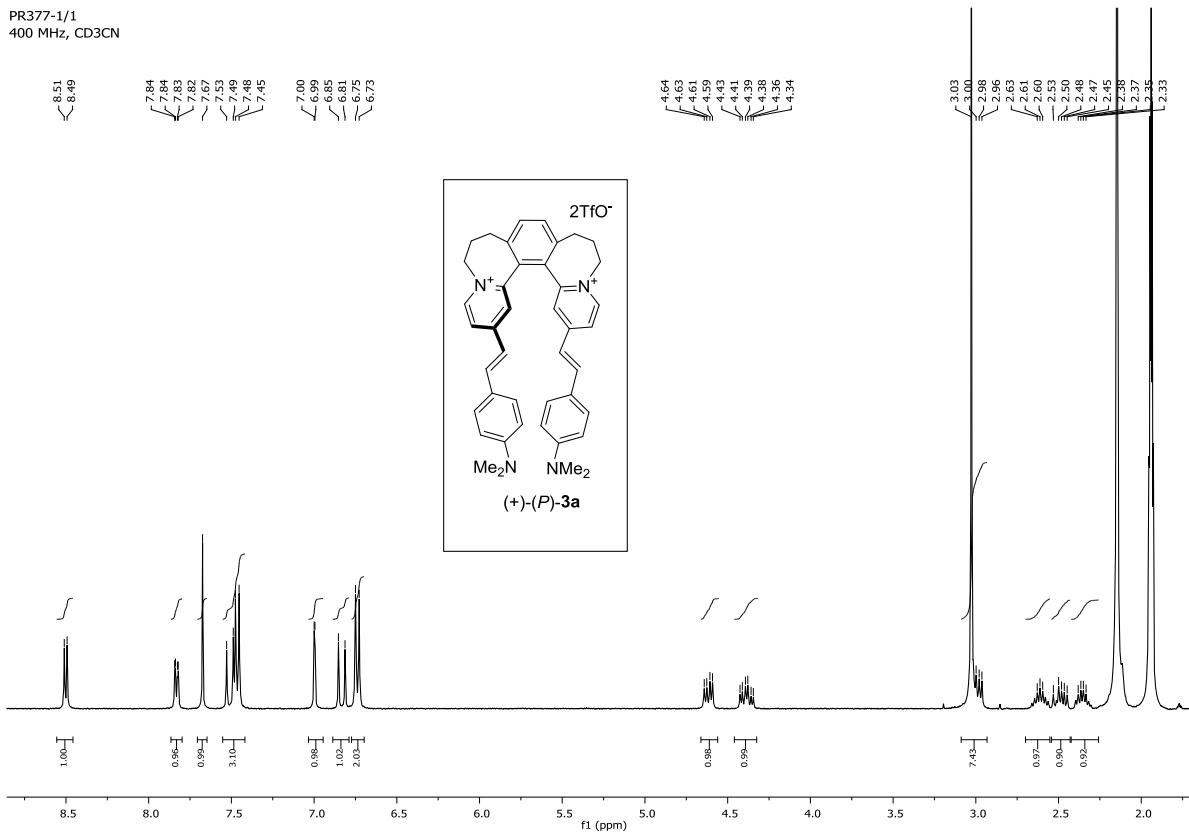
Reyes-PR300.1.fid  
600 MHz, CD3CN



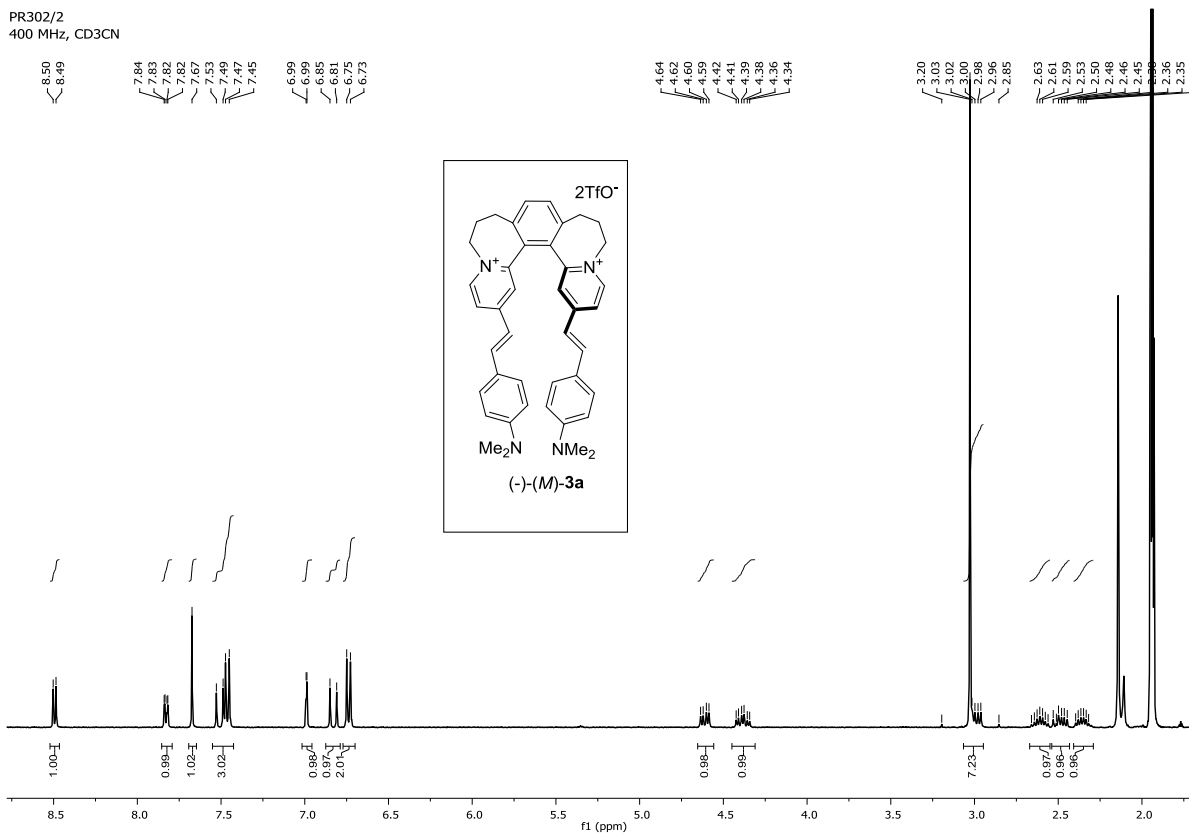
Reyes-PR300.2.fid  
151 MHz, CD3CN



PR377-1/1  
400 MHz, CD3CN

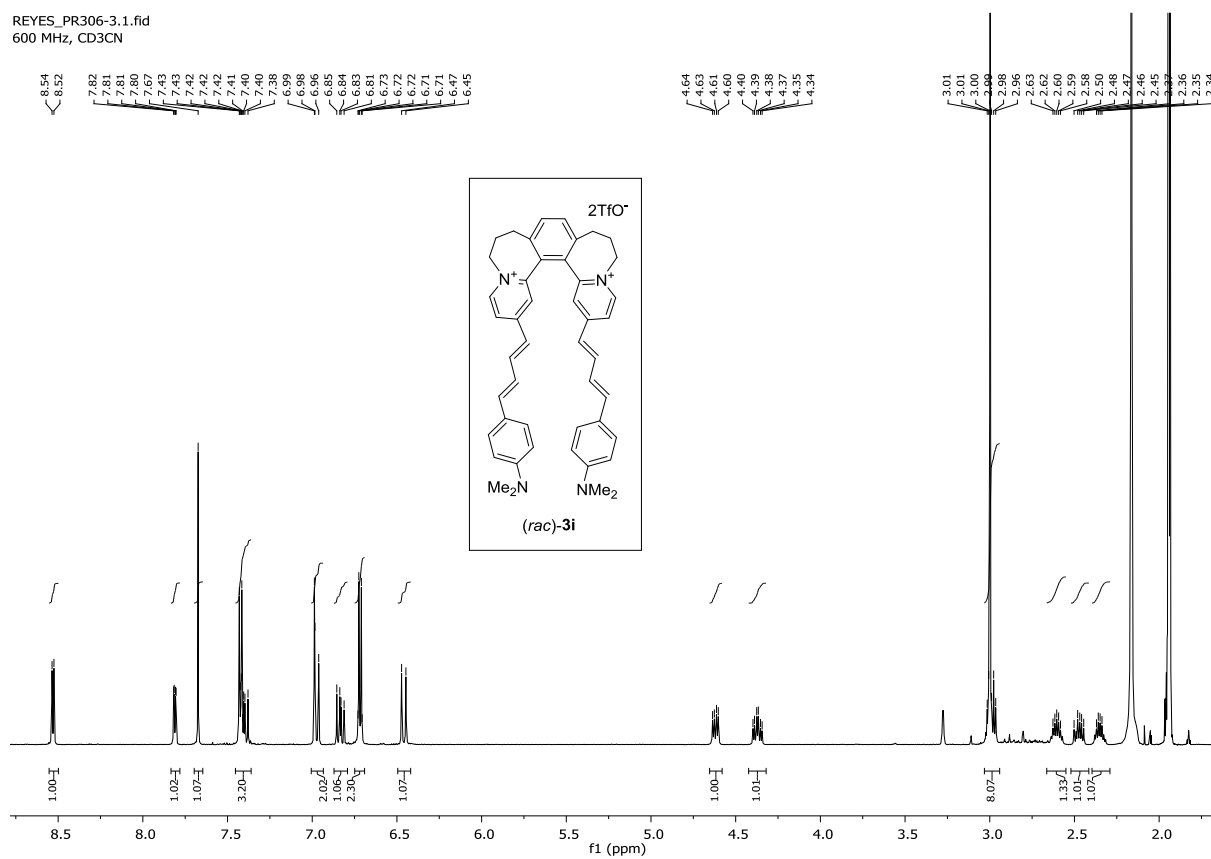


PR302/2  
400 MHz, CD3CN

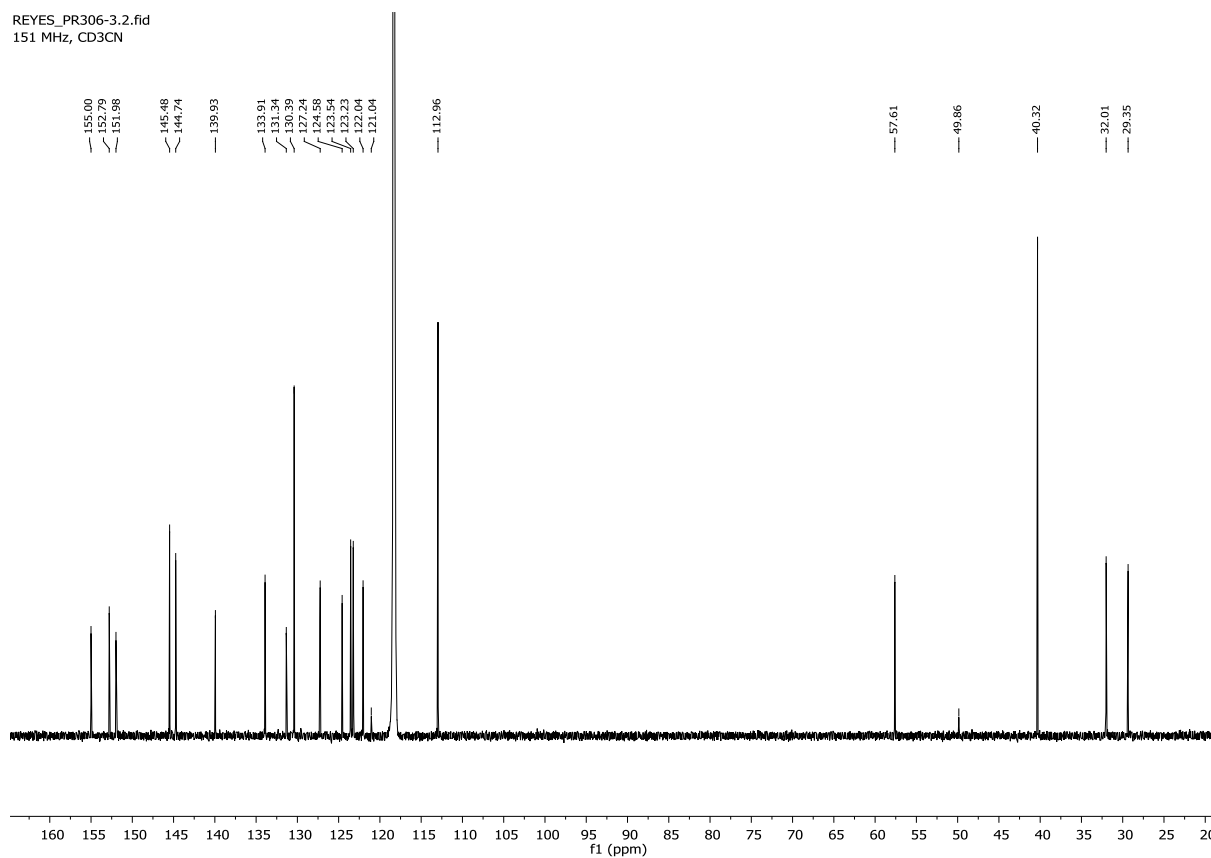




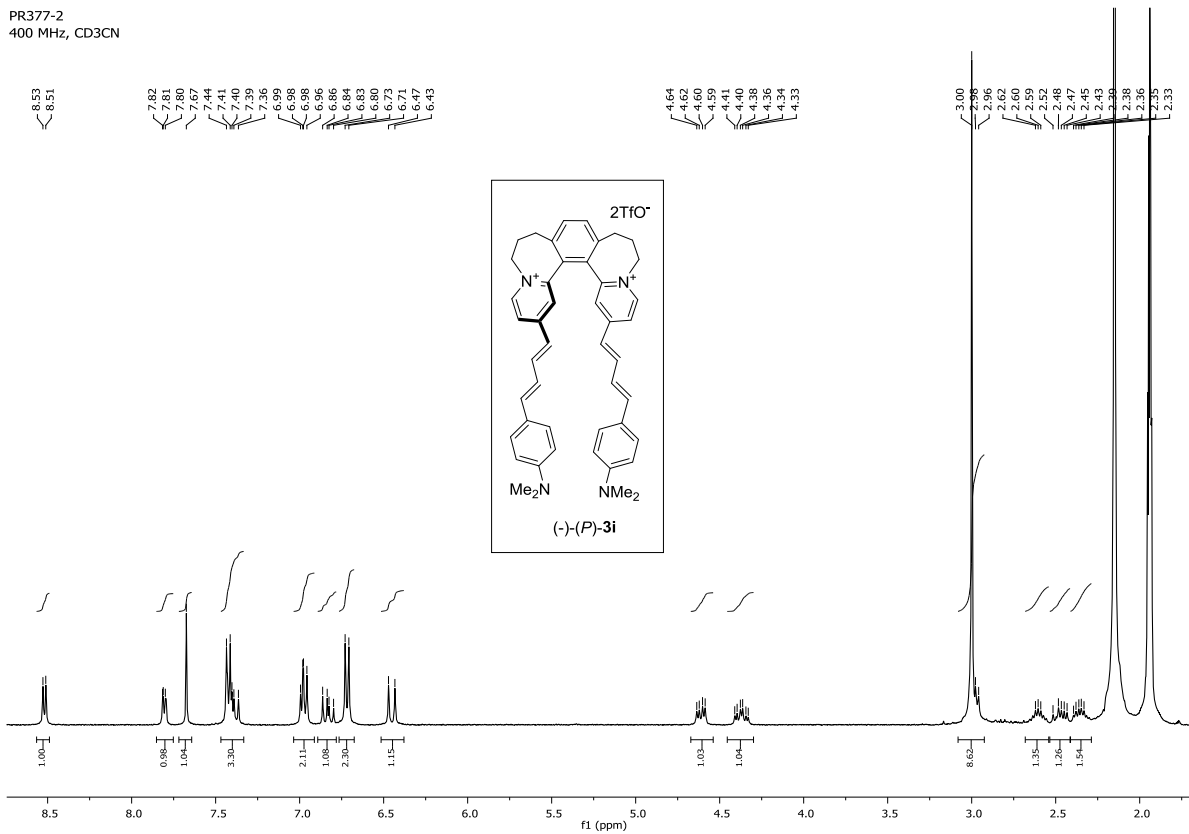
REYES\_PR306-3.1.fid  
600 MHz, CD3CN



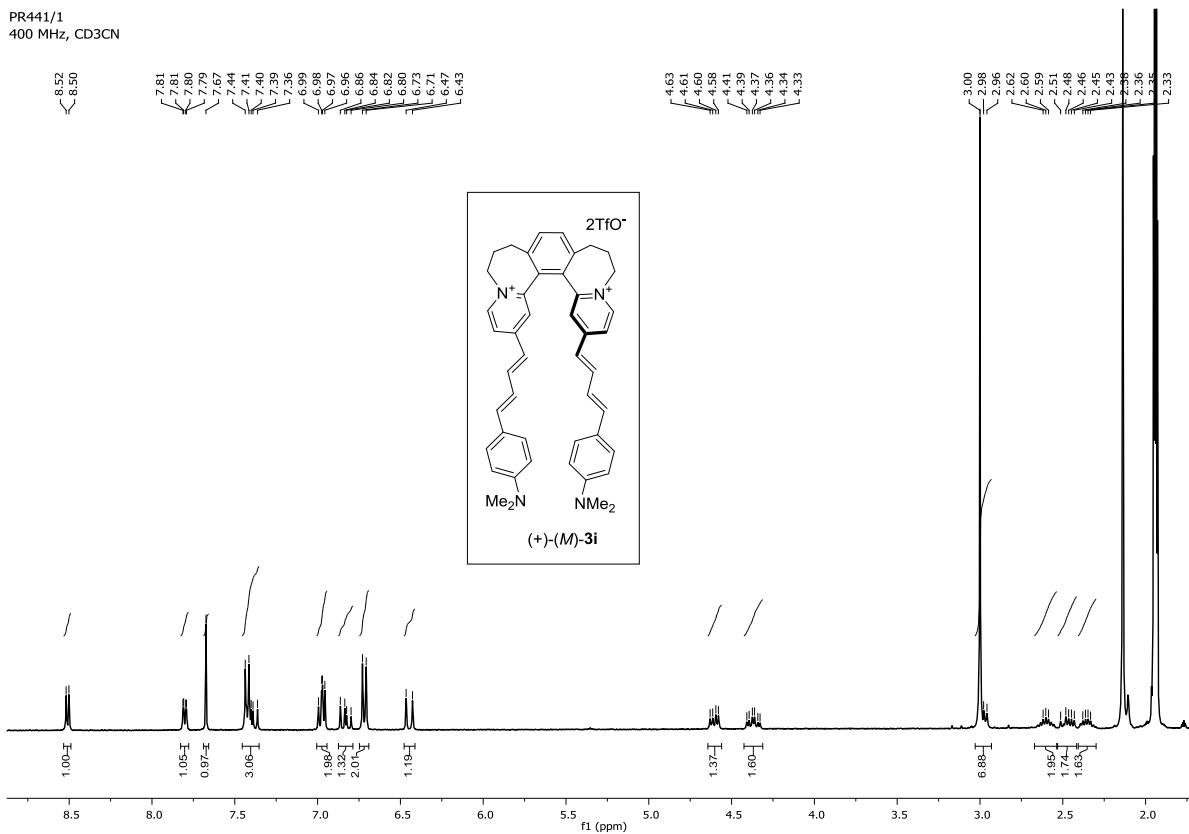
REYES\_PR306-3.2.fid  
151 MHz, CD3CN



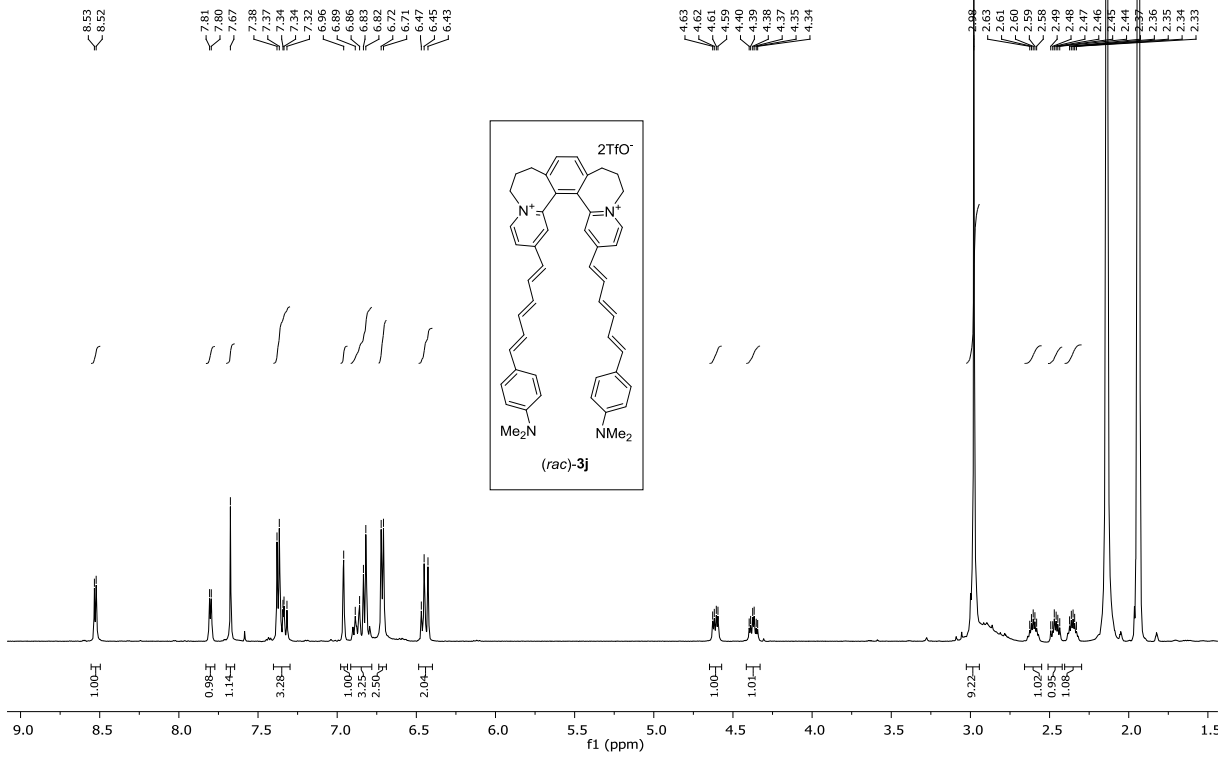
PR377-2  
400 MHz, CD3CN



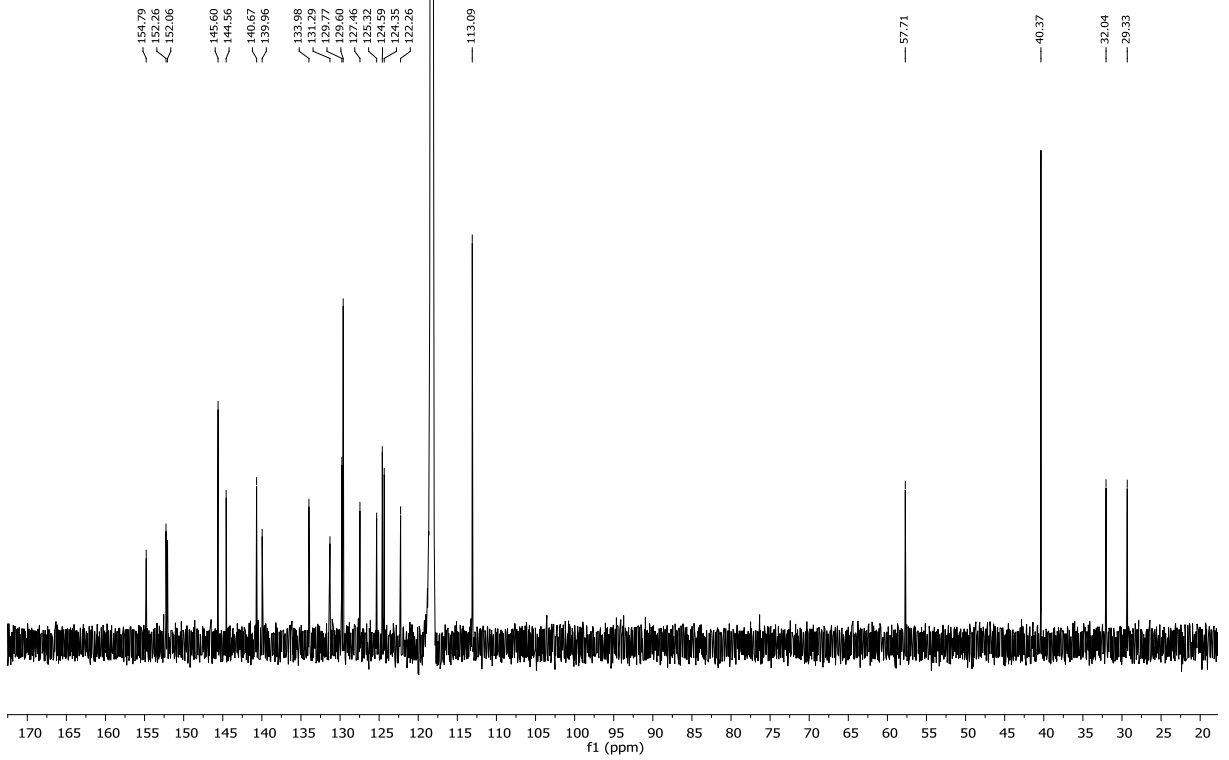
PR441/1  
400 MHz, CD3CN



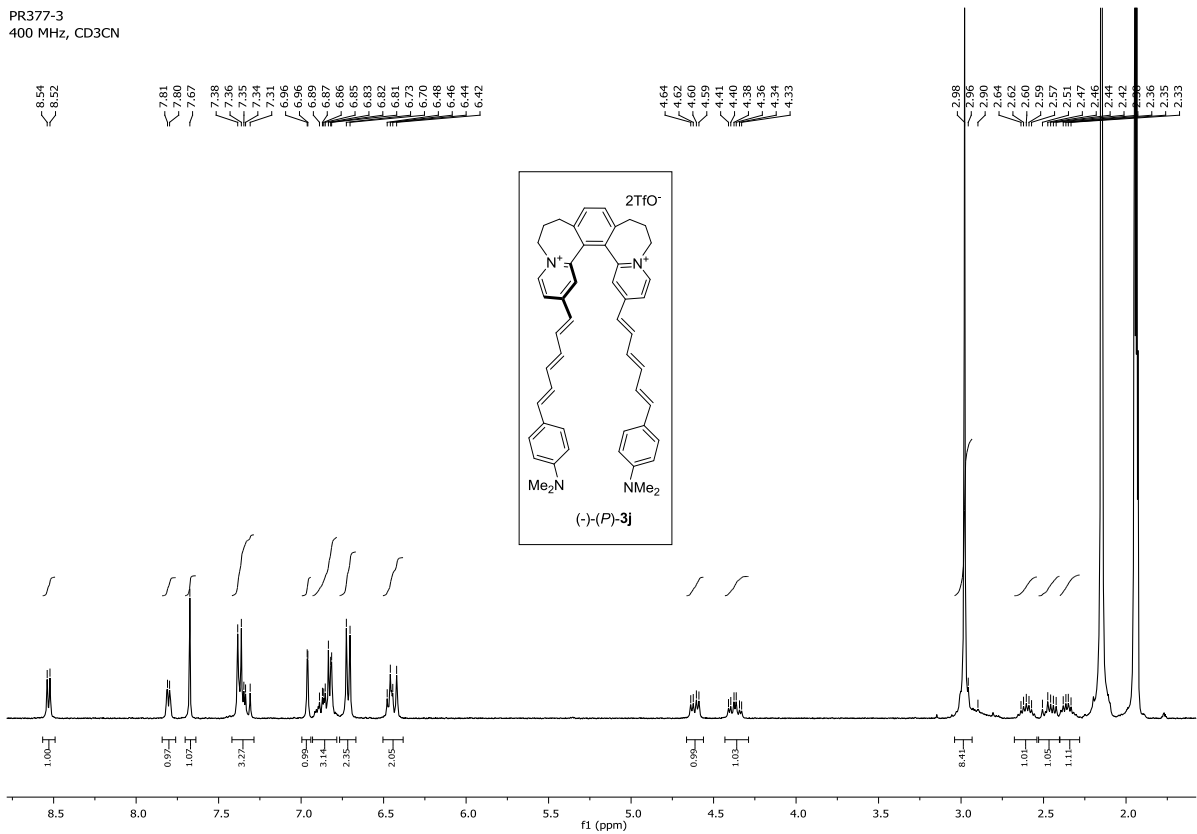
Reyes-PR396\_4.1.fid  
600 MHz, CD3CN



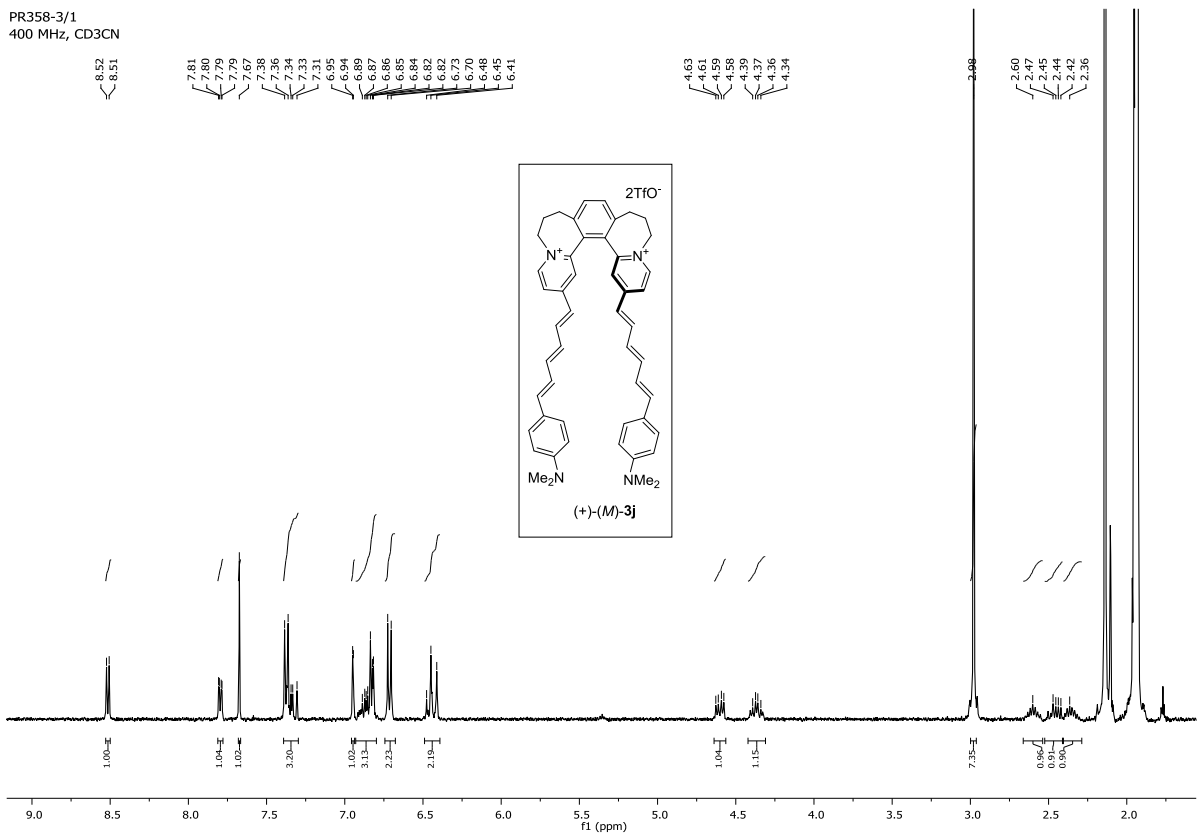
Reyes-PR396\_4.2.fid  
151 MHz, CD3CN



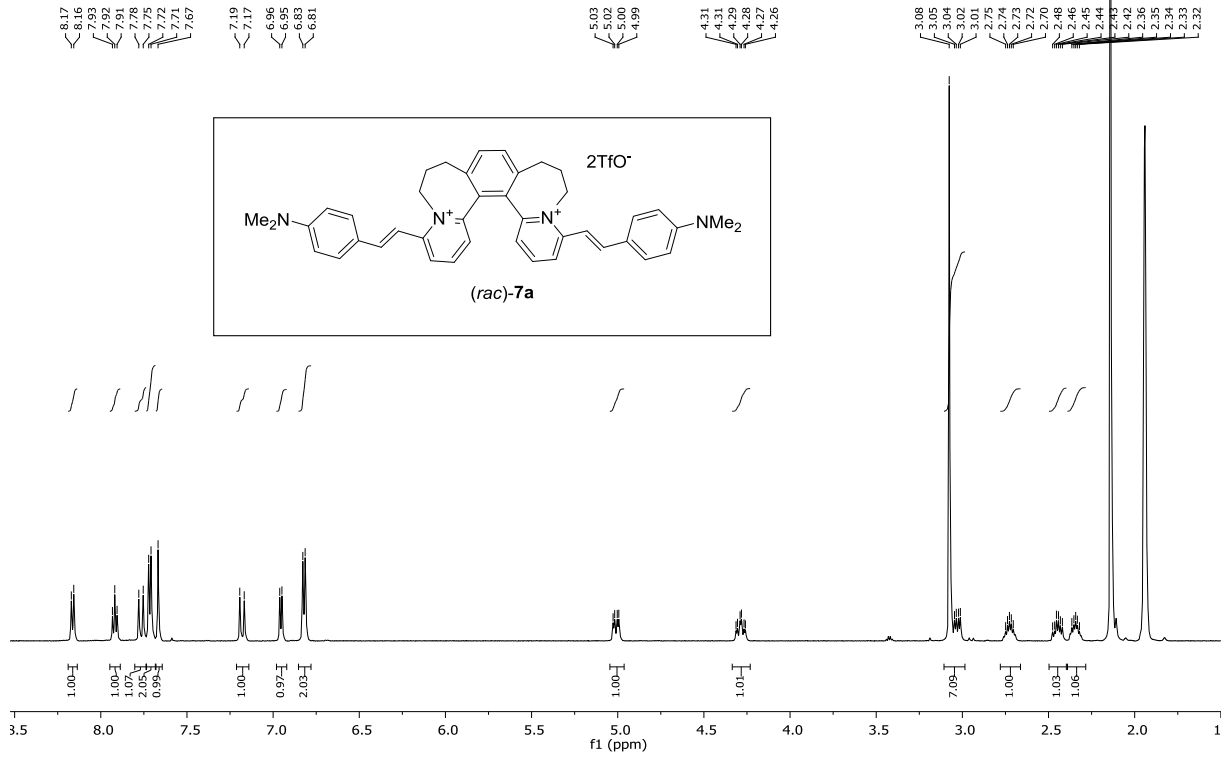
PR377-3  
400 MHz, CD3CN



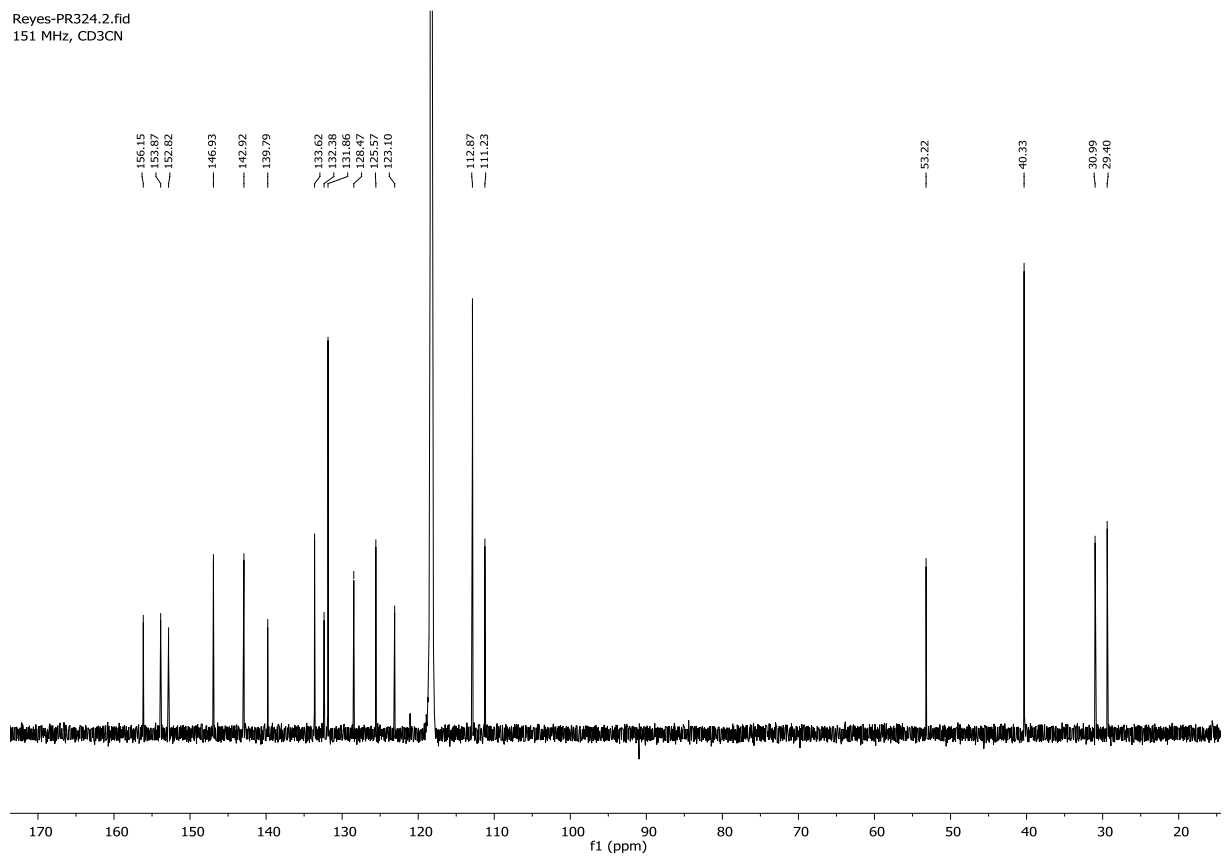
PR358-3/1  
400 MHz, CD3CN



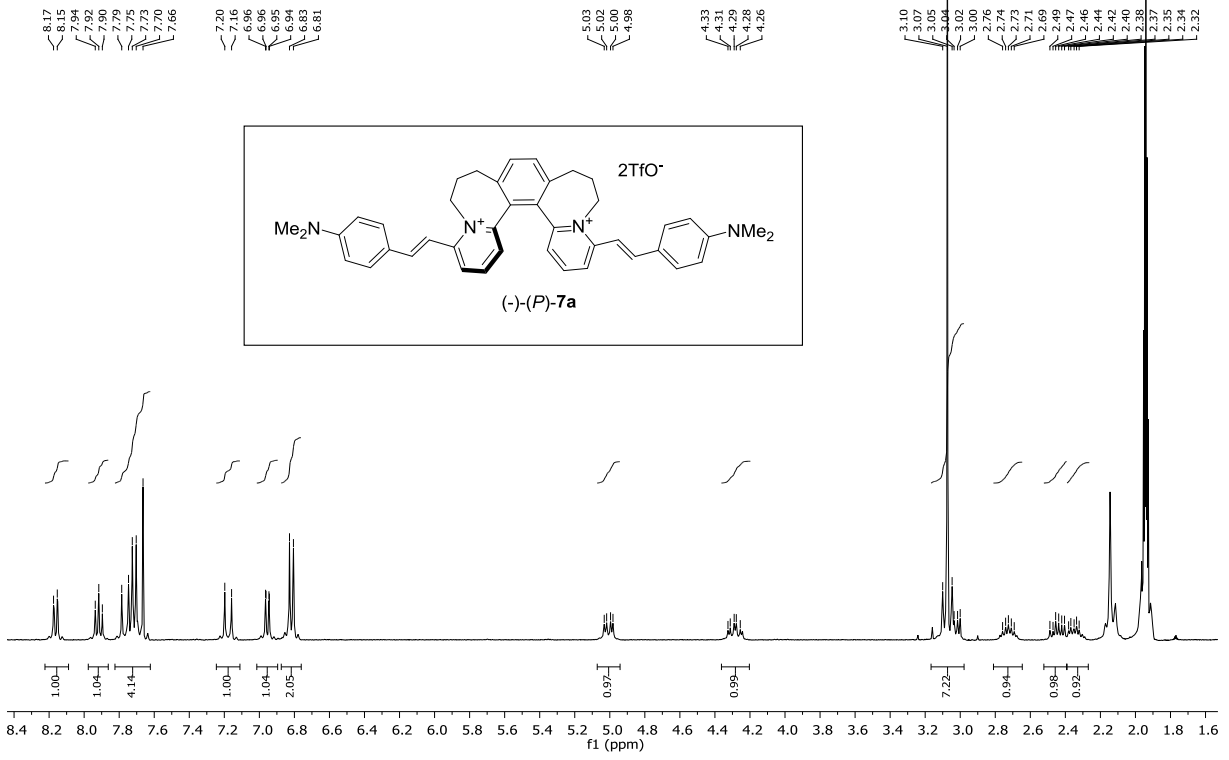
Reyes-PR324.1.fid  
600 MHz, CD3CN



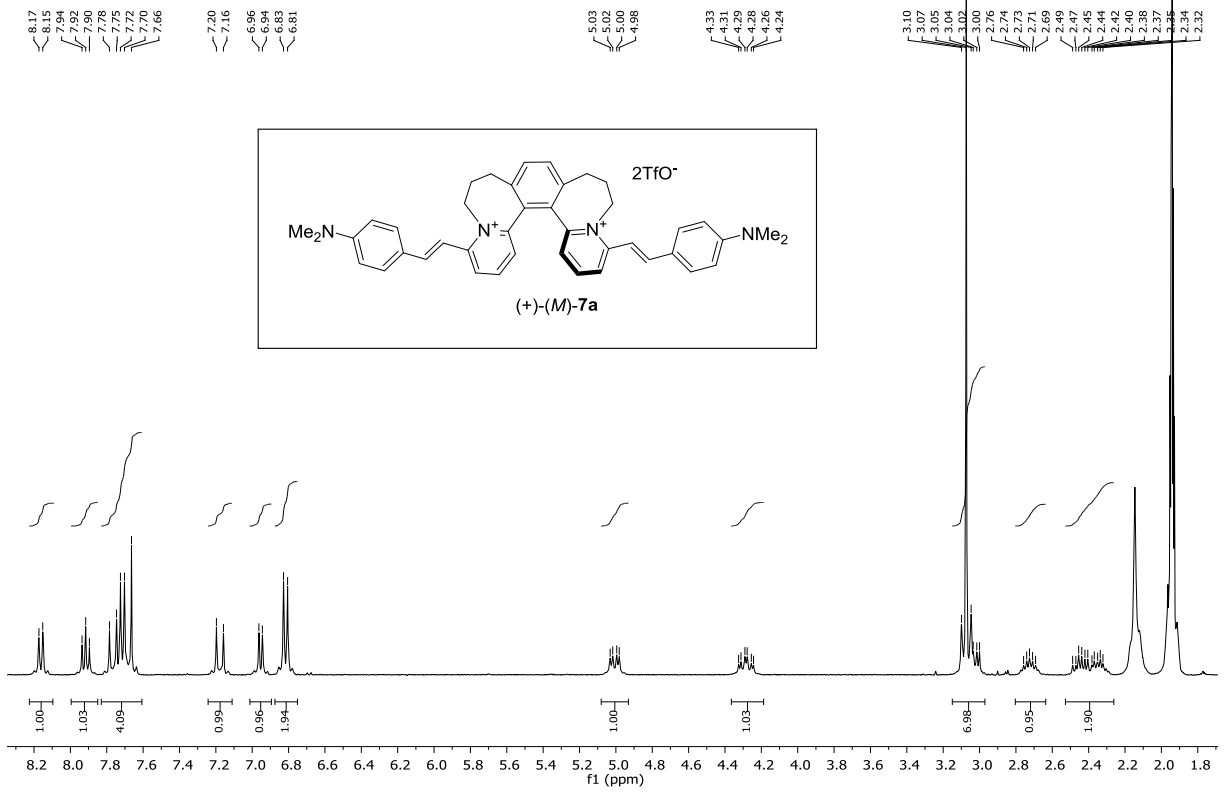
Reyes-PR324.2.fid  
151 MHz, CD3CN



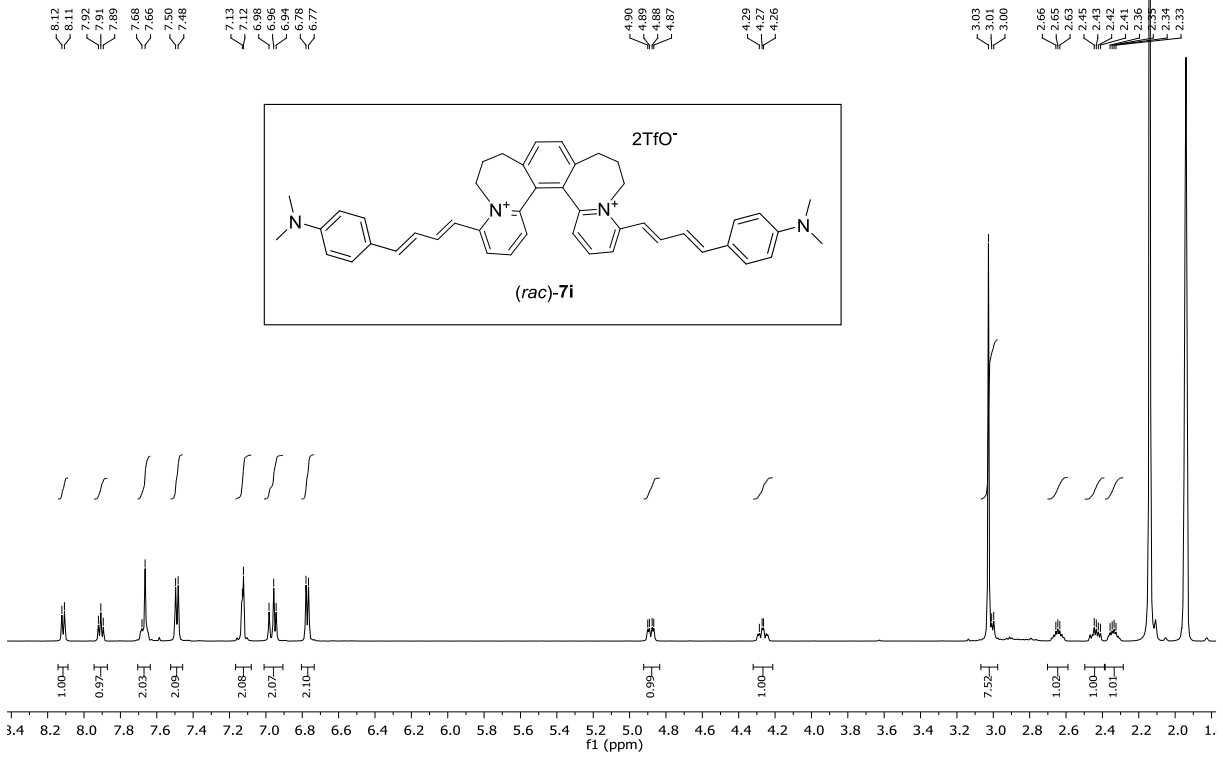
LS922-01  
400 MHz, CD3CN



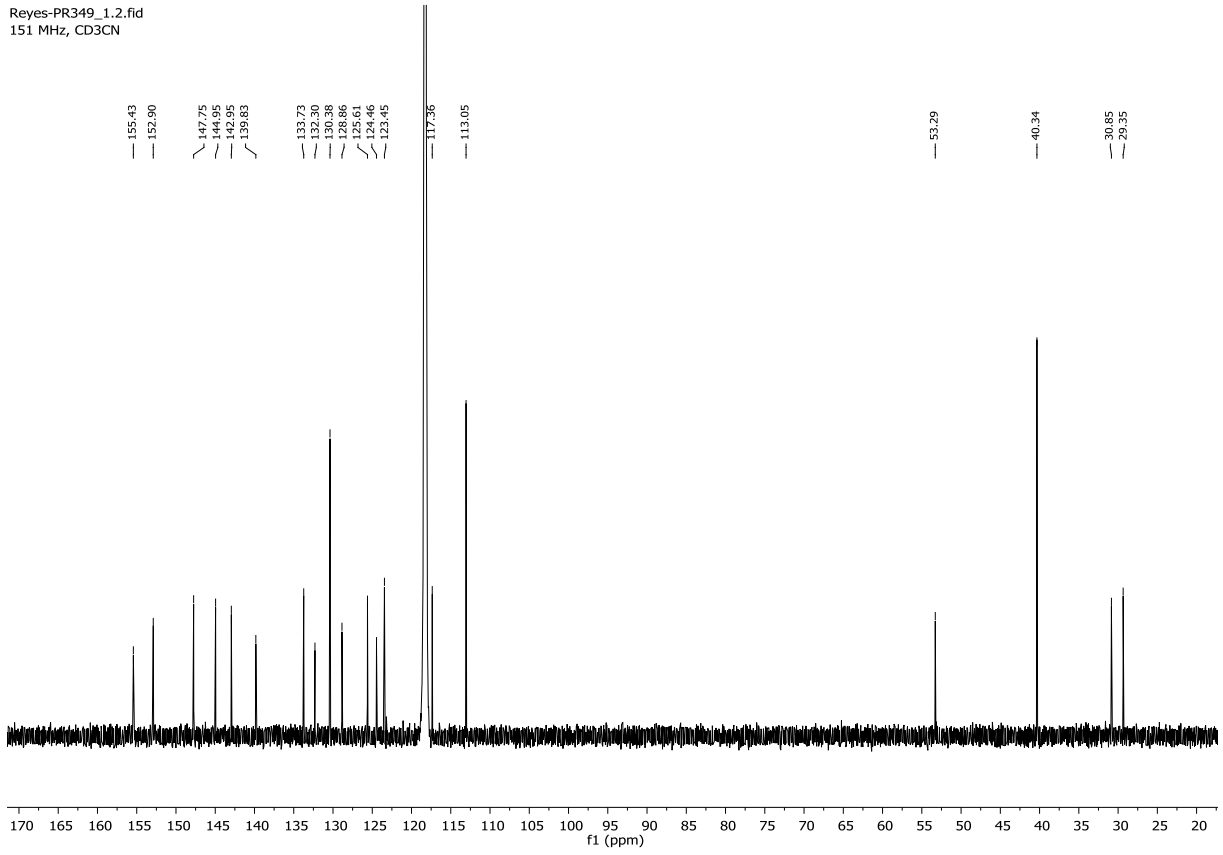
LS766-01  
400 MHz, CD3CN



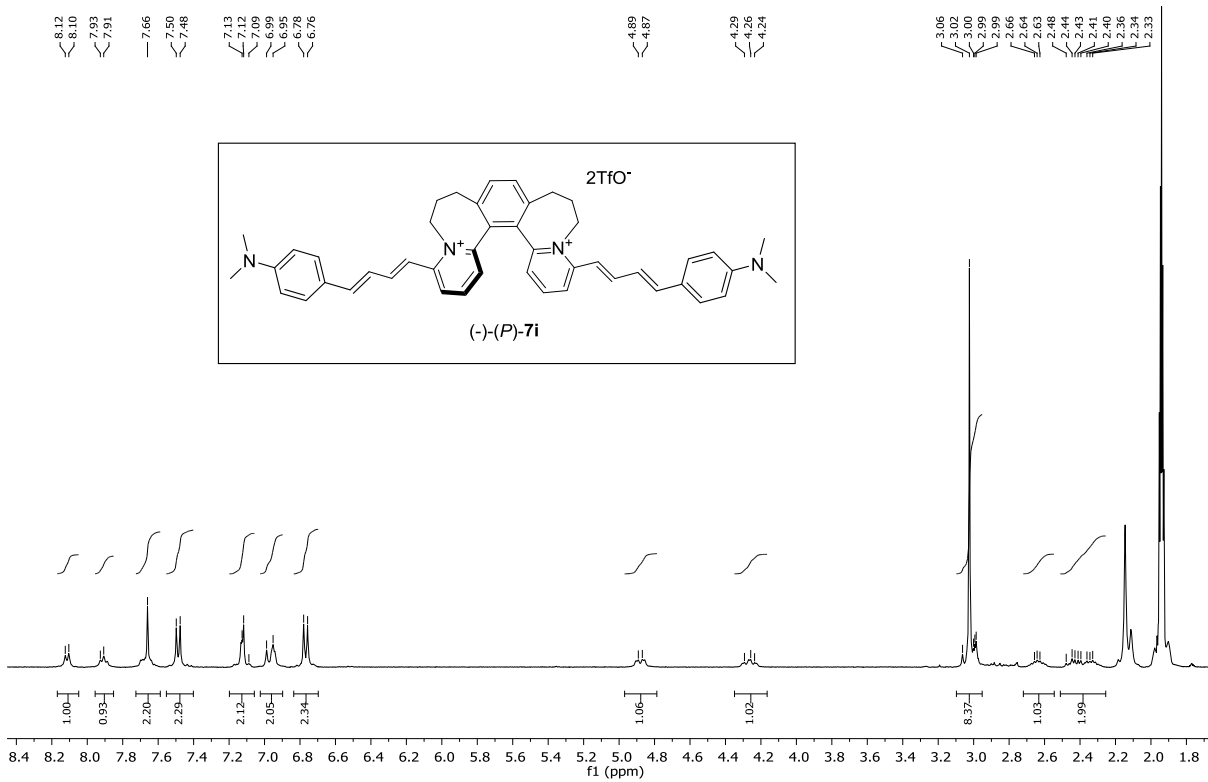
Reyes-PR349\_1.1.fid  
600 MHz, CD3CN



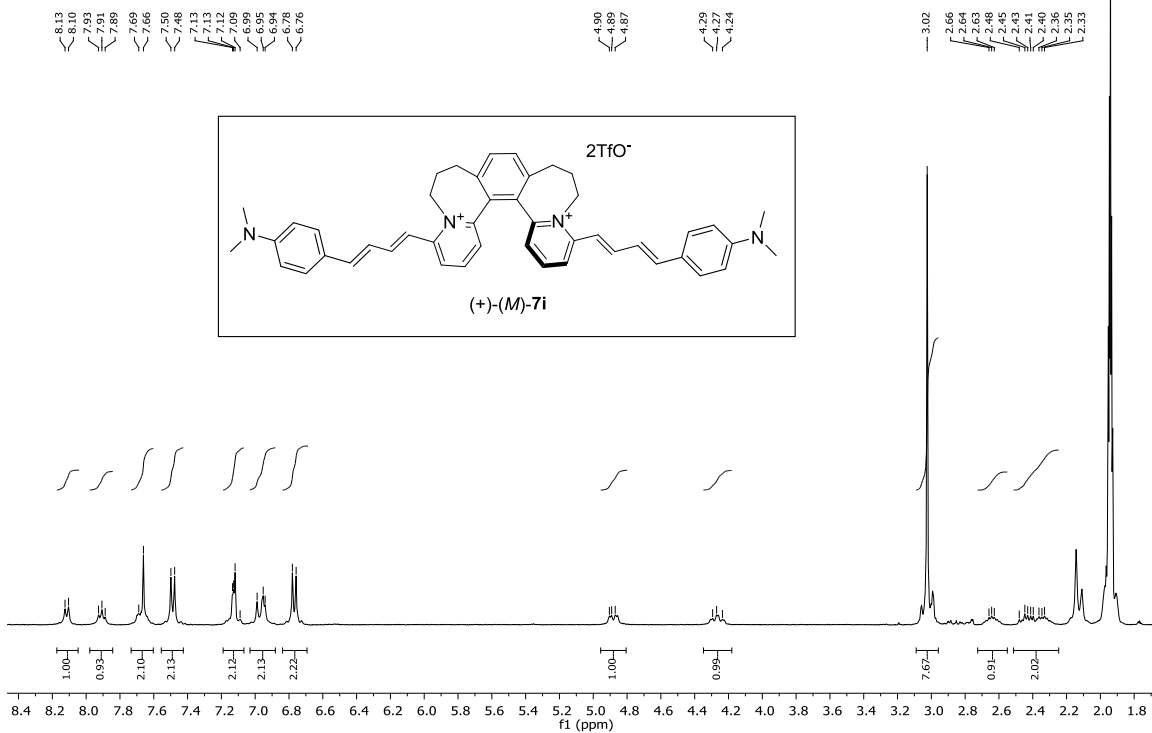
Reyes-PR349\_1.2.fid  
151 MHz, CD3CN



PR481-1.1.fid  
400 MHz, CD3CN

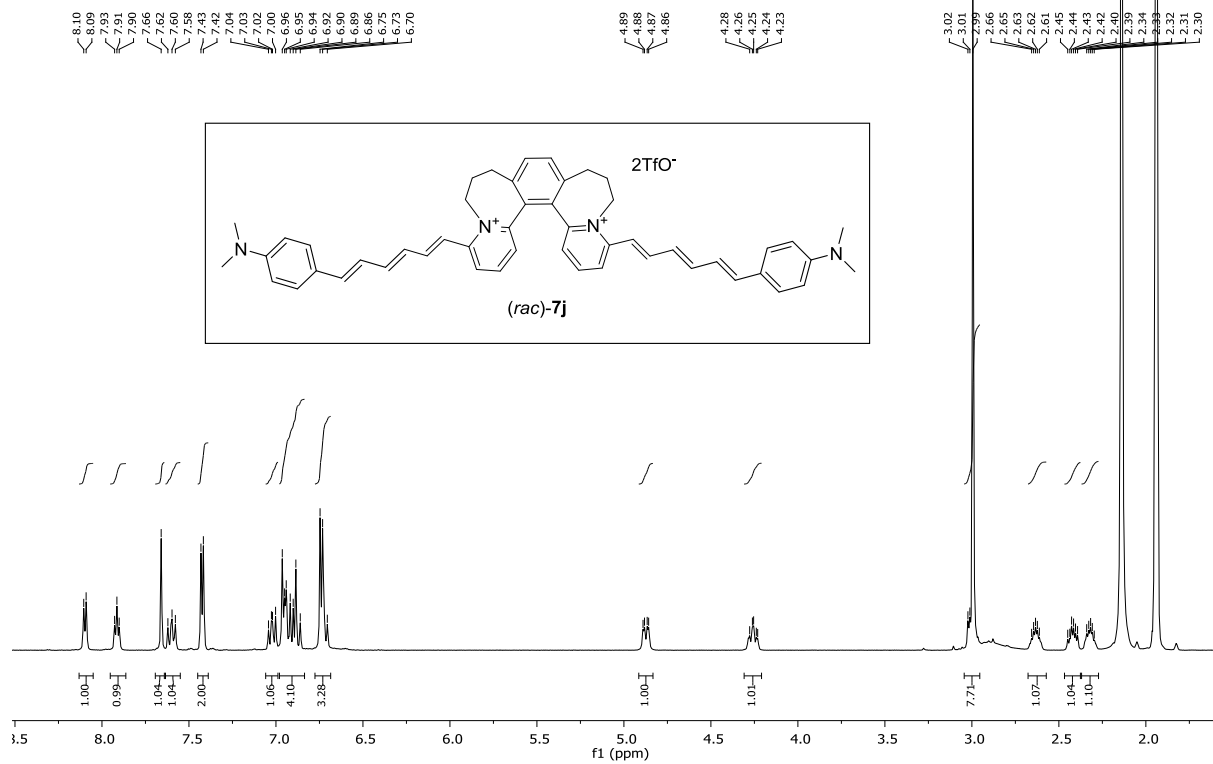


PR482-1.1.fid  
400 MHz, CD3CN

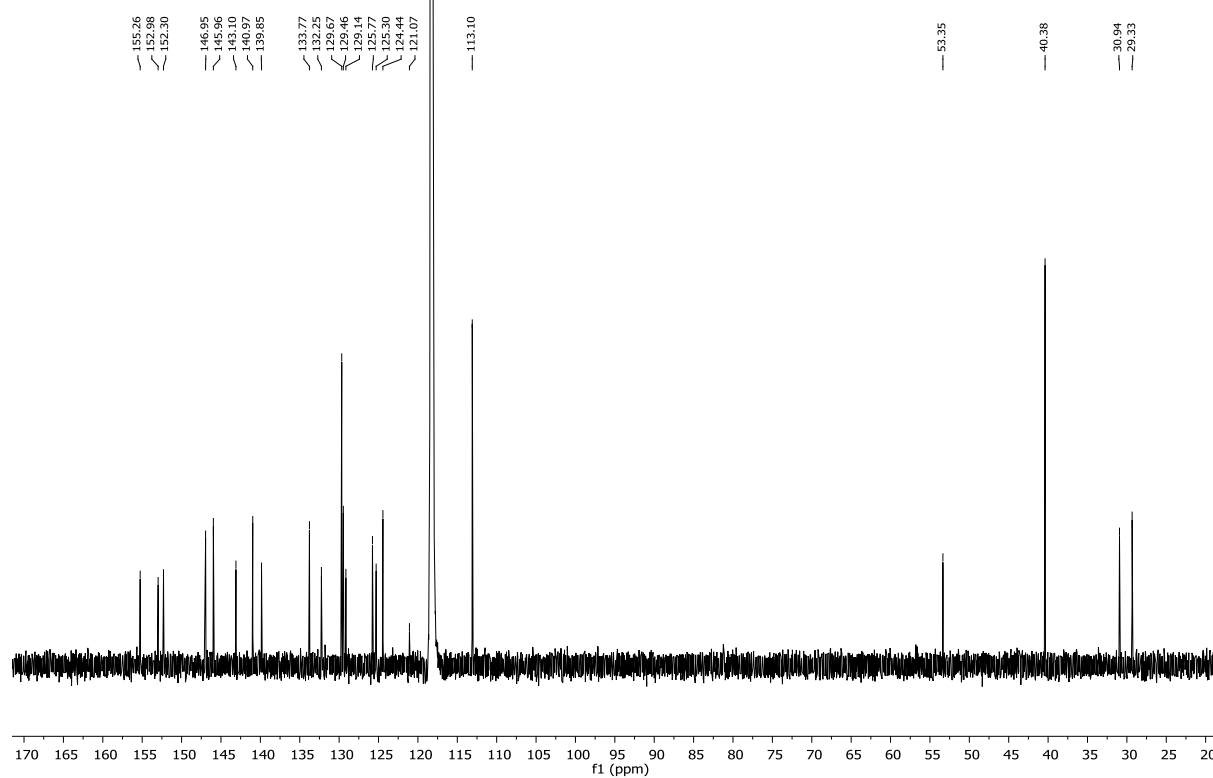




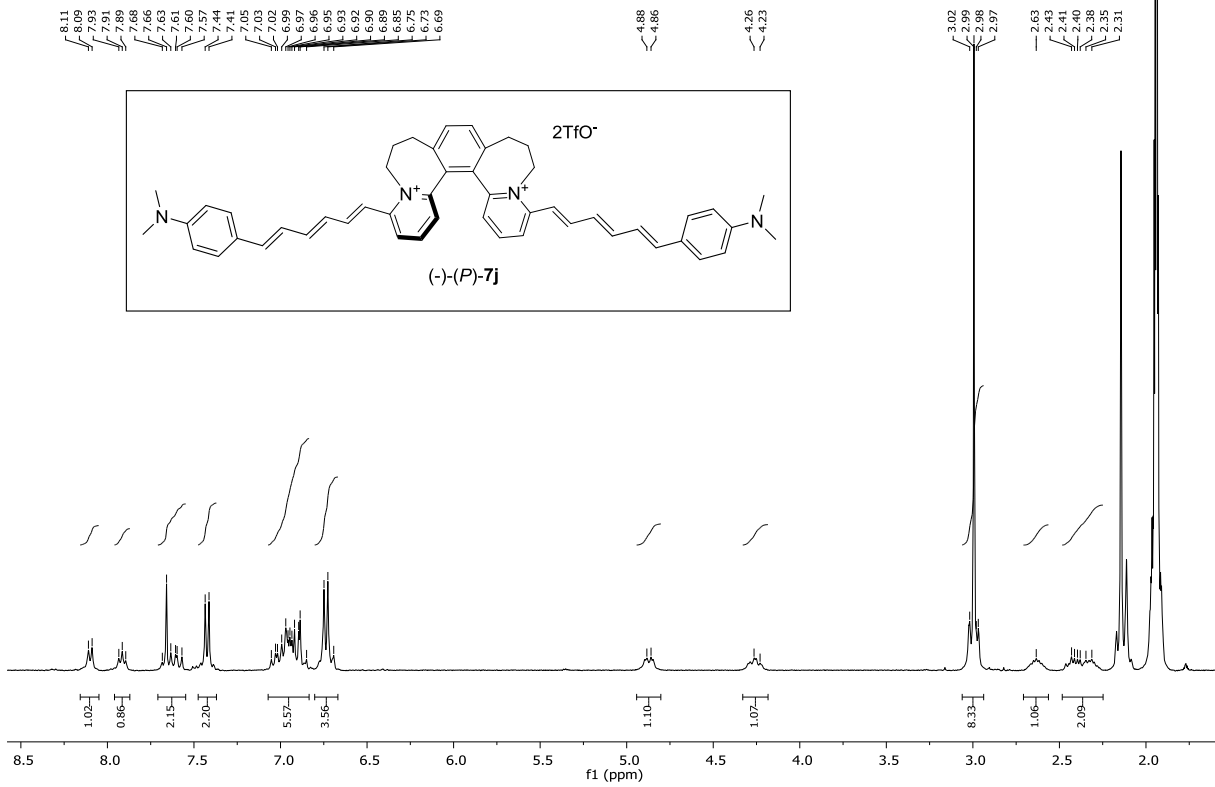
Reyes-PR473\_2.1.fid  
600 MHz, CD3CN



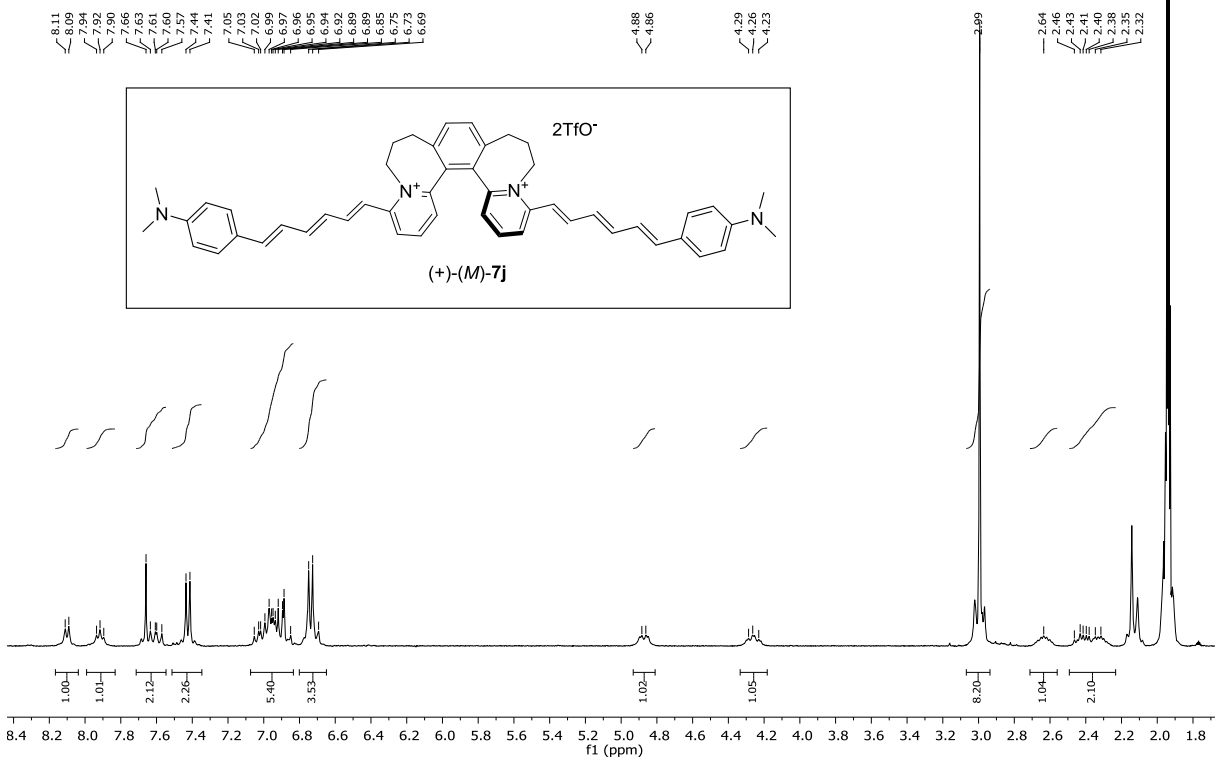
Reyes-PR473\_2.2.fid  
151 MHz, CD3CN



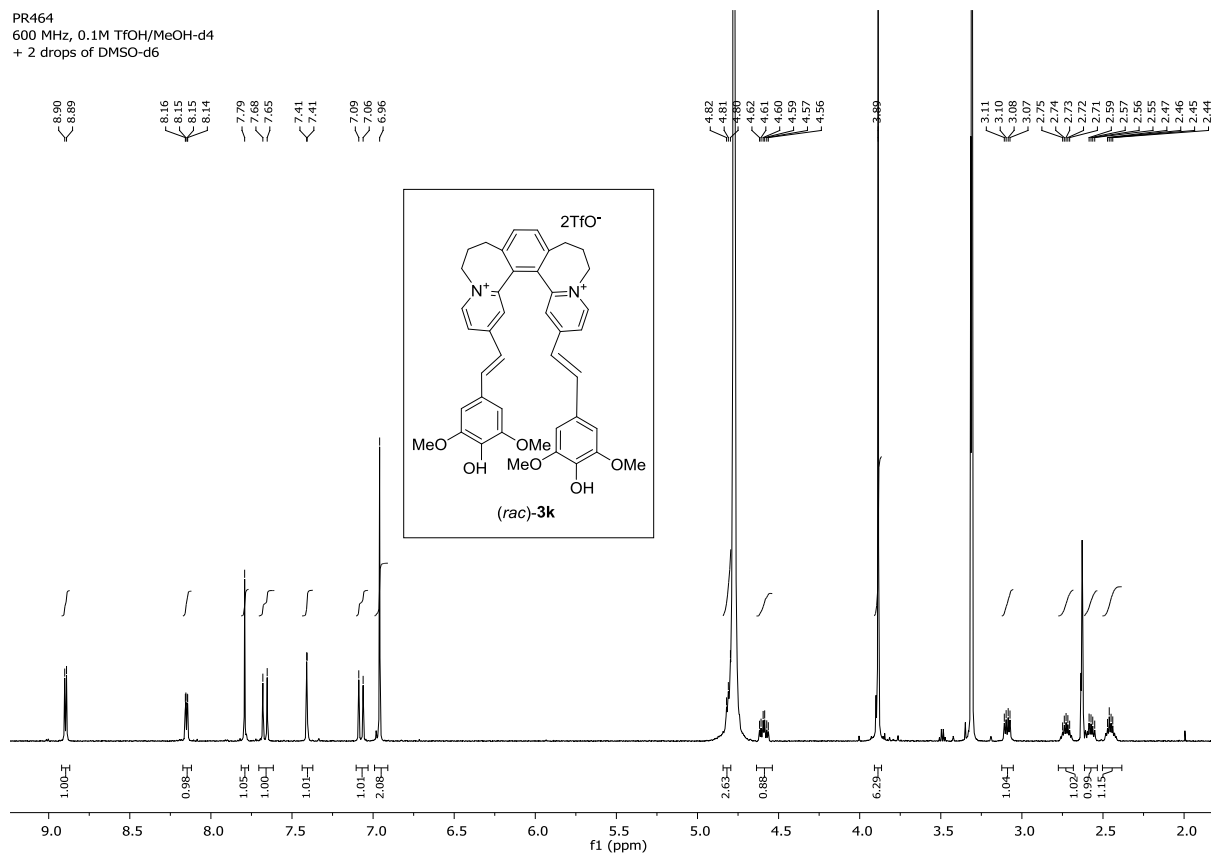
PR481-2.1.fid  
400 MHz, CD3CN



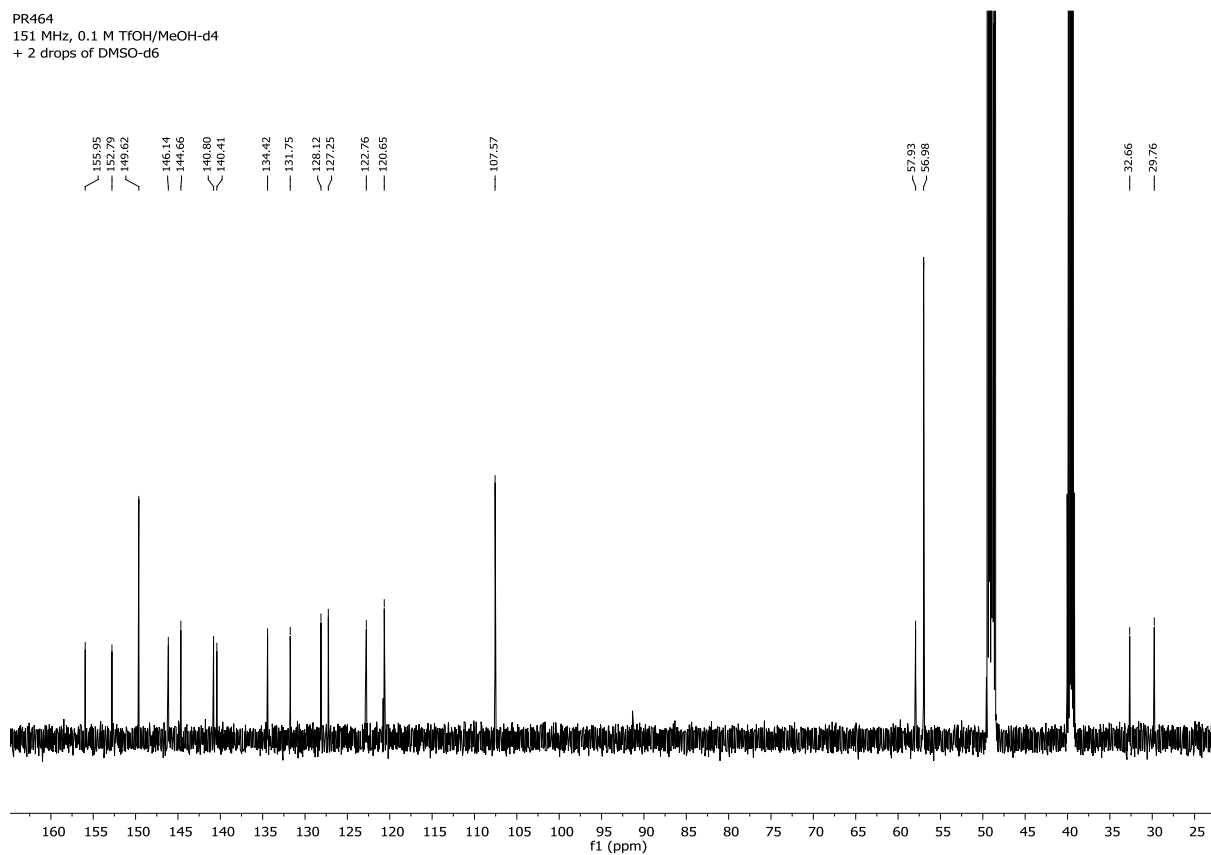
PR482-2.1.fid  
400 MHz, CD3CN



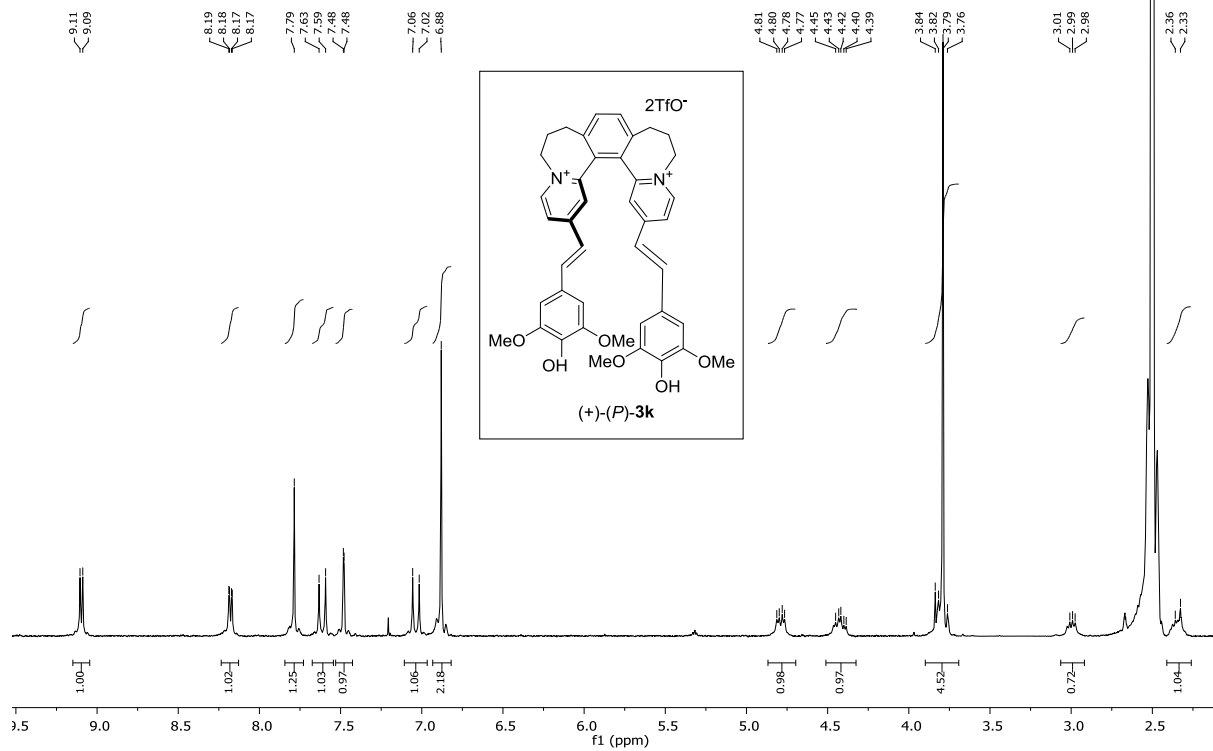
PR464  
600 MHz, 0.1M TFOH/MeOH-d4  
+ 2 drops of DMSO-d6



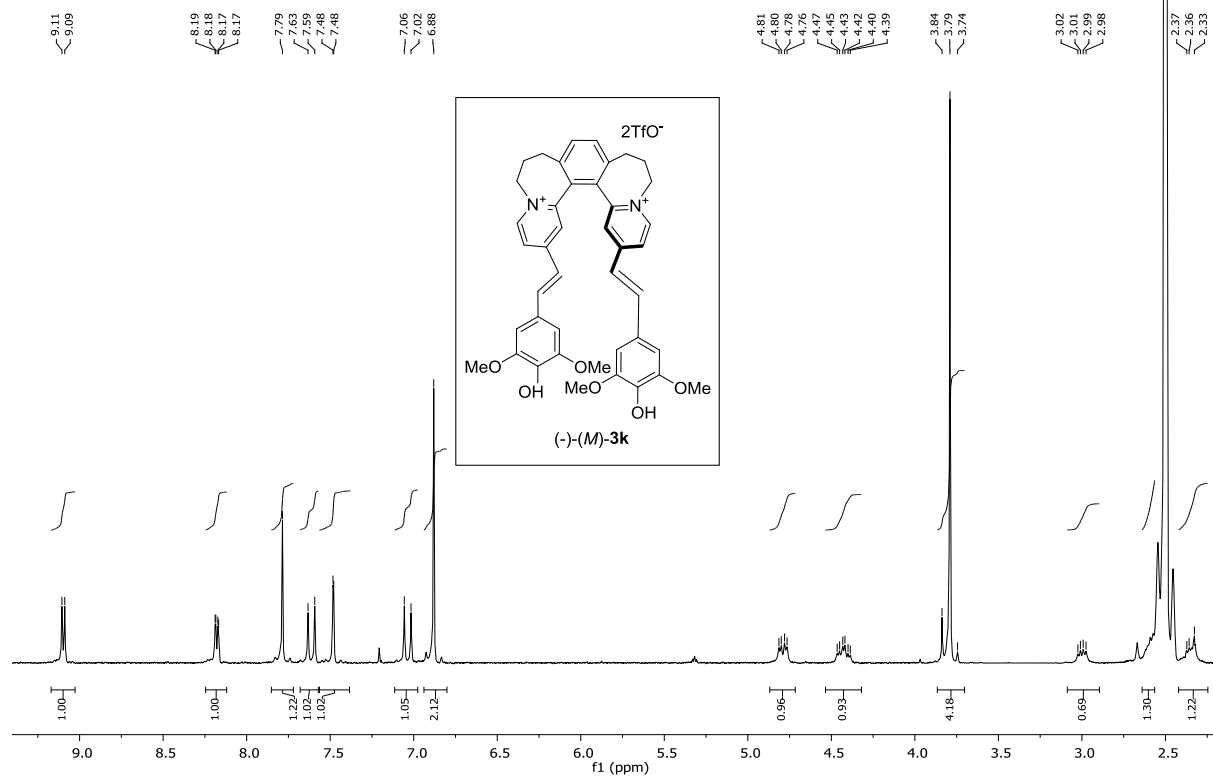
PR464  
151 MHz, 0.1 M TFOH/MeOH-d4  
+ 2 drops of DMSO-d6



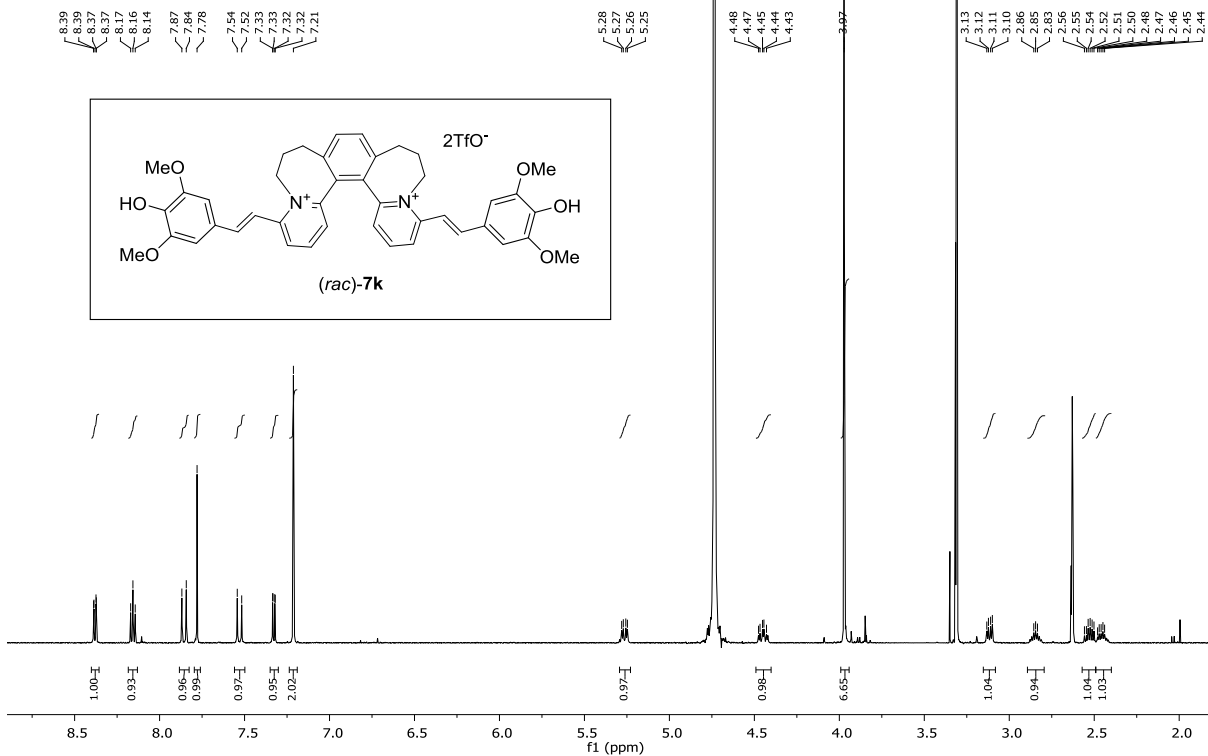
P-PR436  
400 MHz, DMSO-d6  
+ 2 drops of 0.1 M TfOH/MeOH-d4



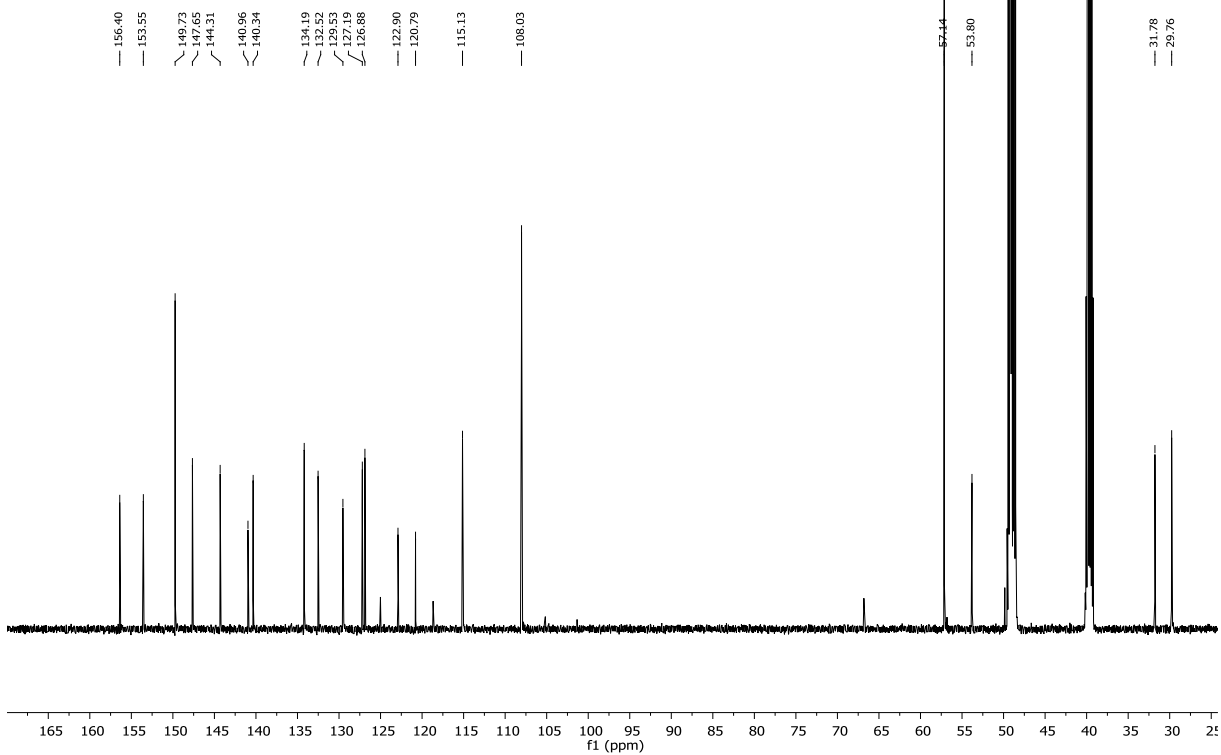
(M)-PR436  
400 MHz, DMSO-d6  
+ 2 drops 0.1M TfOH/MeOH-d4



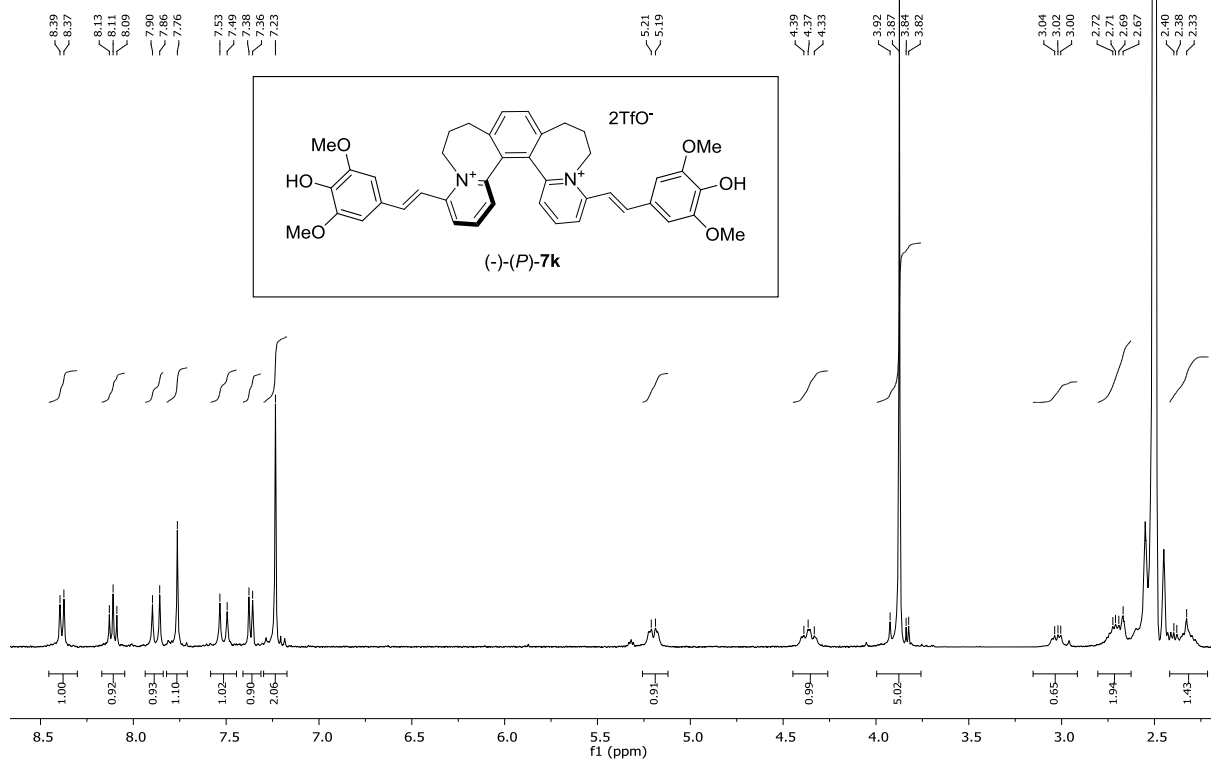
Reyes\_PR465.100.fid  
 600 MHz, 0.1 M TfOH/MeOH-d4  
 + 2 drops DMSO-d6



Reyes\_PR465.101.fid  
 600 MHz, 0.1 M TfOH/MeOH-d4  
 + 2 drops DMSO-d6



(P)-PR468  
 400 MHz, DMSO-d6  
 + 0.1 M TfOH/MeOH-d4



(M)-PR468  
 400 MHz, DMSO-d6  
 + 2 drops 0.1 M TfOH/MeOH-d4

